SYNTHETIC BIOLOGY APPROACHES FOR ENGINEERED LIVING MATERIALS

Charlie Gilbert

Submitted for the Degree of Doctor of Philosophy

Supervised by Dr Tom Ellis
Imperial College London
Department of Bioengineering
Centre for Synthetic Biology and Innovation

March 30th, 2018

Abstract

Nature produces materials with remarkable properties. Starting from single cells, organisms can proliferate and direct the conversion and accumulation of simple raw materials to form large structures. Following pre-programmed genetic rules, the cells that orchestrate the synthesis of these materials exert an incredible degree of control over the morphology of the structures they form. Over the course of evolution, natural biological materials have acquired a staggering range of properties – from electrical conductivity to strong underwater adhesion to thermoplasticity. Lastly, natural biological materials are not inert. The cells that produce these materials and remain associated with them are able to sense and respond to changes in their environment. However, in their natural form, the utility of these materials for applications in human industry and society is limited. Might it be possible to genetically-program living cells to create entirely new and useful biological materials? The emerging field of engineered living materials (ELMs) aims to address this question by recreating and engineering the natural processes of biological material assembly.

Here we explore two distinct strategies for the development of genetically-programmable biological ELMs. Firstly, motivated by a desire to create a modular platform for *de novo* ELM assembly, we developed a strategy enabling extracellular conjugation of proteins secreted by the Gram-positive bacterium, *Bacillus subtilis*. We demonstrate the utility of this system, not only for ELM development, but more generally for the synthetic biology and biotechnology research communities. Secondly, we developed a novel co-culture approach to produce growable bacterial cellulose (BC) materials with genetically-programmed functional properties. Specifically, inspired by the pseudo-natural microbial community of fermented kombucha tea, we recreated kombucha-like co-cultures between an engineerable BC-producing bacterium *Komagataeibacter rhaeticus* and the model organism and synthetic biology host *Saccharomyces cerevisiae*. These approaches therefore lay the groundwork for the development of an entirely new class of materials, ELMs.

Declaration

I herewith certify that all the material in this thesis is my own work, except for quotations from published and unpublished sources which are clearly indicated and acknowledged as such. The source of any picture, diagram or other figure that is not my own work is also indicated.

Contents

List of Figures

List of Tables

Publications resulting from this work

Gilbert, C., Howarth, M., Harwood, C. R., and Ellis, T. (2017) Extracellular Self-Assembly of Functional and Tunable Protein Conjugates from *Bacillus subtilis*. *ACS Synth. Biol. 6*, 957–967.

Acknowledgements

I would like to first thank Tom for being a fantastic supervisor. Not just for providing guidance throughout my PhD project, but also for your genuine commitment to helping me develop as a researcher.

I want to thank the members of the Centre for Synthetic Biology and Innovation who have all helped me in one way or another throughout my time at Imperial – Edina, Joyce, Linda, Rochelle and so many others. In particular I'd like to thank Kealan for always providing stimulating discussion and welcome distraction. I'd like to thank Colin Harwood, Rita Cruz, Chris Sauer and Mark Howarth for giving me guidance at start of my PhD and Tzu-Chieh Tang for being a great collaborator.

To all the members of the Ellis lab – Ali, Franci, George, Glen, Marcus, Ben, and so many others – thank you for all your support and advice, but more importantly, thank you for the great times. I can honestly say that I really enjoyed my time in the lab and we all know that had nothing to do with the science. Thanks to Carlos for being a brilliant mentor and for keeping me going at my lowest point. And thank you to Olivier for being a brilliant menteur and always having time for me. And thanks to Will for being a great mate.

To my family, friends and Chloe, thank you.

1 Introduction

SUMMARY

Natural biological materials exhibit remarkable properties: self-assembly from simple raw materials, autonomous control of morphology, diverse physical and chemical properties, self-repair and the ability to sense-and-respond to environmental stimuli. In their natural form, the utility of these materials for applications in human industry and society is limited. But, could it be possible to genetically program living cells to create entirely new and useful biological materials? Straddling the border between material science and synthetic biology, the emerging field of engineered living materials (ELMs) aims to answer this question. Achieving this grand vision will be a major challenge, requiring the rules governing the formation and function of natural biological materials to be discerned and re-engineered into complex synthetic genetic circuits. However, if realised, this vision could enable a paradigm shift in the production of materials, leading to a future where materials, harnessing the remarkable properties of living cells, are grown rather manufactured. In this section we discuss natural biological materials and ELMs. We also review synthetic biology approaches to develop this new class of material, focussing first on simple microbial model systems and later on more complex systems.

1.1 Biological materials

1.1.1 Defining biological materials

Biological materials are familiar to us from the everyday world – materials like wood, shell or cotton. However, a great many biological materials exist with which we are less familiar – like the ultrahard magnetite teeth of marine molluscs[1], the highly-resilient elastic material resilin found in insect wing ligaments[2] or the electrically-conductive protein fibres produced by certain bacteria[3]. Therefore, it is important to begin by defining exactly what is meant by the term 'biological material'.

In its broadest sense, a 'biological material' could be any substance accumulated or synthesised by an organism. Here, however, we define 'biological materials' as polymeric, fibrous or crystalline structures produced by living cells (Figure 1). These materials can be made up of a number of different biological molecules – including carbohydrates, proteins, lipids or nucleic acids – and can incorporate inorganic species. Biological materials range from homogenous, polymerised species (e.g. spider silk) to complex composites of multiple

Figure 1 Natural biological materials. Examples of natural biological materials. Clockwise from the top left: a bacterial biofilm (image credit: Scott Chimileski and Roberto Kolter, Harvard Medical School, Boston), squid sucker ring teeth (image credit: Shawn Hoon, Flickr), garfish ganoin scales (image credit: Mary Harrsch, Flickr), a chiton showing its mineralised shell (image credit: matt knoth, Flickr), spider silk produced by a net-throwing spider (image credit: Frank Vassen, Flickr) and a cotton boll (image credit: Kimberly Vardeman, Flickr).

chemical species within which living cells are embedded (e.g. whole tissues). Further, biological materials span multiple length scales, from nanostructures like bacterial microcompartments[4], to structures as large as the trunk of a redwood tree or the shell of a giant clam.

1.1.2 Properties of natural biological materials

Humans have found uses for many biological materials as textiles, clothing, construction materials, tools and so on. But over the course of history, many of the biological materials that were once used by humans, have been supplanted by man-made materials such as metals and plastics. However, it is becoming increasingly clear that materials produced by biological systems are capable of matching the properties of man-made materials and, in some cases, surpassing them. Further, natural biological materials exhibit several unique, desirable properties that make them attractive prospects for the production of novel, useful materials. In this section, four unique properties of natural biological materials are described.

Firstly, biological materials are self-assembled or 'grown'. Starting from just a single cell, organisms can proliferate and generate materials on a large scale. So, to produce new material, all that is needed is a single cell and the appropriate nutrients and conditions. On top of that, the growth of biological materials can be fed by relatively simple nutrients, often from sustainable sources. A redwood tree, for instance, is able to convert carbon dioxide, water and simple nutrients into hundreds of tons of wood. Therefore, in contrast to man-made materials, biological materials can manufacture themselves using simple raw materials and the 'seeds' for their growth can be transported with relative ease. One area in which these desirable properties might be of particular value is the field of space exploration. Since the cost of transporting materials into to space is prohibitively expensive – roughly $10,000 per pound – it is impractical to launch all the materials required for construction of habitats, for example. A much more attractive approach would be to transport 'seed' cells or DNA, containing the information required to grow materials *in situ*, using local raw materials[5]. Further, many biological materials are also biodegradable. Considering plastics alone, only around 9% of the ~6 billion metric tons of plastic waste generated up until 2015 have been recycled, with around 79% accumulating in landfills and the natural environment[6]. Biodegradable biological materials therefore represent a far more sustainable potential alternative to many man-made materials.

Secondly, biological materials exhibit a staggering range of functional properties. Across the rich diversity of nature, organisms have evolved to produce a huge number of biological materials to fulfil various functional roles (Table 1). In fact, there are surprisingly few material properties shown by man-made materials that cannot also be found in some natural biological material. Natural biological materials, therefore, can be seen as a vast, largely-untapped resource for the production of a new generation of materials.

Table 1 Examples of natural biological materials with notable functional properties

Biological Material	Functional property
Lotus plant leaves	Ultra-hydrophobicity
Spider silk	Tensile strength comparable to steel
Geobacter protein nanowires	Electrical conductivity
Squid ring teeth	Thermoplasticity
Mussel byssus threads	Strong underwater adhesion
Chiton radula	Ultra-hard abrasion resistant biomineral
Cephalopod skin	Mimcry of natural environment for adaptive camouflage
Gecko setae	Remarkable dry adhesion to almost any surface
Elastin, Resilin	Elasticity with high resilience
Microbes, Fungi, Fireflies, etc.	Bioluminescence

Thirdly, biological materials autonomously form specific structures. In a process known as morphogenesis, cells follow genetically-programmed rules to control the spatial arrangement of the materials they produce. Considering bone, for example, the adult human body contains 206 bones, each composed of broadly the same material: a composite of collagen protein fibres and mineralised calcium phosphate. However, during development, the cells that produce these bones are able to orchestrate the construction of 206 different structures with incredible precision. This is just one of many examples of the exquisite degree of control that cells can exert over the structures of biological materials (Figure 2). Notably, biological material structure is controlled over multiple length scales, from the tissues of large, multicellular organisms all the way down to nanoscale intracellular structures. In fact, in

many cases the fine-control of structure underlies the functional properties of the entire material.

Lastly, biological materials are able to sense and respond to changes in their external environment. Since living cells produce and are often embedded within biological materials, they have the capacity to modify the properties of the material in response to changing conditions. This allows biological materials to perform a number of dynamic tasks, like self-repair or adaption to the environment.

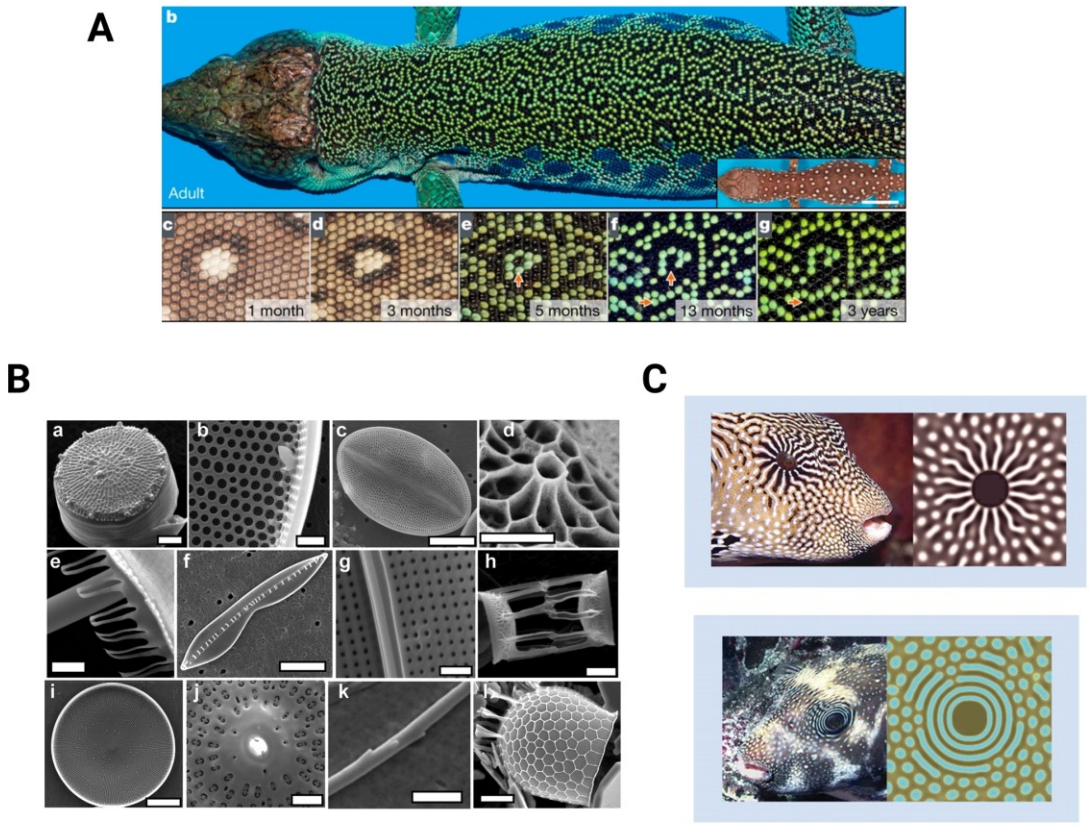

Figure 2 Control of biological material structure. A Patterns of pigmentation in ocellated lizard scales, image reproduced with permission from Manukyan et al. [269] **B** Nanostructured silica cell walls in marine diatoms, image reproduced with permission from Hildebrand et al.[108] **C** Turing patterned pigmentation in popper fish, image reproduced with permission from Massimo Boyer (www.edge-of-reef.com).

1.1.3 Genetically-engineered biological materials

Biological materials possess many advantageous traits that make them attractive prospects as materials of the future. But, since the specific properties of biological materials are dictated by their particular evolutionary context, their utility in human technology is typically limited. Moreover, in many instances it would not be cost effective to source biological materials from their natural source. Spider silk, for example, is a biological material with impressive material properties: tensile strength comparable to steel and elasticity comparable to rubber[7]. But it is not practicable to harvest large quantities of spider silk for industrial purposes.

Since the advent of methods for genetic engineering and recombinant protein expression, there has been growing interest in engineering organisms to produce useful biological materials. Synthesising engineered biological materials in optimised, industrial strains, could create a more cost-effective production pipeline for materials that cannot be harvested from their natural sources. In addition, using genetic engineering specific, desirable properties from natural biological systems could be combined and refactored to produce novel, useful materials.

Over recent decades, numerous natural and engineered biological materials have been produced using recombinant protein expression. Broadly, the same approach is used: recombinant proteins are expressed in engineered hosts, purified and then processed – for instance, by spinning into fibres or casting to form gels – to create the material of interest. Alternatively, non-protein materials can be produced by recombinantly expressing the genes responsible for biosynthesis of the particular material in an engineered host. In fact, recent years have seen this first generation of engineered biological materials nearing a commercial reality. In March 2017, Bolt Threads Inc. sold 49 limited edition ties knitted from recombinant spider silk[8]. In September of the same year Modern Meadow Inc. announced that Zoa™, its prototype fashion line made from recombinant leather, would be exhibited at the Museum of Modern Art in New York[9].

However, these approaches use living cells only to produce a precursor or feedstock for the final material and as such do not take advantage of some the most important properties of biological materials: growability, autonomous structure formation and sense-and-response. The field of synthetic biology may offer the key to meeting this challenge. In general, the

field of synthetic biology aims to recapitulate, reconstitute or repurpose biological systems for useful purposes by genetically programming cells. Inspired by electrical and mechanical engineering disciplines, synthetic biology has focussed on developing standardised, characterised and modular genetic parts and on implementing emerging enabling technologies to facilitate and accelerate genetic engineering. Over recent years, these tools and techniques have been turned to the challenge of engineering biological materials, creating a new class of materials – engineered living materials.

1.1.4 Engineered Living Materials (ELMs)

Natural biological materials exhibit remarkable properties: self-assembly from simple raw materials, autonomous morphogenesis, diverse physical and chemical properties and the ability to sense-and-respond to environmental stimuli. The field of engineered living materials (ELMs) aims to recreate these properties to generate new and useful materials. ELMs are defined as materials in which living cells form an integral part[10–12]. The living component of the material can serve a number of functions: formation of the material itself, contribution of novel functional properties, environment responsiveness, self-healing and so on. As well as living cells, ELMs can be composed of inorganic components, such as synthetic polymer matrices or inorganic compounds. These materials qualify as 'engineered' either if they are composed of living cells that have been genetically-engineered to fulfil some function or if they have been mechanically engineered in some way. For an excellent, comprehensive review of ELMs, readers are referred to Nguyen et al[12].

However, this definition of ELMs includes a large number of partially synthetic composite materials, which once again, do not take full advantage of the some of the most important properties of biological materials – specifically, self-assembly and morphogenetic control. Here we propose a sub-category of ELMs: biological ELMs. We define biological ELMs as engineered living materials, in which the entire material is composed of biologically-derived components and is assembled biologically. As with ELMs, these materials may contain inorganic components. However, to be classified as a biological ELM, any inorganic species must be accumulated or deposited biologically. Indeed, there are many natural examples of biological materials that incorporate a biotic inorganic component, for instance, biomineralized materials like bone or shell. By contrast, ELMs containing synthetic inorganic components – such as polymer scaffolds or nanomaterials – do not qualify as biological ELMs. In addition, the material assembly process must occur through biological self-assembly, so 3D-printed materials, for example, do not qualify as biological ELMs.

The goal of the field of biological ELMs is to genetically engineer biological systems to produce novel, useful materials with programmable properties. Achieving this major challenge could lead to a new paradigm for material production, taking advantage of the remarkable properties of biological materials. However, at the same time biological ELMs represent perhaps the most challenging class of ELMs to engineer. The genetic rules

governing the functional properties and morphogenesis of natural biological materials are still being uncovered. And rationally-engineering these processes will likely require the use of well-characterised genetic parts and circuits from the field of synthetic biology. Indeed, efforts to develop biological ELMs using synthetic biology approaches have only recently begun in earnest. In the remainder of this introduction, we will focus predominantly on biological ELMs and some of the approaches and systems that are being used to engineer this new class of materials. Firstly, we will examine two of the most advanced biological ELM systems developed to date: bacterial biofilm amyloids and bacterial cellulose. Then we will explore more complex biological materials which are emerging as biological ELM systems of the future. Finally, we will review approaches that may allow novel biological ELMs to be built from the bottom-up.

1.2 Bacterial biofilm amyloids and curli fibres

Many of the pioneering efforts to develop biological ELMs have focussed on engineering *E. coli* biofilms. In this section we first discuss some of the natural properties of these simple, genetically-tractable model systems. In addition, we review recent efforts to genetically-program novel, useful properties in this emerging class of biological ELMs.

1.2.1 Structure and properties of natural biofilm amyloids

Amyloids are fibres formed by a diverse group of proteins and are defined by a common β-sheet rich protein structure, the cross-β strand[13,14]. Although originally isolated because of their connection to various human disease states, amyloids are found in diverse organisms, from bacteria to humans[15], and perform numerous functional roles as toxins, adhesins, surface property modifiers and more[16]. The cross-β strand amyloid fibre structure consists of a flattened coil of β-strands that form a continuous hydrogen-bonding network running the length of the fibre. This extended hydrogen-bonding network results in the remarkable material properties of amyloid fibres – such as high tensile strength and Young's modulus[17] – as well as their impressive resistance to degradation by proteases and denaturation[18]. Many bacteria utilise the remarkable properties of amyloids to build biofilms. Bacterial biofilms are essentially composite materials composed of living cells that produce and become embedded within an extracellular matrix. The extracellular matrix itself is composed, chiefly, of polysaccharides and amyloid proteins. In the natural environment, bacteria produce biofilms to enable attachment to surfaces and long-term persistence[19].

The best studied of the bacterial biofilm amyloids are curli fibres. Curli fibres, also known as curli pili, are produced by a number of species of the family *Enterobacteriaciae*, most notably by *E. coli*. Because of their known roles in bacterial pathogenesis, the biogenesis of curli fibres has been extensively studied (Figure 3). Briefly, a host of proteins are expressed from the curli (*csg*) operon and secreted into the *E. coli* periplasm. Here they form a pore in the outer cell membrane through which the major curli subunit CsgA, a 13 kDa protein, is secreted[20]. Once outside the cell, the cell-surface CsgB protein nucleates the conversion of soluble CsgA to the amyloid form and polymerisation proceeds to create curli fibres[21].

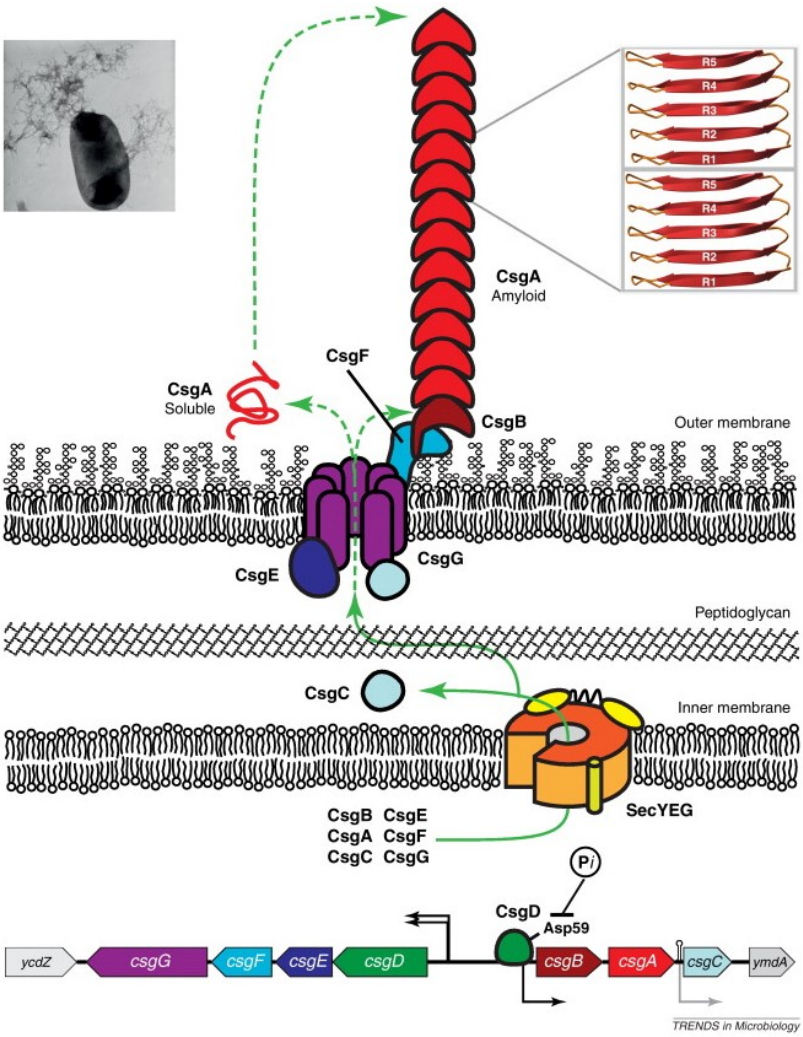

Figure 3 *E. coli* curli fibre biogenesis and structure. Proteins expressed from the *csg* operons enable the extracellular self-assembly of CsgA monomers into amyloid fibres. Inset top left, TEM image of a curli-producing cell. Inset top right, model of the cross β-strand amyloid structure. Image reproduced with permission from Blanco et al. [16]

1.2.2 *E. coli* curli biofilms as biological ELMs

The combination of their polymeric nature, impressive mechanical properties and extracellular production from a genetically-tractable host make *E. coli* Curli fibres ideal targets for biological ELM development. In 2014, two landmark studies showed that new properties can be engineered into *E. coli* bacterial biofilms.

In the first of these studies, curli fibres were inducibly-expressed from a plasmid in *E. coli*. The *E. coli* strain used was mutated to constitutively express the *csg* operon, but lacked the native *csgA* gene[22]. To modify the functional properties of curli fibres, a short hexa-histidine tag was fused to the C-terminus of the CsgA monomer ($CsgA_{His}$). The authors showed that, by adding chemical species that bind this hexa-histidine tag, functionalised biofilms could be created. Using this approach, curli fibres were produced that could bind gold nanoparticles, creating electrically-conductive nanowires. In addition, by co-culturing *E. coli* strains producing CsgA

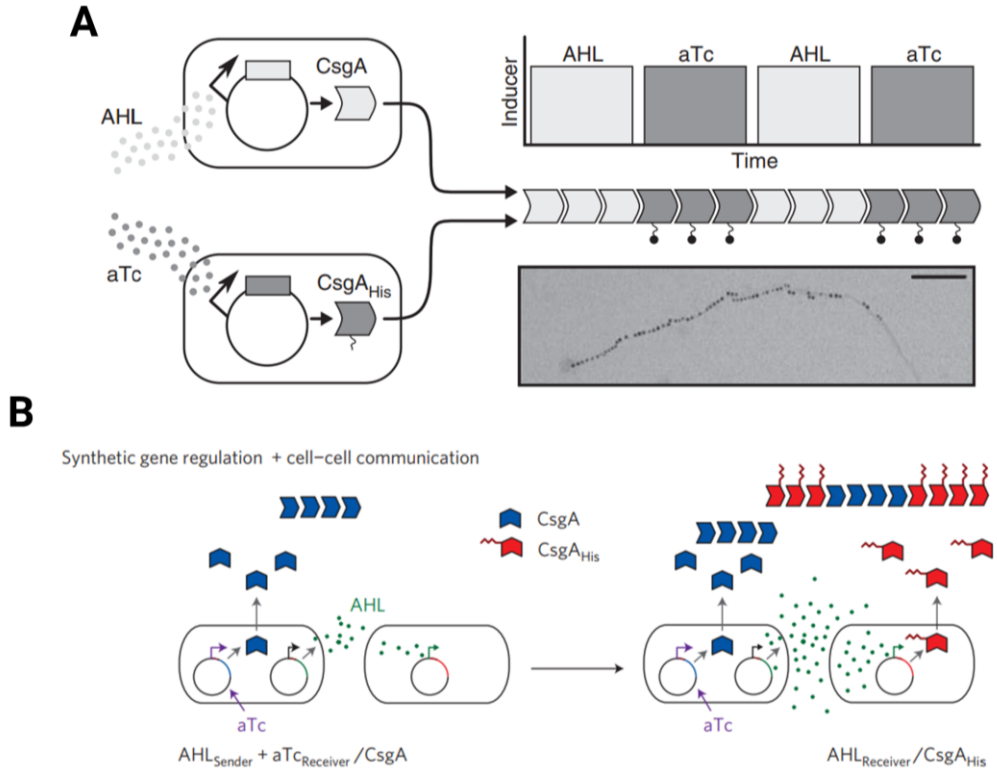

Figure 4 Co-culturing *E. coli* strains producing different CsgA monomers enables external and autonomous patterning. A *E. coli* engineered to express CsgA under AHL induction or $CsgA_{His}$ under aTc induction were co-cultured. Inset is an TEM image of a curli fibre decorated with gold nanoparticles. By adding and removing aTc and AHL, the pattern of different CsgA monomers, and therefore of gold nanoparticles, along curli fibres could be controlled. Image reproduced with permission from Teague et al. [124] **B** By engineering aTc-inducible strains to simultaneously synthesise AHL, autonomous patterning can be genetically-programmed. Image reproduced with permission from Chen et al. [22]

and $CsgA_{His}$ monomers, two-component curli fibres were generated consisting of alternating stretches of both monomers (Figure 4A). The authors showed that the patterning of CsgA and $CsgA_{His}$ monomers within curli fibres could be controlled over multiple length scales by applying gradients of inducers controlling the expression of each protein. Finally, this system was used to demonstrate, for the first time, that living cells can be engineered to autonomously pattern a biological material. To achieve this, the CsgA-secreting strain was engineered to constitutively produce a quorum-sensing molecule, acyl homoserine lactone (AHL), which could activate the expression of $CsgA_{His}$ from a second strain. When co-cultured, these strains initially produced curli fibres consisting predominantly of CsgA monomers, but over time, as AHL accumulated in the culture medium, fibres consisted predominantly of $CsgA_{His}$ monomers (Figure 4B). This engineered cell-cell communication system therefore enabled genetically programmed, autonomous control of the patterning of curli fibres over time.

Soon after this first report, a second study described how a variety of additional novel functional properties can be genetically programmed into *E. coli* biofilms by fusing peptide domains to the CsgA monomer[23]. The system, which the authors call biofilm-integrated nanofiber display (BIND), relies on the fact that peptide domains can be fused to the CsgA monomer without abolishing curli fibre formation. After screening for the optimal fusion site on the CsgA monomer, the authors showed that a panel of peptides, able to bind a variety of species – including ice crystals, carbon nanotubes and magnetite – could be fused to the CsgA monomer without disrupting curli fibre formation. Several candidates were then selected and shown to confer new functional properties to the engineered biofilms: the A3 peptide enabled silver nanoparticle capture, a metal-binding domain allowed stable adhesion to stainless steel and the SpyTag peptide was used to covalently capture tagged fluorescent proteins. The latter approach is of particular interest, here the CsgA subunit was fused to the short SpyTag peptide (13 amino acids) which binds the SpyCatcher protein (84 amino acids). Together the SpyTag-SpyCatcher pair autocatalyse the formation of an intermolecular covalent bond between two amino acid side chains[24]. The authors showed that curli fibres could, therefore, be functionalised in a modular manner, simply by externally adding a protein of interest fused to the SpyCatcher domain.

This SpyTag-SpyCatcher approach has since be extended to create catalytic biofilms. Biofilms were functionalised by expressing SpyTag-displaying curli fibres and incubating with a pre-purified recombinant α-amylase-SpyCatcher fusion protein[25]. In addition, taking advantage of the natural resilience of biofilms to environmental challenges, the authors showed that catalytic biofilms remained active following exposure to a range of pH and organic solvent conditions. A subsequent study expanded this approach by generating a panel of orthogonal protein-protein conjugation domains, as alternatives to the SpyTag-SpyCatcher[26]. It was shown that curli fibres could therefore be conjugated to multiple tagged recombinant proteins obtained directly from crude *E. coli* cell lysates. Using this system, two-enzyme biocatalytic biofilm materials were generated to perform a stereoselective ketone reduction transformation, a potentially industrially-relevant reaction. In addition, to take bacterial biofilm materials closer to industrial applications, a simple, versatile method for scalable production and purification of functionalised curli fibres was recently described[27]. However, one drawback of these approaches is the need for prior production of the functionalising module – the SpyCatcher-enzyme fusion protein. Simultaneous, *in vivo* production of curli fibres and functionalising modules would enable the useful traits of living materials to be leveraged within these systems. For instance, the patterning and relative abundance of different enzymes conjugated to curli fibres could be controlled using genetic circuits. Going forwards, *in vivo* production of functionalised curli fibres could be achieved, for example, by engineering co-secretion of SpyCatcher fusion proteins.

One area that has received particular focus is the creation of electrically-conductive curli fibres. Expanding on previous work, a panel of inorganic-material-nucleating peptides were fused to CsgA and shown to seed the nucleation and formation of gold nanoparticles and, therefore, to create electrically-conductive biofilms[28]. Interestingly, particular peptides directed the mineralisation of gold nanoparticles with different size distributions. Exploiting this phenomenon, the choice of nucleating peptide was then shown to enable tuning of the electrical conductivity of the engineered biofilms. An alternative approach was inspired by the naturally-occurring conductive protein nanowires produced by the bacterium *Geobacter sulfurreducens*[29]. *G. sulfurreducens* produces extracellular protein filaments, in which stretches of aromatic amino acid side chains conduct electrical charge along the length of the filaments[3,30]. Inspired by this natural system, aromatic amino acids were introduced into CsgA

monomers, to create stripes of aromatic side chains running along the length of the resultant curli fibres. The authors found that the resulting curli fibres and bacterial biofilms showed increased electrical conductivity[31].

Another study fused mussel foot proteins (Mfp) to CsgA to a create strong, underwater adhesive material[32]. Mfps are a family of proteins secreted by mussels to form the holdfast, or byssus, with which they adhere to solid surfaces in marine environments[33–35]. Two Mfp proteins, Mfp3 and Mfp5, were genetically fused to CsgA and expressed intracellularly in *E. coli*. The two fusion proteins, CsgA-Mfp3 and CsgA-Mfp5, were then purified and enzymatically-modified, to recreate cross-linkages formed in the natural mussel byssus. Remarkably, the resultant fibres outperformed all previous bio-derived and bio-inspired protein-based underwater adhesives. Notably, this example does not meet the strict definition of a biological ELM, since its production requires external intervention. However, this study clearly illustrates how modular functional protein domains can be fused to one another to create engineered biological materials with novel properties.

In a landmark study leveraging another of the advantages of biological ELMs, *E. coli* biofilms were engineered to act as environmentally-responsive bioremediatory materials[36]. Inspired by a study suggesting curli fibres play a protective role in natural biofilms by absorbing the heavy metal pollutant mercury[37], the authors engineered an *E. coli* strain to produce curli fibres in response to environmental mercury. The CgsA monomer was expressed from a mercury-inducible promoter which becomes active in response to environmentally-relevant concentrations of mercury. The resultant curli fibres were able to efficiently bind and sequester mercury, acting as a sponge to mop up the heavy metal. Notably, this system takes advantage of the ability of living cells to sense and respond to their environment; the bioremediatory biofilm material is only produced in response to the detection of the heavy metal pollutant. As the authors note, in the future, *E. coli* strains engineered to produce the curli fibres in response to a variety of pollutants could be deployed into the environment to sequester multiple pollutants or toxins.

Many of the studies described here use a modular approach to programmably functionalise curli fibres, in which users can pick and choose protein modules with which to decorate curli fibres. A potential limitation of this approach is the requirement for fused protein sequences to retain their function without interfering with the CsgA protein secretion and amyloid

assembly. However, it has been shown that protein sequences of up to at least 260 amino acids can be fused to CsgA without abrogating curli fibre assembly[38]. And in situations where functional protein modules cannot be fused directly to the CsgA monomer, an alternative solution would be to co-secrete SpyTag-displaying CsgA monomers and SpyCatcher-displaying functional protein modules.

1.2.3 The future prospects of biofilm biological ELMs

While impressive progress has been made to create *E. coli* biofilm ELMs, there is great scope to expand these approaches by engineering alternative bacterial biofilm amyloids. For instance, the Gram-positive bacterium *Bacillus subtilis*, another standard synthetic biology host organism, produces biofilms containing amyloid fibres formed from the TasA protein[39]. Indeed, it has already been shown that antigenic peptides and a full-length fluorescent protein could be fused to TasA, without compromising amyloid fibre formation[40]. Notably, *B. subtilis* is one of the preferred host organisms for secretion of recombinant proteins[41]. *B. subtilis* may therefore represent an ideal future candidate for simultaneous secretion of amyloid fibres and functionalisation modules, enabling *in vivo* production of functionalised biofilms. Interestingly, *B. subtilis* biofilms exhibit some remarkable natural properties. Firstly, they are highly hydrophobic – surpassing even the water repellence of Teflon[42] – a property conferred by another secreted protein, BslA[43,44]. And secondly, it has recently been shown that the growth of *B. subtilis* biofilms oscillates in highly-ordered manner[45]. These oscillations were shown to be orchestrated by an unprecedented electrical cell-cell communication system based on K^+ ion flux across the *B. subtilis* cell membrane[46]. Although its environmental relevance remains unproven, this electrical signalling system has been shown, in the lab, to enable recruitment of motile cells to biofilm communities[47] and to allow long-range communication between two distinct biofilms[48]. This new paradigm for bacterial cell-cell communication may therefore represent a useful target for future engineering of *B. subtilis* ELMs. From this single example, it is clear that alternative bacterial biofilm systems have great potential to expand the scope of ELMs. Since homologues of the curli operon have been found in numerous species of bacteria, spanning at least four distinct phyla[49], there may be much more to learn.

1.3 Bacterial cellulose

Another exciting biological ELM system is the model biological material, bacterial cellulose (BC). Thanks in part to the impressive natural properties of BC, there have been growing efforts to genetically-engineer these BC-producing bacteria to produce novel, useful biological materials. In this section, we describe the important properties of BC and BC-producing bacteria and outline various efforts to genetically-engineer BC-bacteria and other microbes to create a new class of biological ELMs.

1.3.1 The structure and properties of bacterial cellulose

Cellulose, a polysaccharide composed of β-(1→4)-linked glucose units, is the most abundant biopolymer on the planet[50]. While best known as the major structural component of many plant tissues, several species of bacteria are also capable of producing cellulose[51]. Plant-derived cellulose has been used by humans for centuries as a sustainable source of clothing, construction materials, paper and so on. But BC exhibits some uniquely advantageous physicochemical properties, such as high crystallinity, high tensile strength, high purity, ultrafine network architecture and biocompatability[52]. As a result, BC has garnered much interest as a feedstock material for industrial applications.

The most prodigious producers of BC are Gram-negative acetic-acid bacteria (AAB), in particular the genera *Gluconacetobacter* and *Komagataeibacter*[53], hereafter referred to generally as BC-producing bacteria. Due to interest in BC, there has been an increasing body of research into the basic cellular physiology of BC-producing bacteria, focussing mainly on *Gluconacetobacter xylinus*. Under static growth in liquid culture, BC-producing bacteria grow predominantly at the air-water interface, where aerobic growth is best supported. As they grow, BC-producing bacteria synthesise and secrete chains of cellulose, which remain attached to the cell surface. The result, referred to as a pellicle, is a floating mat of intertwined cellulose fibrils, within which individual cells are embedded (Figure 5A). Remarkably, BC-producing bacteria are able to synthesise extracellular cellulose reaching yields in excess of 10 grams per litre[54].

Although still not fully understood, a great deal of research has focused on the molecular details of BC biosynthesis. BC-producing bacteria can utilise a variety of carbon sources, operating the pentose phosphate cycle to oxidise carbohydrates and the Krebs cycle to

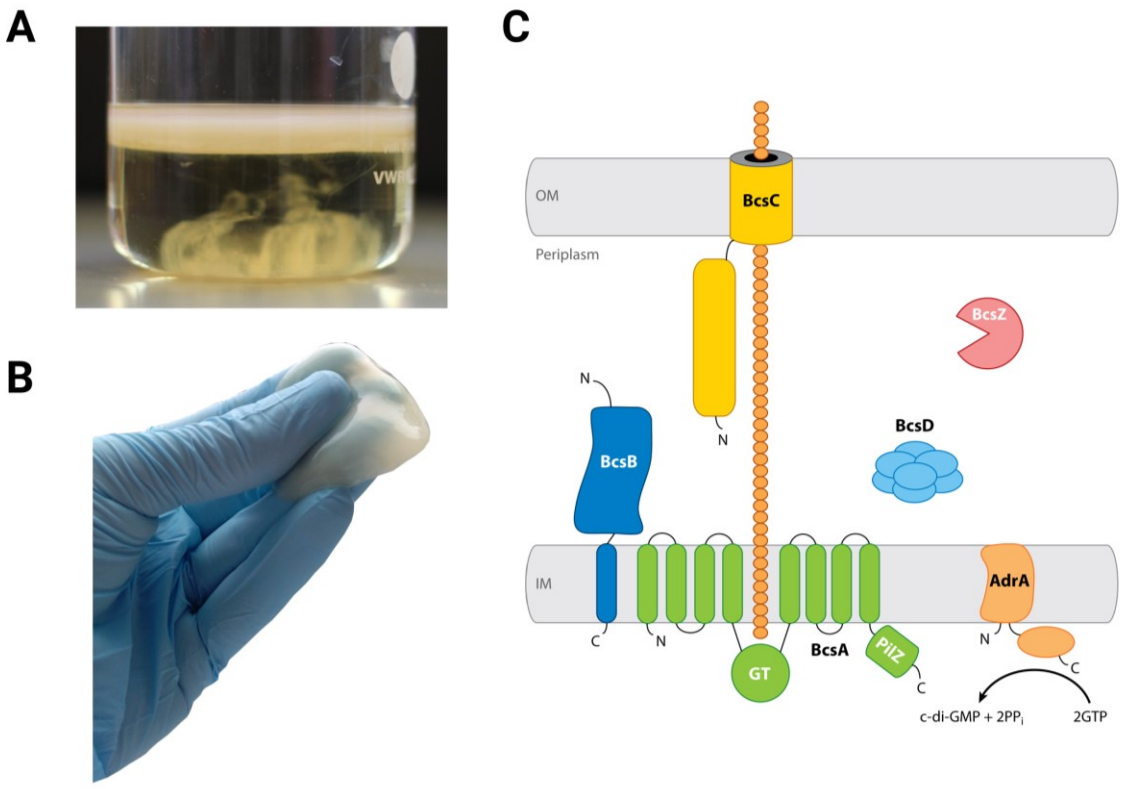

Figure 5 Bacterial cellulose. A When grown statically in liquid media, BC-producing bacteria synthesise a floating mat of cellulose fibres known as a pellicle (white opaque layer). Imaged adapted from Florea et al. [86] **B** Pellicles are flexible and free-standing. **C** BC is synthesised by a membrane-spanning multiprotein complex, the cellulose synthase. Growing glucan chains (orange) and threaded across both membranes to the extracellular environment. Image reproduced with permission from McNamara et al. [270]

oxidise organic acids[55]. Regardless of the carbon source, cellulose biosynthesis is fed by intracellular UDP-glucose monomers. Cellulose synthesis takes place within membrane-spanning, multi-subunit cellulose synthase complexes (Figure 5C). Here, UDP-glucose monomers are added to the growing cellulose chain, while the entire chain is simultaneously translocated across the inner and outer cell membranes[56]. Although many proteins play a role in orchestrating BC synthesis and assembly, the *bcsABCD* operon encodes four essential proteins that make up most of the cellulose synthase complex[54]. BcsA plays a number of roles: it forms part of the pore across the inner membrane, catalyses the polymerisation of UDP-glucose units and enables allosteric regulation of cellulose synthesis by cyclic-di-GMP. BscB also contributes to the formation of the inner membrane pore. BscC, a periplasmic protein, is believed to form β-barrel pore in the outer membrane, through which the glucan chain is threaded. Lastly, a second periplasmic protein, BscD, is believed to be responsible for the correct orientation of cellulose synthase complexes relative to one another.

These remarkable molecular machines are able to polymerise up to 200,000 molecules of glucose per second[57]. Electron microscopy examination of BC-producing cells revealed the presence of ~50 pore-like structures arranged in-line with growing BC fibrils[58,59]. It is believed that these pore-like structures are themselves composed of multiple cellulose synthase complexes, each secreting a single glucan chain. In a process that is yet to be fully elucidated, a single cell is able to simultaneously polymerise, secrete and bundle together around 1000 individual glucan chains into a hierarchy of intermediate structures, finally producing ribbonlike cellulose fibrils, 50-80 nm in width and 1-9 μm in length[55,60]. As with other forms of cellulose, individual glucan chains are strongly held together by a combination of van der Waals' forces and hydrogen-bonds between glucose hydroxyl groups[61]. The resulting BC material is comparatively pure, lacking substances often associated with plant cellulose such as hemicellulose, pectin and lignin. Owing to its high degree of crystallinity – that is, the regular arrangement of glucan chains – BC exhibits excellent mechanical properties: single BC nanofibers have tensile strength estimated to be ~1500 MPa[62] and Young's modulus of ~114 GPa[63]. Further, BC is biocompatible – meaning it is not toxic to human tissue – and biodegradable. Given its desirable material properties, BC has been developed for a variety of potential commercial applications: wound dressings, acoustic diaphragms for headphones and speakers, stabilisers for foams and emulsions, scaffolds for tissue engineering and battery separators.

1.3.2 Bacterial cellulose as a biological ELM

There have been numerous efforts to develop novel BC-based materials with improved material properties. One common approach to develop new BC-based materials is to blend BC with another species to create a composite. In fact, many biological species have been used to modify BC material properties, including spider silk[64], gelatin[65], zein[66], collagen[67], hyaluronan[68], alginate[69], heparin[70,71], antimicrobial peptides[72] and growth factors[73,74]. While some of these species were incorporated into the BC matrix by non-specific forces, others have been specifically bound by fusion to a cellulose-binding domain (CBD) protein[75–77]. These materials are all synthesised *in vitro* using chemical and physical methods, which lack the benefits of biological material assembly. However, recent years have seen more-and-more efforts to harness the benefits of biological assembly by genetically-engineering BC-producing bacteria.

Initial efforts to genetically-engineer BC-producing bacteria focused on improving the yield of BC. In addition to BC, *G. xylinus* is known to produce a second extracellular polysaccharide acetan[78]. In an early attempt to increase BC yields, an acetan biosynthesis gene was disrupted in *G. xylinus*[79] – however, it was found that disrupting acetan biosynthesis in fact reduced BC yield. Other studies used random mutagenesis approaches to isolate high-yielding BC-producing strains[80]. More recently, rational engineering approaches have been used to increase BC production. Knocking out *G. xylinus* glucose dehydrogenase (GDH), which competes with BC biosynthesis for glucose consumption, was shown to boost BC yields[81]. Further, plasmid-based overexpression of the *bcs* operon from a strong, inducible promoter has been shown to increase BC yields from *G. xylinus* by 2-4 fold[82].

In a landmark study, Yadav et al.[83] used a metabolic engineering approach to modify the material properties of BC produced by *G. xylinus*, creating a cellulose-chitin copolymer. Chitin, like cellulose, is a polysaccharide. However, rather than glucose monomers, chitin is made up of chains of N-acetyl-glucosamine (GlcNAc) monomers. The addition of the acetyl amine group to the glucose units results in a stronger hydrogen-bonding network between chitin chains, compared to cellulose, resulting in increased material strength. Since the *G. xylinus* cellulose synthase machinery had previously been shown to be able to incorporate UDP-GlcNAc into BC, the authors hypothesised that producing cytoplasmic UDP-GlcNAc would enable production of a chitin-cellulose copolymer. Indeed, by expressing a *Candida*

albicans three-gene operon for UDP-GlcNAc biosynthesis, it was shown that UDP-GlcNAc could be synthesised and incorporated into growing glucan chains. The resultant chitin-cellulose copolymers were shown to have altered material properties: including decreased crystallinity, increased susceptibility to lysozyme degradation and improved *in vivo* degradability. Another study reported engineering of *G. xylinus* to create curdlan-cellulose composites[84]. Curdlan is a polymer of β-(1→3)-linked glucose monomers, noted for its ability to form gels with applications in the food and biomedical industries. The authors engineered *G. xylinus* to express the *crdS* gene from *Agrobacterium tumefaciens*, which naturally produces large quantities of extracellular curdlan. The CrdS protein is predicted to be the major curdlan synthase enzyme and shares homology with the catalytic BcsA subunit of cellulose synthase[85]. It was found that heterologously-expressed CrdS was able to direct curdlan biosynthesis alongside natural BC production, and the resulting pellicles exhibited altered surface morphology and decreased water permeability.

To aid and expand on these efforts, Florea et al. developed and utilised a modular genetic toolkit to modify a newly-isolated BC-producing strain, *Komagataeibacter rhaeticus*[86]. Compared to other high-producing strains, *K. rhaeticus* was more readily transformed with plasmid DNA. Using the principles of synthetic biology, the authors set out to create a genetic toolkit to facilitate *K. rhaeticus* genetic modification. A panel of modular genetic parts were generated and characterised, including origins of replications, inducible and constitutive promoters, and fluorescent reporter proteins. These genetic tools were then leveraged to engineer control of *K. rhaeticus* BC biosynthesis. An inducible promoter was used to control the expression of an RNA repressor system. Here, an RNA sequence was designed to target the mRNA encoding the enzyme responsible for UDP-glucose synthesis. Once bound to the target mRNA, the RNA recruits a heterologously-expressed *E. coli* Hfq protein, which brings about inhibition of mRNA expression and therefore shuts down BC biosynthesis. This system was not only highly-effective, enabling complete arrest of cellulose synthesis at high levels of induction, but also tunable, enabling intermediate levels of suppression at lower levels of induction. In another demonstration of the utility of this genetic toolkit, it was shown that application of chemical inducers of gene expression could be used to control spatial and temporal patterning of BC (Figure 6A and 6B). Lastly, as an alternative to *in situ* biological functionalisation, BC was functionalised by adding previously

expressed and purified recombinant fluorescent proteins fused to cellulose binding domains (Figure 6C and 6D).

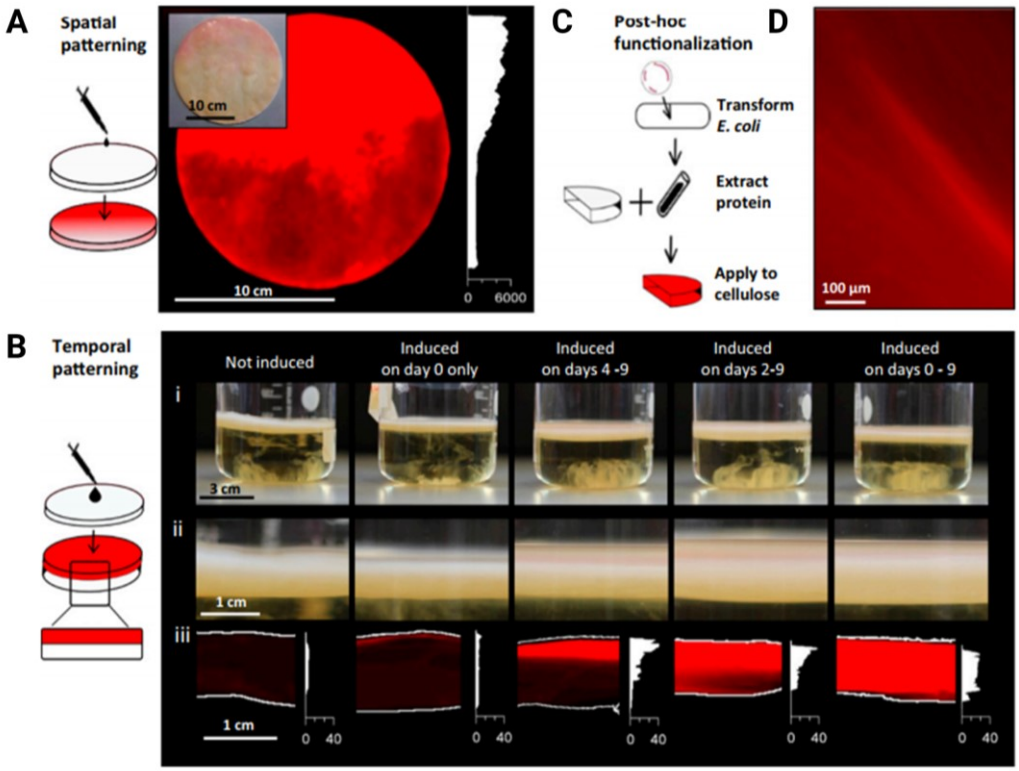

Figure 6 Functionalising and patterning BC materials. By externally adding a chemical inducer of gene expression, in this case mRFP expression, spatial (**A**) and temporal (**B**) patterning of gene expression within BC can be achieved. **C** Schematic showing post-hoc functionalisation by adding proteins to BC. **D** Fluorescence images of post-hoc functionalised BC, in this case with mRFP. Image reproduced with permission from Florea et al. [86] Copyright (2016) National Academy of Sciences

Due to its genetic tractability, relative simplicity and desirable natural material properties BC is an ideal model biological ELM system. But, this is a growing area of study, and so far researchers have only recently begun to explore of what may possible by genetically-engineering new BC material properties. We have seen that BC-producing bacteria can be engineered to synthesise curdlan-cellulose and chitin-cellulose copolymers. However, bacteria naturally produce a vast number of other extracellular polysaccharides, many with important industrial uses[87,88]. Engineering co-secretion of these polysaccharides from BC-producing bacteria could enable the production of a variety of novel copolymer materials. Similarly, numerous reports have demonstrated that purified proteins can be externally added to BC to confer new and useful material properties. In the future, it may be possible to engineer BC-producing bacteria to secrete these proteins themselves and therefore

functionalise BC *in situ*. The creation of modular genetic tools and the recent sequencing of genomes of BC-producing strains[86,89] will play a vital role in achieving these goals.

1.3.3 Co-culture approaches for bacterial cellulose biological ELMs

An alternative approach to create BC-based ELMs relies not on engineering BC-producing bacteria themselves, but instead co-culturing BC-producing bacteria with another engineered microorganism. As we have seen, genetic tools for engineering BC-producing bacteria and detailed molecular characterisation of BC-producing bacteria have only relatively recently been developed. Co-culturing BC-producing bacteria with a model organism for which numerous genetic tools and circuits have been developed may therefore facilitate and accelerate ELM development.

Generally, engineering so-called cellular consortia – co-cultures of two or more microbes – is a topic of increasing interest[90]. Cellular consortia have some broad advantages over mono-cultures, such as improved robustness and the division of labour between individual strains[91]. For example, by distributing the biosynthetic pathway between co-cultured *E. coli* and *S. cerevisiae* production of a precursor of the anticancer drug paclitaxel was enhanced[92]. In addition, as exemplified in bacterial biofilm ELMs, engineered cellular consortia have been shown to enable tunable and autonomous patterning of a biological material[22]. Notably, a similar process occurs in complex natural biological materials. For instance, in skin, keratinocytes produce keratin to give mechanical strength, fibroblasts produce collagen and elastin which further strengthen the extracellular matrix, melanocytes produce melanin to confer colour and Langerhans cells detect and respond to the presence of pathogens.

A similar situation can be envisioned to create novel BC ELMs, where BC-producing bacteria create the scaffold BC matrix and an engineered model organism contributes an additional functional property. Using this approach, a recent study manually incorporated engineered *E. coli* into grown BC[93]. By externally applying *E. coli* cells to the surface of BC part-way through the process of pellicle formation, *E. coli* cells could be entrapped within the growing BC matrix. The authors showed that engineered *E. coli* could be incorporated into BC and could be chemically-induced to express the reporter protein GFP. In a follow-up study, BC pellicles into which *E. coli* had been incorporated were saturated with a pre-purified biopolymer protein, silk fibroin (SF)[94]. Introduction of SF to BC increased the transparency of the resulting material and reduced the escape of incorporated *E. coli* cells. A more complex *E. coli* genetic circuit was then used – a previously-described dual-colour riboswitch, in which addition of a chemical inducer switches GFP expression off and RFP expression on. The authors showed

that this riboswitch system functioned well when incorporated into BC-SF materials. In the future, it is hoped these materials can be developed to act as environmental biosensors, sensing and reporting external stimuli. This approach clearly demonstrates that engineered *E. coli*, co-cultured with BC-producing bacteria can endow new functional properties to BC to create an ELM. However, a limitation of the approach described here is the requirement for external interventions – specifically, the need for manual addition of *E. coli* cultures and pre-purified SF protein to BC. Because of this, some of the advantages of biological material self-assembly are lost. Therefore, a system enabling spontaneous ELM self-assembly by engineered microbes would therefore be preferable.

1.3.4 Kombucha tea – a pseudo-natural co-culture system

Inspiration for another potential strategy for co-culture of a model organism and synthetic biology host with BC-producing bacteria comes from kombucha tea. Many of the highest-yielding BC-producing bacteria were originally isolated from a pseudo-natural fermented tea drink called kombucha. Kombucha is produced by a consortium of bacteria and yeast which act together to ferment sweetened tea – typically green or black tea with 5-15% sucrose[95] (Figure 7A). After several weeks of fermentation, the result is an acidic, mildly effervescent beverage with a fruity flavour. In addition, thanks to the presence of BC-producing bacteria, a large mat of floating BC is formed at the surface of the tea and is used, along with some of the tea liquid, to inoculate fresh batches of kombucha. Kombucha is produced in this way both by home-brewing and on the commercial scale – supporting a growing market currently worth around $600 million USD. Consumption of kombucha tea is purported to have wide-ranging beneficial health effects, however, evidence of this is largely lacking[95].

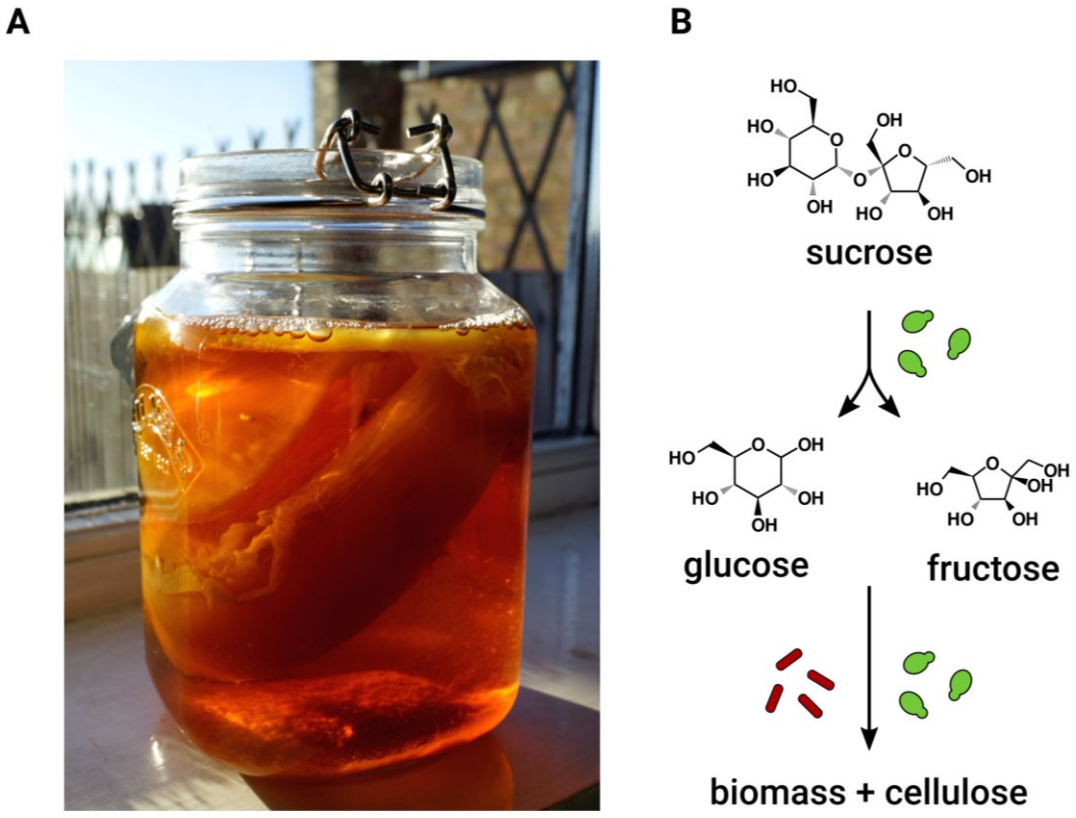

Figure 7 Kombucha tea fermentation. A Image of homebrewed kombucha tea. Newly-formed layers of BC are visible at the surface of the liquid while BC mats produced in previous fermentations are submerged. **B** Proposed metabolic interaction between yeast (green) and bacteria (red) in kombucha fermentations. Yeast convert the carbon source sucrose to glucose and fructose. Both yeast and bacteria then consume glucose and fructose to accumulate biomass and BC.

Recently, there has been growing interest in kombucha as a model microbial system to investigate multi-species cooperation[96]. While the individual species present can vary, kombucha fermentations invariably consist of at least one species of BC-producing acetic acid bacteria and often multiple species of yeast[97]. The BC-producing bacteria – typically from the genera *Gluconacetobacter* and *Komagataeibacter* – are the most abundant microbes in kombucha[98]. Numerous species of yeast have been detected in kombucha, including species of *Zygosaccharomyces*, *Candida*, *Brettanomyces*, *Pichia*, *Torulospora*, *Saccharomyces* and others[99]. Many sources report that the kombucha microbial community is a symbiotic system, however, the exact nature of the interactions between kombucha microbes remains unclear. It is believed that yeasts in kombucha fermentations hydrolyse the majority of carbon source, sucrose, to form extracellular glucose and fructose through the action of the secreted enzyme invertase (Figure 7B)[100]. Yeasts further metabolise glucose and fructose via glycolysis, producing ethanol and creating biomass. Although BC-producing bacteria are able to grow using sucrose as a carbon source, it is believed that they mostly consume glucose, fructose and ethanol produced by the yeasts, and themselves produce acetic acid[101]. In an interesting demonstration of metabolic interactions within the kombucha microbial community, it was reported that ethanol produced by yeast stimulated acetic acid production from bacteria, which reciprocally induced ethanol production from yeast[102]. Others have suggested that the symbiotic relationship may confer mutual benefit, with yeast liberating metabolites to enable bacterial growth and bacteria producing a protective biofilm barrier shielding the culture from UV radiation and microbial invasion[96].

Interestingly, one of the yeast species commonly detected in kombucha is *Saccharomyces cerevisiae*[98]. *S. cerevisiae* is as a model organism and a key host organism for industrial biotechnology and synthetic biology. Consequently, a wealth of genetic tools and molecular biological data are available for *S. cerevisiae*. The *S. cerevisiae* genome has been sequenced and is being reconstructed synthetically as part of an international collaborative effort. *S. cerevisiae* metabolism has been modelled at the genome scale and has been engineered to produce a variety of high-value chemicals, therapeutics and biofuels. Further, *S. cerevisiae* has been engineered to secrete a variety of heterologous proteins and to sense-and-respond to a variety of physical and chemical environmental stimuli. Since *S. cerevisiae* naturally grows in a stable microbial community with BC-producing bacteria, it may be possible to

recreate this co-culture system in the lab and therefore to use *S. cerevisiae* genetic tools to engineer new BC-based biological ELMs. Indeed, the physicochemical properties of BC materials produced by kombucha fermentations have previously been characterised[103]. Kombucha microbial communities have even been exposed to simulated spaceflight and Martian conditions to explore their stability[104].

1.4 Alternative and future biological ELM systems

1.4.1 Biomineralized biological ELMs

Organisms are able to direct and control the mineralisation and deposition of a vast range of minerals into natural biological materials. Further, living cells are able to control the physical and chemical properties of these minerals to a remarkable degree, far surpassing what is possible with man-made materials. Generally, specialised tissues and cells direct the accumulation and deposition of biominerals, controlling the crystal size, shape, location and polymorph. Organic species produced by these cells, such as peptides and polysaccharides, form scaffolds to template crystal deposition and act as soluble modifiers of crystal growth[105]. Since the ability to control inorganic crystal structures is important in the development of materials with applications in optics, microelectronics and catalysis, there is increasing interest in approaches to understand and control the genetic and molecular basis of biomineralization. As with many other biological ELM systems, early efforts to develop genetically-engineered biomineralized materials have largely centred on simple, single-celled organisms.

Diatoms are unicellular, eukaryotic algae noted for their ability to self-assemble intricately-structured silica-mineralised cell walls. Diatoms take up Si from their environment in the form of orthosilicic acid, $Si(OH)_4$, which is abundant in marine and freshwater environments. Subcellular compartments, known as silica deposition vesicles (SDVs) accumulate Si and bring about its polymerisation to silica, SiO_2[106]. Diatoms exert an exquisite degree of control over the fine-structure of the resulting silicified cell walls and produce an incredible diversity of ornate structures (Figure 8). Nanostructured silica materials could have wide-ranging applications as microelectronic and optical devices, microsensors, microbatteries and microfluidic devices[107,108]. Consequently, using the diatom model organism *Thalassiosira pseudonana*, for which genetic transformation methods and a full genome sequence are available, there have been growing efforts to genetically-engineer silica biomineralization[109]. For instance, through genetic fusion to silaffins – a family proteins which participate in silica deposition and remain bound to the silica cell wall – heterologous proteins can be incorporated into biomineralized silica. This approach has been used to decorate and functionalise diatom silica with a number proteins, including GFP, single-chain antibodies[110] and enzymes[111,112]. In an interesting demonstration of the applicability of this approach,

Delalat et al.[111] decorated diatom silica with antibodies to target delivery of drugs loaded within the silica to cancerous human cell lines. It is also hoped that increasing understanding of the molecular basis of silica deposition will enable tunable genetic control of diatom silica morphology[113].

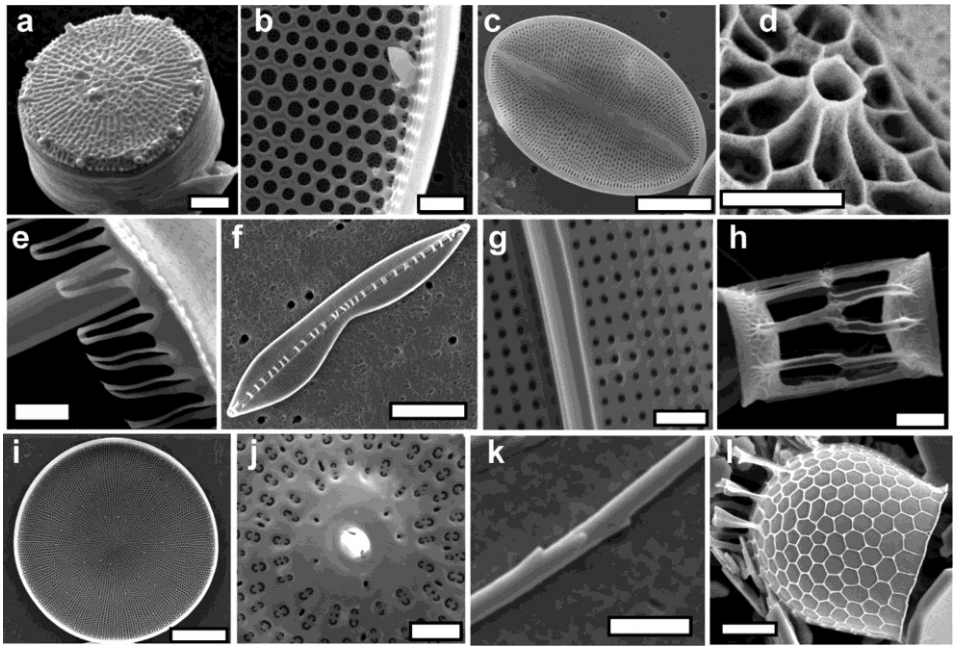

Figure 8 Diatom silica cell walls. Electron microscopy images of isolated silica cell walls from a variety of diatom species. Image reproduced with permission from Hildebrand et al. [108]

Another notable natural instance of biomineralization is the bacterial magnetosome. Many marine and freshwater bacteria accumulate intracellular, membrane-enclosed crystals of magnetite (Fe_3O_4) or greigite (Fe_3S_4). These magnetic crystals enable their parent bacteria to orient themselves along the earth's magnetic field and thereby swim to preferable microenvironments in the water column, a process known as magnetotaxis. In brief, magnetosome biosynthesis occurs by i) invagination and pinching off of the plasma membrane, ii) transport and accumulation of iron to the newly-formed vesicle and iii) controlled nucleation and growth of magnetite or greigite crystals[114]. Various potential applications of magnetosome-producing bacteria can be envisioned. For instance, due to their unique magnetic properties, magnetosome-producing bacteria can be easily both detected and manipulated by external magnetic fields which could be useful in the field of nanorobotics[115]. A number of studies have reported engineering the natural magnetosome-

producing bacterium *Magnetospirillum gryphiswaldense* to create functionalised magnetosomes. The MamC protein localises to the membrane surrounding the magnetite or greigite crystals and is the most abundant magnetosome protein. By genetically fusing heterologous proteins to the MamC protein, magnetosomes have been functionalised *in vivo* with enzymes[116], antibodies[117] and fluorescent proteins[118]. In addition, heterologous expression of magnetosomes was recently demonstrated in the photosynthetic bacterium *Rhodospirillum rubrum*[119]. Expanding the host range of magnetosome expression in this way may facilitate further efforts to engineer novel magnetosome-based nanomaterials.

Going forwards, additional biomineralization systems may be exploited for biological ELM production. In a process known as microbially-induced calcite precipitation (MICP), certain microbes are able to induce the crystallisation of $CaCO_3$ through the action of an enzyme urease[120]. Urease hydrolyses urea to ammonia and carbonate. In the presence of Ca^{2+}, the increase in pH, brought about by the production of ammonia, drives calcium carbonate formation. The urease-producing bacteria themselves then act as nucleation sites for mineralisation. MICP has been proposed as a potential approach to enable concrete self-healing[121], CO_2 capture[121] and capture of groundwater contaminants[122,123]. In the future it may even be possible to rationally engineer complex biomineralized tissues such as bone or shell.

1.4.2 Genetically programming biological ELM morphology

Living cells execute genetically-programmed rules to autonomously control the morphology of natural biological materials. Indeed, many of the impressive physical properties exhibited by natural biological materials are based on their specific structure across multiple length scales. Inspired by these processes, the emerging field 'synthetic morphogenesis' aims to use tools and techniques from synthetic biology to "engineer, program, grow, and maintain biological systems with complex structures"[124]. One embodiment of synthetic morphogenesis is pattern formation[125]. Pattern formation describes the process by which cells become differentiated spatially. Once patterns have formed, cells follow different gene expression programs and can, as a result, produce patterned biological materials. In this section we will examine some natural patterning mechanisms and see how they are being recreated synthetically.

In the French Flag model, a spatial gradient of an external chemical morphogen alters cellular gene expression to create patterns (Figure 9A). This simple system can be built up across multiple dimensions and over hierarchical levels to create complex patterns and structures. The French Flag model is believed to underlie many natural instances of patterning, for instance, in *Drosophila* embryogenesis. In one of the first examples of a synthetic pattern-forming system, *E. coli* cells were engineered to produce fluorescent proteins in response to different concentrations of the quorum-sensing inducer AHL[126].

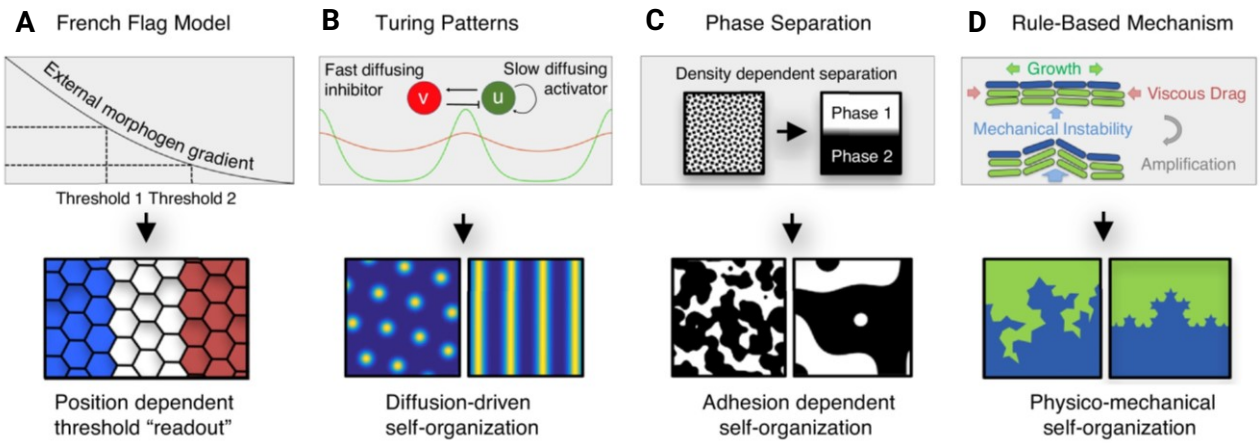

Figure 9 Pattern formation mechanisms. A The French Flag model. **B** Turing pattern formation. **C** Phase separation. **D** Rule-based pattern formation by physico-mechanical interactions. Figure reproduced with permission from Scholes et al. [125]

Synthetic genetic circuits, named 'band detectors', were designed to enable transcriptional activation in response to user-defined AHL concentration ranges. When grown together on agar plates, these band-detector strains formed rings of fluorescence around AHL-synthesising strains[126]. A similar approach was used to demonstrate that multiple morphogens can spatially control gene expression over two- and three-dimensions[127]. Building on these tools, Grant et al. created orthogonal AHL cell-cell communication systems to create long-range signal relays[128]. In an extension of the basic French Flag approach, Boehm et al. created a three-colour French Flag system enabling hierarchical patterning of gene expression from *E. coli*[129]. Engineered cells produced different fluorescent proteins in response to different concentrations of two orthogonal AHL inducers, creating a two-colour pattern. But in addition, each AHL inducer controlled the expression of a split RNA polymerase, which in turn activated the expression of a third fluorescent protein. This second genetic circuit acted like an AND logic gate – activating gene expression only in the presence of both AHL inducers – and created a second level of patterning. The authors propose that, by engineering patterned cells to produce additional orthogonal AHL signalling molecules, higher-order patterning can be achieved in the future. It should be noted that the French Flag system relies on an externally-derived morphogen gradient. Therefore, the systems described here do not strictly result in autonomous patterning. However, in nature, French Flag patterning can be initiated externally. For instance, during *Drosophila* embryo development, maternally-produced morphogen proteins create the anterior-posterior axis, while high-levels of patterning are then generated autonomously.

Turing patterns arise in natural biological systems based on the dynamics of two species: a slow-diffusing species which activates the production of itself and of the other species and a fast-diffusing species which represses the production of the other species (Figure 9B). As a result, stochastic local increases in the levels of the activator are self-reinforcing, while simultaneously creating surrounding regions of repression. Turing patterning is believed to play a widespread role in natural morphogenesis and has been demonstrated to direct zebrafish skin pigmentation, mouse hair follicle formation and vertebrate limb formation[125]. There have been numerous efforts to use the wealth of synthetic biology genetic tools for cell-cell communication to engineer Turing patterns, however, so far none have met with success. So much so, that Turing patterns have been given the tongue-in-cheek moniker "the

graveyard of synthetic biology"[125]! The basis of this difficulty seems to be the narrow range of parameters that must be satisfied to give rise to Turing patterns, especially in terms of the difference in diffusion rates of the activator and the repressor. Many of the current cell-cell communication systems available to synthetic biologists rely on small molecules – peptides and AHLs[130], for example – whose diffusion rates differ only slightly. Borek et al. proposed the use of activating AHLs in combination with gaseous hydrogen peroxide (H_2O_2) as a fast-diffusing, long-range inhibitor[131]. Alternatively, it may be possible to physically restrict the diffusivity of a cell-cell communication species by tethering to the cell surface or by engineering it to bind an underlying material scaffold. Since Turing patterns are truly autonomous and can direct the formation of a variety of structures – stripes, spots and labyrinths – efforts to engineer them will be of great value for the development of biological ELMs and are likely to continue.

The phase separation model creates self-assembled patterns of cells based on differential adhesion between cellular subtypes (Figure 9C). Analogously to the separation of oil and water, cell subtypes that exhibit different propensities for adhesion to one another will become spatially-segregated. If the movement of cells is constrained, incomplete segregation will result in the formation of clusters of each subtype, creating a patterned system. Natural instances of phase separation pattern include the distribution of mussels on solid surfaces, sea urchin blastomere development and *Drosophila* wing disc formation[125]. Cachat et al.[132] used the phase separation model to engineer autonomous patterning of mammalian cells. Mammalian cells were engineered to express cadherins – calcium-dependent cell surface adhesion proteins – enabling specific pairwise cell-cell adhesion[133]. Two self-adhering cell lines were engineered, one expressing GFP and one expressing RFP. When grown in mixed cultures, these cell lines spontaneously sorted into intricate two- and three-dimensional patterns. While this system enables fully autonomous patterning, it does have limitations. Most importantly, the patterns formed cannot be precisely pre-programmed and their specific structures are not reproducible.

A number of other approaches have been described to engineer the morphology of individual, growing *E. coli* colonies. One approach uses the accumulation of an AHL cell-cell communication molecule essentially as a timer, triggering cell-differentiation at a certain stage of colony growth when AHL concentration breaches a particular threshold. Using this

general principle, Payne et al.[134] created a genetic switch, in which a threshold level of AHL results switches off one promoter and switches on another. Consequently, during the growth of single colonies, AHL levels accumulate and eventually flip this genetic switch, creating self-organising ring patterns. In a remarkable extension of this approach, Liu et al.[135] created a genetic circuit in which AHL accumulation leads to suppression of *E. coli* cell motility. Based on the complex interplay of the dynamics of AHL concentration, cell density and nutrient availability, the engineered cells spontaneously self-assemble into stripes of alternating high and low cell density regions. As these engineered cells grow, AHL levels accumulate, switching motility off. This creates a band of high cell density surrounded by bands of low cell density, as cells move in from neighbouring regions, but do not move out. The entire process is iterated to create stripes. In addition, by fine-tuning the expression of a single gene involved in motility, the stripe spacing could be modified.

In an alternative approach, Rudge et al.[136] highlighted the importance of the mechanical and geometric properties of cells in creating rule-based self-organising patterns (Figure 9D). Tracking the interfaces between individual subpopulations in growing bacterial colonies revealed the spontaneous emergence of jagged, fractal patterns. Using mathematical modelling, the authors showed that these patterns were generated by polar cell shape and end-to-end cell division. Indeed, the patterns could be modified by creating a spherical *E. coli* mutant. In the same study, the authors created a spontaneous cell-differentiation system to genetically mark individual subpopulations within a symmetrical colony. Here, *E. coli* cells were transformed with two plasmids harbouring the same origin of replication, each encoding resistance to two antibiotics, one shared, one unique. When grown in media selecting for both the unique antibiotics, cells harboured both plasmids. However, when plated onto solid agar selecting for the shared antibiotic, cells could spontaneously rid themselves of one plasmid. This process results in segregation of the two plasmids early on in colony formation and, therefore, breaks the colony symmetry creating genetically-differentiated subpopulations. In a follow up study, the number of subpopulations was expanded by increasing the number of co-transformed plasmids[137]. This symmetry-breaking system could then be used to engineer domain-specific gene regulation, enabling spatial patterning of metabolite production and of colony morphology.

1.5 Building biological ELMs from the bottom-up

1.5.1 A modular approach to protein-based biological ELMs

The biological ELMs discussed so far are derived from existing biological materials. In each case, the cells that naturally produce these materials have been engineered to add new, useful properties. Since natural biological systems, such as curli fibres and bacterial cellulose, have evolved for specific purposes in their native host, their natural physical and biological properties have limitations. For example, the biosynthesis of bacterial cellulose is highly-regulated in the native host by mechanisms that are not currently fully-understood. Similarly, the physical properties of bacterial biofilms are dictated not only by secreted curli fibres, but also by extracellular polysaccharides and nucleic acids.

To avoid these restrictions, could it instead be possible to rationally engineer the production of a biological ELM from the bottom-up? Engineering biological material formation *de novo* in a simple model organism would offer much greater, user-defined control over the biological ELM material properties. Indeed, a broad framework for such an approach was recently outlined[11] (Figure 10). In this approach, microbes are engineered to express and secrete multiple proteins into the culture medium. Secretion of self-assembling structural proteins – such as CsgA or elastin-like polypeptides (ELPs) – would enable the formation of a polymeric scaffold. Simultaneously, functional protein modules – such as enzymes, adhesion

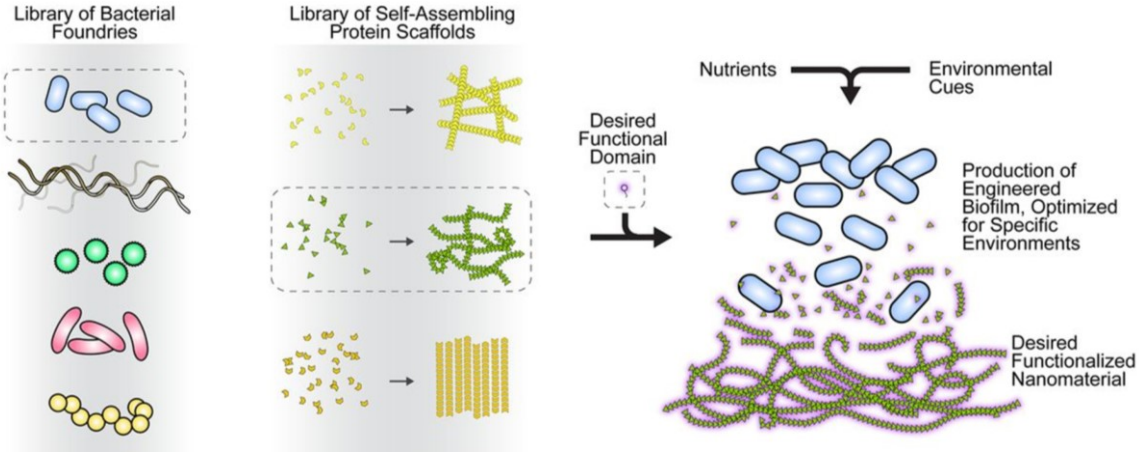

Figure 10 A conceptual approach to *de novo* biological ELM assembly. As outlined by Nguyen et al. in the context of bacterial biofilms, *de novo* biological ELMs could be self-assembled by selecting from a set of bacterial hosts which produce self-assembling protein scaffolds decorated with functional protein domains. Image reproduced with permission from Nguyen et al. [11]

domains or mineralisation peptides – could be secreted and conjugated to the structural protein, creating a functionalised material. Owing to the modular nature of protein domains, the specific properties of the resultant material could be user-defined by picking and choosing the desired structural and functional protein modules. Given the seemingly endless variety in natural structural and functional protein domains, a huge diversity of material properties could, in theory, be achieved using this approach (Table 2).

Table 2 Examples of potential protein components of biological ELMs and their functional properties

Protein	Function	Reference
Elastin + Resilin	Elasticity	138,139
Collagen	Structural properties	140
Keratin	Structural properties	141
Spider Silk Fibroins	Mechanical strength	142,143
Fluorescent proteins	Colour and fluorescence	144
Laccases	Pollutant degradation	145
Mussel foot proteins	Underwater adhesion	35
Mineralisation peptides	Mineral binding and morphology control	146,147
Squid Suckerin	Thermoplasticity	148
Geobacter pili	Electrical conductivity	30
Antibodies + Affibodies	Binding specificity	149
Hydrophobins	Surface hydrophobicity	43
Antimicrobial peptides	Antimicrobial activity	150

One potential embodiment of this system would be to co-culture multiple strains, each engineered to secrete different protein modules. Firstly, this would prevent intracellular conjugation of co-expressed functional and structural proteins. But in addition, a co-culture system could facilitate efforts to genetically-program biological ELM morphogenesis. By using pattern-forming genetic circuits, gene expression from different strains could be differentially regulated, both spatially and temporally. In fact, this approach was used by Chen et al. to control the pattern of CsgA monomers along curli fibres[22].

Despite its potential advantages, engineering such a system is likely to be challenging. Engineering *de novo* biological ELM assembly in this way will require two key processes: i)

efficient secretion of heterologous recombinant proteins ii) stable and spontaneous conjugation of secreted structural and functional protein modules. In the following sections we discuss potential biological systems that could be used to engineer protein secretion and conjugation.

1.5.2 Heterologous protein secretion hosts

Achieving high yield secretion of heterologous proteins has been a major aspiration in biotechnology for many years. As a result, much work has been devoted to developing robust and well-characterised protein secretion hosts. To be suitable for *de novo* biological ELM assembly, it is important that the secretion host employed satisfies two criteria. Firstly, in order to develop a modular system into which many different proteins can be incorporated, the secretion system must be able to handle a variety of proteins. This is a significant challenge since natural secretion systems exhibit differences in the types of protein substrate they can secrete, based on, for instance, folding stability or the presence of cofactors. Secondly, to enable efficient production of biological ELMs, relatively high yields of protein secretion are desirable.

Notably, *E. coli* Sec and Tat pathways can secrete high levels of recombinant protein across the inner membrane. However, secreted proteins are not translocated across the outer membrane and so accumulate in the periplasm. As a result, despite generally being the organism of choice in synthetic biology, *E. coli* is a relatively poor host for heterologous protein secretion. In the remainder of this section we will discuss two model protein secretion host organisms: *Bacillus subtilis* and *Saccharomyces cerevisiae*.

BACILLUS SUBTILIS

The Gram-positive model organism *Bacillus subtilis* is one of the archetypal protein secretion hosts. *B. subtilis* and closely related species are capable of secreting native proteins at remarkably high yields of >20 grams per litre[41]. Indeed these organisms are used for the production of secreted proteins for the detergent, food and beverage industries[151]. In addition, *B. subtilis* has been well-studied for its genetic competence, biofilm formation and ability to sporulate and, as such, is highly genetically tractable.

B. subtilis, like *E. coli*, possesses both Sec and Tat secretion systems (Figure 11). However, as a Gram-positive bacterium, *B. subtilis* is bounded by a single membrane. Therefore, any proteins secreted by the Sec or Tat pathways are translocated directly from the cytoplasm to the extracellular medium. In both the Sec and Tat secretion systems, secreted proteins are directed to the correct translocase by specific N-terminal peptide sequences, known as signal

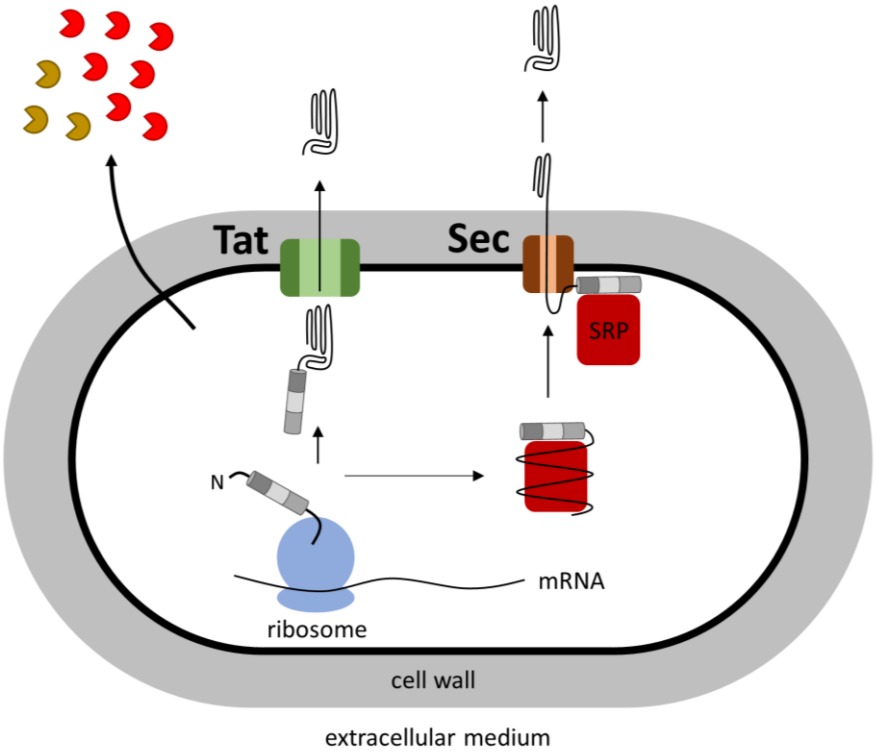

Figure 11 *B. subtilis* protein secretion pathways. Proteins are marked for secretion by the Sec and Tat pathways by the presence of an N-terminal signal peptide (grey cylinder). The Tat pathway secretes fully-folded proteins. The Sec pathway threads unfolded proteins through the membrane. *B. subtilis* naturally secretes ten proteases, three quality control proteases (yellow) and seven feeding proteases (red).

peptides (SPs). Following translocation, both Sec and Tat SPs are cleaved from the rest of the protein by signal peptidases[152].

The Sec and Tat pathways appear to have co-evolved to carry out complementary roles in protein secretion. The Sec pathway, which is responsible for secretion of the vast majority of *B. subtilis* proteins[41], secretes proteins in an unfolded state, threading proteins through a 0.6-0.9 nm pore in the membrane[153]. To accommodate this requirement for unfolded proteins, Sec pathway substrates are translocated co-translationally or bound by chaperones, like the signal recognition peptide (SRP), which maintain the protein in an unfolded state. Once translocated across the membrane, substrates of the Sec pathway must refold to their native state. This requirement for substrate proteins to both remain in an unfolded state and to refold outside the cytoplasm precludes the secretion of many proteins by the Sec pathway, including cofactor-containing proteins, fast-folding proteins, multiprotein complexes and fluorescent proteins[154]. In contrast, the Tat system solely and specifically secretes fully-folded proteins[155]. In fact, many proteins that are incompatible with Sec pathway secretion are well-

secreted by the Tat pathway, including fluorescent proteins[156], cofactor-containing proteins[157] and multiprotein complexes [158]. Further, the Tat pathway actively discriminates against unfolded or partially-folded substrates[159]. However, currently the Sec pathway alone has been used for the secretion of heterologous proteins from *B. subtilis*. Due to the complementary nature of the two pathways, harnessing the Tat system in addition to the Sec system is a major aspiration, but currently one that is yet to be realised.

In theory, by genetically fusing Sec SPs to the N-terminus of heterologous proteins and expressing them in *B. subtilis*, recombinant proteins can be directly delivered to the culture medium. In practice, however, yields of secreted heterologous proteins are far lower than the gram per litre yields attainable with natively-secreted *B. subtilis* proteins. The causes of poor secretion yields are beginning to emerge and so too strategies to relieve these obstacles.

The first issue is the variability in the optimal SP for a given protein. While all SPs share the same tripartite architecture, there are small differences in amino acid sequence between different SPs. Indeed over 170 unique Sec-dependent SPs have been predicted through genome-wide analysis[160]. One challenge is that, for a given heterologous protein, different SPs bring about different secretion yields in an unpredictable manner[161]. This effect is significant and can result in secretion yields that vary over several orders of magnitude[162]. One way, therefore, of optimising SP choice for a given protein is to generate a library of expression cassettes each with a different SP and to screen for high-yield strains[161,162].

In addition, protein folding is believed to play a central role in dictating the success of heterologous protein secretion. Proteins secreted via the Sec pathway must refold once they have been translocated across the cell membrane. However, refolding can be impaired by the polyanionic environment of the cell wall. This problem is exacerbated by the presence of secreted proteases which recognise and degrade unfolded and partially-folded secreted proteins. *B. subtilis* constitutively secretes 7 feeding proteases (NprB, AprE, Epr, Bpr, NprE, Mpr and Vpr) which degrade folded extracellular proteins to provide nutrients for the cell and at least 3 quality control proteases (HtrA, HtrB and WprA) which degrade misfolded proteins in the cell wall[163]. In fact, degradation by these proteases is known to reduce secreted protein yields dramatically. To bypass this problem, strains of *B. subtilis* have been constructed in which these proteases have been deleted from the genome. Indeed these

strains do show significant improvement in the secretion of a heterologous protein, although notably, correct folding of the protein was not assessed in this study[151].

SACCHAROMYCES CEREVISIAE

Saccharomyces cerevisiae yeast is another model organism noted for its high protein secretion capacity. As one of the favoured model eukaryotic organisms, a variety of useful genetic tools and datasets are available for *S. cerevisiae*, including a well-annotated genome, a range of modular genetic toolkits and established methods for industrial scale cultivation. While the *S. cerevisiae* secretory pathway is capable of directing efficient processing and secretion of a variety of proteins, the yields of secreted heterologous proteins are highly-variable and typically much lower than the theoretical maximum yields[164]. Regardless, *S. cerevisiae* is the host of choice for the production of a variety of FDA-approved protein pharmaceuticals, including insulin[165] and the hepatitis B surface antigen[166].

As with other secretory systems, secreted *S. cerevisiae* proteins are directed to the secretory pathway by short N-terminal signal peptides. Typically, the full length native signal peptide of the secreted α-type mating factor (MFα) is used when engineering heterologous protein secretion, as it tends to confer the highest yields. Based on the presence of a signal peptide, proteins are translocated into the endoplasmic reticulum (ER) lumen either co- or post-translationally. Once in the lumen, proteins adopt their native fold, assisted by a number of chaperones. Post-translational modifications, such as glycosylation or GPTI-anchoring, take place here in the ER lumen. At this stage an important quality control step occurs, preventing misfolding or aggregated proteins from proceeding to the next phase of the secretory pathway. Chaperones act as sentinels in the ER, binding to misfolded proteins and directing them for degradation. Particularly high levels of ER stress lead to the activation of the unfolded protein response (UPR). The UPR leads to global changes in gene expression patterns, resulting in increased levels of ER proteolysis and inhibition of the transcription and translocation of target proteins[164]. In the absence of UPR activation, normal secretion proceeds with vesicular transport to the Golgi – where signal peptides are cleaved – and finally to the plasma membrane and extracellular environment.

Although many heterologous proteins can be secreted from *S. cerevisiae*, yields are often suboptimal. Consequently, engineering *S. cerevisiae* strains with increased secretion capacity is a major goal. Because it plays such an important role in determining the efficiency of

heterologous protein secretion, there have been numerous efforts to improve secretion yields by engineering the UPR. However, the results of these studies have been varied. For example, it has been shown that overexpression of one ER chaperone, BiP, is beneficial for the secretion yields of certain proteins, but inhibitory for the yields of others[164]. In an interesting alternative approach, Huang et al. examined and engineered the effect of cellular metabolism on secreted heterologous protein yields[167]. The authors simultaneously examined the global transcriptional responses to protein secretion and yields of protein secretion in a variety of *S. cerevisiae* mutants. Several altered metabolic states were found to be particularly closely-associated with efficient secretion. For instance, high-secreting mutant strains were found to have significantly increased expression of genes involved in thiamine biosynthesis. Using this knowledge, it was shown that heterologous protein secretion yields could be increased by mutating thiamine biosynthesis genes. While it is beyond the scope of this introduction, many other approaches have been employed to engineer increased secretion yields from *S. cerevisiae*. It is becoming increasingly clear from these studies that a global view, taking into account cellular metabolism, vesicular trafficking and genome-wide transcriptional responses, will be required to engineer increased protein secretion from *S. cerevisiae*.

1.5.3 Biological protein conjugation tools

In the context of *de novo* biological ELM assembly, the ideal method for protein-protein conjugation would exhibit several properties: stability, specificity and *in vivo* compatibility. In this section, two potential approaches to protein-protein conjugation for biological ELM assembly are reviewed: the SpyTag-SpyCatcher system and chemical ligation by unnatural amino acid incorporation.

SPYTAG-SPYCATCHER

The SpyTag-SpyCatcher system and its derivatives permit genetically-encoded, covalent, *in vivo* conjugation of recombinant proteins[168]. The SpyTag-SpyCatcher system is derived from the CnaB2 domain of the *Streptococcus pyogenes* cell surface protein FbaB, which adopts a β-sheet rich immunoglobulin-like fold[169]. Once fully folded, CnaB2 autocatalyses the formation of an intramolecular isopeptide bond between a lysine side chain near its N-terminus and an aspartate side chain near its C-terminus, covalently-linking distal parts of the backbone (Figure 12A). To develop the SpyTag-SpyCatcher system the CnaB2 domain was split into two parts: a region encompassing the C-terminal β-strand and its reactive aspartate (SpyTag) and a region encompassing the remainder of the protein including the reactive lysine (SpyCatcher)[24]. The SpyTag and SpyCatcher were shown to be able to come together in solution and form the isopeptide bond, covalently linking the two domains. Therefore, by fusing the SpyTag and SpyCatcher to different recombinant proteins, any two polypeptides can be conjugated. Importantly, the SpyTag-SpyCatcher system results in the formation of a covalent bond between tagged proteins. Consequently, the SpyTag-SpyCatcher system offers potential advantages over alternative, non-covalent protein-protein conjugation systems, such as the α-helical coiled coils[170] or the cohesin-dockerin system[171].

In the few years since its initial description[24] the SpyTag-SpyCatcher system has been applied to the production of engineered *E. coli* biofilm ELMs[22,25], synthetic vaccines[172], thermo-tolerant enzymes[173–175], stably packaged enzymes[176,177] and more[178–180]. Notably, recombinant proteins, to which multiple copies of the SpyTag and SpyCatcher are fused, can be expressed and purified from *E. coli* and then combined to create self-assembling protein hydrogel materials (Figure 12B)[181]. By fusing various proteins between the SpyTag and SpyCatcher domains, a variety of functionalised hydrogel materials have been created, including fluorescent[181], photoresponsive[182] and heavy metal-sequestering materials[183].

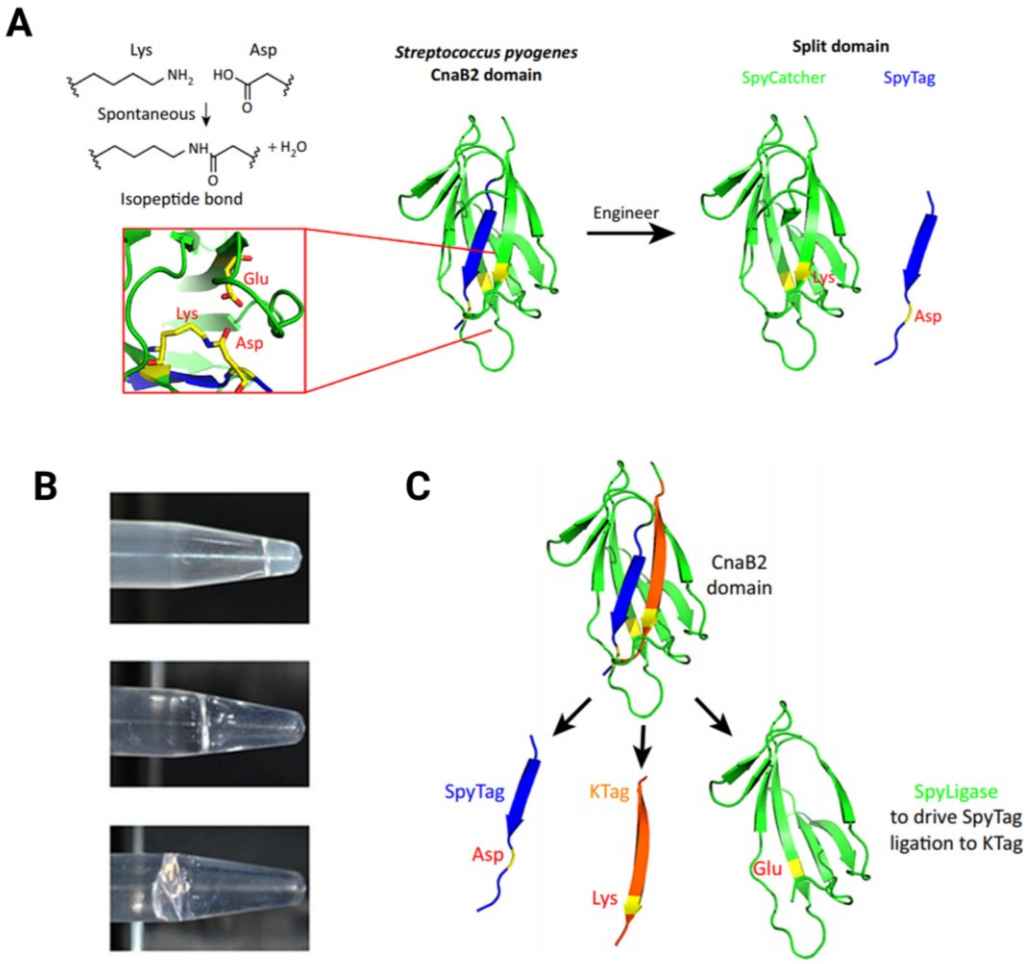

Figure 12 The SpyTag-SpyCatcher and SpyLigase systems for protein-protein conjugation. **A** The SpyTag-SpyCatcher system consists of split domains of the CnaB2 domain. Image adapted from Veggiani et al. [168] **B** Self-assembled protein hydrogel materials, created using the SpyTag-SpyCatcher system. Image adapted from Sun et al. **C** The SpyLigase system was created by further splitting the SpyCatcher domain. Image reproduced with permission from Veggiani et al. [168]

One potential drawback of the SpyTag-SpyCatcher system is the relatively large size of the SpyCatcher domain (84 amino acids). To minimise the size of the conjugation domains, the SpyCatcher itself can be split into two parts: a region encompassing the N-terminal β-strand and its reactive lysine, 'KTag' and the remainder of the protein 'SpyLigase' (Figure 12C)[178]. While the KTag and SpyTag strands cannot alone come together and become linked, it was shown that the SpyLigase component could act as an enzyme, binding the SpyTag and KTag and catalysing isopeptide bond formation. Although the SpyTag-KTag linkage is far less bulky, the reaction is much slower and has yet to be demonstrated to occur *in vivo*.

Recent studies have expanded on the original SpyTag-SpyCatcher system to create orthogonal Tag-Catcher pairs. By following the same process of splitting domains within

intramolecular covalent bond-forming protein, in this instance a homologue of CnaB2 from *Streptococcus dysgalactiae*, Tan et al. created the SdyTag and SdyCatcher$_{\text{DANG short}}$ pair[184]. Similarly, Veggiani et al. engineered the SnoopTag-SnoopCatcher pair from the *Streptococcus pyogenes* RgrA protein[185]. Further, a minimisation approach, similar to that which created the KTag and SpyLigase from SpyCatcher, was applied to the SnoopTag-SnoopCatcher system, enabling conjugation of the short peptides SnoopTagJr and DogTag as catalysed by SnoopLigase[186]. With this expanded protein-protein conjugation toolkit, the Snoop and Spy systems have been leveraged to create linear and branched polymers of recombinant proteins with potential applications in cancer therapy and multi-valent vaccine design[185,187]. In addition, prior to the development of the SpyTag-SpyCatcher system, two Tag-Catcher pairs were generated from the *S. pyogenes* major pilin protein – the pilin-N isopeptag-N pair and the pilin-C isopeptag pair[188].

UNNATURAL AMINO ACID INCORPORATION

One simple approach to protein polymerisation is to use chemical methods to cross-link proteins into multimers and polymers. Chemical linkages that have been used to covalently-link proteins include photoreactive cross-linkages[140], glutaraldehyde cross-linkages[189] and NHS–lysine ε-amine conjugation chemistry[190]. Despite the robust, programmable and site-specific nature of these cross-links, they cannot be genetically-encoded and so require prior purification and treatment of proteins, meaning they cannot be implemented *in vivo*.

However, by incorporating unnatural amino acids (UAAs) into proteins *in vivo*, chemical cross-linking methods can be genetically-encoded. UAA incorporation has been achieved by a variety of similar methods. Generally, an orthogonal aminoacyl-tRNA synthetase/tRNA$^{\text{UAA}}$ pair, which has been engineered to be able to handle a specific UAA, is introduced into the cell. The anticodon loop of the tRNA$^{\text{UAA}}$ is mutated to bind a 'spare' codon – typically the amber UAG codon in *E. coli*. Upon external addition and uptake of the cognate UAA, the aminoacyl-tRNA synthetase charges the tRNA$^{\text{UAA}}$ which then binds the cognate codon during mRNA translation and leads to incorporation of the UAA into the growing polypeptide chain[191]. UAAs can be synthesised to possess specialised functional groups. In particular, UAAs can carry reactive groups that allow for stable, covalent cross-linking of proteins[192–195]. Polymerisation of a monomeric globular protein was recently achieved by incorporating two UAAs – p-azido-L-phenylalanine (pAzF) and p-propargyloxy-L-phenylalanine (pPaF) – into

superfolder green fluorescent protein (sfGFP)[195]. These UAAs were chosen for their ability to become covalently-linked to one another through the Cu(I)-catalysed azido-alkyne cycloaddition (CuAAC) click reaction[196]. When UAA-modified sfGFP monomers were mixed with copper, large aggregates of polymerised protein were produced. Further, by modulating the position and number of UAAs incorporated, linear or branched polymers could be produced.

There are, however, limitations to current strategies for UAA incorporation. A long-standing limitation was the requirement for 'spare' codons. The UAG amber STOP codon in *E. coli* was commonly used. However, in this case the $tRNA^{UAA}$ competes with the native release factor-1 (RF1) for UAG binding, leading to inefficient incorporation and off-target incorporation of the UAA. This obstacle was essentially overcome in a remarkable study – the entirety of *E. coli* UAG codons were replaced with synonymous STOP codons, freeing the UAG codon for UAA incorporation[197]. While currently only employed in *E. coli*, in the future this approach could be applied to other hosts. The final major obstacle to UAA incorporation is the simultaneous incorporation of multiple different UAAs into singe polypeptide chains[198].

UAA incorporation therefore enables genetically-encoded protein-protein conjugation. In addition, the chemical linkages required for conjugation are much smaller than biological alternatives like the SpyTag-SpyCatcher. Going forward, incorporation of UAAs may represent an ideal approach to enabling protein-protein conjugation within biological ELMs. However, this technology is still relatively novel and further obstacles must be overcome to facilitate its application to *de novo* biological ELM development.

1.6 Aims and objectives

The burgeoning field of biological ELMs aims to create an entirely new paradigm for material production. However, realising this vision will require foundational advances to be made, starting with model, tractable systems. The general aim of this PhD project was therefore to develop and expand current approaches to create biological ELMs. We set out to develop and explore two novel biological ELM systems.

Firstly, as described in Chapter 3, we set out to create a modular system for protein secretion and conjugation using the Gram-positive bacterium *Bacillus subtilis*. Achieving programmable protein secretion and conjugation will enable extracellular assembly of protein materials, mimicking examples of natural biological material assembly. Further, creating a modular genetic toolkit for this approach will enable incorporation of numerous different structural and functional proteins, creating materials with user-defined properties. Lastly, we set out to demonstrate that strains secreting different protein components can be co-cultured and that this co-culture system enables tuning of the relative proportions of proteins within resultant conjugates. This novel approach will therefore represent a key step towards engineering the bottom-up, *de novo* assembly of biological ELMs.

Secondly, as described in Chapter 4, we set out to develop a novel approach to engineering BC-based biological ELMs. Inspired by the natural source of many BC-producing bacteria, we planned to recreate kombucha-like co-cultures between two genetically-tractable microbes, *K. rhaeticus* and *S. cerevisiae*. Using such a system, we hoped to harness the wealth of *S. cerevisiae* synthetic biology tools to engineer new biological properties into BC materials.

2 Materials and Methods

2.1 Methods for *B. subtilis* engineering

2.1.1 Strains and plasmids

Bacterial plasmids and strains used in this study are listed in Table 3 and Table 4, respectively. Both *B. subtilis* and *E. coli* were grown in LB medium or 2xYT medium at 37°C under aeration. In all instances media were supplemented with appropriate antibiotics at the following concentrations for *E. coli*: ampicillin 100 µg/mL, chloramphenicol 34 µg/mL, kanamycin 50 µg/mL. For *B. subtilis*, media were supplemented with 5 µg/mL chloramphenicol.

Table 3 Plasmids used in this study

Name	Description	Source
pHT01	*B. subtilis-E.coli* shuttle vector possessing the lacI gene and P_{grac} promoter for IPTG-inducible protein expression	MoBiTec
pHT01-xynA-His6	IPTG-inducible expression of the full length XynA xylanase with a C-terminal His6 tag	This work
pHT01-xynA$_{SP}$-SpyTag-xynA-SpyTag-His6 (**T-Xyn-T**)	IPTG-inducible expression of a fusion protein consisting of an N-terminal XynA signal peptide, an upstream SpyTag, the XynA catalytic core region, a downstream SpyTag and a C-terminal His6 tag	This work
pHT01-xynA$_{SP}$-SpyTag-xynA-SpyCatcher-His6 (**T-Xyn-C**)	IPTG-inducible expression of a fusion protein consisting of an N-terminal XynA signal peptide, an upstream SpyTag, the XynA catalytic core region, a downstream SpyCatcher and a C-terminal His6 tag	This work
pHT01-xynA$_{SP}$-SpyCatcher-xynA-SpyCatcher-His6 (**C-Xyn-C**)	IPTG-inducible expression of a fusion protein consisting of an N-terminal XynA signal peptide, an upstream SpyCatcher, the XynA catalytic core region, a downstream SpyCatcher and a C-terminal His6 tag	This work
pHT01-xynA$_{SP}$-SpyTag-xynA-SpyCatcher^{E77Q}-His6 (**T-Xyn-C'**)	IPTG-inducible expression of a fusion protein consisting of an N-terminal XynA signal peptide, an upstream SpyTag, the XynA catalytic core region, a downstream mutated SpyCatcher (E77Q) and a C-terminal His6 tag	This work
pHT01-celA-His6	IPTG-inducible expression of the full length CelA xylanase with a C-terminal His6 tag	This work
pHT01-celA$_{SP}$-SpyTag-celA-SpyTag-His6 (**T-Cel-T**)	IPTG-inducible expression of a fusion protein consisting of an N-terminal CelA signal peptide, an upstream SpyTag, the CelA catalytic core and carbohydrate-binding module, a downstream SpyTag and a C-terminal His6 tag	This work
pHT01-celA$_{SP}$-SpyTag-celA-SpyCatcher-His6 (**T-Cel-C**)	IPTG-inducible expression of a fusion protein consisting of an N-terminal CelA signal peptide, an upstream SpyTag, the	This work

	CelA catalytic core and carbohydrate-binding module, a downstream SpyCatcher and a C-terminal His6 tag	
pHT01-celA$_{SP}$-SpyCatcher-celA-SpyCatcher-His6 (**C-Cel-C**)	IPTG-inducible expression of a fusion protein consisting of an N-terminal CelA signal peptide, an upstream SpyCatcher, the CelA catalytic core and carbohydrate-binding module, a downstream SpyCatcher and a C-terminal His6 tag	This work
pHT01-xynA$_{SP}$-SpyCatcher-xynA-SpyCatcher (**C-Xyn-C**)	IPTG-inducible expression of a fusion protein consisting of an N-terminal XynA signal peptide, an upstream SpyCatcher, the XynA catalytic core region and a downstream SpyCatcher but lacking a C-terminal His6 tag.	This work
pHT01-celA$_{SP}$-SpyCatcher-celA-SpyCatcher (**C-Cel-C**)	IPTG-inducible expression of a fusion protein consisting of an N-terminal CelA signal peptide, an upstream SpyCatcher, the CelA catalytic core and carbohydrate-binding module and a downstream SpyCatcher but lacking a C-terminal His6 tag.	This work
pHT01-sacB$_{SP}$-ELP$_{20-24}$-His6 (**ELP**)	IPTG-inducible expression of a fusion protein consisting of an N-terminal SacB signal peptide, the ELP$_{20-24}$ sequence and a C-terminal His6 tag.	This work
pHT01-sacB$_{SP}$-SpyTag-ELP$_{20-24}$-SpyTag-His6 (**T-ELP-T**)	IPTG-inducible expression of a fusion protein consisting of an N-terminal SacB signal peptide, an upstream SpyTag, the ELP$_{20-24}$ sequence, a downstream SpyTag and a C-terminal His6 tag.	This work
pHT01-sacB$_{SP}$-SpyTag(DA)- ELP$_{20-24}$-SpyTag(DA)-His6 (**T'-ELP-T'**)	IPTG-inducible expression of a fusion protein consisting of an N-terminal SacB signal peptide, a mutated upstream SpyTag^{DA}, the ELP$_{20-24}$ sequence, a mutated downstream SpyTag^{DA} and a C-terminal His6 tag.	This work
pYTK001	An entry vector taken from the yeast tool kit[199]. New ORF parts were amplified with oligonucleotides introducing *BsaI* sites that dictated the position within ORF assembly and *BsmBI* sites that allow insertion into pYTK001. Once cloned into pYTK001, all ORF parts were verified, sequence and stocked at identical concentrations for subsequent use in BsaI Golden Gate assemblies.	Lee et al.[199]
pCG-A-sacB$_{SP}$-B	An ORF part-containing vector harbouring the signal peptide from SacB with 4 bp overhangs specific for the 'signal peptide' position within an ORF assembly	This work
pCG-A-celA$_{SP}$-B	An ORF part-containing vector harbouring the signal peptide from CelA with 4 bp overhangs specific for the 'signal peptide' position within an ORF assembly	This work
pCG-B-SpyTag-C	An ORF part-containing vector harbouring the SpyTag sequence with 4 bp overhangs specific for the 'upstream SpyPart' position within an ORF assembly	This work
pCG-B-mSpyCatcher-C	An ORF part-containing vector harbouring the minimal SpyCatcher (ΔN1ΔC2[200]) sequence with 4 bp overhangs specific for the 'upstream SpyPart' position within an ORF assembly	This work
pCG-C-celA-D	An ORF part-containing vector harbouring the CelA catalytic core and carbohydrate-binding module sequence with 4 bp overhangs specific for the 'protein of interest' position within an ORF assembly	This work

pCG-C-ELP$_{20-24}$-D	An ORF part-containing vector harbouring the ELP$_{20-24}$ sequence with 4 bp overhangs specific for the 'protein of interest' position within an ORF assembly	This work
pCG-D-SpyTag-His6-E	An ORF part-containing vector harbouring the SpyTag sequence with a His6 tag at its C-terminus and 4 bp overhangs specific for the 'downstream SpyPart' position within an ORF assembly	This work
pCG-D-mSpyCatcher-His6-E	An ORF part-containing vector harbouring the minimal SpyCatcher (ΔN1ΔC2^{200}) sequence with a His6 tag at its C-terminus and 4 bp overhangs specific for the 'downstream SpyPart' position within an ORF assembly	This work
pCG-A-celA^{FULL}-His6-E	An ORF part-containing vector harbouring the full-length CelA sequence with a C-terminal His6 tag. Here special 4 bp overhangs were introduced skip all sub-parts of ORF assembly and allowing 1-part insertion into the entry vector	This work
pCG004	ORF part assembly entry vector derived from pHT01. pCG004 is identical to pHT01 except for two changes. Firstly an unwanted backbone *BsaI* site with the AmpR cassette was removed. Secondly, the multiple-cloning site of pHT01 was replaces with a BsaI dropout part. This part consists of a constitutive GFP mut3b-expression cassette (using the P$_{veg}$ promoter, spoVG RBS and rrnB terminator) flanked by *BsaI* restriction sites. During assembly of ORF parts into pCG004, the GFP-expression cassette is removed and the full-length ORF inserted downstream of the RBS and upstream of the terminator	This work

Table 4 Strains used in this study

Name	Description	Source
Bacillus subtilis WB800N	*trpC2 nprE aprE epr bpr mpr::ble nprB::bsrΔvpr wprA::hyg cm::neo*; NeoR	MoBiTec
Escherichia coli Turbo	F' *proA^{+}B^{+} lacI^{q} ΔlacZM15 / fhuA2 Δ(lac-proAB) glnV galK16 galE15 R(zgb-210::Tn10)*Tet^{S} *endA1 thi-1 Δ(hsdS-mcrB)5*	NEB

2.1.1 Plasmid construction

All plasmids constructed in this study were constructed using standard cloning techniques. Oligonucleotides were obtained from IDT. Restriction endonucleases, Phusion-HF DNA polymerase and T7 DNA ligase were obtained from NEB. Unless stated, all plasmids were transformed into *E. coli* Turbo (NEB) for amplification and verification before transforming into *B. subtilis* WB800N for protein expression and secretion. All constructs were verified by restriction enzyme digestion and Sanger sequencing (Source Bioscience). Amino acid sequences of protein parts used in this study are given in Table 5.

To create the pHT01-xynA-His_6 construct, the native *B. subtilis* xynA ORF was amplified from the genome of *B. subtilis* 168 by colony PCR. Oligonucleotides were designed to introduce a C-terminal His_6 tag as well as upstream *BamHI* and downstream *AatII* restriction enzyme sites. The amplified xynA-His_6 ORF and pHT01 backbone were digested with BamHI and AatII and gel purified and ligated using T4 DNA ligase (NEB).

Using pHT01-xynA-His6 as a starting point, Golden Gate assembly was used to construct pHT01-$xynA_{SP}$-SpyTag-xynA-SpyTag-His_6 (T-Xyn-T), pHT01-$xynA_{SP}$-SpyTag-xynA-SpyCatcher-His_6 (T-Xyn-C) and pHT01-$xynA_{SP}$-SpyCatcher-xynA-SpyCatcher-His_6 (C-Xyn-C). Two versions of the SpyCatcher were synthesised by GeneArt (Life Technologies). A set of SpyCatcher-coding sequences codon-optimised for *B. subtilis* were created and the two most divergent sequences chosen (this was to reduce the risk of recombination within constructs containing two copies of the SpyCatcher). Two versions of the SpyTag were codon-optimised in the same manner and created from overlapping oligonucleotides. Golden Gate assemblies of gel purified PCR products using BsaI were performed as described[201]. SpyTag and/or SpyCatcher sequences were introduced between the xynA signal peptide ($xynA_{SP}$) and xynA enzyme and between the xynA enzyme and His_6 tag. In each instance, 4 bp overhangs were incorporated into glycine-serine (GS) linkers. The backbone was amplified in two halves to allow mutation (and therefore removal) of an unwanted BsaI site in the AmpR cassette.

The pHT01-$xynA_{SP}$-SpyTag-xynA-SpyCatcher^{E77Q}-His_6 (T-Xyn-C') mutant construct was created using pHT01-$xynA_{SP}$-SpyTag-xynA-SpyCatcher-His_6 (T-Xyn-C) as a template. We used BsaI Golden Gate assembly-based mutagenesis to mutate the catalytic glutamate of SpyCatcher to glutamine.

Table 5 Amino acid sequences of parts used in this study

Name	Part Description	Amino acid sequence
XynA	Full length endo-1, 4-β-xylanase from B. subtilis	MFKFKKNFLVGLSAALMSISLFSATASAASTDYWQNWTDGGGIVNAVNGSGGNYSVNWSN TGNFVVGKGWTTGSPFRTINYNAGVWAPNGNGYLTLYGWTRSPLIEYYVVDSWGTYRPTG TYKGTVKSDGGTYDIYTTTRYNAPSIDGDRTTFTQYWSVRQSKRPTGSNATITFSNHVNA WKSHGMNLGSNWAYQVMATEGYQSSGSSNVTVW
CelA	Full length endo-cellulase from *B. subtilis*	MKRSISIFITCLLITLLTMGGMIASPASAAGTKTPVAKNGQLSIKGTQLVNRDGKAVQLK GISSHGLQWYGEYVNKDSLKWLRDDWGITVFRAAMYTADGGYIDNPSVKNKVKEAVEAAK ELGIYVIIDWHILNDGNPNQNKEKAKEFFKEMSSLYGNTPNVIYEIANEPNGDVNWKRDI KPYAEEVISVIRKNDPDNIIIVGTGTWSQDVNDAADDQLKDANVMYALHFYAGTHGQFLR DKANYALSKGAPIFVTEWGTSDASGNGGVFLDQSREWLKYLDSKTISWVNWNLSDKQESS SALKPGASKTGGWRLSDLSASGTFVRENILGTKDSTKDIPETPSKDKPTQENGISVQYRA GDGSMNSNQIRPQLQIKNNGNTTVDLKDVTARYWYKAKNKGQNFDCDYAQIGCGNVTHKF VTLHKPKQGADTYLELGFKNGTLAPGASTGNIQLRLHNDDWSNYAQSGDYSFFKSNTFKT TKKITLYDQGKLIWGTEPN
$XynA_{SP}$	Signal peptide from XynA	MFKFKKNFLVGLSAALMSISLFSATASA
$CelA_{SP}$	Signal peptide from CelA	MKRSISIFITCLLITLLTMGGMIASPASA
$SacB_{SP}$	Signal peptide from *B. subtilis* levansucrase SacB	MNIKKFAKQATVLTFTTALLAGGATQAFA
SpyTag	Zakeri et al.[24]	AHIVMVDAYKPTK
$SpyTag^{DA}$	Zakeri et al.[24]	AHIVMVAAYKPTK
SpyCatcher	Zakeri et al.[24]	GAMVDTLSGLSSEQGQSGDMTIEEDSATHIKFSKRDEDGKELAGATMELRDSSGKTISTW ISDGQVKDFYLYPGKYTFVETAAPDGYEVATAITFTVNEQGQVTVNGKATKGDAHI
$SpyCatcher^{EQ}$	Zakeri et al.[24]	GAMVDTLSGLSSEQGQSGDMTIEEDSATHIKFSKRDEDGKELAGATMELRDSSGKTISTW ISDGQVKDFYLYPGKYTFVQTAAPDGYEVATAITFTVNEQGQVTVNGKATKGDAHI
Minimal SpyCatcher (ΔN1ΔC2)	Li et al.[200]	DSATHIKFSKRDEDGKELAGATMELRDSSGKTISTWISDGQVKDFYLYPGKYTFVETAAP DGYEVATAITFTVNEQGQVTVNG
ELP_{20-24}	Bellingham et al.[202]	FPGFGVGVGGIPGVAGVPGVGGVPGVGGVPGVGIPEAQAAAAAKAAKYGVGTPAAAAAKA AAKAAQFGLVPGVGVAPGVGVAPGVGVAPGVGLAPGVGVAPGVGVAPGVGVAPAIGP
$XynA_{SP}$-SpyTag-XynA-SpyTag-His6	XynA-SpyPart fusion protein	MFKFKKNFLVGLSAALMSISLFSATASAGSAHIVMVDAYKPTKGSASTDYWQNWTDGGGI VNAVNGSGGNYSVNWSNTGNFVVGKGWTTGSPFRTINYNAGVWAPNGNGYLTLYGWTRSP LIEYYVVDSWGTYRPTGTYKGTVKSDGGTYDIYTTTRYNAPSIDGDRTTFTQYWSVRQSK RPTGSNATITFSNHVNAWKSHGMNLGSNWAYQVMATEGYQSSGSSNVTVWGSAHIVMVDA YKPTKGSGHHHHHH
$XynA_{SP}$-SpyTag-XynA-SpyCatcher-His6	XynA-SpyPart fusion protein	MFKFKKNFLVGLSAALMSISLFSATASAGSAHIVMVDAYKPTKGSASTDYWQNWTDGGGI VNAVNGSGGNYSVNWSNTGNFVVGKGWTTGSPFRTINYNAGVWAPNGNGYLTLYGWTRSP LIEYYVVDSWGTYRPTGTYKGTVKSDGGTYDIYTTTRYNAPSIDGDRTTFTQYWSVRQSK RPTGSNATITFSNHVNAWKSHGMNLGSNWAYQVMATEGYQSSGSSNVTVWGSGAMVDTLS GLSSEQGQSGDMTIEEDSATHIKFSKRDEDGKELAGATMELRDSSGKTISTWISDGQVKD FYLYPGKYTFVETAAPDGYEVATAITFTVNEQGQVTVNGKATKGDAHIGSGSGHHHHHH
$XynA_{SP}$-SpyTag-XynA-$SpyCatcher^{EQ}$-His6	XynA-SpyPart fusion protein	MFKFKKNFLVGLSAALMSISLFSATASAGSAHIVMVDAYKPTKGSASTDYWQNWTDGGGI VNAVNGSGGNYSVNWSNTGNFVVGKGWTTGSPFRTINYNAGVWAPNGNGYLTLYGWTRSP LIEYYVVDSWGTYRPTGTYKGTVKSDGGTYDIYTTTRYNAPSIDGDRTTFTQYWSVRQSK RPTGSNATITFSNHVNAWKSHGMNLGSNWAYQVMATEGYQSSGSSNVTVWGSGAMVDTLS GLSSEQGQSGDMTIEEDSATHIKFSKRDEDGKELAGATMELRDSSGKTISTWISDGQVKD FYLYPGKYTFVQTAAPDGYEVATAITFTVNEQGQVTVNGKATKGDAHIGSGSGHHHHHH
$XynA_{SP}$-SpyCatcher-XynA-SpyCatcher-His6	XynA-SpyPart fusion protein	MFKFKKNFLVGLSAALMSISLFSATASAGSGAMVDTLSGLSSEQGQSGDMTIEEDSATHI KFSKRDEDGKELAGATMELRDSSGKTISTWISDGQVKDFYLYPGKYTFVETAAPDGYEVA TAITFTVNEQGQVTVNGKATKGDAHIGSASTDYWQNWTDGGGIVNAVNGSGGNYSVNWSN TGNFVVGKGWTTGSPFRTINYNAGVWAPNGNGYLTLYGWTRSPLIEYYVVDSWGTYRPTG TYKGTVKSDGGTYDIYTTTRYNAPSIDGDRTTFTQYWSVRQSKRPTGSNATITFSNHVNA WKSHGMNLGSNWAYQVMATEGYQSSGSSNVTVWGSGAMVDTLSGLSSEQGQSGDMTIEED SATHIKFSKRDEDGKELAGATMELRDSSGKTISTWISDGQVKDFYLYPGKYTFVETAAPD GYEVATAITFTVNEQGQVTVNGKATKGDAHIGSGSGHHHHHH

$XynA_{SP}$-SpyCatcher-XynA-SpyCatcher	XynA-SpyPart fusion protein	MFKFKKNFLVGLSAALMSISLFSATASAGSGAMVDTLSGLSSEQGQSGDMTIEEDSATHI KFSKRDEDGKELAGATMELRDSSGKTISTWISDGQVKDFYLYPGKYTFVETAAPDGYEVA TAITFTVNEQGQVTVNGKATKGDAHIGSASTDYWQNWTDGGGIVNAVNGSGGNYSVNWSN TGNFVVGKGWTTGSPFRTINYNAGVWAPNGNGYLTLYGWTRSPLIEYYVVDSWGTYRPTG TYKGTVKSDGGTYDIYTTTRYNAPSIDGDRTTFTQYWSVRQSKRPTGSNATITFSNHVNA WKSHGMNLGSNWAYQVMATEGYQSSGSSNVTVWGSGAMVDTLSGLSSEQGQSGDMTIEED SATHIKFSKRDEDGKELAGATMELRDSSGKTISTWISDGQVKDFYLYPGKYTFVETAAPD GYEVATAITFTVNEQGQVTVNGKATKGDAHI
$CelA_{SP}$-SpyTag-CelA-SpyTag-His6	CelA-SpyPart fusion protein	MKRSISIFITCLLITLLTMGGMIASPASAGSAHIVMVDAYKPTKGSAGTKTPVAKNGQLS IKGTQLVNRDGKAVQLKGISSHGLQWYGEYVNKDSLKWLRDDWGITVFRAAMYTADGGYI DNPSVKNKVKEAVEAAKELGIYVIIDWHILNDGNPNQNKEKAKEFFKEMSSLYGNTPNVI YEIANEPNGDVNWKRDIKPYAEEVISVIRKNDPDNIIIVGTGTWSQDVNDAADDQLKDAN VMYALHFYAGTHGQFLRDKANYALSKGAPIFVTEWGTSDASGNGGVFLDQSREWLKYLDS KTISWVNWNLSDKQESSSALKPGASKTGGWRLSDLSASGTFVRENILGTKDSTKDIPETP SKDKPTQENGISVQYRAGDGSMNSNQIRPQLQIKNNGNTTVDLKDVTARYWYKAKNKGQN FDCDYAQIGCGNVTHKFVTLHKPKQGADTYLELGFKNGTLAPGASTGNIQLRLHNDDWSN YAQSGDYSFFKSNTFKTTKKITLYDQGKLIWGTEPNGSAHIVMVDAYKPTKGSHHHHHHG S
$CelA_{SP}$-SpyTag-CelA-SpyCatcher-His6	CelA-SpyPart fusion protein	MKRSISIFITCLLITLLTMGGMIASPASAGSAHIVMVDAYKPTKGSAGTKTPVAKNGQLS IKGTQLVNRDGKAVQLKGISSHGLQWYGEYVNKDSLKWLRDDWGITVFRAAMYTADGGYI DNPSVKNKVKEAVEAAKELGIYVIIDWHILNDGNPNQNKEKAKEFFKEMSSLYGNTPNVI YEIANEPNGDVNWKRDIKPYAEEVISVIRKNDPDNIIIVGTGTWSQDVNDAADDQLKDAN VMYALHFYAGTHGQFLRDKANYALSKGAPIFVTEWGTSDASGNGGVFLDQSREWLKYLDS KTISWVNWNLSDKQESSSALKPGASKTGGWRLSDLSASGTFVRENILGTKDSTKDIPETP SKDKPTQENGISVQYRAGDGSMNSNQIRPQLQIKNNGNTTVDLKDVTARYWYKAKNKGQN FDCDYAQIGCGNVTHKFVTLHKPKQGADTYLELGFKNGTLAPGASTGNIQLRLHNDDWSN YAQSGDYSFFKSNTFKTTKKITLYDQGKLIWGTEPNGSDSATHIKFSKRDEDGKELAGAT MELRDSSGKTISTWISDGQVKDFYLYPGKYTFVETAAPDGYEVATAITFTVNEQGQVTVN GGSHHHHHHGS
$CelA_{SP}$-SpyCatcher-CelA-SpyCatcher-His6	CelA-SpyPart fusion protein	MKRSISIFITCLLITLLTMGGMIASPASAGSDSATHIKFSKRDEDGKELAGATMELRDSS GKTISTWISDGQVKDFYLYPGKYTFVETAAPDGYEVATAITFTVNEQGQVTVNGGSAGTK TPVAKNGQLSIKGTQLVNRDGKAVQLKGISSHGLQWYGEYVNKDSLKWLRDDWGITVFRA AMYTADGGYIDNPSVKNKVKEAVEAAKELGIYVIIDWHILNDGNPNQNKEKAKEFFKEMS SLYGNTPNVIYEIANEPNGDVNWKRDIKPYAEEVISVIRKNDPDNIIIVGTGTWSQDVND AADDQLKDANVMYALHFYAGTHGQFLRDKANYALSKGAPIFVTEWGTSDASGNGGVFLDQ SREWLKYLDSKTISWVNWNLSDKQESSSALKPGASKTGGWRLSDLSASGTFVRENILGTK DSTKDIPETPSKDKPTQENGISVQYRAGDGSMNSNQIRPQLQIKNNGNTTVDLKDVTARY WYKAKNKGQNFDCDYAQIGCGNVTHKFVTLHKPKQGADTYLELGFKNGTLAPGASTGNIQ LRLHNDDWSNYAQSGDYSFFKSNTFKTTKKITLYDQGKLIWGTEPNGSDSATHIKFSKRD EDGKELAGATMELRDSSGKTISTWISDGQVKDFYLYPGKYTFVETAAPDGYEVATAITFT VNEQGQVTVNGGSHHHHHHGS
$CelA_{SP}$-SpyCatcher-CelA-SpyCatcher	CelA-SpyPart fusion protein	MKRSISIFITCLLITLLTMGGMIASPASAGSDSATHIKFSKRDEDGKELAGATMELRDSS GKTISTWISDGQVKDFYLYPGKYTFVETAAPDGYEVATAITFTVNEQGQVTVNGGSAGTK TPVAKNGQLSIKGTQLVNRDGKAVQLKGISSHGLQWYGEYVNKDSLKWLRDDWGITVFRA AMYTADGGYIDNPSVKNKVKEAVEAAKELGIYVIIDWHILNDGNPNQNKEKAKEFFKEMS SLYGNTPNVIYEIANEPNGDVNWKRDIKPYAEEVISVIRKNDPDNIIIVGTGTWSQDVND AADDQLKDANVMYALHFYAGTHGQFLRDKANYALSKGAPIFVTEWGTSDASGNGGVFLDQ SREWLKYLDSKTISWVNWNLSDKQESSSALKPGASKTGGWRLSDLSASGTFVRENILGTK DSTKDIPETPSKDKPTQENGISVQYRAGDGSMNSNQIRPQLQIKNNGNTTVDLKDVTARY WYKAKNKGQNFDCDYAQIGCGNVTHKFVTLHKPKQGADTYLELGFKNGTLAPGASTGNIQ LRLHNDDWSNYAQSGDYSFFKSNTFKTTKKITLYDQGKLIWGTEPNGSDSATHIKFSKRD EDGKELAGATMELRDSSGKTISTWISDGQVKDFYLYPGKYTFVETAAPDGYEVATAITFT VNEQGQVTVNG
$SacB_{SP}$-$ELP_{20\text{-}24}$-His6	$ELP_{20\text{-}24}$ secretion construct	MNIKKFAKQATVLTFTTALLAGGATQAFAGSFPGFGVGVGGIPGVAGVPGVGGVPGVGGV PGVGIPEAQAAAAAKAAKYGVGTPAAAAAKAAAKAAQFGLVPGVGVAPGVGVAPGVGVAP GVGLAPGVGVAPGVGVAPGVGVAPAIGPGSHHHHHHGS
$SacB_{SP}$-SpyTag-$ELP_{20\text{-}24}$-SpyTag-His6	$ELP_{20\text{-}24}$-SpyPart fusion protein	MNIKKFAKQATVLTFTTALLAGGATQAFAGSAHIVMVDAYKPTKGSFPGFGVGVGGIPGV AGVPGVGGVPGVGGVPGVGIPEAQAAAAAKAAKYGVGTPAAAAAKAAAKAAQFGLVPGVG VAPGVGVAPGVGVAPGVGLAPGVGVAPGVGVAPGVGVAPAIGPGSAHIVMVDAYKPTKGS HHHHHHGS
$SacB_{SP}$-$SpyTag^{DA}$-$ELP_{20\text{-}24}$-$SpyTag^{DA}$-His6	$ELP_{20\text{-}24}$-SpyPart fusion protein	MNIKKFAKQATVLTFTTALLAGGATQAFAGSAHIVMVAAYKPTKGSFPGFGVGVGGIPGV AGVPGVGGVPGVGGVPGVGIPEAQAAAAAKAAKYGVGTPAAAAAKAAAKAAQFGLVPGVG VAPGVGVAPGVGVAPGVGLAPGVGVAPGVGVAPGVGVAPAIGPGSAHIVMVAAYKPTKGS HHHHHHGS

To suit our cloning needs we created a modular DNA assembly toolkit based on Golden Gate assembly (Figure 23). Four separate ORF parts were defined: a signal peptide part, an upstream SpyPart, a central protein of interest part and a downstream SpyPart. Each position was defined by the sequence of specific 4 bp overhangs generated by BsaI digestion upstream and downstream of the part. Where fewer than four ORF parts are desired in the final construct, the 4 bp overhangs were modified accordingly. ORF parts were cloned into a Golden Gate assembly part vector, pYTK001, where they were sequence-verified and stocked for subsequent assemblies. Stocked parts used in this study are summarised in Figure 24, their sequences given in Table 6 and are available from Addgene.

We also created an entry vector derived from pHT01, called pCG004, itself assembled by BsaI Golden Gate assembly. The pHT01 backbone was amplified by PCR – again in two halves to allow removal of the unwanted BsaI site – and a dropout part introduced downstream of the P_{grac} promoter and upstream of the terminator. The dropout part consists of a constitutive GFP mut3b[203] expression cassette flanked by BsaI restriction sites. Successful Golden Gate assembly will result in removal of the GFP expression cassette and therefore visual (green-white) screening of transformants. The GFP expression cassette was created using the P_{veg} promoter and spoVG RBS, specifically chosen for their activity in both *E. coli* and *B. subtilis* – and therefore allowing transformation of Golden Gate assemblies into either strain.

We used our Golden Gate assembly system to construct pHT01-celA-his_6 (CelA), pHT01-$celA_{SP}$-SpyTag-celA-SpyTag-His_6 (T-Cel-T), pHT01-$celA_{SP}$-SpyTag-celA-SpyCatcher-His_6 (T-Cel-C) and pHT01-$celA_{SP}$-SpyCatcher-celA-SpyCatcher-His_6 (C-Cel-C). To minimise the size of these constructs we used SpyCatcherΔN1ΔC2, which has superfluous amino acids trimmed from its N- and C-termini[200] (mSpyCatcher). Since repeated attempts to clone the pHT01-$celA_{SP}$-SpyCatcher-celA-SpyCatcher-His_6 (C-Cel-C) plasmid into *E. coli* resulted in identical mutations of the upstream SpyCatcher, it was cloned directly into *B. subtilis* WB800N and sequence-verified. We also used our Golden Gate assembly system to construct pHT01-$sacB_{SP}$-ELP_{20-24}-His_6 (ELP) and pHT01-$sacB_{SP}$-SpyTag-ELP_{20-24}-SpyTag-His_6 (T-ELP-T).

BsaI Golden Gate assembly-based mutagenesis was used to construct: the mutated pHT01-$sacB_{SP}$-$SpyTag^{DA}$-ELP_{20-24}-$SpyTag^{DA}$-His_6 (T'-ELP-T') (from pHT01-$sacB_{SP}$-SpyTag-ELP_{20-24}-SpyTag-His_6), the His_6 tag-lacking pHT01-$xynA_{SP}$-SpyCatcher-xynA-SpyCatcher (from pHT01-$xynA_{SP}$-SpyCatcher-xynA-SpyCatcher-His_6) and the His_6 tag-lacking pHT01-$celA_{SP}$-

SpyCatcher-celA-SpyCatcher (from pHT01-celA$_{SP}$-SpyCatcher-celA-SpyCatcher-His$_6$). Similar to the construct from which it was derived, pHT01-celA$_{SP}$-SpyCatcher-celA-SpyCatcher repeatedly showed mutations when cloned into *E. coli* and so was instead cloned directly into *B. subtilis* WB800N and sequence-verified.

Table 6 Golden gate assembly parts used in this study and available from Addgene. BsaI restriction enzyme recognition sites are shown in bold and overhangs are highlighted.

Name	Description	Addgene #
A-sacB$_{SP}$-B	Signal peptide part sequence encoding the *B. subtilis sacB* gene signal peptide	87370

GGTCTCAGGATATGAACATCAAAAAGTTTGCAAAACAAGCAACAGTATTAACCTTTACTACCGCACTGCTGGCAGGAGGCGCAACTCAAGCGTTT
GCGGGAAGCC**GAGACC**

A-celA$_{SP}$-B	Signal peptide part sequence encoding the *B. subtilis celA* gene signal peptide	87371

GGTCTCAGGATATGAAACGGTCAATCTCTATTTTTATTACGTGTTTATTGATTACGTTATTGACAATGGGCGGCATGATAGCTTCGCCGGCATCA
GCAGGAAGCT**GAGACC**

A-xynA$_{SP}$-B	Signal peptide part sequence encoding the *B. subtilis xynA* gene signal peptide	87372

GGTCTCAGGATATGTTTAAGTTTAAAAAGAATTTCTTAGTTGGATTATCGGCAGCTTTAATGAGTATTAGCTTGTTTTCGGCAACCGCCTCTGCA
GG**AAGC**C**GAGACC**

B-SpyTag-C	Upstream SpyPart sequence encoding the SpyTag	87373

GGTCTCAAAGCGCTCATATTGTAATGGTTGATGCTTATAAACCGACGAAGGGCTCAT**GAGACC**

B-mSpyCatcher-C	Upstream SpyPart sequence encoding the minimal SpyCatcher	87374

GGTCTCAAAGCGATTCAGCTACGCATATAAAATTTTCTAAACGGGACGAAGACGGCAAGGAACTGGCGGGTGCTACTATGGAACTCCGGGACTCA
TCGGGAAAAACTATAAGCACGTGGATCAGCGATGGACAAGTCAAGGACTTTTACCTTTACCCTGGCAAGTACACATTCGTCGAAACGGCTGCTCC
GGATGGATATGAAGTGGCAACAGCTATTACATTCACGGTTAACGAACAGGGGCAGGTCACCGTGAACGGGGGCTCAT**GAGACC**

D-SpyTag-His6-E	Downstream SpyPart sequence encoding the SpyTag with a C-terminal His6-tag	87375

GGTCTCAGGCAGCGCCCACATCGTTATGGTAGACGCGTACAAACCTACAAAGGGAAGCCATCATCATCATCATCACGGCAGCTAAGTTCT**GAGAC
C**

D-mSpyCatcher-His6-E	Downstream SpyPart sequence encoding the minimal SpyCatcher with a C-terminal His6-tag	87376

GGTCTCAGGCAGCGACTCCGCGACACACATCAAATTTAGCAAGCGTGATGAGGATGGGAAAGAATTAGCCGGCGCAACGATGGAACTTCGGGATT
CGAGCGGAAAGACGATTTCGACGTGGATTTCAGATGGCCAAGTCAAAGATTTTTACCTGTATCCGGGAAAATATACATTTGTCGAAACGGCAGCA
CCAGATGGATATGAGGTCGCAACAGCTATTACATTTACGGTGAATGAGCAAGGACAAGTCACGGTTAATGGCGGAAGCCATCATCATCATCATCA
CGGCAGCTAAGTTCT**GAGACC**

pCG004	Entire plasmid sequence of the entry vector pCG004	87377

TATCTAAAACAAACACTTTAACATCTGAGTCAATGTAAGCATAAGATGTTTTTCCAGTCATAATTTCAATCCCAAATCTTTTAGACAGAAATTCT
GGACGTAAATCTTTTGGTGAAAGAATTTTTTTATGTAGCAATATATCCGATACAGCACCTTCTAAAAGCGTTGGTGAATAGGGCATTTTACCTAT
CTCCTCTCATTTTGTGGAATAAAAATAGTCATATTCGTCCATCTACCTATCCTATTATCGAACAGTTGAACTTTTTAATCAAGGATCAGTCCTTT
TTTTCATTATTCTTAAACTGTGCTCTTAACTTTAACAACTCGATTTGTTTTTCCAGATCTCGAGGGTAACTAGCCTCGCCGATCCCGCAAGAGGC
CCGGCAGTCAGGTGGCACTTTTCGGGGAAATGTGCGCGGAACCCCTATTTGTTTATTTTTCTAAATACATTCAAATATGTATCCGCTCATGAGAC
AATAACCCTGATAAATGCTTCAATAATATTGAAAAAGGAAGAGTATGAGTATTCAACATTTCCGTGTCGCCCTTATTCCCTTTTTTGCGGCATTT
TGCCTTCCTGTTTTTGCTCACCCAGAAACGCTGGTGAAAGTAAAAGATGCTGAAGATCAGTTGGGTGCACGAGTGGGTTACATCGAACTGGATCT
CAACAGCGGTAAGATCCTTGAGAGTTTTCGCCCCGAAGAACGTTTTCCAATGATGAGCACTTTTAAAGTTCTGCTATGTGGCGCGGTATTATCCC
GTATTGACGCCGGGCAAGAGCAACTCGGTCGCCGCATACACTATTCTCAGAATGACTTGGTTGAGTACTCACCAGTCACAGAAAAGCATCTTACG
GATGGCATGACAGTAAGAGAATTATGCAGTGCTGCCATAACCATGAGTGATAACACTGCGGCCAACTTACTTCTGACAACGATCGGAGGACCGAA
GGAGCTAACCGCTTTTTTGCACAACATGGGGGATCATGTAACTCGCCTTGATCGTTGGGAACCGGAGCTGAATGAAGCCATACCAAACGACGAGC
GTGACACCACGATGCCTGTAGCAATGGCAACAACGTTGCGCAAACTATTAACTGGCGAACTACTTACTCTAGCTTCCCGGCAACAATTAATAGAC
TGGATGGAGGCGGATAAAGTTGCAGGACCACTTCTGCGCTCGGCCCTTCCGGCTGGCTGGTTTATTGCTGATAAATCTGGAGCCGGTGAGCGTGG
TTCTCGCGGTATCATTGCAGCACTGGGGCCAGATGGTAAGCCCTCCCGTATCGTAGTTATCTACACGACGGGGAGTCAGGCAACTATGGATGAAC
GAAATAGACAGATCGCTGAGATAGGTGCCTCACTGATTAAGCATTGGTAACTGTCAGACCAAGTTTACTCATATATACTTTAGATTGATTTAAAA
CTTCATTTTTAATTTAAAAGGATCTAGGTGAAGATCCTTTTTGATAATCTCATGACCAAAATCCCTTAACGTGAGTTTTCGTTCCACTGAGCGTC
AGACCCCGTAGAAAAGATCAAAGGATCTTCTTGAGATCCTTTTTTTCTGCGCGTAATCTGCTGCTTGCAAACAAAAAAACCACCGCTACCAGCGG
TGGTTTGTTTGCCGGATCAAGAGCTACCAACTCTTTTCCGAAGGTAACTGGCTTCAGCAGAGCGCAGATACCAAATACTGTCCTTCTAGTGTAG
CCGTAGTTAGGCCACCACTTCAAGAACTCTGTAGCACCGCCTACATACCTCGCTCTGCTAATCCTGTTACCAGTGGCTGCTGCCAGTGGCGATAA
GTCGTGTCTTACCGGGTTGGACTCAAGACGATAGTTACCGGATAAGGCGCAGCGGTCGGGCTGAACGGGGGGTTCGTGCACACAGCCCAGCTTGG
AGCGAACGACCTACACCGAACTGAGATACCTACAGCGTGAGCTATGAGAAAGCGCCACGCTTCCCGAAGGGAGAAAGGCGGACAGGTATCCGGTA
AGCGGCAGGGTCGGAACAGGAGAGCGCACGAGGGAGCTTCCAGGGGGAAACGCCTGGTATCTTTATAGTCCTGTCGGGTTTCGCCACCTCTGACT
TGAGCGTCGATTTTTGTGATGCTCGTCAGGGGGGCGGAGCCTATGGAAAAACGCCAGCAACGCGGCCTTTTTACGGTTCCTGGCCTTTTGCTGGC
CTTTTGCTCACATGTTCTTTCCTGCGTTATCCCCTGATTCTGTGGATAACCGTATTACCGCCTTTGAGTGAGCTGATACCGCTCGCCGCAGCCGA
ACGACCGAGCGCAGCGAGTCAGTGAGCGAGGAAGCGGAAGAGCGCCCAATACGCATGCTTAAGTTATTGGTATGACTGGTTTTAAGCGCAAAAAA
AGTTGCTTTTTCGTACCTATTAATGTATCGTTTTAGAAAACCGACTGTAAAAAGTACAGTCGGCATTATCTCATATTATAAAAGCCAGTCATTAG
GCCTATCTGACAATTCCTGAATAGAGTTCATAAACAATCCTGCATGATAACCATCACAAACAGAATGATGTACCTGTAAAGATAGCGGTAAATAT
ATTGAATTACCTTTATTAATGAATTTTCCTGCTGTAATAATGGGTAGAAGGTAATTACTATTATTATTGATATTTAAGTTAAACCCAGTAAATGA
AGTCCATGGAATAATAGAAAGAGAAAAAGCATTTTCAGGTATAGGTGTTTTGGGAAACAATTTCCCCGAACCATTATATTTCTCTACATCAGAAA
GGTATAAATCATAAAACTCTTTGAAGTCATTCTTTACAGGAGTCCAAATACCAGAGAATGTTTTAGATACACCATCAAAAATTGTATAAAGTGGC
TCTAACTTATCCCAATAACCTAACTCTCCGTCGCTATTGTAACCAGTTCTAAAAGCTGTATTTGAGTTTATCACCCTTGTCACTAAGAAAATAAA
TGCAGGGTAAAATTTATATCCTTCTTGTTTTATGTTTCGGTATAAAACACTAATATCAATTTCTGTGGTTATACTAAAAGTCGTTTGTTGGTTCA
AATAATGATTAAATATCTCTTTTCTCTTCCAATTGTCTAAATCAATTTTATTAAAGTTCATTTGATATGCCTCCTAAATTTTTATCTAAAGTGAA
TTTAGGAGGCTTACTTGTCTGCTTTCTTCATTAGAATCAATCCTTTTTTAAAAGTCAATATTACTGTAACATAAATATATATTTTAAAAATATCC
CACTTTATCCAATTTTCGTTTGTTGAACTAATGGGTGCTTTAGTTGAAGAATAAAAGACCACATTAAAAAATGTGGTCTTTTGTGTTTTTTTAAA
GGATTTGAGCGTAGCGAAAAATCCTTTTCTTTCTTATCTTGATAATAAGGGTAACTATTGCCGATCGTCCATTCCGACAGCATCGCCAGTCACTA
TGGCGTGCTGCTAGCGCCATTCGCCATTCAGGCTGCGCAACTGTTGGGAAGGGCGATCGGTGCGGGCCTCTTCGCTATTACGCCAGCTGGCGAAA
GGGGGATGTGCTGCAAGGCGATTAAGTTGGGTAACGCCAGGGTTTTCCCAGTCACGACGTTGTAAAACGACGGCCAGTGAATTCGAGCTCAGGCC
TTAACTCACATTAATTGCGTTGCGCTCACTGCCCGCTTTCCAGTCGGGAAACCTGTCGTGCCAGCTGCATTAATGAATCGGCCAACGCGCGGGGA
GAGGCGGTTTGCGTATTGGGCGCCAGGGTGGTTTTTCTTTTCACCAGTGAGACGGGCAACAGCTGATTGCCCTTCACCGCCTGGCCCTGAGAGAG
TTGCAGCAAGCGGTCCACGCTGGTTTGCCCCAGCAGGCGAAAATCCTGTTTGATGGTGGTTAACGGCGGGATATAACATGAGCTGTCTTCGGTAT
CGTCGTATCCCACTACCGAGATATCCGCACCAACGCGCAGCCCGGACTCGGTAATGGCGCGCATTGCGCCCAGCGCCATCTGATCGTTGGCAACC
AGCATCGCAGTGGGAACGATGCCCTCATTCAGCATTTGCATGGTTTGTTGAAAACCGGACATGGCACTCCAGTCGCCTTCCCGTTCCGCTATCGG
CTGAATTTGATTGCGAGTGAGATATTTATGCCAGCCAGCCAGACGCAGACGCGCCGAGACAGAACTTAATGGGCCCGCTAACAGCGCGATTTGCT
GGTGACCCAATGCGACCAGATGCTCCACGCCCAGTCGCGTACCGTCTTCATGGGAGAAAATAATACTGTTGATGGGTGTCTGGTCAGAGACATCA
AGAAATAACGCCGGAACATTAGTGCAGGCAGCTTCCACAGCAATGGCATCCTGGTCATCCAGCGGATAGTTAATGATCAGCCCACTGACGCGTTG
CGCGAGAAGATTGTGCACCGCCGCTTTACAGGCTTCGACGCCGCTTCGTTCTACCATCGACACCACCACGCTGGCACCCAGTTGATCGGCGCGAG
ATTTAATCGCCGCGACAATTTGCGACGGCGCGTGCAGGGCCAGACTGGAGGTGGCAACGCCAATCAGCAACGACTGTTTGCCCGCCAGTTGTTGT
GCCACGCGGTTGGGAATGTAATTCAGCTCCGCCATCGCCGCTTCCACTTTTTCCCGCGTTTTCGCAGAAACGTGGCTGGCCTGGTTCACCACGCG
GGAAACGGTCTGATAAGAGACACCGGCATACTCTGCGACATCGTATAACGTTACTGGTTTCATCAAAATCGTCTCCCTCCGTTTGAATATTTGAT
TGATCGTAACCAGATGAAGCACTCTTTCCACTATCCCTACAGTGTTATGGCTTGAACAATCACGAAACAATAATTGGTACGTACGATCTTTCAGC
CGACTCAAACATCAAATCTTACAAATGTAGTCTTTGAAAGTATTACATATGTAAGATTTAAATGCAACCGTTTTTTCGGAAGGAAATGATGACCT
CGTTTCCACCGGAATTAGCTTGGTACCAGCTATTGTAACATAATCGGTACGGGGGTGAAAAAGCTAACGGAAAAGGGAGCGGAAAAGAATGATGT
AAGCGTGAAAAATTTTTTATCTTATCACTTGAAATTGGAAGGGAGATTCTTTATTATAAGAATTGTGGAATTGTGAGCGGATAACAATTCCCAAT
TAAAGGAGGAAGGGGATAGAGACCGGGCCTTTCTGCGTTTATATACTAGAGAATTTTGTCAAAATAATTTTATTGACAACGTCTTATTAACGTTG
ATATAATTTAAATTTTATTTGACAAAAATGGGCTCGTGTTGTACAATAAATGTTACTAGAGAAAGGTGGTGAATACTAGATGCGTAAAGGAGAAG
AACTTTTCACTGGAGTTGTCCCAATTCTTGTTGAATTAGATGGTGATGTTAATGGGCACAAATTTTCTGTCAGTGGAGAGGGTGAAGGTGATGCA
ACATACGGAAAACTTACCCTTAAATTTATTTGCACTACTGGAAAACTACCTGTTCCATGGCCAACACTTGTCACTACTTTCGGTTATGGTGTTCA
ATGCTTTGCGAGATACCCAGATCATATGAAACAGCATGACTTTTTCAAGAGTGCCATGCCCGAAGGTTATGTACAGGAAAGAACTATATTTTTCA
AAGATGACGGGAACTACAAGACACGTGCTGAAGTCAAGTTTGAAGGTGATACCCTTGTTAATAGAATCGAGTTAAAAGGTATTGATTTTAAAGAA
GATGGAAACATTCTTGGACACAAATTGGAATACAACTATAACTCACACAATGTATACATCATGGCAGACAAACAAAAGAATGGAATCAAAGTTAA
CTTCAAAATTAGACACAACATTGAAGATGGAAGCGTTCAACTAGCAGACCATTATCAACAAAATACTCCAATTGGCGATGGCCCTGTCCTTTTAC
CAGACAACCATTACCTGTCCACACAATCTGCCCTTTCGAAAGATCCCAACGAAAAGAGAGATCACATGGTCCTTCTTGAGTTTGTAACAGCTGCT
GGGATTACACATGGCATGGATGAACTATACAAATAATAATACTAGAGCCAGGCATCAAATAAAACGAAAGGCTCAGTCGAAAGACTGGGCCTTTC
GTTTTATCTGTTGTTTGTCGGTGAACGCTCTCTACTAGAGTCACACTGGCTCACCTTCGGGTGGGCCTTTCTGCGTTTATATACTAGAGATCCGT
TTAGGCTGGGCGGTGATAGCTTCTCGTTCAGGCAGTA**GGTCTC**AGTTCTAAGACGTCCCCGGGGCAGCCCGCCTAATGAGCGGGCTTTTTTCACG
TCACGCGTCCATGGAGATCTTTGTCTGCAACTGAAAAGTTTATACCTTACCTGGAACAAATGGTTGAAACATACGAGGCTAATATCGGCTTATTA
GGAATAGTCCCTGTACTAATAAAATCAGGTGGATCAGTTGATCAGTATATTTTGGACGAAGCTCGGAAAGAATTTGGAGATGACTTGCTTAATTC
CACAATTAAATTAAGGGAAAGAATAAAGCGATTTGATGTTCAAGGAATCACGGAAGAAGATACTCATGATAAAGAAGCTCTAAAACTATTCAATA
ACCTTACAATGGAATTGATCGAAAGGGTGGAAGGTTAATGGTACGAAAATTAGGGGATCTACCTAGAAAGCCACAAGGCGATAGGTCAAGCTTAA
AGAACCCTTACATGGATCTTACAGATTCTGAAAGTAAAGAAACAACAGAGGTTAAACAAACAGAACCAAAAAGAAAAAAAGCATTGTTGAAAACA
ATGAAAGTTGATGTTTCAATCCATAATAAGATTAAATCGCTGCACGAAATTCTGGCAGCATCCGAAGGGAATTCATATTACTTAGAGGATACTAT
TGAGAGAGCTATTGATAAGATGGTTGAGACATTACCTGAGAGCCAAAAAACTTTTTATGAATATGAATTAAAAAAAAGAACCAACAAAGGCTGAG
ACAGACTCCAAACGAGTCTGTTTTTTTTAAAAAAAATATTAGGAGCATTGAATATATATTAGAGAATTAAGAAAGACATGGGAATAAAAATATTTT

AAATCCAGTAAAAATATGATAAGATTATTTCAGAATATGAAGAACTCTGTTTGTTTTTGATGAAAAAACAAACAAAAAAAATCCACCTAACGGAA
TCTCAATTTAACTAACAGCGGCCAAACTGAGAAGTTAAATTTGAGAAGGGGAAAAGGCGGATTTATACTTGTATTTAACTATCTCCATTTTAACA
TTTTATTAAACCCCATACAAGTGAAAATCCTCTTTTACACTGTTCCTTTAGGTGATCGCGGAGGGACATTATGAGTGAAGTAAACCTAAAAGGAA
ATACAGATGAATTAGTGTATTATCGACAGCAAACCACTGGAAATAAAATCGCCAGGAAGAGAATCAAAAAAGGGAAAGAAGAAGTTTATTATGTT
GCTGAAACGGAAGAGAAGATATGGACAGAAGAGCAAATAAAAAACTTTTCTTTAGACAAATTTGGTACGCATATACCTTACATAGAAGGTCATTA
TACAATCTTAAATAATTACTTCTTTGATTTTTGGGGCTATTTTTTAGGTGCTGAAGGAATTGCGCTCTATGCTCACCTAACTCGTTATGCATACG
GCAGCAAAGACTTTTGCTTTCCTAGTCTACAAACAATCGCTAAAAAAAATGGACAAGACTCCTGTTACAGTTAGAGGCTACTTGAAACTGCTTGAA
AGGTACGGTTTTATTTGGAAGGTAAACGTCCGTAATAAAACCAAGGATAACACAGAGGAATCCCCGATTTTTAAGATTAGACGTAAGGTTCCTTT
GCTTTCAGAAGAACTTTTAAATGGAAACCCTAATATTGAAATTCCAGATGACGAGGAAGCACATGTAAAGAAGGCTTTAAAAAAGGAAAAAGAGG
GTCTTCCAAAGGTTTTGAAAAAAGAGCACGATGAATTTGTTAAAAAAATGATGGATGAGTCAGAAACAATTAATATTCCAGAGGCCTTACAATAT
GACACAATGTATGAAGATATACTCAGTAAAGGAGAAATTCGAAAAGAAATCAAAAAACAAATACCTAATCCTACAACATCTTTTGAGAGTATATC
AATGACAACTGAAGAGGAAAAAGTCGACAGTACTTTAAAAAGCGAAATGCAAAATCGTGTCTCTAAGCCTTCTTTTGATACCTGGTTTAAAAACA
CTAAGATCAAAATTGAAAATAAAAATTGTTTATTACTTGTACCGAGTGAATTTGCATTTGAATGGATTAAGAAAAGATATTTAGAAACAATTAAA
ACAGTCCTTGAAGAAGCTGGATATGTTTTCGAAAAAATCGAACTAAGAAAAGTGCAATAAACTGCTGAAGTATTTCAGCAGTTTTTTTTATTTAG
AAATAGTGAAAAAAATATAATCAGGGAGGTATCAATATTTAATGAGTACTGATTTAAATTTATTTAGACTGGAATTAATAATTAACACGTAGACT
AATTAAAATTTAATGAGGGATAAAGAGGATACAAAAATATTAATTTCAATCCCTATTAAATTTTAACAAGGGGGGGATTAAAATTTAATTAGAGG
TTTATCCACAAGAAAAGACCCTAATAAAATTTTTACTAGGGTTATAACACTGATTAATTTCTTAATGGGGGAGGGATTAAAATTTAATGACAAAG
AAAACAATCTTTTAAGAAAAGCTTTTAAAAGATAATAATAAAAAGAGCTTTGCGATTAAGCAAAACTCTTTACTTTTTCATTGACATTATCAAAT
TCATCGATTTCAAATTGTTGTTGTATCATAAAGTTAATTCTGTTTTGCACAACCTTTTCAGGAATATAAAACACATCTGAGGCTTGTTTTATAAA
CTCAGGGTCGCTAAAGTCAATGTAACGTAGCATATGATATGGTATAGCTTCCACCCAAGTTAGCCTTTCTGCTTCTTCTGAATGTTTTTCATATA
CTTCCATGGGTATCTCTAAATGATTTTCCTCATGTAGCAAGGTATGAGCAAAAAGTTTATGGAATTGATAGTTCCTCTCTTTTTCTTCAACTTTT
T

2.1.3 Protein expression and co-culturing

In all instances, glycerol stocks of *Bacillus subtilis* strains were first spread onto selective LB plates from which single colonies were used to inoculate 5 mL 2xYT liquid cultures. After 16 h of growth, strains were back-diluted 1/50 into 5 mL of fresh 2xYT medium. Where indicated, protein expression was induced with 1 mM IPTG. Expression culturing was performed for between 2 h and 8 h, depending on the individual experiment. To collect secreted protein fractions, cultures were centrifuged at 3220 x g for 10 min and supernatants harvested.

2.1.4 SDS-PAGE and Western blotting

Since the concentration of proteins in the culture supernatant is relatively low, trichloroacetic acid (TCA) precipitation was performed to concentrate samples (by a factor of 10) prior to analysis by SDS-PAGE and Western blotting. Secreted proteins in the supernatant were precipitated by adding 100 µL of 4°C 100% TCA to 900 µL of culture supernatant and incubating for 16 h at 4°C. Precipitated proteins were centrifuged at 16900 x g for 10 min at 4°C, washed with 1 mL of ice-cold acetone, centrifuged again at 16900 x g for 10 min at 4°C and finally air-dried. Protein-containing pellets were then resuspended in 90 µL of 1x SDS-PAGE sample buffer (0.2 M Tris-HCl pH 6.8, 2% SDS, 10% glycerol, 0.01% bromophenol blue + 2 mM DTT) and boiled for 10 min at 100°C. To prepare cellular protein samples, 1 OD unit of culture was harvested by centrifuged at 16900 x g for 10 min. The cell pellet was resuspended in 150 µL of lysis buffer (10 mM TRIS-HCl, 20% sucrose, 10 mM EDTA, 50 mM NaCl, 2.5 $mg.mL^{-1}$ lysozyme, pH 8.1) and incubated at 37°C for 30 min. After incubation, 37.5 µL of 5x SDS-PAGE sample buffer was added and samples were boiled for 10 min at 100°C.

SDS-PAGE gels – with differing separating gel percentages depending on the size of proteins analysed – were run as standard and proteins stained using SimplyBlue SafeStain (Thermo). Alternatively, proteins were transferred to a PVDF membrane for immunodetection using a mouse anti-His_6 primary antibody (BioLegend clone: J099B12) at 0.1 µg/mL concentration and an alkaline phosphatase-conjugated anti-mouse secondary antibody (Promega) at 0.13 µg/mL concentration. Bound antibodies were detected using a BCIP-NBT colorimetric kit (Life Technologies).

2.1.5 Enzyme activity assays

Assays for xylanase and cellulase activities were performed using the EnzChek Cellulase Substrate (Thermo) and EnzChek Ultra Xylanase Assay Kit (ThermoFisher). Substrate solutions were prepared according to the manufacturer's instructions. In both assays 50 µL supernatant samples were pipetted into a Costar 96-well Cell Culture Plate (Corning) and 50 µL substrate solutions added simultaneously with a multi-channel pipette. Samples were immediately analysed on a Synergy HT plate reader – both assays report enzyme activity through a fluorogenic substrate (filter wavelengths: excitation 485/20 nm, emission 530/25 nm). All assays were performed at room temperature with biological triplicates. In order to calculate xylanase and cellulase enzyme activities, standard curves were prepared using known amounts of xylanase (*T. lanuginosus* Xylanase, Sigma X2753) and cellulase (*T. reseii* Cellulase, Sigma C2730) enzymes. For standard curves and for actual samples, enzyme reaction rates were calculated from the gradient over the linear region of a graph plotting

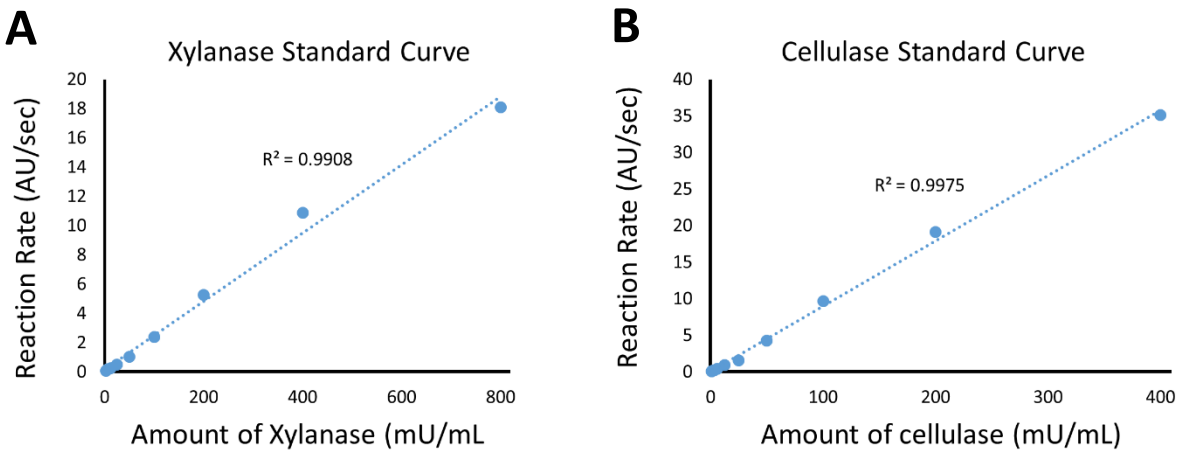

Figure 13 Xylanase and Cellulase enzyme standard curves. A Xylanase enzyme standard curve. As described in the Methods section, known amounts of a xylanase enzyme were assayed using the EnzChek xylanase assay kit. Reaction rates were calculated over the initial, linear region of a graph of plotting fluorescence AU over time. **B** Cellulase enzyme standard curve. As described in the Methods section, known amounts of a cellulase enzyme were assayed using the EnzChek cellulase substrate. Reaction rates were calculated over the initial, linear region of a graph of plotting fluorescence AU over time.

fluorescence AU over time. Where appropriate, enzyme activities were calculated using the standard curves shown in Figure 13A and 13B.

2.1.6 Protein purification

Protein purifications were performed using HisPur Ni-NTA Spin Columns (ThermoFisher), with 0.2 mL resin bed volume, according to the manufacturer's instructions. Prior to purification, 3 mL samples of culture supernatant were first mixed with a 10x concentrated

equilibration solution (500 mM NaH_2PO_4, 2.15 M Sodium Chloride, 100 mM imidazole, pH 8.0) to enable efficient binding of His6-tagged proteins to the Ni-NTA resin. A total of 2 mL of supernatant was passed over the Ni-NTA resin in three batches of 666 µL, with each incubated with the resin for 15 min prior to collecting flow through. Three washes were performed with 666 µL of wash buffer (50 mM NaH_2PO_4, 300 mM Sodium Chloride, 20 mM imidazole, pH 8.0) followed by elution in 500 µL of elution buffer (50 mM NaH_2PO_4, 300 mM Sodium Chloride, 250 mM imidazole, pH 8.0).

2.1.7 Enzyme thermo-tolerance assays

To assess the ability of different proteins to withstand boiling, supernatants samples were exposed to specified temperature programs using a ProFlex PCR System (ThermoFisher) thermal cycler. Following boiling, samples were cooled a rate of 3 °C/sec to 4°C, re-equilibrated to room temperature and assayed for xylanase activity. Data were presented as plots showing the accumulation of fluorescent product over time. In addition, reaction rates were calculated by taking gradient over the linear (early) region of the fluorescence-time plots. The percentage of enzyme activity retained after boiling was calculated by comparing reactions rates between samples subjected to 25 °C for 10 min and samples subjected to 100 °C for 10 min (or otherwise stated).

2.1.8 Co-culture conditions, co-purifications and enzyme assays

Two-strain co-cultures were performed with strains expressing SpyTag-CelA-SpyTag-His_6 and SpyCatcher-XynA-SpyCatcher proteins. Seed cultures in 2xYT medium were grown for 16 h and used to inoculate co-cultures. Inductions were performed by inoculating 5 mL 2xYT medium containing 1 mM IPTG with 50 µL of each strain, or 100 µL of each strain for monocultures. Supernatant samples were harvested after 6 h and 8 h of incubation at 37 °C and analysed by SDS-PAGE and Western blotting.

Three-strain co-cultures were performed with strains expressing C-Xyn-C, C-Cel-C and various ELP_{20-24}-containing proteins. In this instance triplicate seed cultures in 2xYT medium were grown for 16 h. Since seed cultures consistently reached similar optical densities (OD_{600} = 4.5 – 5.5), identical inoculation volumes were used for each replicate during inductions.

To compare the ability of the T-ELP-T, the mutant T'-ELP-T' and the ELP proteins to co-purify xylanase and cellulase activities, 40 µL of overnight cultures of each of the three strains were

inoculated into 5 mL 2xYT medium containing 1 mM IPTG. After 8 h of incubation at 37 °C supernatants were harvested and analysed by Western blotting using an anti-His_6 antibody. In addition, IMAC purifications of His_6-tagged proteins in the supernatant were performed as described above.

To test the ability to tune the composition of protein-protein conjugates, a number of different three-strain co-cultures were prepared in which the ratio of strains expressing the C-Xyn-C and C-Cel-C proteins was varied. The T-ELP-T-expressing strain inoculation was fixed at 40 µL. The total inoculation volume of strains expressing the C-Xyn-C and C-Cel-C proteins was fixed at 80 µL and varied: 0%:100% (0 µL:80µL), 2%:98% (1.6 µL:78.4 µL), 10%:90% (8 µL:72 µL), 25%:75% (20 µL:60 µL), 50%:50% (40 µL:40 µL) 75%:25% (60 µL:20 µL), 90%:10% (72 µL:8 µL), 98%:2% (78.4 µL:1.6 µL) and 100%:0% (80 µL:0 µL). After 8 h of incubation at 37 °C supernatants were harvested and, again, IMAC purifications of His_6-tagged proteins in the supernatant were performed as described above.

Purified protein samples were analysed by xylanase and cellulase activity assays to determine the relative levels of co-purified protein. Reaction rates were calculated by determining the gradient of the linear region of the fluorescence-time plots. The 'maximum activity' was defined as that detected from co-cultures inoculated with 100% (80 µL) of the strain expressing the C-Xyn-C or C-Cel-C protein and percentage activities were calculated based on this value.

2.2 Methods for engineered *S. cerevisiae-K. rhaeticus* co-culture

2.2.1 Strains, constructs and DNA assembly

Strains and DNA constructs used in this study are listed in Table 7 and Table 8, respectively. All plasmids constructed in this study were constructed using standard cloning techniques. Oligonucleotides were obtained from IDT. Restriction endonucleases, Phusion-HF DNA polymerase and T7 DNA ligase were obtained from NEB. Unless stated, all plasmids were transformed into *E. coli* turbo (NEB) for amplification and verification before transforming into *S. cerevisiae* for protein expression and secretion. All constructs were verified by restriction enzyme digestion and Sanger sequencing (Source Bioscience).

Table 7 Strains used in this study

Name	Description	Source
Escherichia coli Turbo	F' *proA⁺B⁺ lacI^q ΔlacZM15 / fhuA2 Δ(lac-proAB) glnV galK16 galE15 R(zgb-210::Tn10)*Tet^S *endA1 thi-1 Δ(hsdS-mcrB)5*	NEB
Saccharomyces cerevisiae BY4741	MATa his3Δ1 leu2Δ0 met15Δ0 ura3Δ0	Winston et al.[204]
Komagataeibacter rhaeticus iGEM	BC-producing bacterium isolated from kombucha tea	Florea et al.[205]
K. rhaeticus Kr RFP	Constitutive mRFP expression. *K. rhaeticus* transformed with J23110-mRFP1-331Bb.	Florea et al.[205]
S. cerevisiae Sc GFP	Constitutive GFP expression. BY4741 transformed with integrative plasmid pWS195.	Will Shaw, Ellis lab
S. cerevisiae yCG01	Constitutive GFP secretion. BY4741 transformed with integrative plasmid pCG01	This study
S. cerevisiae yCG02	Constitutive GFP-CBD secretion. BY4741 transformed with integrative plasmid pCG02	This study
S. cerevisiae yCG04	Constitutive BLA secretion. BY4741 transformed with integrative plasmid pCG04	This study
S. cerevisiae yCG05	Constitutive BLA-CBD secretion. BY4741 transformed with integrative plasmid pCG05	This study
S. cerevisiae yGPY093	β-estradiol inducible GFP expression. BY4741 transformed with integrative plasmid pGPY093.	Georgios Pothoulakis, Ellis lab
S. cerevisiae yWS890	MFα-inducible GFP expression. BY4741 transformed with integrative plasmid pWS890.	Will Shaw, Ellis lab

Table 8 Plasmid used in this study

Name	Description	Source
J23110-mRFP1-331Bb	Constitutive mRFP1 expression from the pSEVA-331Bb backbone plasmid. Expression is driven by the low strength J23110 promoter. Addegene #78277	Florea et al.[205]
pWS195	YTK single gene cassette plasmid for constitutive GFP expression, pTDH3-sfGFP-tTDH1. Backbone enabling propagation in *E. coli* and integration at the URA3 locus in *S. cerevisiae*	Will Shaw, Ellis lab
pYTK001	YTK entry vector into which new DNA parts can be cloned using BsmBI golden gate reactions, verified and stored for later assemblies.	Lee et al.[201]
pYTK096	Pre-assembled YTK plasmid containing genetic elements enabling cloning in E. coli and later integrative transformation into the URA3 locus in *S. cerevisiae*. Golden gate assembly allows insertion of YTK type 2-3-4 parts.	Lee et al.[201]
pCG01	YTK single gene cassette plasmid for constitutive GFP secretion, pTDH3-MFα-sfGFP-tTDH1. Backbone enabling propagation in *E. coli* and integration at the URA3 locus in *S. cerevisiae*	This study
pCG02	YTK single gene cassette plasmid for constitutive GFP-CBD secretion, pTDH3-MFα-sfGFP-CBDcex-tTDH1. Backbone enabling propagation in *E. coli* and integration at the URA3 locus in *S. cerevisiae*	This study
pCG04	YTK single gene cassette plasmid for constitutive BLA secretion, pTDH3-MFα-BLA-tTDH1. Backbone enabling propagation in *E. coli* and integration at the URA3 locus in *S. cerevisiae*	This study
pCG05	YTK single gene cassette plasmid for constitutive BLA-CBD secretion, pTDH3-MFα-BLA-CBD-tTDH1. Backbone enabling propagation in *E. coli* and integration at the URA3 locus in *S. cerevisiae*	This study
pGPY093	YTK multi gene cassette plasmid for β-estradiol inducible GFP expression, cassette 1: pREV1-Z_3EV-tTDH1, cassette 2: pGAL1^{6xZ3BS}-sfGFP-tTDH1. Backbone enabling propagation in *E. coli* and integration at the URA3 locus in *S. cerevisiae*	Georgios Pothoulakis, Ellis lab

S. cerevisiae constructs for strains yCG01, yCG02, yCG04 and yCG05 were cloned using the yeast toolkit (YTK) system developed by the Dueber lab[201]. The YTK system uses Golden Gate assembly to combine pre-assembled, defined parts into single gene cassettes and multi-gene cassettes. The final positions of pre-assembled parts within constructs are determined by the sequences of 4 bp overhangs created by digestion with type IIS restriction enzymes (BsaI or BsmBI). Users can therefore pick and choose from pre-assembled promoter, terminator and protein-coding parts to create expression cassettes. The combination of parts used to create strains yCG01, yCG02, yCG04 and yCG05 are shown in Table 9. These parts

were cloned into a pre-assembled backbone plasmid, pYTK096, containing genetic elements enabling cloning in *E. coli* and later integrative transformation into the URA3 locus in *S. cerevisiae*. Type 2, 3 and 4 parts were cloned into the pre-assembled backbone. To create more complex fusion proteins, additional subparts were used (e.g. 3a and 3b parts). The sequences of new parts created for the purposes of this study are shown in Table 10. New parts were codon optimised for *S. cerevisiae* expression, synthesised commercially (GeneArt) and cloned into the YTK system entry vector, pYTK001, for storage and verification. All other parts were taken from the YTK. Golden gate assembly reactions were performed as described in Lee et al.[201]. Plasmid maps and insert sequences are shown in detail in Appendix 1. Other strains, including Sc GFP, yWS890 and yGPY093, were similarly constructed using the YTK system and kindly provided by colleagues in the Ellis lab.

Table 9 YTK parts used to create *S. cerevisiae* expression constructs

Plasmid	2	3a	3b	4a	4b
yCG01	pTDH3	MFα prepro SP	TEM1 BLA	tTDH1	
yCG02	pTDH3	MFα prepro SP	TEM1 BLA	CBDcex	tTDH1
yCG04	pTDH3	MFα prepro SP	sfGFP	tTDH1	
yCG05	pTDH3	MFα prepro SP	sfGFP	CBDcex	tTDH1

Table 10 DNA sequences of new YTK parts created in this study BsaI restriction enzyme sites required for golden gate assembly are underlined, 4 bp overhangs are highlighted in red.

Name	Sequence	YTK part definition
MFα prepro	GGTCTCATATGAGATTTCCTTCAATTTTTACTGCAGTTTTATTCGCAGCATCCTCCGCATTAGCT GCTCCAGTCAACACTACAACAGAAGATGAAACGGCACAAATTCCGGCTGAAGCTGTCATCGGTTA CTTAGATTTAGAAGGGGATTTCGATGTTGCTGTTTTGCCATTTTCCAACAGCACAAATAACGGGT TATTGTTTATAAATACTACTATTGCCAGCATTGCTGCTAAAGAAGAAGGGGTATCTTTGGATAAA AGAGGTTCTTGAGACC	3a
TEM1 BLA	GGTCTCATTCTCACCCAGAAACGCTGGTGAAAGTAAAAGATGCTGAAGATCAGTTGGGTGCACGA GTGGGTTACATCGAACTGGATCTCAACAGCGGTAAGATCCTTGAGAGTTTTCGCCCCGAAGAACG TTTTCCAATGATGAGCACTTTTAAAGTTCTGCTATGTGGCGCGGTATTATCCCGTATTGACGCCG GGCAAGAGCAACTCGGTCGCCGCATACACTATTCTCAGAATGACTTGGTTGAGTACTCACCAGTC ACAGAAAAGCATCTTACGGATGGCATGACAGTAAGAGAATTATGCAGTGCTGCCATAACCATGAG TGATAACACTGCGGCCAACTTACTTCTGACAACGATCGGAGGACCGAAGGAGCTAACCGCTTTTT TGCACAACATGGGGGATCATGTAACTCGCCTTGATCGTTGGGAACCGGAGCTGAATGAAGCCATA CCAAACGACGAGCGTGACACCACGATGCCTGTAGCAATGGCAACAACGTTGCGCAAACTATTAAC TGGCGAACTACTTACTCTAGCTTCCCGGCAACAATTAATAGACTGGATGGAGGCGGATAAAGTTG CAGGACCACTTCTGCGCTCGGCCCTTCCGGCTGGCTGGTTTATTGCTGATAAATCTGGAGCCGGT GAGCGTGGGTCCCGCGGTATCATTGCAGCACTGGGGCCAGATGGTAAGCCCTCCCGTATCGTAGT TATCTACACGACGGGGAGTCAGGCAACTATGGATGAACGAAATAGACAGATCGCTGAGATAGGTG CCTCACTGATTAAGCATTGGGGATCCTGAGACC	3b
CBDcex	GGTCTCAATCCGGCGGACCCGCTGGGTGCCAAGTGTTATGGGGGGTCAATCAGTGGAATACTGGT TTCACGGCTAACGTCACTGTCAAGAACACTTCCTCTGCCCCTGTTGACGGCTGGACACTAACTTT CAGTTTCCCATCCGGTCAACAGGTTACCCAGGCATGGTCCTCCACTGTAACTCAATCCGGTAGTG CTGTCACTGTAAGGAATGCACCTTGGAATGGCAGCATCCCTGCCGGAGGGACTGCACAATTCGGC TTCAACGGGAGTCACACCGGTACAAACGCGGCTCCAACAGCATTCAGCCTAAACGGTACGCCATG CACCGTAGGGGGTAGTACTGGTTAACTCGAGTGGCTGAGACC	4a

2.2.2 Culture conditions and media

Yeast extract peptone dextrose (YPD) and yeast extract peptone sucrose (YPS) media were prepared with 10 g/L yeast extract, 20 g/L peptone and 20 g/L glucose or sucrose. Synthetic complete (SC) dropout media were prepared with 1.4 g/L yeast synthetic dropout medium supplements, 6.8 g/L yeast nitrogen base without amino acids and 20 g/L glucose. Depending on the required selection, SC media were supplemented with stock solutions of one or more of uracil (final concentration 2 g/L), tryptophan (final concentration 50 mg/L), histidine (final concentration 50 mg/L) and leucine (final concentration 0.1 g/L). Hestrin–Schramm (HS) media were prepared with 5 g/L yeast extract, 5 g/L peptone, 2.7 g/L Na_2HPO_4, 1.5 g/L citric acid and 20 g/L glucose or sucrose. Where required, media were supplemented with 20 g/L bacteriological agar. Note: partway through this study, a switch was made between sources of peptone for co-culture medium preparation from peptone from casein, to peptone from soybean. It was noted that peptone from soybean resulted in higher and more consistent pellicle yields. Specifically, results in Figure 29, Figure 30 and Figure 32 were generated using peptone from casein and all other results were generated using peptone from soybean.

E. coli was grown in LB medium at 37°C, supplemented with appropriate antibiotics at the following concentrations: chloramphenicol 34 µg/mL, kanamycin 50 µg/mL. For biomass accumulation, *K. rhaeticus* was grown at 30°C in yeast extract peptone dextrose (YPD) medium supplemented with 34 µg/mL chloramphenicol and 1% (v/v) cellulase from *T. reseii* (Sigma Alrich, C2730). Notably, we found that the growth of *K. rhaeticus* liquid cultures was significantly more reliable when inoculated from glycerol stock, rather than from colonies. Therefore, unless otherwise indicated, all *K. rhaeticus* cultures were inoculated from glycerol stocks. *S. cerevisiae* was grown at 30°C in rich YPD medium or selective, SC medium lacking the appropriate supplements, each supplemented with 50 µg/mL kanamycin.

2.2.3 Co-culture condition screen

Triplicate samples of *K. rhaeticus* Kr RFP were inoculated from glycerol stocks into 5 mL YPD medium supplemented with cellulase (1% v/v) and grown in shaking conditions for 3 days. Triplicate samples of *S. cerevisiae* Sc GFP were inoculated from plates into 5 mL YPD medium and grown in shaking conditions for 24 hours. To prepare screens, *K. rhaeticus* and *S. cerevisiae* were inoculated into 2 mL volumes of YPD, YPS, HS-glucose or HS-sucrose media

in 24-well cell culture plates. *K. rhaeticus* cultures were diluted 1/50 into fresh media. *S. cerevisiae* cultures were inoculated over a range of dilutions: 1/100, 1/1000, 1/10,000, 1/100,000 and 1/1,000,000. To enable pellicle formation, plates were incubated for 4 days under static conditions at 30°C. After 4 days of incubation, cultures were photographed under identical conditions. Where present, pellicle layers were removed from the culture surface and photographed.

2.2.4 Standard co-culture protocol

Triplicate samples of *K. rhaeticus* were inoculated from glycerol stocks into 5 mL YPD medium supplemented with cellulase (1% v/v) and grown in shaking conditions for 3 days. Triplicate samples of *S. cerevisiae* were inoculated from plates into 5 mL YPD medium and grown in shaking conditions for 24 hours. To enable inoculation of co-cultures with equivalent cell densities of different samples, OD_{600} measurements were made and used to normalise pre-culture densities. *K. rhaeticus* pre-cultures were centrifuged at 3220 x g for 10 min and cell pellets resuspended in sufficient volume of YPS medium to result in a final OD_{600} of 2.5. *S. cerevisiae* pre-cultures were diluted in YPS medium to a final OD_{600} of 0.01. To prepare final co-cultures, resuspended *K. rhaeticus* samples were diluted 1/50 and pre-diluted *S. cerevisiae* samples were diluted 1/100 into fresh YPS medium. In instances where strains were inoculated into various different final media, *K. rhaeticus* pellets were resuspended in PBS buffer and *S. cerevisiae* cultures were pre-diluted in PBS buffer. To prepare optiprep-containing co-cultures, optiprep (D1556, Sigma-Aldrich) was added to YPS media to a final concentration of 45% (v/v). Co-cultures were grown in 55 mm petri dishes (15 mL) or 12 well cell culture plates (4 mL). Co-cultures were incubated for 3 days at 30°C under static conditions. For even pellicle formation, it is important to ensure that culture vessels are not disturbed during the incubation period.

2.2.5 Determining BC pellicle yields

To determine the yields of BC pellicles, pellicle layers were removed from the surfaces of cultures and dried using the 'sandwich method'. Here, pellicles were sandwiched between two sheets of greaseproof paper and then further sandwiched between multiple sheets of absorbent paper and finally placed under a heavy weighted object. After 24 hours, fresh sheets of absorbent paper were added and pellicles were then left for an additional 24 hours. Pellicles dried in this way were then weighed to determine pellicle yields. Importantly,

pellicles were not treated with NaOH to lyse and remove cells embedded within the BC matrix.

This method was used to follow the yields of pellicle formation over time. Here, multiple co-cultures were prepared in triplicate using Sc GFP and Kr RFP strains and the standard co-culture procedure. Co-cultures were grown in 12 well plate format. At indicated time points, pellicle layers were removed to be dried and weighed.

This method was also used to compare the pellicle yield between *K. rhaeticus* mono-culture and co-culture with *S. cerevisiae*. Here, mono-cultures of *K. rhaeticus* (Kr RFP) were prepared in YPD medium and in co-culture with *S. cerevisiae* (Sc GFP) in YPS medium, using the standard co-culture protocol. After 3 days of incubation at 30°C, pellicle layers were removed to be dried and weighed.

2.2.6 Co-culture passage

To test whether co-cultures could be passaged, initial co-cultures between *S. cerevisiae* (Sc GFP) and *K. rhaeticus* (Kr RFP) were prepared in triplicate in 15 mL YPS cultures using the standard co-culture protocol. After 3 days incubation at 30°C, photographs were taken of the resultant cultures. To initiate new rounds of growth, pellicle layers were removed and the liquid below mixed by aspiration and diluted 1/100 into fresh samples of 15 mL YPS. This process was repeated over 16 rounds.

To confirm that the initial strain of GFP-expressing *S. cerevisiae* (Sc GFP) was maintained during passage, samples were plated at the end of each round. Samples from both the liquid below the pellicle and the pellicle layer itself were plated at various dilutions onto YPD-kanamycin plates. To enable plating, pellicles were digested by shaking gently for 16 hours at 4°C in 15 mL of PBS buffer with 2% (v/v) cellulase from *T. reseii* (Sigma Alrich, C2730). After 48 hours of incubation at 30°C, plates were imaged for GFP fluorescence. Dilutions were selected which enabled visualisation of single colonies. Initially plates were imaged using a Fujifilm FLA-5000 Fluorescent Image Analyser. However, due to equipment malfunction, later plates were photographed under a transluminator.

2.2.7 Determining cell distribution in co-cultures

Cell distributions were determined by plating samples of cells onto solid media and counting the resultant colonies. Pellicle samples were first rinsed by inverting ten times in 15 mL PBS and then digested by shaking gently for 16 hours at 4°C in 15 mL of PBS buffer with 2% (v/v) cellulase from *T. reseii* (Sigma Alrich, C2730). Samples were diluted at various levels into PBS. For *S. cerevisiae* cell counts, samples were plated onto YPD-kanamycin media. For *K. rhaeticus* cell counts, samples were plated onto SC media lacking all four supplements essential for *S. cerevisiae* growth (histidine, leucine, tryptophan and uracil). In all instances, Kr RFP and Sc GFP strains were used. Therefore, to ensure the colonies counted were the target strains, plates were scanned for fluorescence using a Fujifilm FLA-5000 Fluorescent Image Analyser. Plate cell counts were used to calculate the original colony forming units (cfu) per unit volume for liquid samples. However, since the exact volumes of pellicle were not measured prior to degradation, it was not possible to calculate the *exact* cell counts in cfu per unit volume. To enable a rough approximation of the cell counts per unit volume, pellicle volumes were estimated at fixed levels and these values were used to calculate estimated cfu per unit volume. For 15 mL cultures, pellicle volumes were estimated at 4 mL and for 4 mL cultures in 12 well plates pellicle volumes were estimated at 1 mL.

To compare cell counts from mono-cultures and co-cultures of *K. rhaeticus* and *S. cerevisiae*, pre-cultures of *K. rhaeticus* Kr RFP were pelleted and resuspended in PBS buffer and pre-cultures of *S. cerevisiae* Sc GFP were diluted in PBS buffer, according to the standard co-culture procedure. Various co-cultures and mono-cultures were then prepared in different media in 15 mL volumes. After 3 days incubation at 30°C, pellicle and liquid samples were prepared, diluted and plated for cell counts.

To determine the reproducibility of co-culture cell counts, co-cultures were prepared according to the standard co-culture protocol in 15 mL cultures on three separate occasions. After 3 days incubation at 30°C, pellicle and liquid samples were prepared, diluted and plated for cell counts.

To determine cell counts in BC balls, balls were degraded by gently mixing for 16 hours at 4°C in 1 mL of PBS buffer with 2% (v/v) cellulase from *T. reseii* (Sigma Alrich, C2730). Degraded ball samples were diluted and plated for cell counts as above. To estimate the cell counts of *S. cerevisiae* in cfu per unit volume, a ball diameter of 3 mm was assumed.

2.2.8 Fluorescence microscopy

Images of pellicles were prepared using a 20x objective lens mounted on a Nikon Eclipse Ti inverted microscope. Slices of pellicle were mounted on slides with the bottom face of the pellicle facing downwards. To visualise samples, a phase filter (Ph1) was used to enhance contrast. GFP fluorescence images were taken using 480 nm excitation and 535 nm emission wavelengths. The NIS-elements microscope imaging software was used for initial image capture and ImageJ was used for downstream image analysis and stacking of GFP and brightfield images.

2.2.9 Growing BC balls

To prepare BC balls co-cultures, *S. cerevisiae* and *K. rhaeticus* pre-cultures were diluted and resuspended, respectively, as described in the standard co-culture protocol (section **2.2.5**). Resuspended *K. rhaeticus* pre-cultures were inoculated into 5 mL of YPS or YPD media with a dilution of 1/50. Diluted *S. cerevisiae* pre-cultures were inoculated into 5 mL of YPS or YPD media with a dilution of 1/100 or 1/1000, creating final total dilutions of approximately $1/10^5$ or $1/10^6$. These 5 mL cultures were then grown for 2 days at 30°C with shaking at 250 rpm. After incubation, balls were removed from cultures, photographed, imaged under light microscopy or degraded for cell count estimation.

2.2.10 Supernatant nitrocefin assay

For culture supernatant assays, WT BY4741, yCG04 and yCG05 *S. cerevisiae* strains were grown in triplicate overnight in YPD liquid medium with shaking. After 16 hours growth, liquid cultures were back-diluted to final OD_{600} = 0.01 in 5 mL fresh YPS medium and grown for 24 hours with shaking. The resultant cultures were centrifuged at 3220 x g for 10 min and the supernatant fractions harvested. Supernatant samples were pipetted in 50 µL volumes into the wells of a 96 well plate. The colorimetric substrate, nitrocefin (484400, Merck-Millipore), was resuspended in DMSO to create a 10 mg/mL working stock. This stock was diluted to 50 µg/mL in nitrocefin assay buffer (50 mM sodium phosphate, 1 mM EDTA, pH 7.4). To start the reaction, 50 µL of nitrocefin at 50 µg/mL was added to each of the samples simultaneously and the absorbance at 490 nm was measured over time. Active β-lactamase converts nitrocefin to a red substrate, increasing the absorbance of light at 490 nm. Therefore, to calculate the relative β-lactamase activity in samples, the rate of change in the

absorbance of light at 490 nm was determined. Specifically, the product formation rates were calculated from the gradient over the linear region of a graph plotting fluorescence AU over time.

2.2.11 Pellicle nitrocefin assays

For initial pellicle assays (Figure 37), WT BY4741, yCG04 and yCG05 *S. cerevisiae* strains were co-cultured with *K. rhaeticus* (Kr RFP) in triplicate, according to the standard co-culture protocol. Following 3 days growth, pellicles were removed and washed in 15 mL PBS buffer for 30 min with shaking at 150 rpm. Square pieces of pellicle, measuring 5 mm x 5 mm, were then cut using a scalpel. The remainder of the pellicle was dried using the sandwich method, described in section **2.2.6**. Once dried, pellicles were again cut to produce 5 mm x 5 mm pieces. Dried pellicle pieces were rehydrated by adding 25 µL of PBS buffer and incubating for 30 min. Assays for both wet and dried samples were run by adding 10 µL of nitrocefin, diluted to 1 mg/mL in PBS buffer, to each of the pellicle pieces simultaneously. Initial assays were performed at room temperature. Photographs were taken of pellicles over the course of 35 min to follow the colour change. To provide a quantitative measure of colour change, the ImageJ (NIH) image analysis software was used. Images were first split into individual colour channels. Since yellow-to-red colour change is caused by an increase in the absorbance of green light wavelengths, the green channel was selected. To quantify the yellow-to-red colour change, the green channel intensity was then measured from greyscale-inverted images of pellicle slices over time. Since preliminary results showed that WT pellicles exhibited no colour change, the signal from WT pellicles was used as a baseline value to correct for background levels of green channel intensity.

To determine absolute levels of β-lactamase activity in wet and dried pellicles, a similar protocol was used to create standard curves. Standard curves were prepared using a commercial *E. coli* β-lactamase enzyme (ENZ-351, ProSpec). First, pellicles grown with WT BY4741 *S. cerevisiae* were washed in nitrocefin assay buffer buffer (50 mM sodium phosphate, 1 mM EDTA, pH 7.4). Pieces measuring 5 mm x 5 mm were cut and weighed to enable determination of the approximate volume of liquid within the pellicle. The remainder of the pellicles were dried using the sandwich method. Once dried, 5 mm x 5 mm pieces of pellicle were cut for dried pellicle standard curves. Dried pellicle pieces were rehydrated by adding 20 µL of nitrocefin assay buffer. Pre-diluted standard β-lactamase samples were then

added to pellicle pieces in 5 µL volumes and allowed to diffuse throughout the BC for 30 min. To initiate the reaction, 5 µL aliquots of nitrocefin, diluted to 2 mg/mL in nitrocefin assay buffer, were added to each of the pellicle pieces simultaneously. Samples were incubated at 25°C and photographs taken over the course of the reaction. Again, ImageJ was used to quantify the yellow-to-red colour change at given time points. Time points were chosen to maximise the dynamic range, without reaching saturation. For wet pellicles, it was necessary to use the measured weight of pellicle slices to determine the actual final concentration of the standard β-lactamase. Standard curves are shown in Figure 39. Standard curves using fresh wet pellicles, dried pellicles and dried pellicles stored for 1 month at room temperature were all prepared according to this method.

Alongside standard curves, pellicles grown with yCG05 *S. cerevisiae* were analysed using an identical protocol. To enable cross comparison with standard curves, negative samples (pellicles from co-cultures with WT *S. cerevisiae*) and positive samples (pellicles from co-cultures with WT *S. cerevisiae* to which a known amount of β-lactamase standard had been added) were run with samples. For samples to which no standard β-lactamase was added, 5 µL of nitrocefin assay buffer was added to maintain equal final liquid volumes. Photographs taken at identical time points were then used with standard curves to calculate absolute values of β-lactamase activity. Again, ImageJ was used to quantify the yellow-to-red colour change. For wet pellicles, it was necessary to use the measured weight of pellicle slices to determine the actual final concentration of enzyme. Again, fresh wet pellicles, dried pellicles and dried pellicles stored for 1 month at room temperature were all assayed according to this method.

2.2.12 β-lactamase activity retention assay

To determine the retention of β-lactamase within BC following multiple rounds of washes, nitrocefin assays were performed. Pieces measuring 5 mm x 5 mm were cut from dried pellicles grown with yCG04 and yCG05. All pellicle pieces were rehydrated by incubating in 1mL of PBS buffer. Pieces were subjected to a variable number of wash steps, where pellicle pieces were incubated in 4 mL PBS buffer at 25°C and 150 rpm for 30 min. After washing, pellicles were assayed for β-lactamase activity. Negative samples (pellicles from co-cultures with WT *S. cerevisiae*) and positive samples (pellicles from co-cultures with WT *S. cerevisiae* to which a known amount of β-lactamase standard had been added) were run alongside all

samples. For samples to which no standard β-lactamase was added, 5 µL of PBS buffer was added to maintain equal final liquid volumes. As before, assays were initiated by adding 5 µL of nitrocefin, diluted to 2 mg/mL in PBS buffer, to each of the pellicle pieces simultaneously. Since the number of samples that can be run in parallel is limited, samples were run in batches based on the number of washes. Again, ImageJ was used to quantify the yellow-to-red colour change at given time points. To enable cross-comparison between different assay runs, negative samples were used to subtract background signals and positive samples were used to normalise signals. To ensure that yellow-to-red colour change values were within a range in which there is a linear relationship between β-lactamase activity and the yellow-to-red colour change signal, a standard curve was run. The standard curve (r^2 = 0.9571) confirmed that detected yellow-to-red colour change values fell within the linear range.

2.2.13 BC balls nitrocefin assay

BC balls were grown using the standard BC balls protocol (**2.2.10**) with WT BY4741, yCG04 and yCG05 *S. cerevisiae* strains. Triplicate samples were first washed by incubating in 1 mL of PBS buffer with incubation at 25°C and 150 rpm for 30 min. Afterwards BC balls were placed into fresh 30 µL spots of PBS buffer. Assays were initiated by simultaneously adding 5 µL of nitrocefin, diluted to 2 mg/mL in PBS buffer, to each spot. Reactions were allowed to proceed at room temperature. Photographs were taken after 15 min of incubation.

2.2.14 Assaying GFP secretion into supernatant and pellicles

As preliminary test of ability of yCG01 and yCG02 to secrete GFP, individual colonies were grown in 5 mL YPD medium for 48 hours. As a negative control strain, non-fluorescent yCG04 was used. After 48 hours growth, cultures were centrifuged at 3220 x g for 10 min and supernatant samples imaged for fluorescence under a transluminator.

To test whether *S. cerevisiae* could secrete detectable levels of GFP into BC materials, co-cultures were prepared in triplicate according to the standard co-culture protocol using WT BY4741, yCG01 and yCG02 strains. Co-cultures were grown in 4 mL volumes in 12 well plates. Since GFP secretion yields were anticipated to be low, co-cultures were allowed to grow for either 7 days or 14 days before imaging. After incubation, pellicles were washed by incubating for 30 min in 15 mL PBS buffer. Washed pellicles were then imaged for GFP using Fujifilm FLA-5000 Fluorescent Image Analyser. Images were analysed and modified for

presentation using ImageJ (NIH). Specifically, brightness and contrast were adjusted, equally for all samples, to the point at which the background fluorescence of pellicles grown with WT *S. cerevisiae* was just visible.

2.2.15 Preparing and assaying biosensor pellicles

As a preliminary test of *S. cerevisiae* sense-and-response in BC pellicles, co-cultures were prepared in triplicate according to the standard co-culture protocol using WT BY4741 and yGPY093 strains. Co-cultures were inoculated into 4 mL YPS-optiprep medium in 12 well cell culture plates. After 3 days of growth, pellicles were removed and washed by incubating at 25°C with shaking at 150 rpm in 15 mL PBS. Pellicles were then placed in fresh 15 mL of YPD medium in the presence or absence of 5 nM β-estradiol (E8875, Sigma-Aldrich) and incubated for 24 hours at 30°C and 150 rpm. Large quantities of cells had 'escaped' from biosensor pellicles, making the medium surrounding the pellicles turbid. Therefore, to remove loosely-associated cells, pellicles were washed twice by incubating at for 30 min at 25°C and 150 rpm in 15 mL of PBS buffer. Finally, pellicles were imaged simultaneously for GFP fluorescence under a transluminator.

Similarly, dried biosensor pellicles were prepared were prepared in triplicate according to the standard co-culture protocol using WT BY4741 and yGPY093 or WT BY4741 and yWS890 strains. Co-cultures were inoculated into 4 mL YPS-optiprep medium in 12 well cell culture plates. After 3 days of growth, pellicles were dried using the 'sandwich method' (see section **2.2.6**). Dried pellicles were then placed in fresh 15 mL of YPD medium in the presence or absence of 5 nM β-estradiol (E8875, Sigma-Aldrich) or 50 nM *S. cerevisiae* α–mating factor (RP01002, GenScript) and incubated 24 hours at 30°C statically. Static growth was chosen to more closely mimic a potential in-the-field application. Since static growth result in far less growth in the surrounding liquid, pellicles were only briefly washed by inverting ten times in 15 mL PBS buffer. Finally, pellicles were imaged side-by-side for GFP fluorescence under a transluminator.

2.2.16 Determining the viability of *S. cerevisiae* in dried BC pellicles

Co-cultures were prepared in triplicate according to the standard co-culture protocol using Sc GFP and Kr RFP. Co-cultures were inoculated into 4 mL YPS-optiprep medium in 12 well cell culture plates. Counts of viable *S. cerevisiae* cells within wet and dried pellicles were determined as described in section **2.2.8**. Dried pellicles were also stored for 1 month at room temperature, and then degraded and plated onto YPD medium. Since one of the triplicate samples produced no colonies, we could not calculate estimated cell counts within pellicles. However, images are presented of the three plates to show that viable cells were indeed recovered from the other two samples (Figure 44).

3 Extracellular self-assembly of functional and tunable protein conjugates from *Bacillus subtilis*

SUMMARY

The ability to stably and specifically conjugate recombinant proteins to one another is a powerful approach for engineering multifunctional enzymes, protein therapeutics and novel biological materials. While many of these applications have been illustrated through *in vitro* and *in vivo* intracellular protein conjugation methods, extracellular self-assembly of protein conjugates offers unique advantages: simplifying purification, reducing toxicity and burden, and enabling tunability. Exploiting the recently described SpyTag-SpyCatcher system, we describe here how enzymes and structural proteins can be genetically-encoded to covalently conjugate in culture media following programmable secretion from *Bacillus subtilis*. Using this novel approach, we demonstrate how self-conjugation of a secreted industrial enzyme, XynA, dramatically increases its resilience to boiling and we show that cellular consortia can be engineered to self-assemble functional protein-protein conjugates with tunable composition. This novel genetically-encoded modular system provides a flexible strategy for protein conjugation harnessing the substantial advantages of extracellular self-assembly.

AIMS

- Determine if the SpyTag-SpyCatcher system can be used to program extracellular conjugation of proteins secreted by *Bacillus subtilis*
- To develop a modular toolkit of genetic parts to facilitate extracellular protein-protein conjugation
- To demonstrate that strains secreting different proteins can be co-cultured to produce protein-protein conjugates with tunable composition
- To explore potential applications of extracellular protein-protein conjugation

3.1 Introduction

In section **1.5.1** a conceptual approach to *de novo* biological ELM self-assembly was outlined. In contrast to the majority of efforts to create and engineer biological ELMs, this strategy aims to build a material from the bottom-up using rational design. The approach consists of two steps: i) secretion of proteins from co-cultures of engineered microbes and ii) spontaneous conjugation of secreted proteins in the extracellular environment. By secreting and conjugating both structural proteins, which self-assemble to form a scaffold material, and functional proteins, which confer desired additional material properties, this modular system would enable self-assembly of biological ELMs with programmable properties.

However, an approach enabling extracellular self-assembly of protein-protein conjugates would not only be of value to biological ELM development. Proteins themselves are modular biological components whose functions can be combined, augmented and repurposed by bringing them together in new ways. Not only is this a key driver in the evolution of novel cellular processes[206], but it is also a powerful approach in the creation of a variety of biotechnological products. Co-localizing enzymes from a single metabolic pathway can be used to enhance metabolic fluxes in biosynthesis[180,207]. Vaccine efficacy can be improved by conjugating antigens to specific presentation proteins[172,208,209]. Therapeutic proteins can be stabilised or targeted to specific tissues and cells by fusing them to appropriate protein partners[210,211].

A modular, genetically-programmable *in vivo* approach to protein-protein conjugation could replace the costly and technically-demanding methods previously used to conjugate proteins. The ability to program self-assembly of protein-protein complexes from microorganisms in this way could simultaneously accelerate the development of novel biotechnological products and facilitate their spontaneous on-site growth, obviating the need for external manipulation.

Genetic fusion is a simple and direct method for conjugating proteins together, but is limited in the size, topology and repetitiveness of conjugates that can be formed[212]. Conversely, chemical conjugation methods enable multivalent and extensible protein-protein conjugation, but typically require prior purification and treatment of proteins and so cannot be implemented *in vivo*[190,195,213,214]. By contrast, biological conjugation methods such as the

SpyTag-SpyCatcher system[24], enable both genetically-programmed *in vivo* self-assembly and the formation of a variety of topologies[185,215,216].

As outlined in detail in section **1.5.3**, the SpyTag-SpyCatcher system[24] directs specific, covalent conjugation of proteins through two short polypeptide tags: the SpyTag and SpyCatcher. The larger partner, the SpyCatcher, adopts an immunoglobulin-like fold that specifically binds the SpyTag and autocatalyses the formation of an intermolecular isopeptide bond between two amino acid side chains. Notably, in the few years since its initial description[24], the SpyTag-SpyCatcher system has been applied to the production of programmable and customisable materials[22,25,27,181,217], synthetic vaccines[172], thermo-tolerant enzymes[173–175], stably packaged enzymes[176,177] and more[178–180,218–222].

However, thus far, the SpyTag-SpyCatcher system has only ever been deployed within the cell or *in vitro*, following purification of individual components. Yet for a variety of applications, it would be advantageous for proteins to be secreted prior to spontaneous conjugation. Firstly, extracellular production greatly simplifies downstream processing and purification of products[223], improving industrial scale cost-effectiveness. In addition, secreting the monomeric components of protein polymers avoids the cytotoxicity and misfolding commonly associated with their intracellular expression, facilitating applications such as protein material production[224]. Lastly, by engineering microbes to secrete proteins that form complexes outside the cell, it becomes possible to compartmentalise the production of individual proteins within separate strains in a co-culture. Engineering so-called 'cellular consortia' to perform co-operative biological tasks in this way has attracted increasing interest in recent years due to the substantial potential advantages it offers[90,91]. For instance, engineered cellular consortia allow the division of labor between co-cultured strains, meaning less burden is placed on each individual cell. In addition, by separately engineering individual strains within co-cultures, cellular consortia have been shown to facilitate the optimisation of biological processes and to enable tunable and autonomous patterning of biomaterials[22,91,92,225,226].

A modular platform enabling programmable, spontaneous self-assembly of extracellular protein-protein conjugates would therefore be of great value not only for *de novo* biological ELM design but also more widely in the biotechnology and synthetic biology research communities. With this aim, we sought to engineer simultaneous protein secretion and SpyTag-SpyCatcher-mediated protein conjugation using *Bacillus subtilis*. We designed and

built recombinant fusion proteins consisting of separate protein modules specifying function, secretion and conjugation and demonstrate here that these modules are active and direct secretion and extracellular conjugation without perturbing enzymatic activity. Lastly, we illustrate the utility and applicability of our approach in two scenarios: engineering secreted, thermo-tolerant enzymes for industrial biotechnology and tuning the assembly of functional, secreted protein conjugates by cellular consortia.

3.2 Results and Discussion

3.2.1 Expression, secretion and conjugation of SpyTag-SpyCatcher fusion proteins

To first determine the feasibility of our approach – combining SpyTag-SpyCatcher conjugation and *B. subtilis* protein secretion – we fused together protein-encoding DNA modules specifying secretion, conjugation and function into single open reading frames (ORFs) within gene expression cassettes. Four protein modules, each connected by two amino acid glycine-serine linkers, were defined: an N-terminal secretion signal peptide, an upstream SpyPart – either SpyTag (T) or SpyCatcher (C) – then a user-defined protein of interest and a C-terminal His_6-tagged SpyPart (Figure 14A).

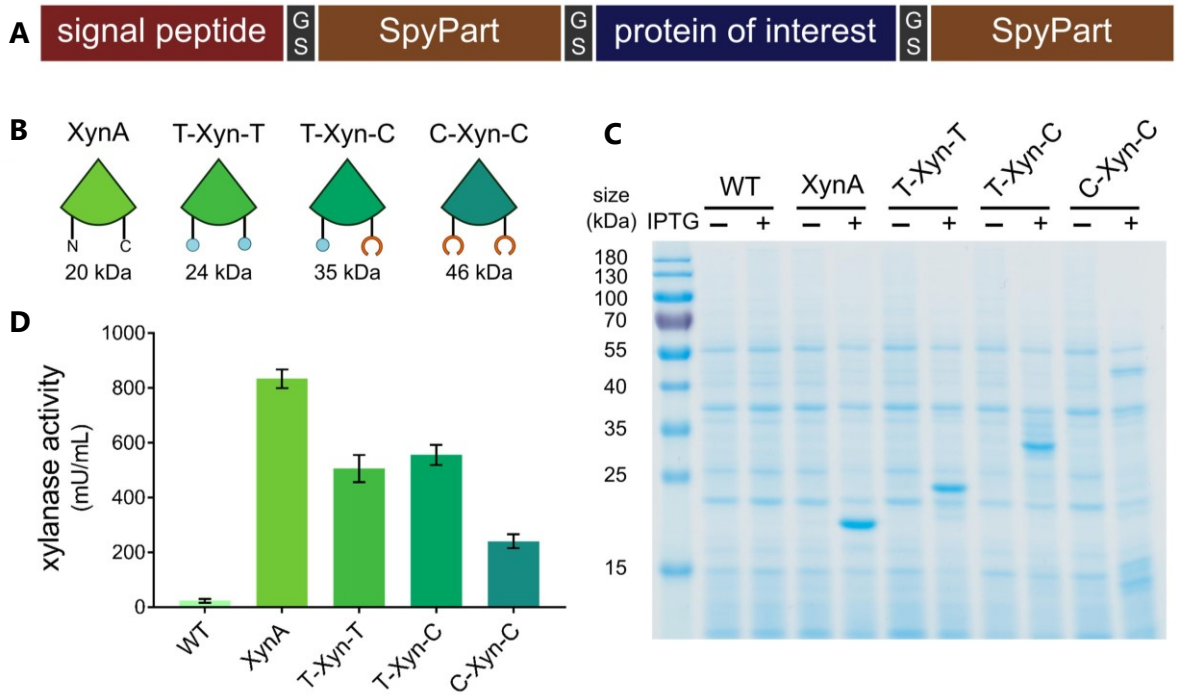

Figure 14 Design, secretion and activity of SpyTag-SpyCatcher XynA fusion proteins. A Protein-encoding DNA modules specifying secretion, conjugation and function were fused into single ORFs separated by 2-amino acid glycine-serine linkers. **B** Four recombinant proteins based on XynA were designed: the full-length xylanase XynA, SpyTag-XynA-SpyTag (T-Xyn-T), SpyTag-XynA-SpyCatcher (T-Xyn-C) and SpyCatcher-XynA-SpyCatcher (C-Xyn-C). All possess the native XynA signal peptide at their N-termini as well as a C-terminal His6 tag. **C** Culture supernatants from uninduced (-) and IPTG-induced (+) cultures were 10x concentrated by TCA precipitation prior to SDS-PAGE analysis with Coomassie staining. All four proteins were well-expressed and secreted. Untransformed B. subtilis WB800N (WT) was included as a negative control. **D** Culture supernatants were analysed for xylanase activity using a fluorogenic substrate. All samples exhibited xylanase activity, indicating secretion of active fusion proteins. Product formation rates were calculated over 10 minutes from triplicate samples (data represent the mean ± 1 SD).

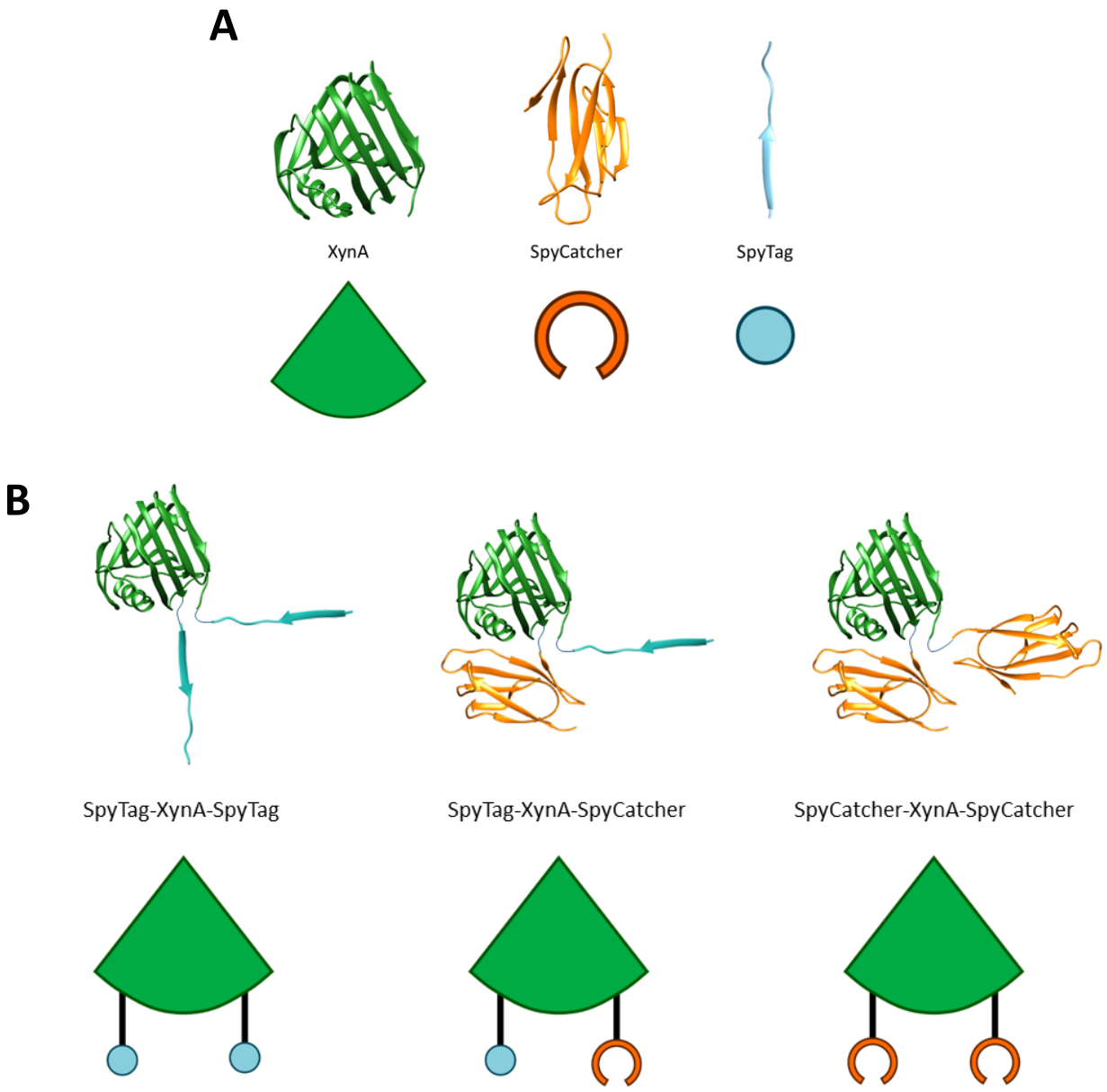

Figure 15 XynA fusion protein schematics. A X-ray crystal structures of XynA (PDB ID: 2DCY), SpyCatcher and SpyTag (both base on PDB ID: 4MLI) are shown alongside the graphic representations used elsewhere in this study. The N- and C-termini of XynA (following removal of the N-terminal signal peptide) are very close to one another: 3.8 Å as measured between the N-terminal nitrogen and C-terminal C_α atoms (using Chimera, UCSF). **B** Approximate structures of XynA-SpyPart fusion proteins and graphic representations used throughout this study. Note that the structures shown were *not* experimentally determined and are purely for illustrative purposes. SpyParts are fused the N- and C-termini of XynA through flexible 2 amino acid glycine-serine linkers. Due the close proximity of the SpyParts, cyclisation reactions are possible.

Using this design, we first generated a series of fusion proteins based on the native, secreted *B. subtilis* endo-xylanase, XynA (Figure 14B and Figure 15), a hemicellulose-degrading enzyme with uses in industry. The native XynA signal peptide was preserved at the N-terminus and SpyParts were fused either side of the XynA enzyme core to create three proteins: T-Xyn-T, T-

Xyn-C and C-Xyn-C (Figure 14B). As a control, a construct expressing the full-length XynA with a C-terminal His_6-tag was also created. All constructs were cloned downstream of the strong IPTG-inducible P_{grac} promoter in pHT01, a *B. subtilis-E. coli* shuttle vector. Each of these fusion proteins was successfully expressed and secreted from *B. subtilis* (Figure 14C and Figure 16) and retained xylanase activity (Figure 14D).

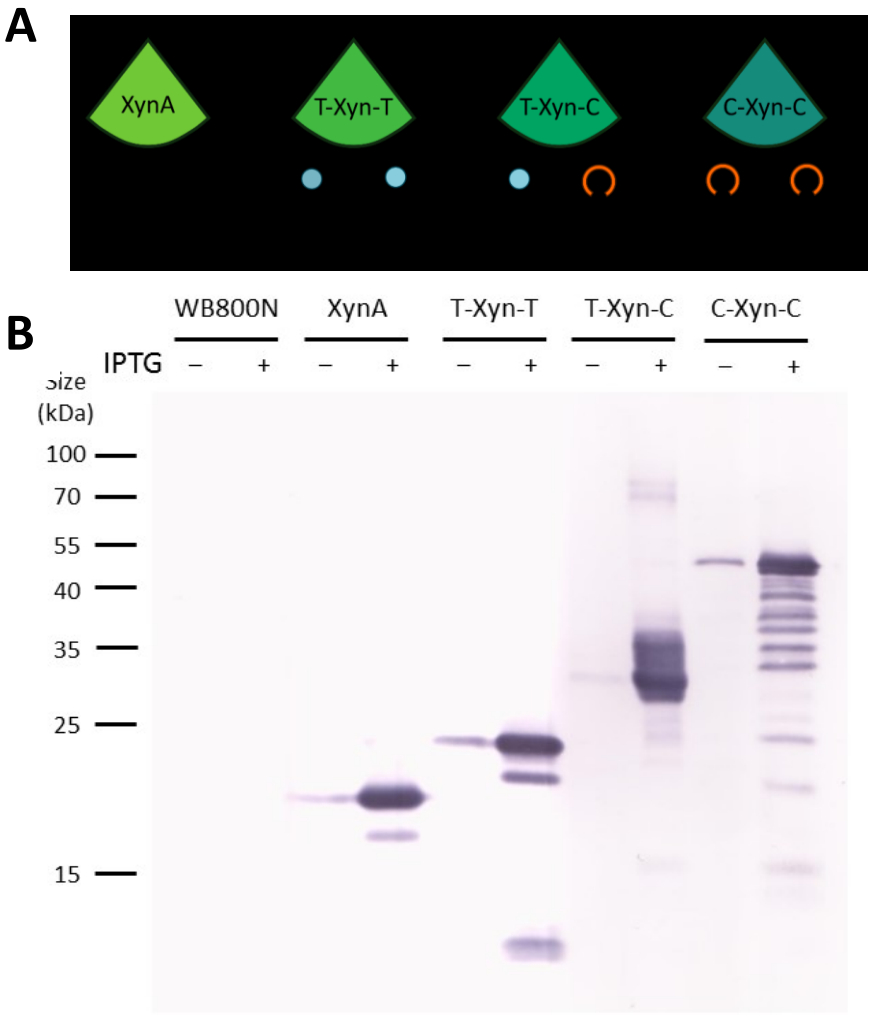

Figure 16 XynA fusion protein construct expression and secretion. A Constructs analysed below and their approximate molecular weights. **B** Western blot analysis of secreted XynA fusion proteins. Four fusion proteins based on XynA were designed: XynA, SpyTag-XynA-SpyTag (T-Xyn-T), SpyTag-XynA-SpyCatcher (T-Xyn-C) and SpyCatcher-XynA-SpyCatcher (C-Xyn-C). Each possessed the native XynA signal peptide at the N-terminus as well as a C-terminal His_6 tag. Each recombinant protein was expressed from the IPTG-inducible *B. subtilis-E. coli* shuttle vector pHT01. After 6 h growth culture supernatants were collected and analysed by SDS-PAGE for protein expression. Supernatants from uninduced (-) and IPTG-induced (+) cultures were 10x concentrated by TCA precipitation prior to Western blotting using an anti-His_6 primary antibody. The background strain *B. subtilis* WB800N possessing no plasmid is included as a negative control. All constructs are well-expressed and secreted. There is also clearly some leaky expression from the P_{grac} promoter even in the absence of IPTG induction. In addition all constructs are subject to varying degrees of proteolysis – resulting in lower molecular weight species.

To determine whether fusion of SpyParts to XynA affected its secretion, we analysed cellular and secreted protein samples by Western blot (Figure 17). For the T-Xyn-T and C-Xyn-C proteins, fusion of SpyParts had little influence on both the level of protein retained within the cell and the secreted protein yield compared to the native XynA protein. By contrast, significantly increased levels of T-Xyn-C fusion protein are detected within the cellular fraction

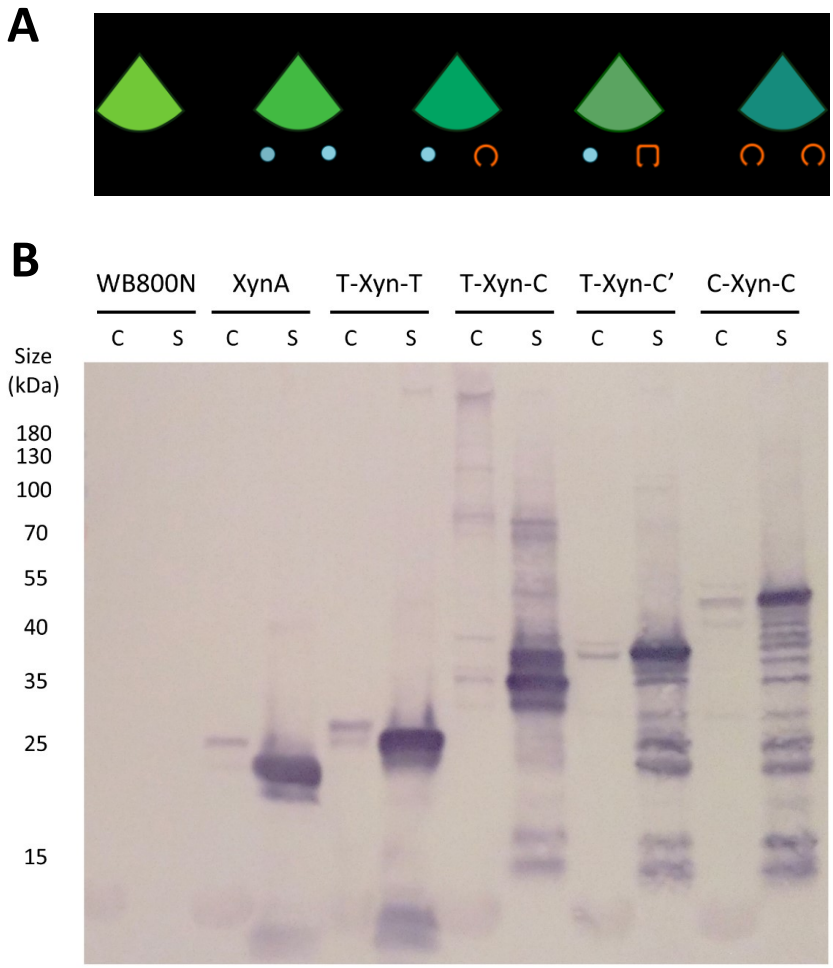

Figure 17 Cellular and secreted fractions of XynA fusion proteins. A Schematic of XynA fusion proteins analysed and their approximate molecular weights. **B** Anti-His_6 western blot analysis of cellular (C) and secreted (S) fractions of XynA fusion protein-expressing strains: WB800N WT strain, XynA, SpyTag-XynA-SpyTag (T-Xyn-T), SpyTag-XynA-SpyCatcher (T-Xyn-C), the mutated SpyTag-XynA-SpyCatcher^{EQ} (T-Xyn-C') and SpyCatcher-XynA-SpyCatcher (C-Xyn-C). Induction was performed for 8 h, after which cellular and secreted fractions were prepared as described in Methods section. Here 5 µL of cellular and 10 µL of secreted samples were loaded on an SDS-PAGE gel. In all samples a clear band is seen in the secreted fraction and varying degrees of proteolytic degradation are apparent. In addition, faint bands are visible within all cellular fractions. The slight difference in apparent molecular weight between cellular and secreted fractions corresponds to the removal of the approximately 1 kDa XynA signal peptide. Notably the T-Xyn-C cellular fraction also contains higher molecular weight species corresponding well to the expected sizes for T-Xyn-C dimers (~70 kDa), trimers (~125 kDa) and larger species (>180 kDa). Since these species are not detected in the cellular fraction of T-Xyn-C' expressing strain, they are likely to correspond to polymers of T-Xyn-C trapped within the cell. The T-Xyn-C and T-Xyn-C' proteins exhibit slightly different mobilities not accounted for by the single amino acid mutation – for more details see Results and Discussion section "Engineering XynA thermo-tolerance by SpyRing cyclisation".

in the form of higher molecular weight species. The electrophoretic mobility of these species correspond to polymers of T-Xyn-C and their presence is not detected with a mutated version of T-Xyn-C in which the SpyTag-SpyCatcher conjugation reaction is prevented, suggesting a small fraction of the expressed T-Xyn-C protein polymerises within the cell impeding secretion. However, the majority of expressed T-Xyn-C protein is secreted, with yields comparable to XynA, T-Xyn-T and C-Xyn-C (Figure 14C and 14D).

To verify the activity of the secreted SpyTag and SpyCatcher motifs, we first purified the His_6-tagged T-Xyn-T and C-Xyn-C proteins from *B. subtilis* culture supernatant using immobilised metal ion affinity chromatography (IMAC) (Figure 18). Purified proteins were mixed (Figure 19) and analysed by Western blot (Figure 19B). Immediately upon mixing, covalently-conjugated polymeric species were formed, indicating that SpyTag and SpyCatcher were functional. After longer periods of incubation, the majority of monomers were converted to a polymeric form.

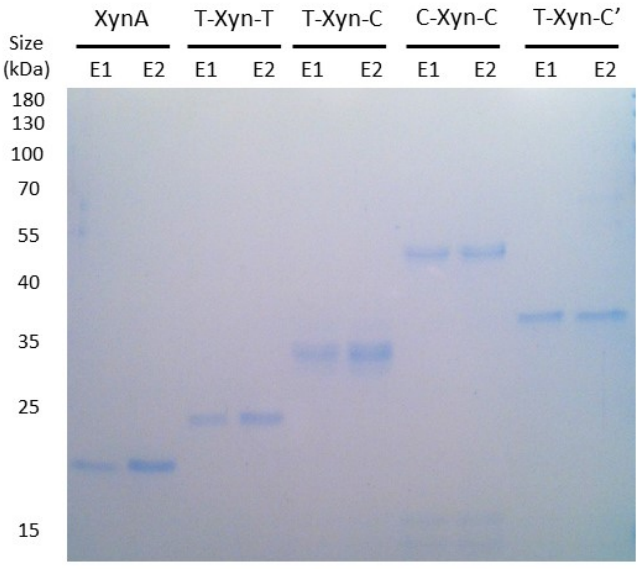

Figure 18 SDS-PAGE analysis of purified XynA fusion proteins. Various XynA fusion proteins were purified from the culture supernatant by IMAC purification: the full-length xylanase XynA, SpyTag-XynA-SpyTag (T-Xyn-T), SpyTag-XynA-SpyCatcher (T-Xyn-C), SpyCatcher-XynA-SpyCatcher (C-Xyn-C) and SpyTag-XynA-SpyCatcher^{E77Q} (T-Xyn-C'). Samples were bound to the Ni-NTA resin and after washing were eluted in two separate 250 µL fractions, E1 and E2. We added 4 µL of 5x SDS-PAGE sample buffer to 16 µL of E1 and E2 samples and then boiled for 10 min. 10 µL samples were loaded and separated by SDS-PAGE with subsequent Coomassie staining. Purification was successful for each protein, with little detectable contaminating species present. Since roughly equal yields were obtained in both the E1 and E2 fractions for each protein, the fractions were pooled for downstream investigations. Approximate molecular weights of each species were: XynA ~20 kDa, T-Xyn-T ~ 24 kDa, T-Xyn-C ~35 kDa, C-Xyn-C ~46 kDa and T-Xyn-C' ~35 kDa. The difference in mobility of T-Xyn-C and T-Xyn-C' proteins due to cyclisation is very apparent here.

To determine whether SpyTag and SpyCatcher were active under co-culture, strains expressing T-Xyn-T and C-Xyn-C were grown alone or together and supernatant samples analysed by Western blot (Figure 20B). A species with mobility corresponding to a dimer was detected after two hours of co-culture, indicating that SpyTag and SpyCatcher are indeed functional under co-culture conditions. Detection of polymeric species over longer periods of co-culture was visible, but hampered by inherent proteolysis from the two extracellular proteases native to *B. subtilis* WB800N and by smearing of bands at higher molecular weights.

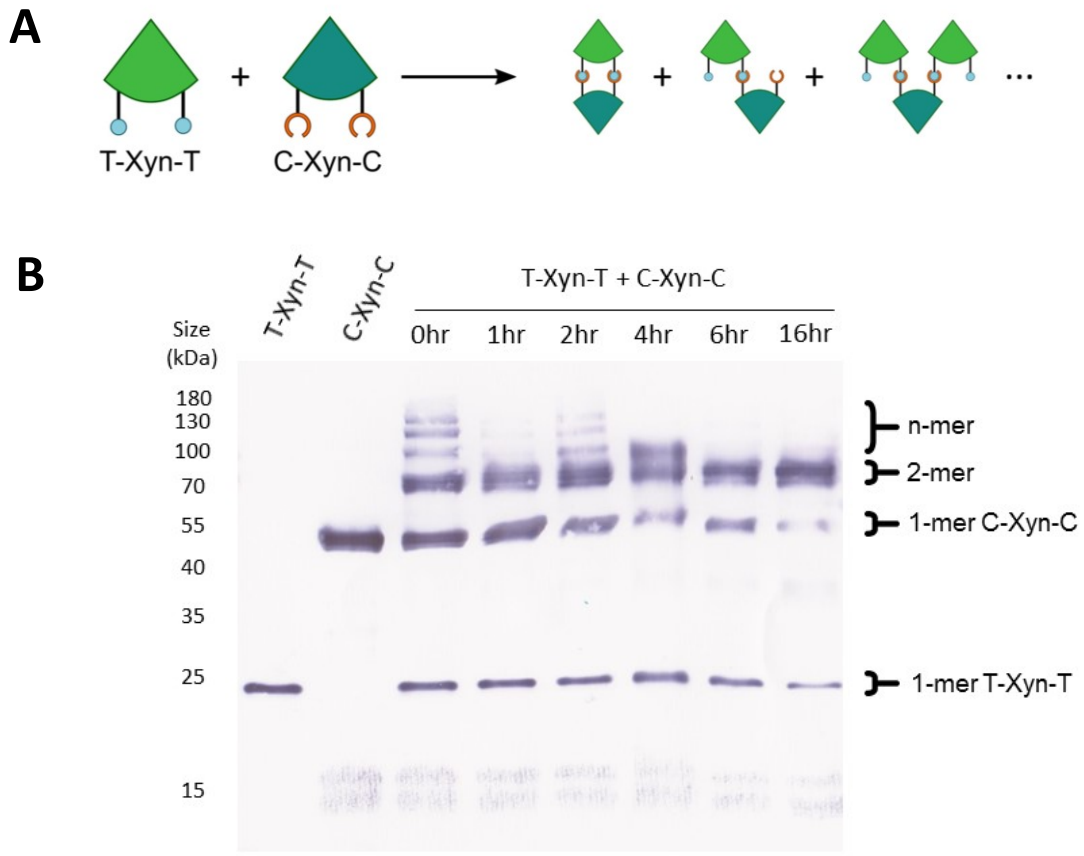

Figure 19 SpyTag-SpyCatcher-mediated conjugation of purified proteins. A Schematic showing the possible reaction products between T-Xyn-T and C-Xyn-C. **B** Purified T-Xyn-T and C-Xyn-C proteins were mixed 1:1 in a total volume of 20 µL and incubated at 25°C for indicated time periods, after which Western blotting was performed on all samples as well as unmixed samples of each protein. Clear evidence of polymerisation (high molecular weight species) is evident even when mixed samples were boiled immediately after mixing. Interestingly, over time, the presence of species larger than dimers appears to decrease, while dimers appear to constantly increase in abundance. The reasons for this are not clear. However, we speculate that, at the point of linkage between two proteins, there is a bifurcation between two pathways: circularisation and linear polymerisation. Since larger, polymerised species tend to be less efficiently transferred to the PVDF membrane during Western blotting, linear polymer species disappear over time as their size grows. Circularised dimers in contrast cannot grow larger over time and so appear to steadily increase in abundance. Regardless, it is clear that over time increasing amounts of monomer species become conjugated, with the reaction reaching near-completion (consumption of all of the C-Xyn-C monomer) after 16 h. Approximate molecular weights of each species were: T-Xyn-T ~ 24 kDa, C-Xyn-C ~46 kDa and T-Xyn-T + C-Xyn-C dimers ~70 kDa.

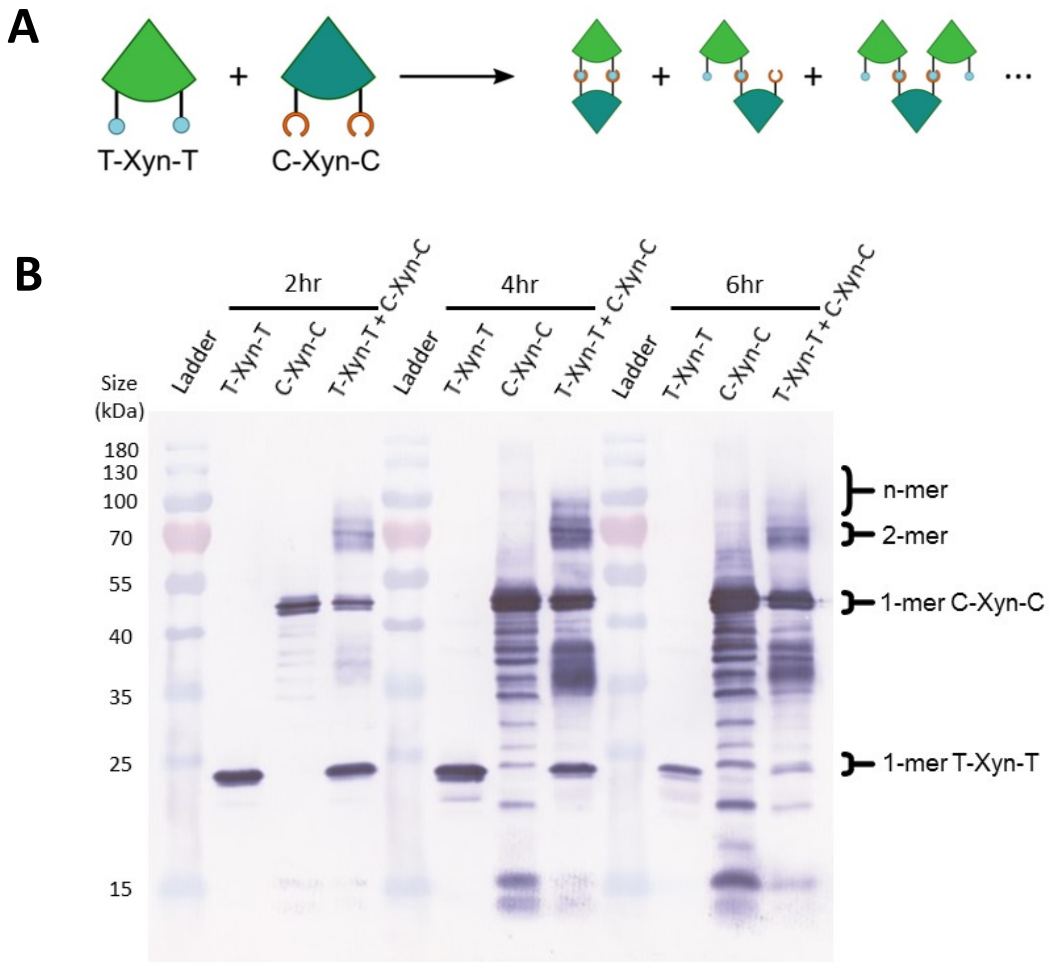

Figure 20 SpyTag-SpyCatcher-mediated conjugation of secreted proteins during co-culture. A Schematic showing the possible reaction products between T-Xyn-T and C-Xyn-C. **B** Strains expressing SpyTag-XynA-SpyTag (T-Xyn-T) and SpyCatcher-XynA-SpyCatcher (C-Xyn-C) were grown alone and in coculture. At various time points, supernatant samples were harvested, concentrated 10x by TCA precipitation and analysed by Western blotting using an anti-His_6 antibody. Figure 2C is a cropped version of this blot. Samples were run alongside the PageRuler Prestained Protein Ladder (Thermo) which produces light blue and red bands. After 2 h of coculture, clear evidence of dimeric species can be seen. However, longer incubations produce less clear results due to the high levels of proteolysis, particularly for the CXC construct. At 4 h dimeric and possibly trimeric species are apparent. After 6 h smearing and proteolysis prevents reliable data interpretation. However, the majority of the monomeric T-Xyn-T protein appears to have been consumed after 6 h, indicating that the SpyTag-SpyCatcher conjugation is near-complete. Approximate molecular weights of each species were: T-Xyn-T ~ 24 kDa, C-Xyn-C ~46 kDa and T-Xyn-T + C-Xyn-C dimers ~70 kDa.

3.2.2 Engineering XynA thermo-tolerance by SpyRing cyclisation

To demonstrate the utility of this technique for protein engineering, we tested the ability of the SpyTag-SpyCatcher reaction to improve the thermo-tolerance of XynA through SpyRing cyclisation following secretion. Protein cyclisation by linkage of the N- and C-termini has been shown to increase the ability of enzymes to tolerate exposure to high temperatures – a highly-desirable trait for many industrial enzymes – and can be achieved through a number of methods[227–230]. The SpyRing system works through fusion of the SpyTag and SpyCatcher, respectively, at the N- and C-termini of a protein, leading to covalent cyclisation that dramatically improves the ability of globular proteins to refold to native structures following exposure to high temperatures[231]. While protein cyclisation methods, such as the SpyRing system, have been previously shown to improve the thermo-tolerance of enzyme expressed intracellularly from *E. coli* – including a study focussing on *B. subtilis* XynA[230] – secretion of thermo-tolerant enzymes might significantly increase the cost-effectiveness of industrial scale production.

In addition to strains secreting the full length XynA and T-Xyn-C proteins, we engineered a strain to secrete a protein bearing the mutated SpyCatcher^{E77Q} (C′) unable to form the covalent isopeptide linkage with the SpyTag[24], T-Xyn-C′ (Figure 21A-C). Due to the close proximity of the N- and C-termini of XynA (within 1 nm, Figure 15) we anticipated that the SpyTag and SpyCatcher of the T-Xyn-C protein would be capable of reacting intramolecularly to cyclise XynA. While competing polymerisation reactions are also possible (Figure 21C), we expected cyclisation to be the major product, as seen with other SpyRing cyclisations[173], particularly since the concentration of the T-Xyn-C protein is relatively low in the culture medium.

To confirm cyclisation, which is known to perturb the mobility of proteins during gel electrophoresis[173], we compared the electrophoretic mobility of T-Xyn-C to that of the mutant T-Xyn-C′. Consistent with SpyRing cyclisation, the T-Xyn-C and T-Xyn-C′ proteins exhibited substantially different mobilities under gel electrophoresis (Figure 21D). To next determine whether SpyRing cyclisation confers thermo-tolerance to XynA by preventing irreversible aggregation (Figure 21E), we subjected supernatant samples from cultures secreting the native

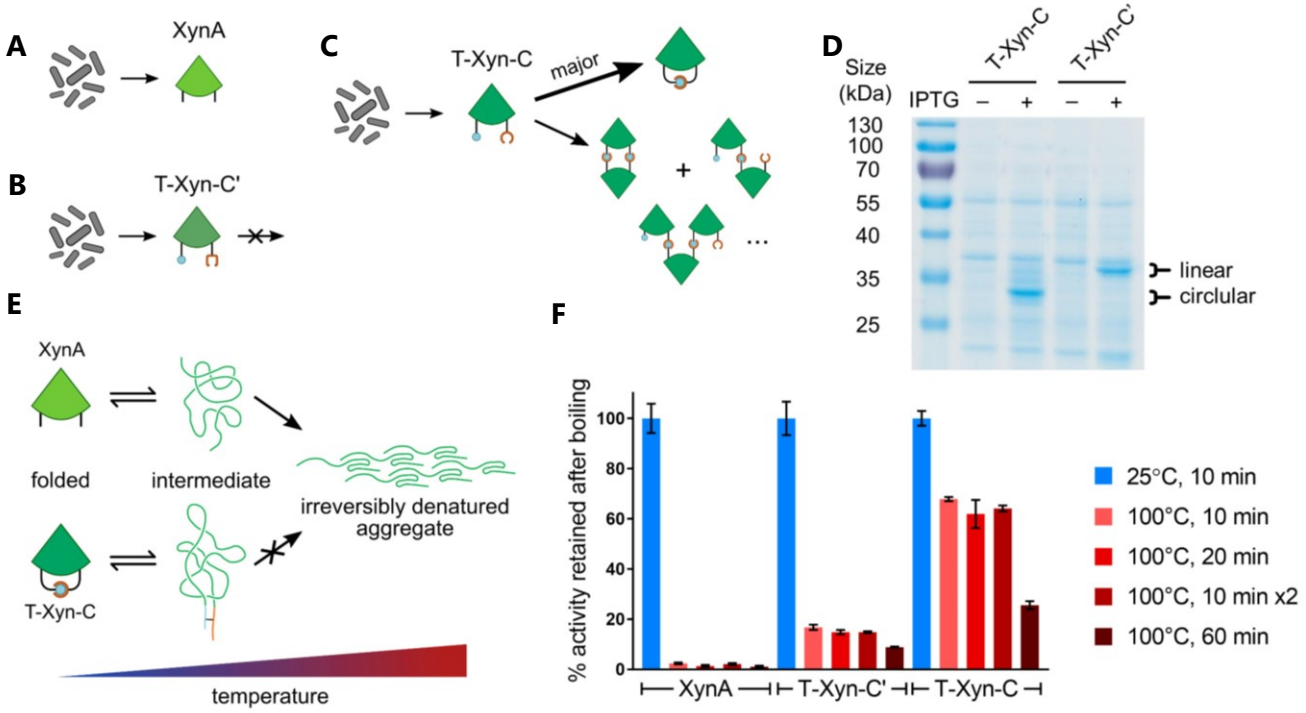

Figure 21 SpyRing cyclisation confers XynA thermo-tolerance. Strains expressing XynA **A**, the mutant SpyTag-XynA-SpyCatcherE77Q (T-Xyn-C′) **B** and SpyTag-XynA-SpyCatcher (T-Xyn-C) **C** were created. The T-Xyn-C protein is able to cyclise through SpyRing cyclisation. **D** Comparison of the electrophoretic mobility of T-Xyn-C and T-Xyn-C′ proteins by SDS-PAGE with Coomassie staining (expected molecular mass ~ 35 kDa). A clear difference in electrophoretic mobility of the two proteins is seen, consistent with covalent cyclisation of T-Xyn-C. **E** SpyRing cyclisation works by covalently conjugating the N and C-termini of a globular protein. Upon boiling, the folded protein begins to unfold. The SpyRing system is believed to prevent the irreversible transition of partially unfolded intermediates to denatured aggregates and therefore enable refolding when the temperature is lowered. **F** Culture supernatants from strains expressing XynA, T-Xyn-C′ and T-Xyn-C were subjected to a variety of high-temperature programs and subsequently assayed for xylanase activity. The T-Xyn-C protein shows dramatically increased tolerance to a variety of high temperature programs compared to XynA and T-Xyn-C′. Samples were analysed in triplicate, data represent the mean ± 1 SD.

XynA, T-Xyn-C′ and T-Xyn-C proteins to a variety of high-temperature conditions. After cooling to 4°C these samples were then assayed for xylanase activity (Figure 21F). All supernatants exhibited similar levels of xylanase activity following incubation at 25°C (Figure 22). However, following exposure to high-temperature conditions, only supernatants containing T-Xyn-C retained substantial levels of xylanase activity (Figure 21F). After exposure to 100°C for 10 min, T-Xyn-C retained 67.9% ±0.9 of its xylanase activity in contrast to negligible activity (2.4% ±0.3) for XynA, and a similar protective effect was also seen across a variety of other high-temperature programs. Consistent with previous studies[173], a mild protective effect was also observed for the mutant control T-Xyn-C′. This is likely due to the relatively strong, non-covalent interactions between SpyTag and SpyCatcher mutants[24].

Owing to its ease of implementation and the availability of guidelines for its design[231], the SpyRing system is an attractive tool for improving the stability of enzymes. The SpyRing

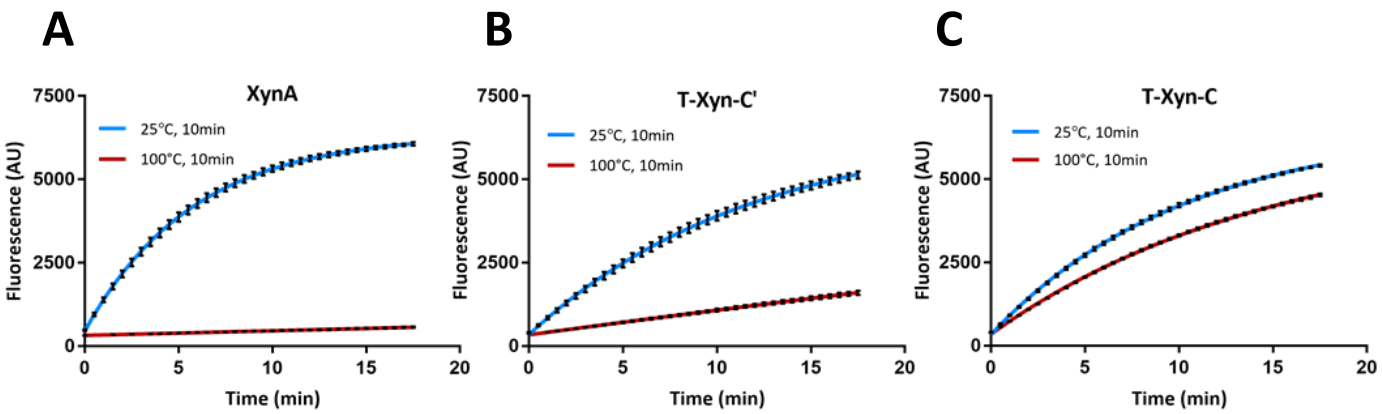

Figure 22 Representative xylanase assay traces following high-temperature exposure. Here culture supernatants from strains expressing **A** XynA, **B** T-Xyn-C' and **C** T-Xyn-C were subjected to 25°C or 100°C for 10 minutes, cooled to 4°C then equilibrated to room temperature and finally assayed for xylanase activity. Product formation rates were calculated over the linear region of the curves to produce the data in Figure 21F. Samples were analysed in triplicate, data represent the mean ± 1 SD.

cyclisation system has previously been harnessed to improve the thermo-tolerance of a number of intracellularly expressed enzymes with industrial relevance[174,175]. However, since extracellular production of proteins for biotechnology could vastly improve cost-effectiveness, our strategy offers a novel, attractive approach to the production and stabilisation of industrially-relevant enzymes. Notably, xylanases with improved thermal stability are of great interest to industry, offering an eco-friendly alternative to the chemicals used in the paper pulp bleaching process[232] and as an additive to improve animal feed digestibility[233]. Further, *B. subtilis* naturally secretes a number of other enzymes with industrial uses, including amylases, proteases and lipases. Therefore, a similar approach might be applicable to these enzymes, enabling the secretion of additional thermo-tolerant industrial enzymes.

3.2.3 A modular method for extracellular protein-protein conjugation from cellular consortia

Having demonstrated secretion and conjugation of XynA fusion proteins, we next looked to exploit our approach to conjugate alternative proteins of biotechnological interest from engineered cellular consortia. To facilitate assembly of plasmid constructs, we first designed a Golden Gate assembly genetic toolkit (Figure 23). This strategy allowed simple, one-step assembly of ORFs encoding an N-terminal signal peptide for secretion, an upstream SpyPart, a user-defined protein of interest and a C-terminal His_6-tagged SpyPart. Parts were initially

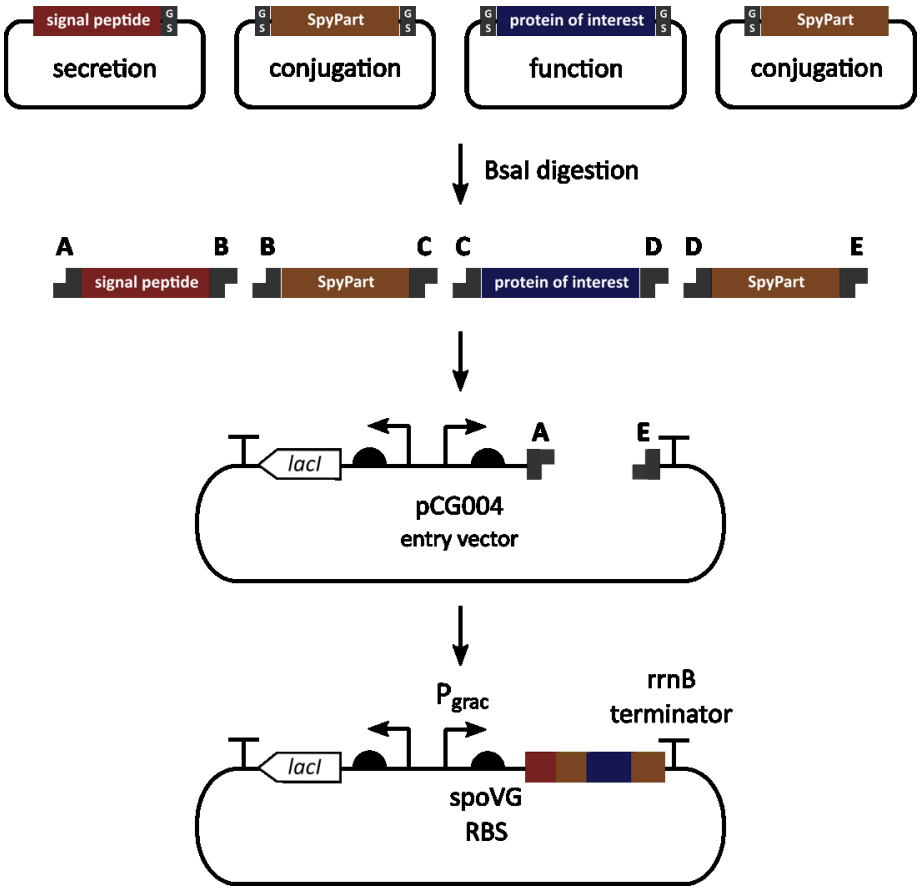

Figure 23 Golden Gate assembly method design and composition. Protein modules were pre-cloned into the part plasmids, sequence-verified and stocked. Four separate positions within the final ORF were defined based on the sequence of upstream and downstream 4 bp overhangs generated by BsaI digestion. Signal peptide parts were cloned with an upstream 'A' and downstream 'B' overhang, upstream SpyParts were cloned with an upstream 'B' and downstream 'C' overhang, protein of interest parts were cloned with an upstream 'C' and downstream 'D' overhang and downstream SpyParts were cloned with an upstream 'D' and downstream 'E' overhang. Internal overhangs were designed to incorporate two amino acid glycine-serine linkers between ORF parts. Assembly of ORF parts into an entry vector based on pHT01 (pCG004) enabled one-step construction of protein expression constructs. pCG004 possesses a 'dropout' part downstream of the P_{grac} promoter and spoVG ribosome binding site (RBS) and upstream of the rrnB terminator. The dropout part consists of a constitutive GFP expression cassette flanked by BsaI restriction sites producing an upstream 'A' overhang and downstream 'E' overhang. Successful Golden Gate assemblies will therefore result in removal of the GFP expression cassette enabling visual (green-white) screening of transformants.

cloned into entry vectors from which they can be verified, stocked and re-used for future assemblies (Figure 24). Stocked parts were then assembled directly into the pHT01 IPTG-inducible expression vector ready for use in *B. subtilis*.

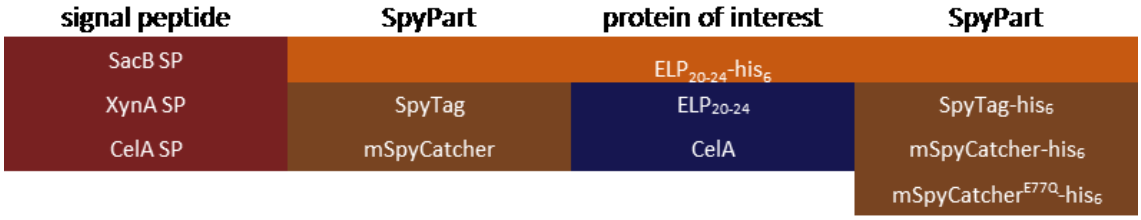

Figure 24 Genetic parts cloned and verified during the course of this study. Additional parts not used in this study have also been created. Where required, 4 bp overhangs can be modified to allow assembly of 2 or 1 ORF parts into the entry vector (e.g. the ELP_{20-24}-His_6 part was cloned with an upstream 'B' overhang and downstream 'E' overhang). Sequences of selected parts and the entry vector pCG004 are included in Table 6 and deposited on Addgene.

Using this system, we created a series of plasmid constructs for secretion of recombinant proteins based on a second native, secreted *B. subtilis* enzyme, the endo-cellulase, CelA (Figure 25). Like xylanases, cellulases have attracted interest in variety of industrial contexts, notably for their ability to degrade plant biomass, a sustainable potential feedstock for bio-commodity production[234,235]. In fact, creating multi-enzyme complexes of synergistic plant biomass-

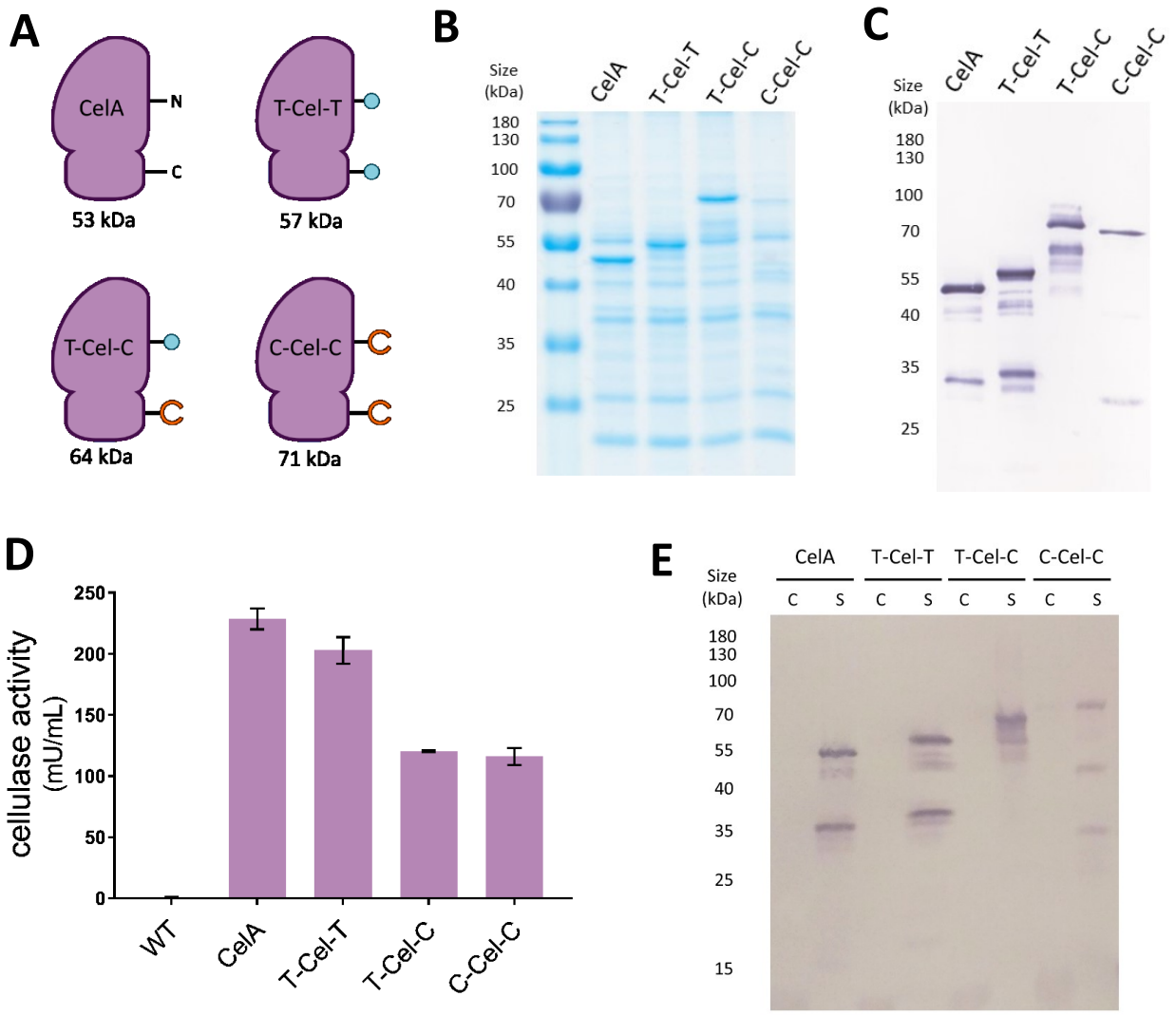

Figure 25 Design, secretion and activity of SpyPart-CelA fusion proteins. A Four recombinant proteins based on CelA were designed: the full-length cellulase CelA, SpyTag-CelA-SpyTag (T-Cel-T), SpyTag-CelA-SpyCatcher (T-Cel-C) and SpyCatcher-CelA-SpyCatcher (C-Cel-C). Each possessed the native CelA signal peptide at the N-terminus as well as a C-terminal his_6 tag. Each recombinant protein was expressed from the IPTG-inducible *B. subtilis-E. coli* shuttle vector pHT01 and culture supernatant analysed by SDS-PAGE for protein expression. Supernatants from IPTG-induced cultures grown for 6 h were 10x concentrated by TCA precipitation prior to **B** SDS-PAGE with Coomassie staining and **C** western blot analysis using an anti-his_6 primary antibody. All constructs were well-expressed at roughly equal yields, although some proteolytic degradation is evident. Interestingly, the majority of the T-Cel-C protein appears to have lower than expected mobility. This is consistent with cyclisation through reaction of the SpyTag and SpyCatcher. **D** Culture supernatants were analysed for cellulase activity using a fluorogenic substrate. Cellulase activity was calculated using a standard curve, as described in the Methods section, from triplicate samples, data represent the mean ± 1 SD. **E** Anti-His_6 western blot analysis of cellular (C) and secreted (S) fractions of each of the CelA fusion proteins. Induction was performed for 8 h, after which cellular and secreted fractions were prepared as described in Methods section. Here 5 µL of cellular and 10 µL of secreted samples were loaded on an SDS-PAGE gel.

degrading enzymes such as CelA and XynA, has previously been shown to enhance the degradation of complex cellulosic substrates[236]. As with XynA, we found that SpyParts could be fused to the N- and C-termini of CelA without disrupting secretion, directed by the native CelA secretion signal peptide (Figure 25B and 25C) or enzyme activity (Figure 25D). Additionally, fusion of SpyParts to CelA had no effect on the levels of protein retained within the cell (Figure 25E). Interestingly, in contrast to T-Xyn-C, the T-Cel-C protein did not appear to be retained within the cell due to self-polymerisation. Further, these SpyParts were active and directed covalent linkage of XynA and CelA fusion proteins under co-culture to form protein-protein conjugates (Figure 26).

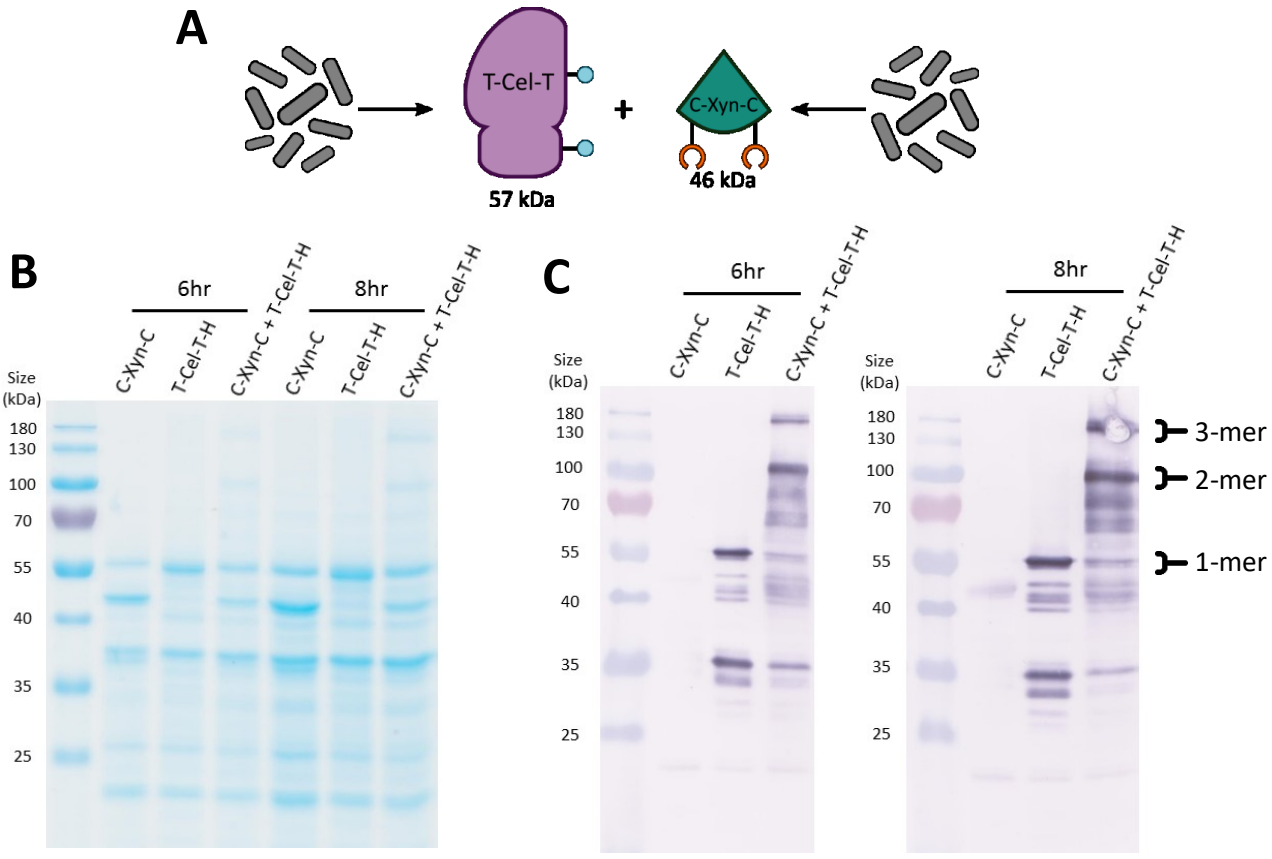

Figure 26 Two-strain co-cultures of T-Cel-T and C-Xyn-C produce protein-protein conjugates. A Schematic showing the two-strain coculture setup and design of SpyTag-CelA-SpyTag-his$_6$ (T-Cel-T) and SpyCatcher-XynA-SpyCatcher (C-Xyn-C). Mono-cultures and a two-strain co-culture of strains expressing each protein were prepared. Supernatant samples were collected after incubation for 6 h and 8 h and concentrated 10x by TCA precipitation. Concentrated samples were analysed by **B** SDS-PAGE with Coomassie staining and **C** western blotting with an anti-His$_6$ primary antibody. Notably, since only the T-Cel-T construct possesses a His$_6$ tag, the C-Xyn-C protein is not detectable by western blotting. While SDS-PAGE analysis produces relatively faint bands, clear evidence of conjugation of T-Cel-T and C-Xyn-C is visible by western blotting. Species with apparent molecular weights corresponding to dimers and trimers are discernible (expected molecular weights: T-Cel-T + C-Xyn-C ~103 kDa, T-Cel-T + 2(C-Xyn-C) ~149 kDa and 2(T-Cel-T) + C-Xyn-C ~160kDa).

The ability to co-localise cooperative enzymes – ones that act in concert on a single substrate or in a pathway – has been shown to improve metabolic fluxes and is consequently a useful approach in metabolic engineering[180,207]. Indeed, this is an strategy employed in nature; certain bacteria able to metabolise plant biomass produce large, extracellular multi-protein complexes known as cellulosomes, consisting of numerous synergistically-acting enzymes[171]. Notably, in efforts to engineer recombinant microbes capable of growth on plant biomass, two- and three-protein 'designer-cellulosomes' have previously been assembled *in vitro* and *in vivo* by co-culturing protein-secreting bacterial strains through the cohesin-dockerin interaction[237,238], a non-covalent protein-protein interaction[239]. However, in contrast to the cohesin-dockerin system, the covalent nature of SpyTag-SpyCatcher-based protein conjugation offers significant advantages, improving stability, removing the requirement for native protein folding and facilitating application in wider range of scenarios – for instance, the enzyme thermo-tolerance engineering demonstrated in this study.

To begin to the feasibility of our approach to create *de novo* biological ELMs, we wished to test whether a heterologous structural protein could be secreted and conjugated from *B. subtilis*. Therefore, we created a plasmid construct for expression and secretion of an elastin-like polypeptide (ELP) fused to SpyParts. The ELP used here, $ELP_{20\text{-}24}$, is a short ~10 kDa polypeptide derived from human tropoelastin, consisting of one hydrophilic domain flanked by two hydrophobic domains[202]. Owing to its short size, $ELP_{20\text{-}24}$, does not undergo coacervation – an ELP-specific form of phase separation – under conditions used here.

Three fusion proteins based on $ELP_{20\text{-}24}$ were generated, each with an N-terminal signal peptide from the *B. subtilis* SacB protein (which provided the good secretion yields during initial testing) and a C-terminal His_6 tag. The first construct, ELP, consisted of $ELP_{20\text{-}24}$ alone, lacking any SpyParts, the second construct, T-ELP-T, consisted of the ELP protein fused to upstream and downstream SpyTags and lastly a mutated version of T-ELP-T was generated in which the isopeptide bond-forming aspartate residue of each SpyTag was mutated to alanine (T'-ELP-T'), preventing covalent conjugation with SpyCatcher[24] (Figure 27). Each of these proteins was well-expressed and secreted, although significant amounts of all three proteins were retained in the cellular fraction (Figure 27B). In addition, plasmids expressing the C-Xyn-C and C-Cel-C proteins were modified to remove their C-terminal His_6 tags.

Strains expressing T-ELP-T and the mutant T′-ELP-T′ were then co-cultured with strains expressing the C-Xyn-C and C-Cel-C proteins. Supernatant samples from monocultures of each of the strains and from three-strain co-cultures were analysed by Western blot with an anti-His_6 antibody (Figure 27C). The T-ELP-T and the mutant T′-ELP-T′ proteins were well-expressed and secreted. When cultured together with the C-Xyn-C and C-Cel-C proteins, the mobility of the mutant T′-ELP-T′ was unaffected, whereas almost all of the secreted T-ELP-T

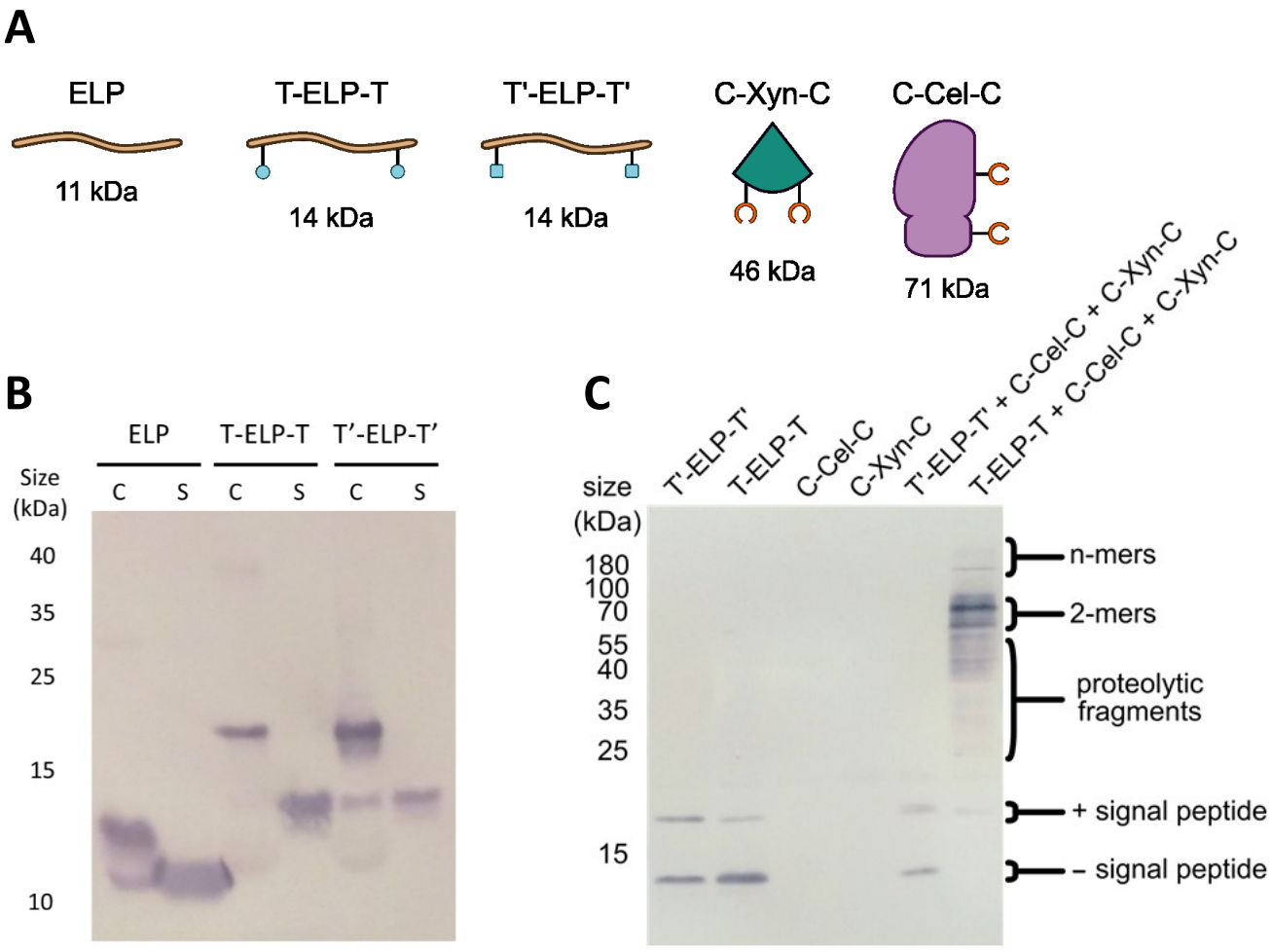

Figure 27 Protein-protein conjugate formation from a three-strain co-culture. A The four recombinant proteins used here: $ELP_{20\text{-}24}$, SpyTag-$ELP_{20\text{-}24}$-SpyTag-his_6 (T-ELP-T) and $SpyTag^{DA}$-$ELP_{20\text{-}24}$-$SpyTag^{DA}$-his_6 (T′-ELP-T′), SpyCatcher-XynA-SpyCatcher lacking a C-terminal His_6 tag (C-Xyn-C), SpyCatcher-CelA-SpyCatcher lacking a C-terminal His_6 tag (C-Cel-C). Approximate molecular weights of each species are also given (calculated assuming removal of N-terminal signal peptides). **B** Anti-His_6 western blot analysis of cellular (C) and secreted (S) fractions of ELP fusion protein-expressing strains. Induction was performed for 8 h, after which cellular and secreted fractions were prepared as described in Methods section. Here 5 µL of cellular and 10 µL of secreted samples were loaded on and SDS-PAGE gel. In all samples clear bands are seen in both the cellular and secreted fractions. The difference in apparent molecular weight between cellular and secreted fractions corresponds to the removal of the ~3 kDa SacB signal peptide. **C** Culture supernatants from strains expressing Xyn, Cel and ELP recombinant proteins alone or under co-culture were analysed by western blotting with an anti-His_6 antibody. Since only the $ELP_{20\text{-}24}$-containing constructs possess C-terminal His_6 tags, only these species are detected. Under three-strain co-cultures, almost the entirety of T-ELP-T is incorporated into protein-protein conjugates with C-Cel-C and C-Xyn-C, an interaction dependent on the SpyTag-SpyCatcher reaction.

protein was incorporated into dimeric and trimeric species (Figure 27C and 27D), verifying conjugation by the Spy system.

In both two-protein and three-protein co-culture conjugations demonstrated here, the major products formed are dimer species, along with a minority of oligomer species (Figure 26E and Figure 27D). For specific applications, it will be preferable to precisely control the multimeric state and topology of conjugates formed. Following design rules from *in vitro* studies, our modular toolkit could therefore be adapted for user-defined extracellular self-assembly of dimers[24], circular, tadpole and star oligomers[215], catenanes[216] and polymers[181,217].

3.2.4 Tuning conjugation through consortia composition

A key advantage of engineering cellular consortia to carry out a biological process, is that the balance between different sub-processes can be tuned simply by tuning the relative productivity of different strains within the co-culture. To demonstrate this, we set out to tune the relative amounts of C-Xyn-C and C-Cel-C conjugated to T-ELP-T, simply by tuning the relative inoculation ratios of the producer strains in three-strain co-cultures. To quantify the relative amounts of C-Xyn-C and C-Cel-C conjugated to T-ELP-T, we performed co-purifications using the C-terminal His_6 tag fused to ELP proteins. As outlined in Figure 28B, following three-strain co-culture growth, His_6-tagged ELP proteins were isolated from the culture supernatant by IMAC purification, and any SpyTag-SpyCatcher conjugated proteins were co-purified along with them while unbound proteins were washed off. The relative levels of C-Xyn-C and C-Cel-C conjugated to T-ELP-T were then quantified via enzyme activity assays.

We performed several three-strain co-cultures in which the inoculum volume of the T-ELP-T expressing strain was fixed and the inoculation proportions of C-Xyn-C and C-Cel-C expressing strains varied. Enzyme activity was detected in all purified fractions, demonstrating the formation of functional protein conjugates (Figure 28C). We found that the proportions of CelA and XynA proteins incorporated into the extracellular protein-protein conjugates could be finely tuned simply by adjusting the proportions of the strains in the initial inoculations (Figure 28C). Furthermore, the relative enzyme activities of these complexes closely matched the relative inoculation proportions over a range of conditions. Additional co-purifications with two negative control strains, a strain expressing the mutant T'-ELP-T' only capable of non-covalent binding and a strain expressing secreted ELP lacking SpyTags, verified that the conjugation between all three proteins in the culture medium was specifically SpyTag-SpyCatcher-mediated as both controls showed dramatically reduced cellulase (Figure 28D) and xylanase (Figure 28E) levels. We thus verified our ability to tune the relative proportions of XynA and CelA incorporated into protein-protein conjugates simply by tuning their relative inoculation ratios.

This system thus offers a simple way to both assemble functional protein-protein conjugates and to fine-tune their properties. This approach could be useful in any scenario in which the proportions of individual components of protein-protein conjugates influences the desired functions. For instance, when co-localising co-operative enzymes to improve flux through a

metabolic pathway – as with the previously-mentioned 'designer cellulosomes' – tuning enzyme proportions may enable improved yields by increasing the levels of enzymes catalysing rate-limiting steps or decreasing the levels of enzymes producing toxic pathway intermediates.

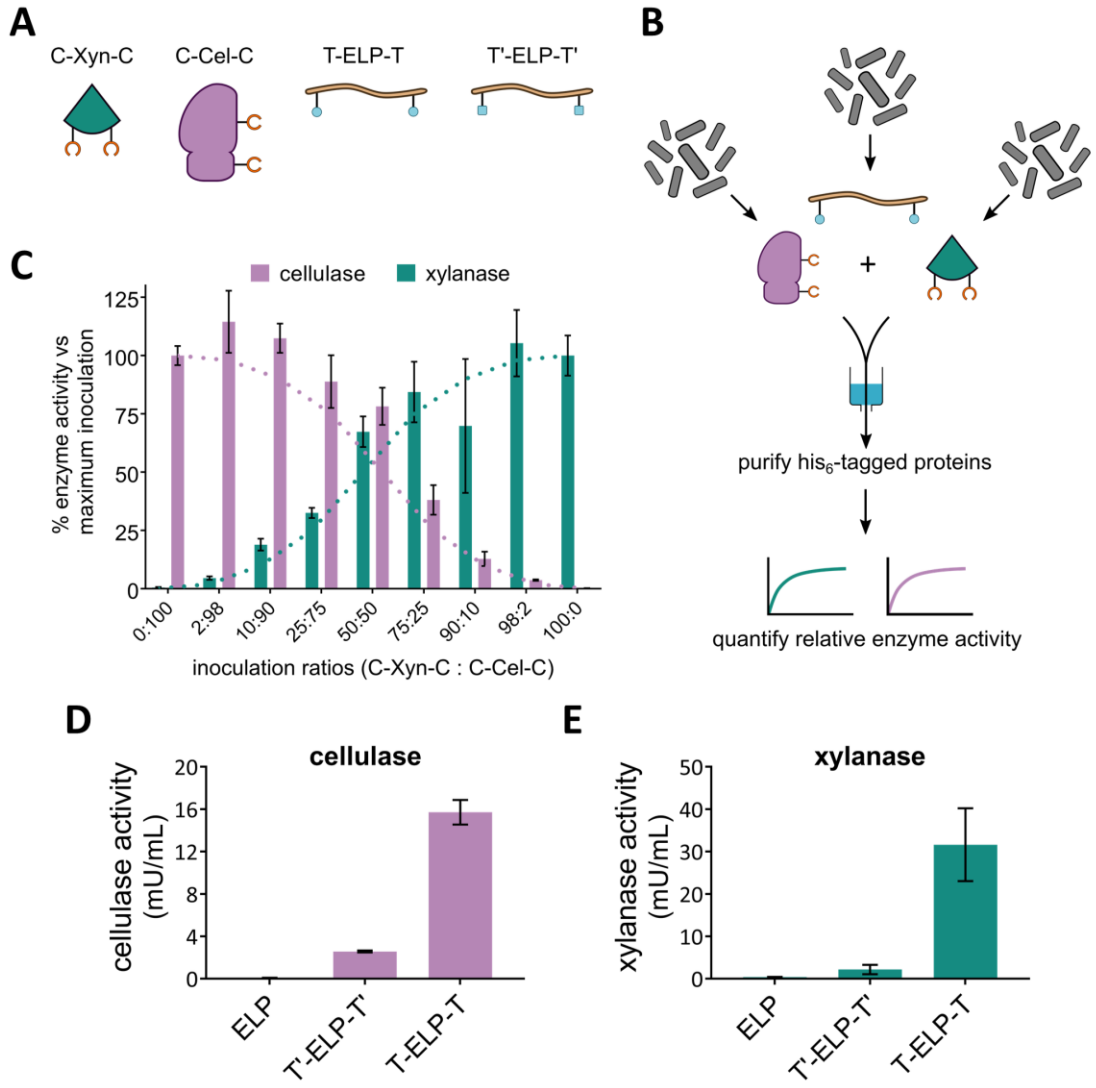

Figure 28 Tuning the composition of protein-protein conjugates. A The four recombinant proteins used here: SpyCatcher-XynA-SpyCatcher lacking a C-terminal His6 tag (C-Xyn-C), SpyCatcher-CelA-SpyCatcher lacking a C-terminal His6 tag (C-Cel-C), SpyTag-ELP20-24-SpyTag-His6 (T-ELP-T) and SpyTagDA-ELP20-24-SpyTagDA-His6 (T'-ELP-T'). Molecular weights of each species are also given (calculated assuming removal of N-terminal signal peptides). **B** Schematic illustrating the co-purification experiment. **C** By modulating the proportion of cells expressing the C-Xyn-C (teal dotted line) inoculated compared to the proportion of cells expressing the C-Cel-C (lilac dotted line) inoculated, the relative levels of xylanase and cellulase activities (represented by the teal and lilac bars, respectively) co-purified with T-ELP-T could be tuned across a variety of different inoculation ratios (samples prepared in triplicate, data represent the mean ± 1 SD). The y-axis plots percentage of enzyme activity calculated relative to the 'maximum activity' – i.e. that detected from co-cultures inoculated with 100% of the strain expressing the C-Xyn-C or C-Cel-C protein. Co-purification of cellulase **D** and xylanase **E** activity was repeatable and dependent on the SpyTag-SpyCatcher reaction, as co-purification sharply decreased when performed with an ELP construct lacking SpyTags (ELP) or with mutated SpyTags (T'-ELP-T'). Samples prepared in triplicate, data represent the mean ± 1 SD.

3.3 Conclusion

Here we have demonstrated the feasibility of combining protein secretion with SpyTag-SpyCatcher-mediated protein conjugation. To illustrate the immediate applicability of this approach, we first coupled SpyRing cyclisation with protein secretion, enabling one-step extracellular production and stabilisation of the endo-xylanase, XynA. Additionally, we applied our method to engineer extracellular production of self-assembling protein-protein conjugates from cellular consortia. Finally, we showed that this approach allows the relative proportions of proteins incorporated into protein-protein conjugates to be fine-tuned simply by varying their relative inoculation ratios in co-cultures, rather than requiring any additional genetic engineering such as promoter swapping. We have therefore shown, for the first time, that the SpyTag-SpyCatcher system can be deployed extracellularly *in vivo* and in co-cultures. Importantly, as outlined in section **1.5.1**, this approach should accelerate future efforts to engineer *de novo* biological ELMs.

Beyond the work presented here, the productivity of different strains within co-cultures could be further controlled by coupling expression with additional genetic circuits, such as inducible switches and quorum sensing systems[130]. Indeed, these tools have been previously harnessed within cellular consortia to program temporal and spatial control over monomer patterning within amyloid fibrils[22]. In addition, transferring the strategy to alternative secretion hosts – such as the yeasts *Saccharomyces cerevisiae* and *Pichia pastoris* – would enable the secretion of a much broader range of heterologous proteins, relieving the need for compatibility with *B. subtilis*. As our approach is modular in design there is also great scope for integrating further components to broaden potential applications, such as alternative functional components or biological protein conjugation methods[170,185,239,240]. Lastly, while the work here focuses exclusively on bivalent proteins – those possessing two SpyParts – incorporating additional SpyParts into fusion proteins could facilitate the formation of extended, branching polymeric networks and hydrogels[181,217].

Programming protein conjugation and self-assembly within the extracellular environment offers great promise in the effort to generate novel industrial enzymes, multi-protein complexes and biological materials: improving production cost-effectiveness, reducing cellular burden and toxicity and enabling patterning and tunability through engineered cellular consortia. The modular approach described here therefore offers a platform for the

development of not only of biological ELMs, but also of novel biotechnological products to meet real-world challenges.

4 Growing functional biomaterials with engineered, kombucha-inspired co-cultures

SUMMARY

Natural biological materials exhibit remarkable properties: self-assembly from simple raw materials, autonomous morphogenesis, diverse physical and chemical properties and the ability to sense-and-respond to environmental stimuli. The field of engineered living materials (ELMs) aims to recreate these properties to generate new and useful materials. Owing to its impressive material properties, high natural yield and genetic tractability, bacterial cellulose (BC) is an ideal natural biological material for ELM development. However, there remains a paucity of genetic tools and circuits with which to engineer BC-producing bacteria. Inspired by the pseudo-natural microbial community of fermented kombucha tea, we set out to recreate kombucha-like co-cultures between an engineerable BC-producing bacterium *Komagataeibacter rhaeticus* and the model organism and synthetic biology host *Saccharomyces cerevisiae*. We first established and characterised a method for stable co-culture of *K. rhaeticus* and *S. cerevisiae*, in which the two species exhibited a symbiotic interaction. Using this system, we show that *S. cerevisiae* can be engineered to secrete an enzyme into BC, generating a grown, functionalised material. In addition, our system enables engineered biosensor *S. cerevisiae* strains to be incorporated into BC, creating grown, functional biosensor materials. This novel co-culture approach therefore enables growth of BC-based ELMs with programmable properties.

AIMS

- Recreate and characterise BC-producing, kombucha-like co-cultures of *Komagataeibacter rhaeticus* and *Saccharomyces cerevisiae*
- Engineer the *S. cerevisiae* component of co-cultures to secrete proteins to functionalise BC
- Engineer the *S. cerevisiae* component of co-cultures to sense-and-respond to environmental stimuli

4.1 Introduction

From the standpoint of materials science, natural biological materials exhibit some impressive traits. Firstly, they can be grown starting from small numbers of initial cells and using simple raw materials. Secondly, they have evolved to exhibit a huge range of remarkable material properties – from electrical conductivity to strong underwater adhesion to thermoplasticity. Thirdly, the organisms which produce these materials can control their morphology, directing the autonomous self-assembly of intricate structures over multiple length scales. Finally, the living cells that produce and are associated with these materials can sense changes in their environment and respond appropriately to modify the material properties in some way.

Straddling the border between material science and synthetic biology, the emerging field of engineered living materials (ELMs) aims to harness the desirable traits of natural biological materials to generate novel, useful materials[10–12]. Although current definitions of ELMs encompass biohybrid materials, consisting of both biological and synthetic components, a long-standing aim is to create fully-biological ELMs in which living cells are genetically-programmed to self-assemble materials with desired properties. Achieving this major challenge could lead to a new paradigm for material production, taking advantage of the remarkable properties of biological material assembly.

To this end, several recent reports have described approaches to create biological ELMs, focussing, in particular, on simple, genetically-tractable model microbial systems. As outlined in section **1.2**, *E. coli* biofilm nanomaterials have attracted great interest as model ELM systems. Curli fibres, amyloid polymers of the secreted CsgA protein, are a major component of the extracellular structural matrix of *E. coli* biofilms[16]. By engineering the CsgA monomer and controlling its expression, biofilm ELMs with electrical conductivity[31], autonomous patterning[22], metal adhesion[23] and environmental sense-and-response functions[36] have been grown. In addition, functionalised ELMs have been created by growing curli biofilms modified to display a short peptide tag enabling subsequent covalent capture of enzymes and fluorescent proteins. However, a limitation of this approach is the requirement for prior expression and external addition of functional protein components. Moreover, even under optimised conditions, the yields of *E. coli* biofilm ELMs remain restricted to tens of milligrams per litre of culture, limiting scalability[241].

As an alternative to *E. coli* biofilms, bacterial cellulose (BC) is emerging as an ideal, model ELM system. Various species of Gram-negative acetic acid bacteria – particularly members of the *Komagataeibacter* and *Gluconacetobacter* genera – are able to produce large quantities of extracellular cellulose. When grown in static liquid culture, these BC-producing bacteria secrete cellulose, in the form of numerous individual glucan chains bundled into ribbon-like fibrils. Over the course of several days, a thick floating mat of entangled BC fibrils forms, known as a pellicle, within which the BC-producing bacteria become embedded. As a material, BC exhibits impressive properties, including high crystallinity, high tensile strength, biodegradability and biocompatibility. Consequently, BC has garnered much interest as a feedstock material for industrial applications, including wound dressings, acoustic diaphragms for headphones and speakers, stabilisers for foams and emulsions, and scaffolds for tissue engineering and battery separators. Since it is also relatively pure and produced in high yields – reaching in excess of 10 grams per litre – BC is an ideal blank slate material for ELM development.

Despite the lack of established genetic tools for BC-producing bacteria, recent years have seen growing efforts to genetically engineer BC-producing bacteria to modify BC material properties. Initial studies focussed on increasing BC yields[80,81]. More recently, BC-producing bacteria have been engineered to produce additional non-native polysaccharides, creating chitin-cellulose[83] and curdlan-cellulose[84] co-polymer materials. To aid and expand on these efforts, Florea et al. developed and utilised a modular genetic toolkit to modify a newly-isolated BC-producing strain, *Komagataeibacter rhaeticus*[86]. A panel of modular genetic parts were developed and used to engineer control of BC production and spatial and temporal control of gene expression from *K. rhaeticus*. Further, BC materials were functionalised by manually adding recombinant proteins fused to cellulose binding domains (CBDs). Once again, this approach required prior expression and external addition of functional protein components.

Although engineering BC-producing bacteria will likely continue to be a fruitful approach to developing BC-based ELMs, we wondered whether an alternative, co-culture approach could accelerate these efforts. Specifically, we set out to co-culture BC-producing bacteria with a standard synthetic biology host organism, for which a wealth of genetic tools and circuits are available. We speculated that division of labour between BC-producing bacteria and a co-

cultured host conferring novel functional properties, might expand the possibilities for BC-based ELMs. In fact, previous work has shown that engineered *E. coli* can be incorporated into BC materials by manually adding cells to growing pellicle layers[93]. This approach was used to create BC-based ELMs in which engineered *E. coli* could sense-and-respond to chemical inducers[94]. However, this approach requires external intervention. By contrast, we wished to develop a stable co-culture system, enabling spontaneous self-assembly or growth of ELMs with programmable properties.

To achieve this, we took inspiration from the natural source of many of the highest-producers of BC, kombucha tea. Kombucha tea is a fermented beverage produced by the action of a microbial community of bacteria and yeast. Invariably this cellular consortium consists of at least one species of BC-producing bacteria and often multiple species of yeast. In fact, there is growing interest in kombucha as a model microbial system to investigate multi-species cooperation[96]. Notably, one of the yeast species often found in kombucha fermentations is the model eukaryotic and standard synthetic biology host organism *Saccharomyces cerevisiae*[242].

Therefore, we set out to recreate kombucha-like co-cultures of an engineerable BC-producing bacterium, *K. rhaeticus*, and the synthetic biology host organism *S. cerevisiae*. By screening various conditions, we established and characterised a method for stable co-culture in which *K. rhaeticus* and *S. cerevisiae* exhibited a symbiotic interaction. Using our co-culture system, we programmed *S. cerevisiae* to secrete an enzyme into BC, generating a grown, functionalised material. In addition, by modifying the density of co-culture media, engineered biosensor *S. cerevisiae* strains could be incorporated into BC, creating grown biosensor materials.

4.2 Results and Discussion

4.2.1 Establishing S. cerevisiae-K. rhaeticus co-culture conditions

Our first aim was to recreate kombucha-like co-cultures between *S. cerevisiae* and *K. rhaeticus*. We selected two engineered strains previously developed in the Ellis lab, a *S. cerevisiae* strain constitutively expressing GFP from a strong promoter (referred to here as Sc GFP) and a *K. rhaeticus* strain constitutively expressing mRFP from a mid-strength promoter (referred to here as Kr RFP). These strains were chosen to allow detection of both strains within co-cultures through fluorescence measurements and therefore to facilitate downstream experiments.

Since the ideal conditions for co-culture were unknown, we initially screened a panel of co-culture conditions for growth of both strains. Specifically, *K. rhaeticus* and *S. cerevisiae* were grown separately in liquid culture and then inoculated together into different media at a range of different inoculation ratios. Four different culture media were selected: standard rich yeast medium with glucose (YEP-glucose, also known as YPD) or sucrose (YEP-sucrose, also known as YPS) as the carbon source and standard medium for cultivation of BC-producing bacteria with glucose (HS-glucose) or sucrose (HS-sucrose) as the carbon source. As *K. rhaeticus* exhibits a comparatively slow growth rate compared to *S. cerevisiae*, we fixed the inoculation density of *K. rhaeticus* at a relatively high level (1/50 dilution of pre-culture) and varied the inoculation density of *S. cerevisiae* over five orders of magnitude ($1/10^2$ to $1/10^6$ dilution of pre-culture). After 4 days of incubation in multiwell plates, images were taken of cultures (Figure 29A and 29C) and of isolated pellicles, where present (Figure 29B and 29D).

We found that, in isolation, *S. cerevisiae* grew well in all media types, forming a dense sediment at the base of the culture well. In contrast, in both HS-based and YEP-based media, *K. rhaeticus* grew poorly in sucrose-containing media compared to glucose-containing media, as shown by the absence of pellicle formation in sucrose media (Figure 29B and 29D), suggesting *K. rhaeticus* is unable to utilise sucrose as an effective carbon source. Broadly, *K. rhaeticus* produced thicker pellicles in YEP-based media compared to HS-based media (Figure 29B and 29D), consistent with the fact that YEP medium is more nutrient-rich than HS.

In glucose media, co-inoculating *S. cerevisiae* at relatively high final cell densities abolished pellicle formation (Figure 29B and 29D). Since the final cell density of *K. rhaeticus* was kept

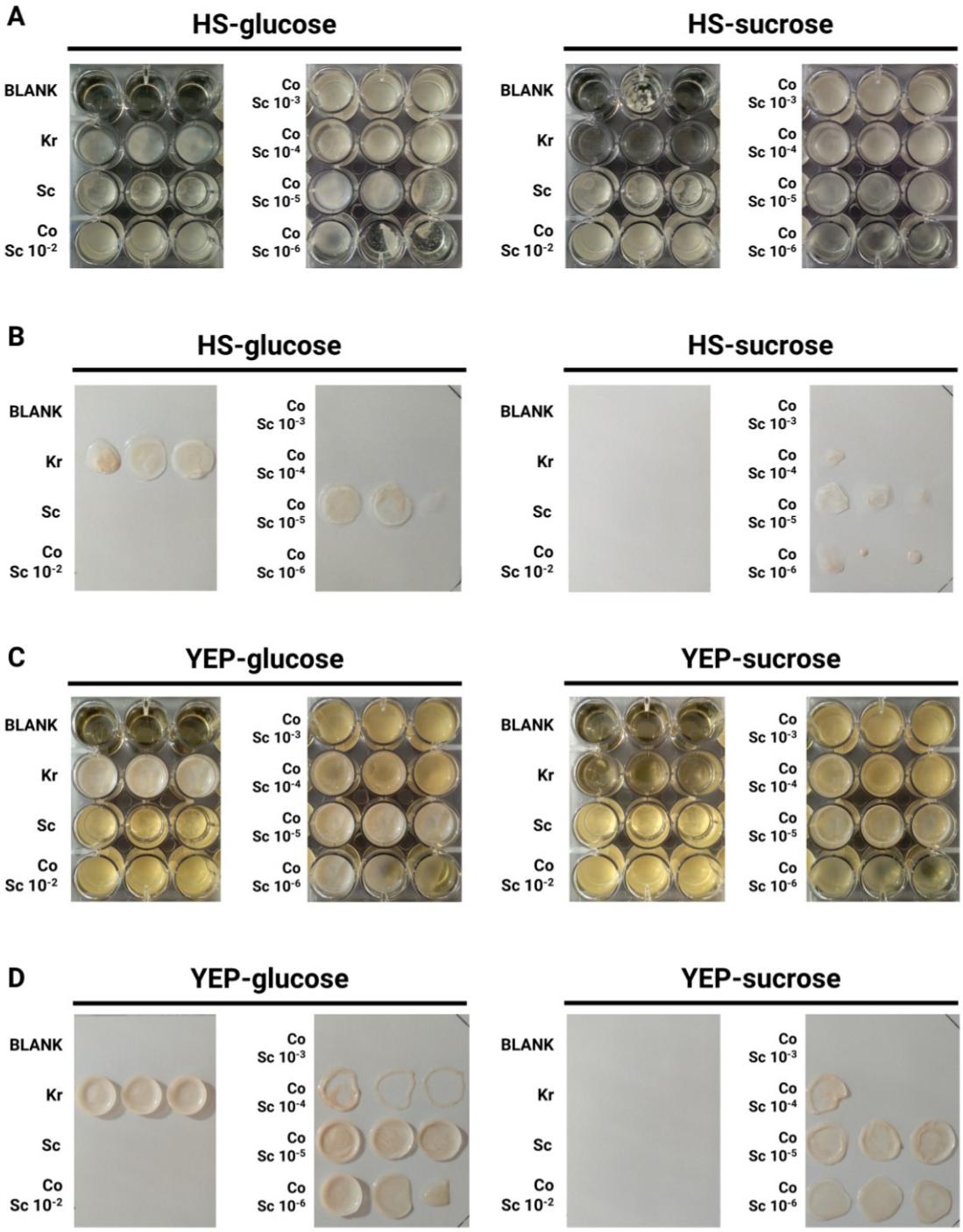

Figure 29 Images of cultures and pellicles from the co-culture condition screen. *S. cerevisiae* (Sc) and *K. rhaeticus* (Kr) were inoculated in mono-culture or co-culture (Co) in rich yeast media (YEP) or BC-producing bacteria media (HS) with either glucose or sucrose as the carbon source. For co-cultures, the Sc pre-cultures were diluted into fresh medium over a range from 1/100 (Sc 10^{-2}) to $1/10^6$ (Sc 10^{-6}). In mono-culture, Sc pre-cultures was diluted 1/100 and Kr pre-cultures was diluted 1/50. As a control for contamination, wells were included in which no cells were inoculated (BLANK). After 4 days incubation at 30°C, images were taken of cultures and then of isolated pellicle layers, where present. Cultures (**A**) and pellicles (**B**) produced in HS media and cultures (**C**) and pellicles (**D**) produced in YEP media.

constant, this observation suggests that *S. cerevisiae* can either outcompete *K. rhaeticus* or somehow suppress pellicle formation. Consistent with this, at lower *S. cerevisiae* inoculum densities (e.g. at $1/10^5$ dilution of *S. cerevisiae* pre-culture), pellicle formation was restored in both HS-glucose and YEP-glucose media. The presence of a visible sediment at the base of the culture wells – seen only with *S. cerevisiae* and not *K. rhaeticus* – suggested this dilution constituted a balance between *S. cerevisiae* and *K. rhaeticus* final cell densities at which the two strains are able to 'share' nutrients. Interestingly, at an even lower inoculum density of *S. cerevisiae*, $1/10^6$ dilution, pellicles appeared thinner than those formed than at $1/10^5$ dilution, suggesting that *S. cerevisiae* may have some stimulatory effect on production.

As described, in both HS-sucrose and YEP-sucrose media, *K. rhaeticus* failed to produce a pellicle in mono-culture. However, when co-inoculated with *S. cerevisiae* at low inoculum densities (at $1/10^4$-$1/10^6$ dilutions of *S. cerevisiae* pre-culture), *K. rhaeticus* exhibited improved growth and pellicle formation (Figure 29B and 29D). This observation implies that, during co-culture in sucrose media, *S. cerevisiae* results in the accumulation of some metabolite which is subsequently utilised as a carbon source by *K. rhaeticus*. As with glucose media, we also observed that higher inoculation volumes of *S. cerevisiae* abolished pellicle formation, again consistent with either nutrient competition or suppression of BC production by *S. cerevisiae*.

Following our initial screening approach, we next wished to develop a standardised co-culture protocol that could be used for all subsequent investigations (Figure 30A). In this approach, liquid cultures of *K. rhaeticus* and *S. cerevisiae* are grown and diluted to fixed cell densities in the co-culture. Based on our initial screen, we chose a final cell density of *S. cerevisiae* corresponding to a dilution of approximately $1/10^5$ and maintained *K. rhaeticus* at a relatively high final cell density. To confirm observations from our screen, we used this protocol to set up mono-cultures and co-cultures of each of *S. cerevisiae* (Sc GFP) and *K. rhaeticus* (Kr RFP) in YEP-glucose (YPD) and YEP-sucrose (YPS) media (Figure 30B). After 3 days of growth, *S. cerevisiae* in mono-culture had once again grown well in both media types, forming a sediment at the base of culture wells. Similarly, mono-cultures of *K. rhaeticus* behaved as in the screen, forming thick pellicles in YEP-glucose and no pellicles in YEP-sucrose. Finally, when co-cultured, both strains were able to grow together in both YEP-glucose and YEP-sucrose, as determined by the presence of thick pellicles as well as the

formation of a sediment at the base of the culture well. Notably, it was observed once again that the presence of *S. cerevisiae* in YEP-sucrose medium conferred a strong growth benefit to *K. rhaeticus*. Co-culture in YEP-sucrose following this protocol was therefore defined as our standard co-culture condition.

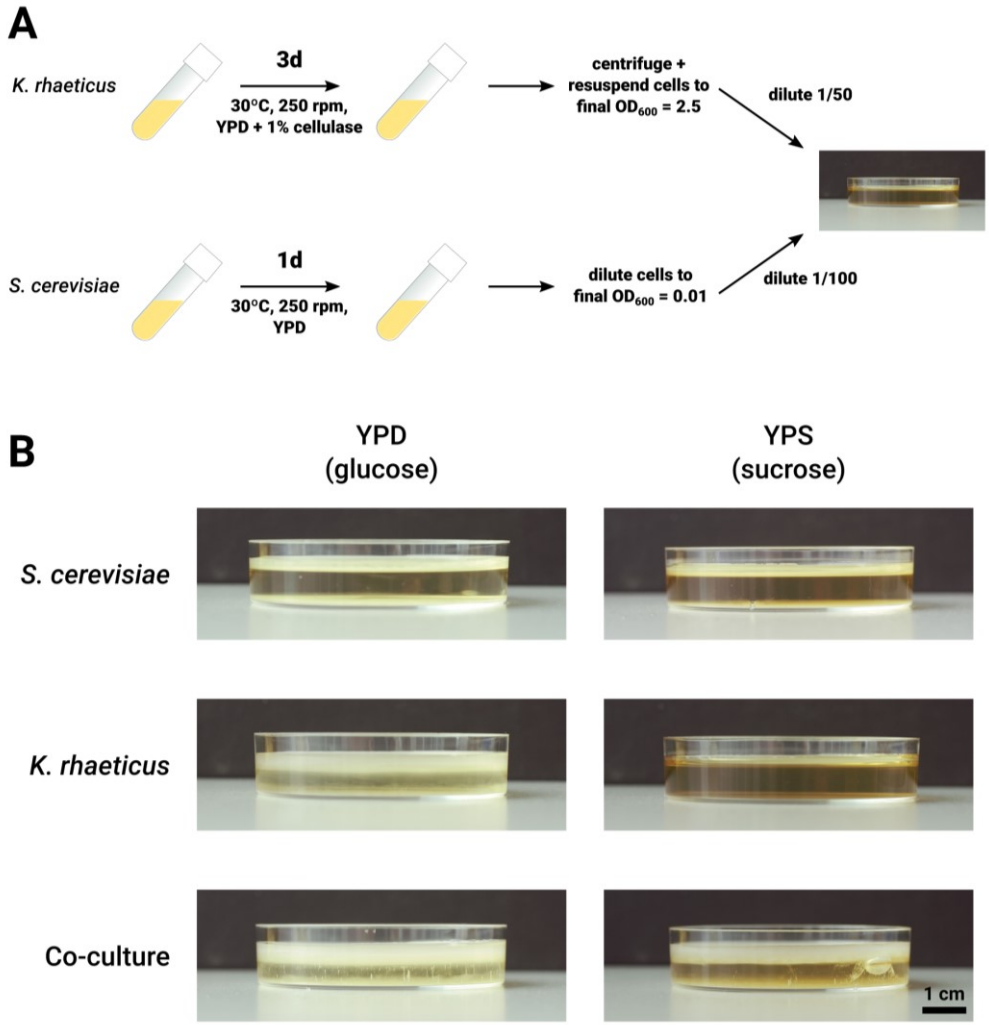

Figure 30 Defining and testing a standard protocol for co-culturing *S. cerevisiae* and *K. rhaeticus*. A Schematic outlining the standard co-culture protocol. *K. rhaeticus* and *S. cerevisiae* are grown in mono-culture under agitation. *K. rhaeticus* cultures are then centrifuged and resuspended in YEP-sucrose (YPS) medium to a final OD_{600} = 2.5 – this step removes trace amounts of cellulase enzyme and normalises cell density. *S. cerevisiae* cultures are normalised by diluting to an OD_{600} = 0.01 in YPS. Normalised *K. rhaeticus* and *S. cerevisiae* cultures are then inoculated into fresh YPS by diluting 1/50 and 1/100, respectively. **B** Images of mono-cultures and co-cultures grown for 3 days. *S. cerevisiae* grows well in both YPD and YPS media, forming a sediment at the base of the culture. *K. rhaeticus* grew well in YPD medium, forming a thick pellicle layer at the air-water interface, but failed to form a pellicle in YPS medium. When co-cultured, in both YPD and YPS, a thick pellicle layer was formed as well as a sediment layer at the base of the culture, indicating both *S. cerevisiae* and *K. rhaeticus* had grown.

Given our aim of establishing a robust method for co-culturing *S. cerevisiae* alongside *K. rhaeticus*, we felt that the observed beneficial interaction between *K. rhaeticus* and *S. cerevisiae* in sucrose media would be a useful trait. Specifically, since *K. rhaeticus* growth is dependent on the growth of *S. cerevisiae*, these co-culture conditions effectively ensure that *K. rhaeticus* cannot outcompete *S. cerevisiae*. This situation resembles a commensal symbiotic relationship, where one partner benefits from the interaction while the other is unaffected. Or alternatively, the interaction may represent a parasitic symbiotic relationship, in which one partner benefits from the interaction while the other is detrimentally affected. A more desirable co-culture system would incorporate an obligate mutualistic symbiosis, where both species are unable to survive without the other. In this case, neither species can outcompete the other, resulting in a stable co-culture system. In fact, such metabolic co-dependencies can be engineered to create coexisting microbial consortia[243]. Indeed, in the future, it may be possible to engineer similar obligate mutualistic interactions within this co-culture system. Further, metabolic dependencies, such as this, are not only useful in creating stable microbial consortia, but also are of great interest in the field of synthetic ecology, which aims to construct and understand artificial communities of microbes. Our co-culture system may therefore represent an ideal model system for investigating and engineering microbe-microbe interactions.

4.2.2 Co-culture characterisation

Having defined standard conditions for growing co-cultures, we next wished to characterise various co-culture properties to help guide biomaterial engineering approaches. Firstly, the pellicle yield from co-cultures of *S. cerevisiae* Sc GFP and *K. rhaeticus* Kr RFP over time was measured. Co-cultures were inoculated simultaneously and allowed to grow over the course of several days. At each time point, pellicles were removed and dried using the 'sandwich method'. Notably, pellicles were not treated with NaOH to lyse and remove cells embedded within the BC matrix. Pellicle formation was first detectable at low yields after 2 days and reaches a maximum after 3 days (Figure 31A). Therefore, for all subsequent experiments, a 3 day incubation was selected for co-culture cultivation.

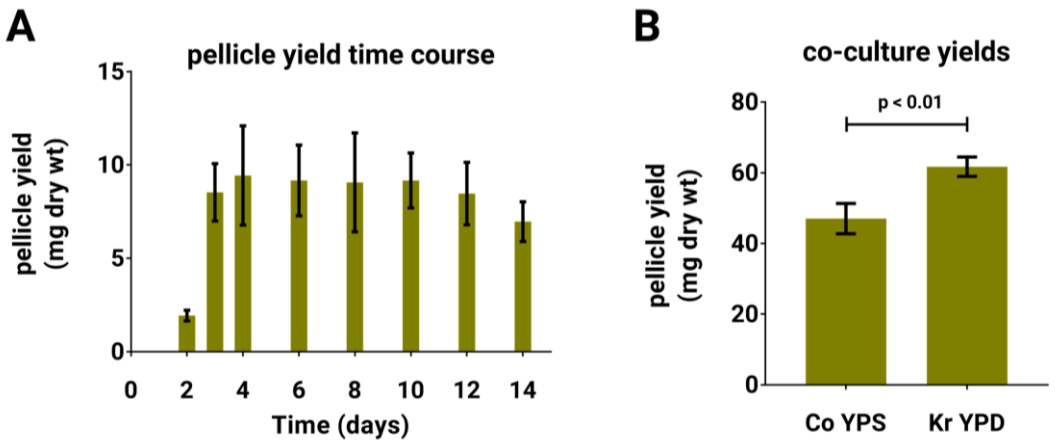

Figure 31 Measuring co-culture pellicle yields. A To follow BC production dynamics over time, co-cultures were prepared following our standard protocol and left to incubated over several days. At each time point, pellicle layers were removed and dried, since pellicles consist of ~99% water. Once dried, pellicles were weighed to determine the pellicle yield. Notably, since pellicles were not treated to lyse and remove cells, this measurement includes contribution from both BC yield and entrapped cells. Pellicle yield rapidly increased between 2 and 3 days, at which point it plateaus. Samples prepared in triplicate, data represent the mean ±1 SD. **B** Pellicle yields were compared between *K. rhaeticus* mono-culture and co-culture. Since *K. rhaeticus* grows poorly in sucrose media, mono-culture was performed in YPD (Kr YPD) and compared to co-culture in YPS (Co YPS). Co-culture was found to result in only a slight, but significant decrease in pellicle yield. Samples prepared in triplicate, $p<0.01$ from unpaired, two-tailed t-test, data represent the mean ±1 SD.

Since the growth of *K. rhaeticus* is likely based on some metabolic interaction with *S. cerevisiae* in YEP-sucrose medium, we wondered how the pellicle yield in our co-culture conditions compared to *K. rhaeticus* grown in YEP-glucose medium in mono-culture. To test this, mono-cultures of *K. rhaeticus* Kr RFP in YEP-glucose were grown alongside co-cultures

of *S. cerevisiae* Sc GFP and *K. rhaeticus* Kr RFP in YEP-sucrose and pellicle yields were measured as above. In YEP-glucose mono-culture *K. rhaeticus* produced a pellicle yield of 61.7 ± 2.7 mg compared to 47.0 ± 4.3 mg when grown in co-culture in YEP-sucrose (Figure 31B). One possible explanation for this mild reduction in pellicle yield would be that *K. rhaeticus* is utilising some derivative of sucrose produced by *S. cerevisiae* as its carbon source. Therefore, in comparison to mono-culture, *K. rhaeticus* in co-culture would have a reduced amount of carbon source available to it.

Since yeast and bacterial communities are stable over many cycles of growth during kombucha tea fermentation, we next set out to determine to what extent our co-culture system constitutes a stable co-culture. Specifically, we wondered whether *K. rhaeticus* and *S. cerevisiae* could coexist over multiple generations without either strain outcompeting the other. In order to assay long-term co-culture dynamics, we used a serial passage approach, in which the liquid below mature pellicles was inoculated into fresh media and allowed to grow for 3 days (Figure 32A). This process was repeated over 16 rounds (48 days) (Figure 32B). During each round of serial passage cultures produced pellicles, confirming the presence of *K. rhaeticus* throughout serial passage. Since *K. rhaeticus* is unable to grow effectively in YEP-sucrose medium, we inferred that *S. cerevisiae* was also maintained throughout serial passage. To confirm this and to rule out the possibility of contamination with another yeast species, samples from the liquid below the pellicle and from pellicles degraded with commercial cellulase enzyme were plated onto YPD plates and the resultant colonies imaged for GFP expression (Figure 32C). We observed that the original *S. cerevisiae* strain, Sc GFP, was indeed maintained throughout the 16 rounds of serial passage. Further data from our collaborators (Tzu-Chieh Tang, MIT) has shown that, after the first round of passage, the pellicle yield is decreased and *S. cerevisiae* cell count increased compared to the original culture. However, for all subsequent rounds of passage, these parameters remained relatively constant. Interestingly, serial passage is essentially the same process used to brew kombucha tea, where a small amount of culture is reserved from each batch to initiate the next round of fermentation. Therefore, we confirmed that *K. rhaeticus* and *S. cerevisiae* form a stable, kombucha-like co-culture under these conditions.

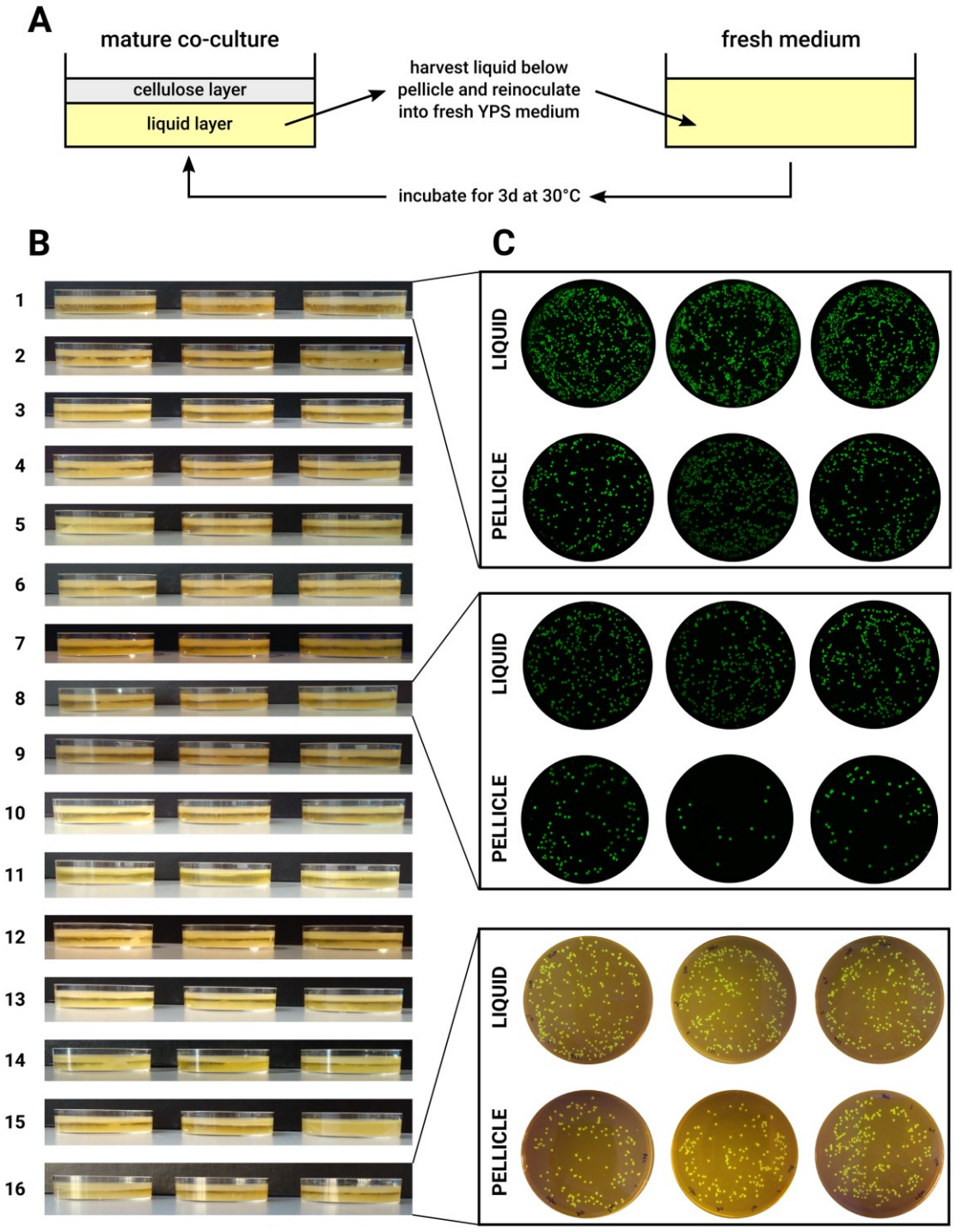

Figure 32 Investigating co-culture stability by passage. A Co-cultures of *S. cerevisiae* Sc GFP and *K. rhaeticus* Kr RFP were passaged by iteratively back-diluting liquid from below the pellicle layer in mature co-cultures into fresh YPS medium. **B** At each stage, mature pellicles were imaged. Pellicle formation was constant, indicating *K. rhaeticus* was growing well. In addition, a clear sediment was formed below the pellicle, consistent with *S. cerevisiae* growth. **C** To confirm the presence of the initial *S. cerevisiae* strain, which expresses GFP, in passage co-cultures, samples of the liquid below the pellicle (LIQUID) and enzymatically-degraded pellicles (PELLICLE) were plated and imaged for GFP fluorescence. In the interest of clarity, plates from only three time points are shown here. The appearance of the final time point is different as it was imaged for fluorescence using different equipment (fluorescence scanning versus imaging under a transluminator). All images showed that the initial GFP-expressing *S. cerevisiae* strain was maintained throughout passage.

A key factor affecting the downstream development of BC-based biological ELMs is the distribution of *S. cerevisiae* and *K. rhaeticus* within the co-cultures. For instance, in order to engineer cells to autonomously pattern a material as it grows or to create a biosensor material, it is crucial that those cells are embedded within the material layer. Consequently, we wished to determine the distribution of *K. rhaeticus* and *S. cerevisiae* between the liquid below the pellicle and the pellicle layer itself. Simultaneously, we wished to compare the distribution and densities of cells between mono-cultures and co-cultures. Therefore, mono-cultures and co-cultures were prepared and counts of viable cells obtained from the liquid and pellicle layers for both *K. rhaeticus* Kr RFP (Figure 33A) and *S. cerevisiae* Sc GFP (Figure 33B). Importantly, as described in greater detail in section **2.2.7**, since the degraded pellicle volume was not measured, cell counts in pellicles were estimated by assuming a fixed pellicle volume. In all conditions, we found that the majority of *K. rhaeticus* cells are found in the pellicle layer, while the majority of *S. cerevisiae* cells are found in the liquid layer. Consequently, although *K. rhaeticus* grows to similar cell densities in the liquid layer in YEP-glucose and YEP-sucrose, the total cell density of *K. rhaeticus* cell is much lower in YEP-sucrose as no pellicle was formed in this condition. Notably, in mono-culture in YEP-glucose, *K. rhaeticus* reached similar estimated cell densities in both the pellicle and liquid layers compared to growth in co-culture in YEP-sucrose (Figure 33A). By contrast, *S. cerevisiae* grew to a significantly reduced overall density when co-cultured with *K. rhaeticus* in YEP-sucrose compared to mono-culture in YEP-sucrose (Figure 33B). Taken together these results indicate that *K. rhaeticus* either competes with *S. cerevisiae* for some nutrient in the medium or creates conditions in the co-culture that inhibit *S. cerevisiae* growth. However, *S. cerevisiae* is still able to grow to reasonably high cell densities under co-culture conditions, reaching a cell density in the liquid layer of 1.78×10^7 cells/mL ($\pm$ 2.42×10^6 cells/mL).

Importantly, as described above, the propensity for *S. cerevisiae* to grow in the liquid layer rather than the pellicle layer might preclude the use of *S. cerevisiae* for certain applications – for example, controlling pattern formation or creating biosensor materials. In addition, fluorescence microscopy showed that *S. cerevisiae* cells that were present in the pellicle layer exhibited a highly-variable distribution across the pellicle (Figure 33C). Since applications such as autonomous material patterning require an even distribution of engineered cells across the material, this represents a limitation of the co-culture system in its current state.

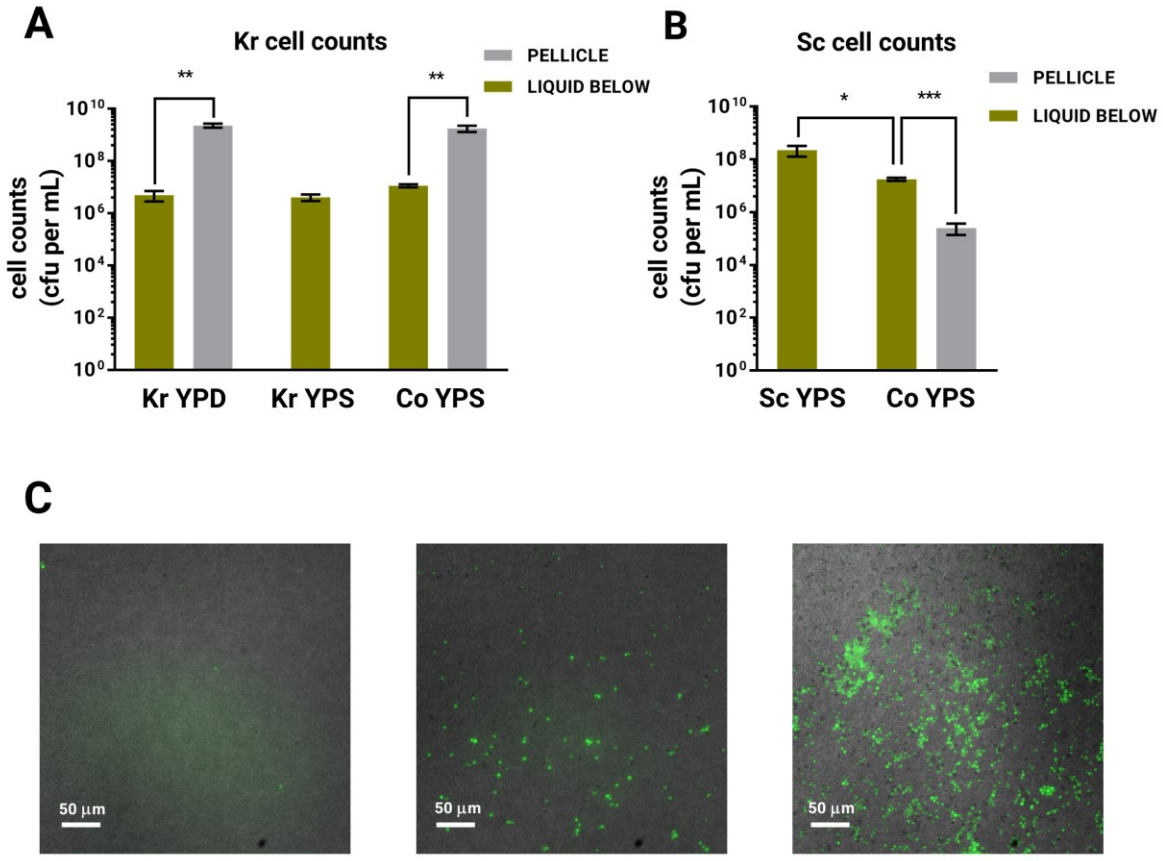

Figure 33 Analysing the cell distribution within co-cultures. By plating and counting cells, the numbers cells of present in the two phases of co-cultures – the liquid layer (LIQUID BELOW) and the pellicle (PELLICLE) layer – were determined. **A** Cell counts of *K. rhaeticus* grown in mono-culture in YPD (Kr YPD) or YPS (Kr YPS) or in co-culture with *S. cerevisiae* in YPS (Co YPS). Samples prepared in triplicate, p-values calculated by unpaired, two-tailed t-test data (* $p < 0.05$, ** $p < 0.005$ and *** $p < 0.0005$), data represent the mean ±1 SD. **B** Estimated cell counts of *S. cerevisiae* in mono-culture in YPS (Sc YPS) or in co-culture with K. rhaeticus in YPS (Co YPS). Samples prepared in triplicate, p-values calculated by unpaired, two-tailed t-test data (* $p < 0.05$, ** $p < 0.005$ and *** $p < 0.0005$), data represent the mean ±1 SD. **C** Fluorescence microscopy images of pellicles. Three separate regions of the same pellicle are shown, illustrating the variability in the density of GFP-expressing *S. cerevisiae* cells within the pellicle. Brightfield and GFP images were taken using a 20x objective and merged.

Finally, to give an idea of the robustness of our co-culture method, we set out to determine the reproducibility of co-culture properties. To achieve this, identical co-cultures were prepared following the standard protocol on three separate occasions and two parameters were measured: pellicle yields and cell counts. These two parameters were chosen as they are likely to significantly impact any downstream applications. For instance, if *S. cerevisiae* is engineered to secrete proteins into the pellicle, both the cell density of *S. cerevisiae* in the co-culture and the pellicle yield will strongly influence the final titres of secreted protein. We found that pellicle yields tended to be consistent within triplicate samples, but variable between co-cultures set up on different occasions (Figure 34A). As before, cell counts were determined by plating liquid from below the pellicle and degraded pellicle samples onto selective media and imaging plates under fluorescence (Figure 34B). Estimated cell counts for *K. rhaeticus* were consistent in the pellicle layer, where the majority of cells were detected, but varied by up to an order of magnitude in the liquid layer (Figure 34C and 34E). There were no significant differences (using a cut-off of $p < 0.05$ by unpaired, two-tail t-test) between the cell counts of *K. rhaeticus* in the pellicle layer. While a significant difference ($p < 0.05$ by unpaired, two-tail t-test) was only seen between measurements on the second and third measurements for the cell counts of *K. rhaeticus* in the liquid layer (Figure 34C). Similarly, *S. cerevisiae* cell counts were consistent in the liquid layer, where the majority of cells were detected, but more variable in the pellicle layer (Figure 34D and 34F). Statistically-significant differences were observed between *S. cerevisiae* cell counts in both the pellicle and liquid layers (Figure 34D).

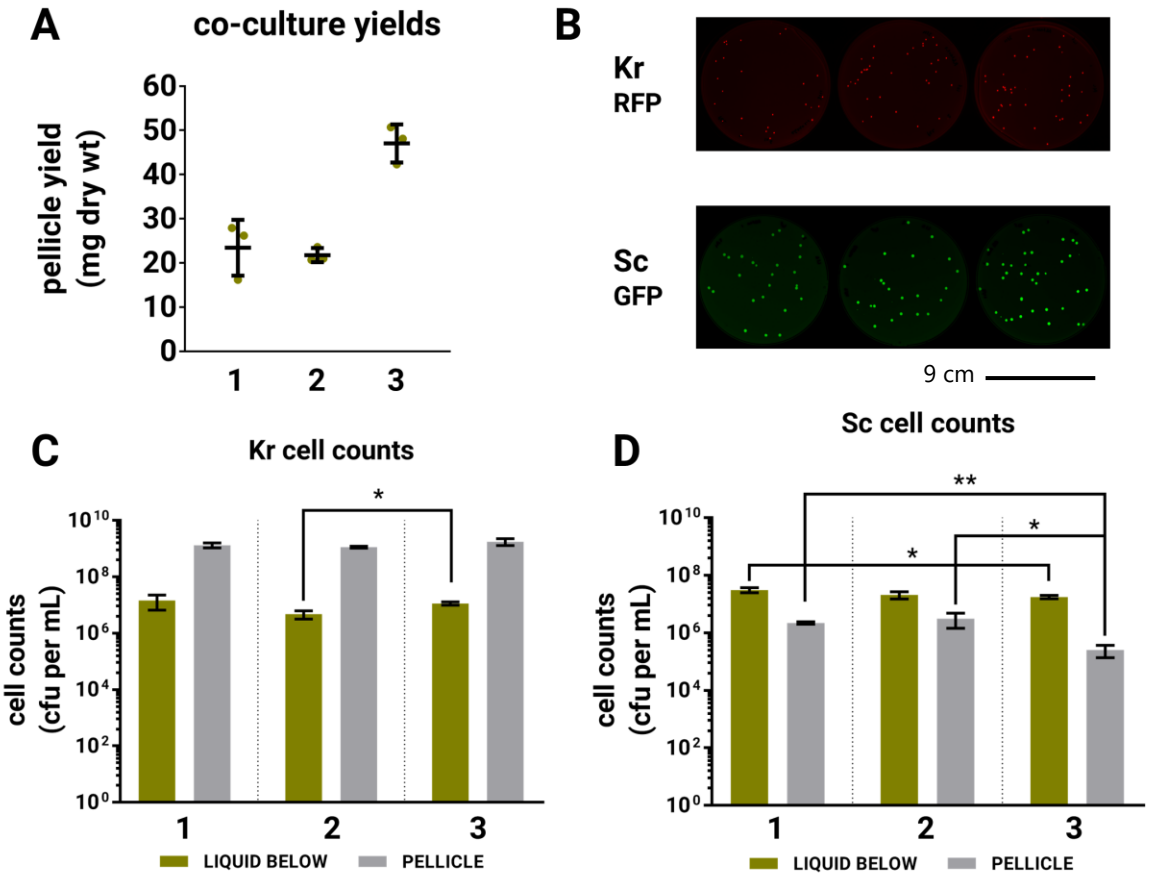

E Kr cell counts

	liquid			pellicle		
	1	2	3	1	2	3
mean cell counts (cfu/mL)	1.47E+07	4.75E+06	1.14E+07	1.33E+09	1.14E+09	1.77E+09
standard deviation (cfu/mL)	8.02E+06	1.53E+06	1.46E+06	2.60E+08	8.43E+07	4.82E+08

F Sc cell counts

	liquid			pellicle		
	1	2	3	1	2	3
mean cell counts (cfu/mL)	3.10E+07	2.09E+07	1.78E+07	2.23E+06	3.16E+06	2.53E+05
standard deviation (cfu/mL)	6.24E+06	5.80E+06	2.42E+06	2.08E+05	1.70E+06	1.15E+05

Figure 34 Reproducibility of co-culture pellicle yields and cell densities. A Pellicle yields were measured on three separate occasions. For each repeat samples were prepared in triplicate, horizontal bars represent the mean ±1 SD, green circles represent the values of individual samples. **B** Cell counts from co-cultures were prepared on three separate occasions by plating onto selective media and scanning for RFP fluorescence for *K. rhaeticus* and GFP fluorescence for *S. cerevisiae*. Cell counts were recorded from both the liquid and pellicle layers for both *K. rhaeticus* (**C**) and *S. cerevisiae* (**D**). Samples were prepared in triplicate, p-values calculated by unpaired, two-tailed t-test data (* $p < 0.05$ and ** $p < 0.005$), data represent the mean ±1 SD. Since logarithmic scales can mask some of the variation, numerical values of cell counts are included for both *K. rhaeticus* (**E**) and *S. cerevisiae* (**F**).

4.2.3 Approaches to incorporate *S. cerevisiae* within BC

As outlined above, the majority of *S. cerevisiae* cells in our co-cultures are found in the liquid layer below the pellicle, potentially limiting biological ELM engineering efforts. Consequently, we wished to explore alternative growth conditions that might increase the proportion of *S. cerevisiae* cells incorporated into the BC. While we have so far exclusively considered culture under static conditions, it is well-documented that BC production also occurs under agitation. For instance, when grown in standard 'shaking' conditions without the addition of cellulase enzyme, *K. rhaeticus* and other BC-producing bacteria form ball-shaped particles of cellulose. We hypothesised that, since agitation will also maintain *S. cerevisiae* cells in suspension, co-culture under shaking conditions might therefore result in the formation of BC 'balls' containing *S. cerevisiae*. In order to test this possibility, co-cultures of *K. rhaeticus* Kr RFP and *S. cerevisiae* Sc GFP were prepared in two different media (YPD and YPS) with *S. cerevisiae* at two different final cell densities. Images of cultures were then taken after 2 days growth under shaking conditions (Figure 35A). Particles of BC were formed under all conditions tested, however, growth in YPD yielded the largest and most regular BC balls. In all cases the culture surrounding the balls was turbid, suggesting the presence of *S. cerevisiae*. Balls produced under these conditions varied in size from approximately 1-4 mm in diameter (Figure 35B). In order to determine if *S. cerevisiae* had indeed grown alongside *K. rhaeticus* and become incorporated into the BC balls, light microscopy was used to compare balls produced from *K. rhaeticus* mono-culture (Figure 35C) with BC balls produced from *K. rhaeticus* co-culture with *S. cerevisiae* (Figure 35D). Compared to the smooth surface observed with the ball produced from *K. rhaeticus* mono-culture, the ball produced from co-cultures exhibited a speckled, granular appearance due to the presence of *S. cerevisiae* cells within the BC. To verify this observation and to provide a quantitative estimate of the cell numbers present, BC balls degraded with cellulase enzyme were spread onto agar plates and counts made of GFP-expressing *S. cerevisiae* cells (Figure 35E). BC balls were found to contain an average of 2.90×10^5 cfu/ball ($\pm 7.41 \times 10^4$), assuming a ball diameter of 3 mm, corresponding to a cell density of 2.07×10^7 cfu/mL ($\pm 5.29 \times 10^6$). Notably, this *S. cerevisiae* cell density is similar to that observed in the liquid layer below the pellicle during static co-culture (1.78×10^7 cfu/mL $\pm$ 2.42×10^6). Growth under shaking conditions therefore offers an alternative co-culture approach, enabling efficient incorporation of *S. cerevisiae* into BC.

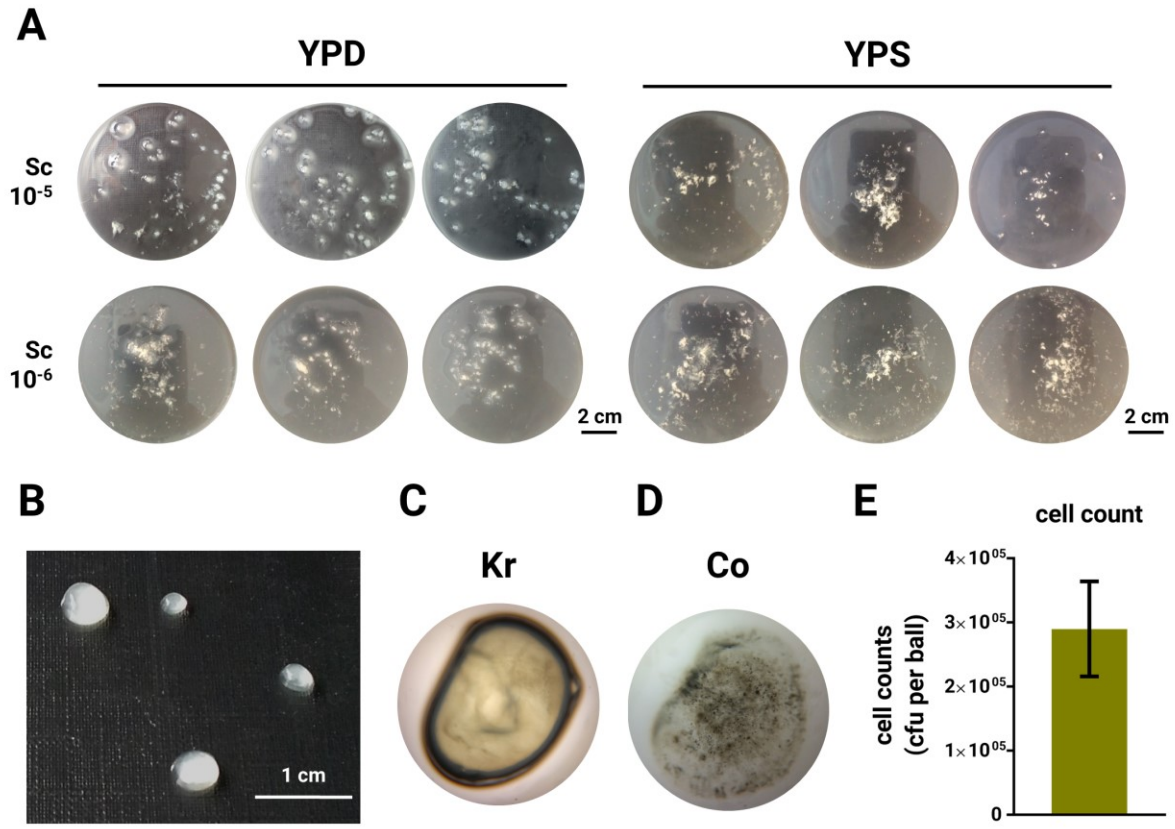

Figure 35 Formation and characterisation of BC balls produced by co-culture agitation. A Images of BC particles formed by co-culturing *K. rhaeticus* and *S. cerevisiae* in YPD and YPS media. Two final cell densities of *S. cerevisiae* were tested by diluting the pre-culture either $1/10^5$ (Sc 10^{-5}) or $1/10^6$ (Sc 10^{-6}) into co-cultures. In all cultures BC particles are visible, however, growth in YPD at the *S. cerevisiae* dilution of 10^{-5} yielded the largest and most consistently ball-shaped particles. **B** Close-up images of balls formed from growth in YPD with an *S. cerevisiae* dilution of 10^{-5}. Light microscopy images taken of balls produced by *K. rhaeticus* mono-culture (**C**) or co-culture with *S. cerevisiae* (**D**), using a 10x objective lens. The ball produced by co-culture has a speckled appearance, suggesting *S. cerevisiae* cells are incorporated within the BC matrix. **E** To confirm that *S. cerevisiae* cells are contained within the BC matrix, balls produced by co-culture were enzymatically-degraded, plated and counts made of fluorescent cells. Samples prepared in triplicate, data represent mean ±1 SD.

However, the BC balls produced in this approach tended to be small and of highly variable sizes, limiting potential applications. Since previous studies have shown that the speed of agitation influences the size of balls, in the future there may be scope to refine this method and improve the properties of the resultant balls.

By contrast to the BC balls approach, static culture is a simpler method and, in theory, can be easily modified to suit larger production scales by increasing culture top surface area. Therefore, we wished to find a co-culture method that would enable efficient incorporation of *S. cerevisiae* within BC, while remaining compatible with static cultivation. *S. cerevisiae* settles to the bottom of culture vessels because the density of the cells is greater than that of

water: ~1.11 g/mL compared to 1 g/mL[244]. Therefore, we hypothesised that, if the density of the culture medium were increased to >1.11 g/mL, *S. cerevisiae* cells would float to the surface rather than sinking and so become incorporated into the newly-forming pellicle at the air-water interface. In collaboration with our collaborators (Tzu-Chieh Tang, MIT), we tested whether optiprep, a non-toxic, aqueous solution of 60% iodixanol with a density of 1.32 g/mL, could be adding to culture medium in order to increase its density. Based on an initial screen performed by our collaborators, a concentration of 45% (v/v) optiprep was found to sufficiently modify the density of culture media so that *S. cerevisiae* cells floated rather than sedimenting. In order to confirm these observations, co-cultures of *S. cerevisiae* (Sc GFP) and *K. rhaeticus* (Kr RFP) were prepared in standard YPS medium and in YPS + 45% optiprep (v/v) and images taken of the cultures. Pellicles were formed under both conditions with little apparent thickness of the resulting pellicles (Figure 36A). However, when pellicles were removed, there was a complete absence of sediment in the YPS + optiprep medium, in contrast to the dense sediment observed in standard YPS medium (Figure 36B). Further, compared to the smooth, homogenous surface of pellicles formed in YPS, pellicles formed in YPS + optiprep had a speckled appearance (Figure 36C). Taken together, these results suggest that addition of optiprep to the co-culture medium results in *S. cerevisiae* cells becoming buoyant and therefore incorporated into the pellicle layer. To confirm this observation, estimated counts of *S. cerevisiae* cells within pellicles from co-cultures with or without optiprep were determined. Indeed, addition of optiprep resulted in a ~200-fold increase in estimated cell count from 2.44×10^5 cfu/mL ($\pm 1.98 \times 10^5$) to 4.60×10^7 cfu/mL ($\pm 1.06 \times 10^7$). Addition of optiprep to co-culture medium therefore represents a simple approach to direct the incorporation of *S. cerevisiae* cells into the growing BC material layer under static conditions. A disadvantage of this approach is the cost of optiprep (£270 for 250 mL from Sigma Aldrich), which is likely to be a significant barrier to cost-effective scale-up. However, future work to explore alternative approaches – for instance, using a cheaper density-modifying reagent or genetically-encoding *S. cerevisiae* incorporation into the pellicle – could overcome this potential obstacle. Interestingly, increasing sucrose concentration in aqueous solution increases density, in fact, at a concentration of ~25% (w/v), sucrose solutions have a density equal to that of YPS + 45% optiprep. Although co-culture at such high sucrose concentration has not been demonstrated – all co-cultures described here use 2% sucrose – this may represent a more cost-effective approach to

increasing co-culture medium density. Although the density of the medium would change as sucrose is consumed, *S. cerevisiae* cells that are incorporated into a growing BC layer early on may be stably held within the cellulose fibre matrix.

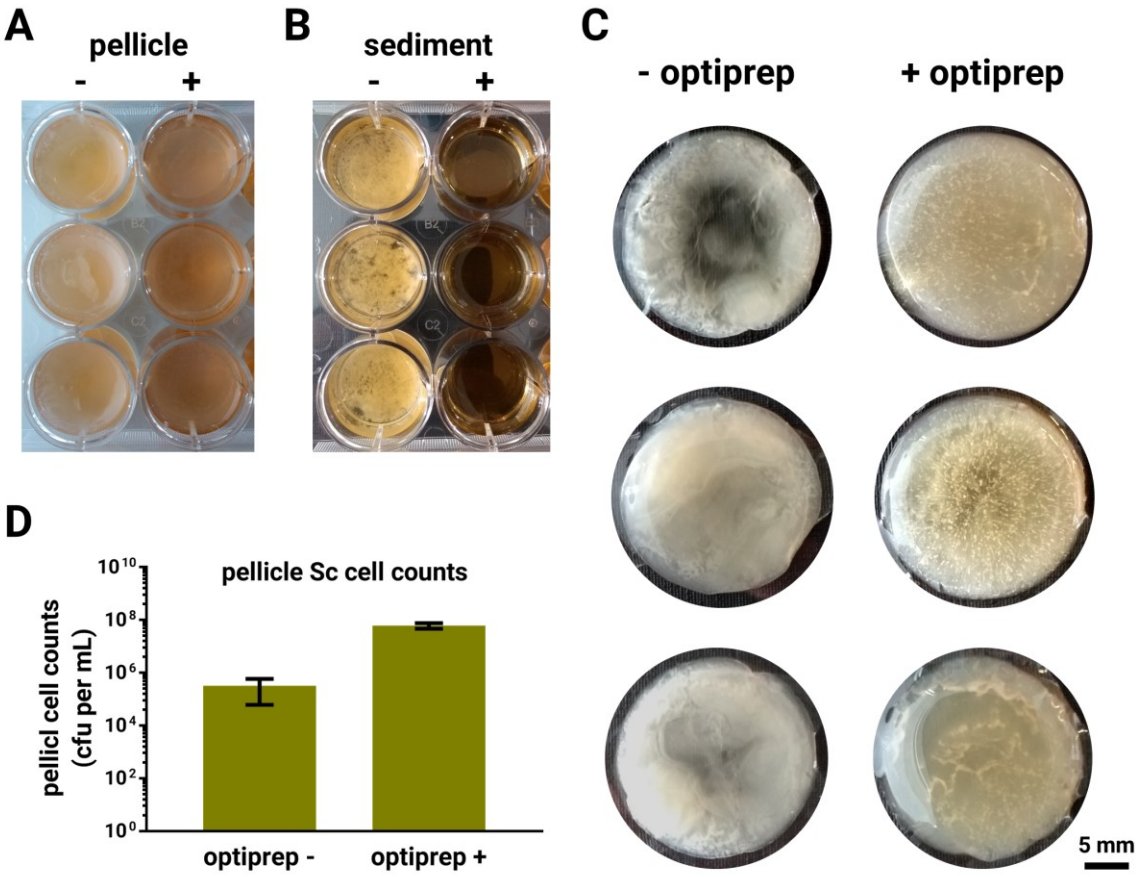

Figure 36 Addition of optiprep to co-culture medium enables incorporation of *S. cerevisiae* into the BC matrix under static growth. Co-cultures were prepared in YPS media with (+) or without (-) 45% optiprep. Images taken showing the pellicles formed at the air-water interface (**A**), of the liquid below the pellicle, following pellicle removal (**B**) and of the isolated pellicles (**C**). A clear difference is seen in the liquid below the pellicles, where the dense formed in standard co-cultures is completely absent in co-cultures to which optiprep has been added. Pellicles isolated from co-cultures with optiprep have a speckled appearance. **D** To confirm that optiprep results in *S. cerevisiae* incorporation within the BC matrix, pellicles from co-cultures with and without optiprep were enzymatically-degraded, plated and counts made of fluorescent cells. Samples prepared in triplicate, data represent mean ±1 SD.

4.2.4 Engineering BC material functionalisation

Having achieved our initial aim of recreating engineerable kombucha-like co-cultures, we next set out to engineer *S. cerevisiae* strains to add new biological functions to BC materials. Since *S. cerevisiae* is well-known as an effective recombinant protein secretion host, we first asked if *S. cerevisiae* strains could be engineered to secrete functional proteins into the BC material during co-culture (Figure 37A). To test this, a protein that had been previously-demonstrated to be secreted from *S. cerevisiae* was selected, the β-lactam hydrolysing enzyme, β-lactamase (BLA). Specifically, the catalytic region of *E. coli* TEM1 BLA, lacking the native signal peptide was chosen. Using the yeast toolkit (YTK) system[201], the BLA catalytic region was cloned downstream of the *S. cerevisiae* mating factor alpha (MFα) prepro secretion signal peptide under the control of a strong constitutive promoter (pTDH3) (Figure 37B). This construct was then integrated into *S. cerevisiae* genome to create strain yCG04. However, since the BC layer constitutes only a fraction of the total volume of the co-culture, only a fraction of the secreted BLA would be expected to be incorporated into the BC layer. Therefore, a second strain (yCG05) was engineered in which a cellulose-binding domain (CBD) was fused to the C-terminus of BLA (Figure 37B). In theory, addition of a CBD should increase the amount of secreted protein in the BC layer and so improve the efficiency of functionalisation. While numerous CBDs have been described in the literature, CBDcex[245] (the 112 amino acid region from the C-terminus of the Cex exoglucanase from *Cellulomonas fimi*) was chosen based on previous work demonstrating its ability to bind BC[86].

We first sought to confirm that our engineered strains were able to secrete functional BLA enzyme. Therefore, the wild type, BLA-secreting and BLA-CBD-secreting *S. cerevisiae* strains were grown in mono-culture in YPS medium with agitation for 24 hours. Supernatants were harvested from these cultures and then screened using the nitrocefin β-lactamase assay. The nitrocefin assay provides a colourimetric readout of β-lactamase activity; the yellow nitrocefin substrate is converted to a red product under the action of β-lactamase, which can be quantified by measuring light absorbance at 490 nm. Supernatants from both BLA and BLA-CBD secreting strains showed significantly increased β-lactamase activity compared to that of the WT strain (Figure 37C). Interestingly, the activity detected from the BLA-CBD secreting strain was reduced compared to the BLA secreting strain. Since this assay was

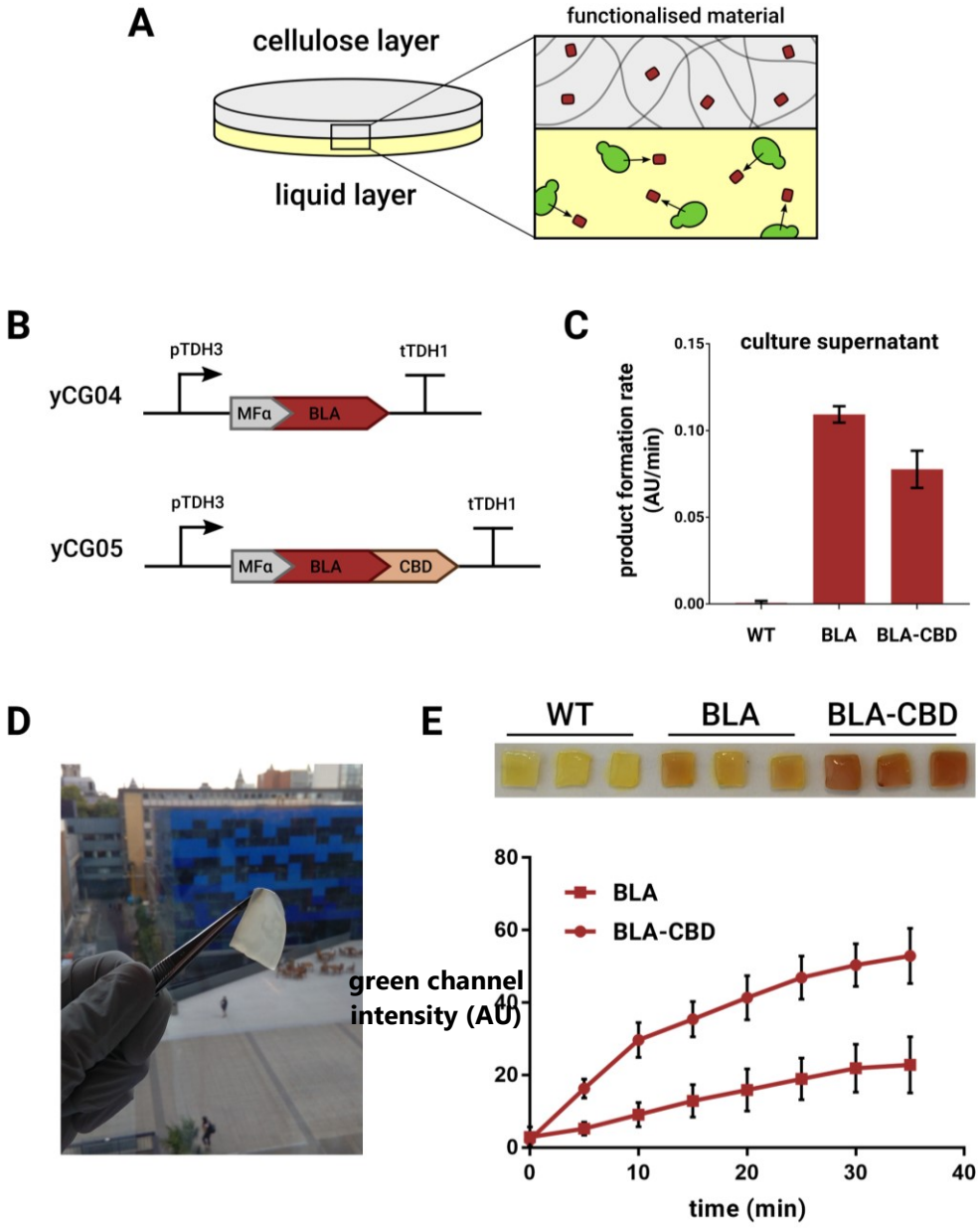

Figure 37 Secretion of β-lactamase from *S. cerevisiae* to functionalise the BC material. A Schematic illustrating the concept of functionalisation. *S. cerevisiae* cells, the majority of which are found in the liquid layer, secrete a protein which then becomes incorporated into the BC layer, conferring a new functional property to the material. **B** BLA-secreting strains yCG04 (BLA) and yCG05 (BLA-CBD). **C** Culture supernatants from WT, BLA and BLA-CBD strains were assayed for β-lactamase activity using the colourimetric nitrocefin substrate. The product formation rate was measured using a plate reader. Samples prepared in triplicate, data represent the mean ±1 SD. **D** Co-cultures were prepared with WT, BLA and BLA-CBD strains and pellicles removed and washed. **E** The nitrocefin assay, which produces a yellow-to-red colour change in the presence of active β-lactamase, was performed with pellicle samples and images taken at five minute intervals. Shown here is the reaction after ten minutes. **F** The yellow-to-red colour change was then quantified as green channel intensity using ImageJ image analysis software. Samples prepared in triplicate, data represent the mean ±1 SD.

performed using undiluted supernatants from 24-hour cultures, the enzyme activity will be affected by multiple factors. Therefore, the observed decrease in β-lactamase activity for the BLA-CBD secreting strain could be due to decreased growth rate, decreased secreted protein yields or an effect of fusion of the CBD to BLA enzyme decreasing its activity by causing steric hindrance, for example.

Having demonstrated that our engineered *S. cerevisiae* strains can secrete active BLA, we next wished to test whether they could be co-cultured with *K. rhaeticus* to produce a grown, functionalised material. Co-cultures were prepared under standard conditions with wild type BY4741, BLA-secreting (yCG04) or BLA-CBD-secreting (yCG05) strains and the resultant native, wet pellicles (Figure 37D) were screened for β-lactamase activity using the nitrocefin assay. While pellicles from co-cultures with WT *S. cerevisiae* showed no colour change from yellow to red, a clear signal was observed with pellicles from co-cultures with BLA-secreting and BLA-CBD-secreting strains (Figure 37E and 37F). Notably, the fusion of the CBD to the BLA C-terminus resulted in an increase in the observed β-lactamase signal. Therefore, although fusion of the CBD appears to result in a decreased yield of secreted BLA in mono-culture, it results in an increase in the proportion of secreted enzyme that becomes incorporated into the pellicle layer and so a greater degree of functionalisation.

This demonstrates that *S. cerevisiae* can indeed be engineered to functionalise a grown BC material using our co-culture method. While the primary aim of this experiment was to serve as a proof of principle, there are in fact some immediate potential biotechnological applications of this approach. For instance, attaching enzymes to a support material – a process known as 'enzyme immobilisation' – is a method used to improve the cost-effectiveness of industrial biocatalysts, facilitating purification of the product from the enzyme and often improving the stability and reusability of the enzyme. Immobilised enzymes are already used in a variety of industrial processes: lactase in lactose-free milk production[246], glucose isomerase in high-fructose corn syrup production[247] and lipases in the interesterification of food fats and oils[248]. Our approach enables catalytic materials to be grown rather than produced manually and could therefore be more cost-effective than current immobilised enzyme production methods.

Since native pellicles have a water content of ~99%, we wondered if functionalised materials needed to be kept in their hydrated state for the BLA enzyme to remain active. To explore this idea, pellicles produced by co-culturing *K. rhaeticus* with WT, BLA-secreting (yCG04) and BLA-CBD-secreting (yCG05) *S. cerevisiae* strains were dried by sandwiching them between sheets of absorbent paper towel to create thin, paper-like materials (Figure 38A). Dried pellicles were then rehydrated and screened for β-lactamase activity using the nitrocefin assay. Remarkably, dried pellicles from co-culture with BLA-secreting and BLA-CBD-secreting strains converted the yellow substrate to the red product, indicating the presence of active β-lactamase within the material (Figure 38B and 38C). Again, a greater signal was observed in pellicles from co-culture with the BLA-CBD secreting strain compared to the BLA secreting strain.

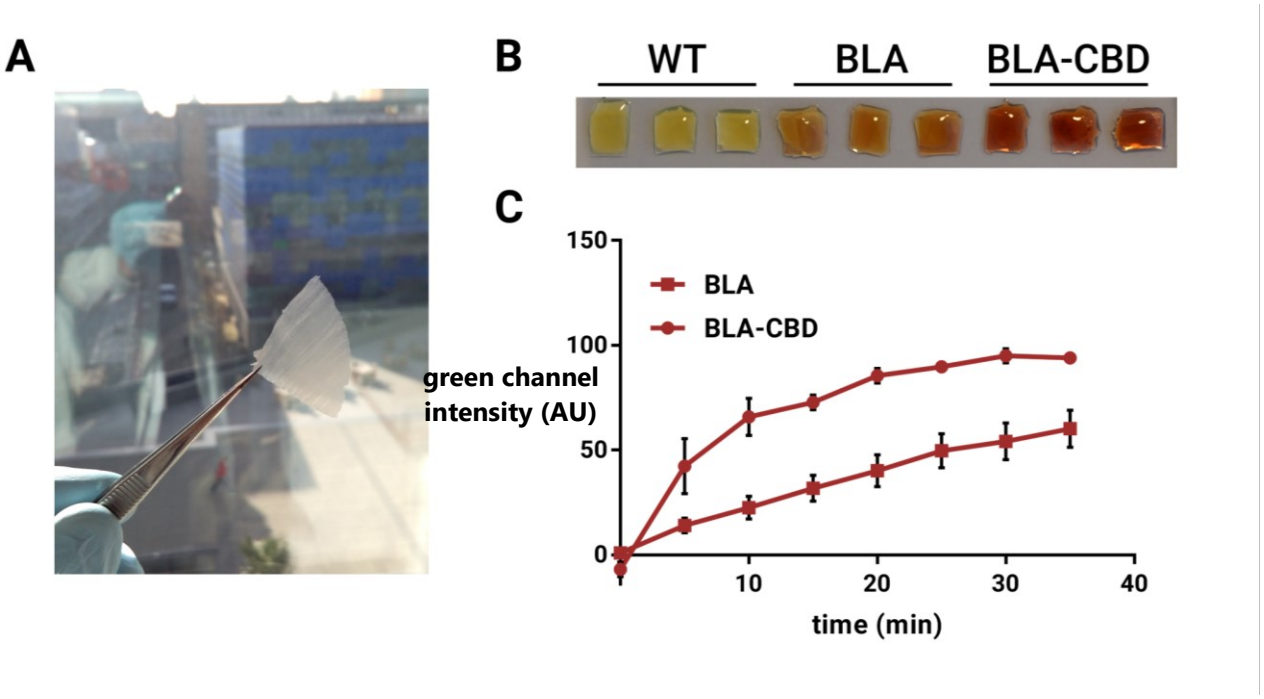

Figure 38 Dried functionalised materials retain β-lactamase activity. A Photograph of a dried pellicle. **B** The nitrocefin assay, which produces a yellow-to-red colour change in the presence of active β-lactamase, was performed with dried pellicle samples and images taken at five minute intervals. Pellicles grown with BY4741 (WT), yCG04 (BLA) and yCG05 (BLA-CBD) *S. cerevisiae* strains were analysed. Shown here is the reaction after ten minutes**. C** The yellow-to-red colour change was then quantified as green channel intensity using ImageJ image analysis software. Samples prepared in triplicate, data represent the mean ±1 SD.

To enable comparison of the absolute levels of β-lactamase activity between wet pellicles and dried pellicles, the nitrocefin assay was repeated alongside standard curves with a commercial BLA enzyme (Figure 39). Interestingly, the drying process had little effect on the activity of BLA in the material: 29.8 ±3.7 mU/mm^2 before drying and 27.3 ±4.4 mU/mm^2 after. Further, the assay was performed following storage of functionalised BC for 1 month at room temperature. Remarkably, after long-term storage under ambient conditions, the pellicles retained β-lactamase activity, although activity was reduced to around a third of the original level (Figure 39A). Nonetheless, this shows that functionalised materials can be grown and stored at room temperature, retaining their activity for later rehydration and deployment.

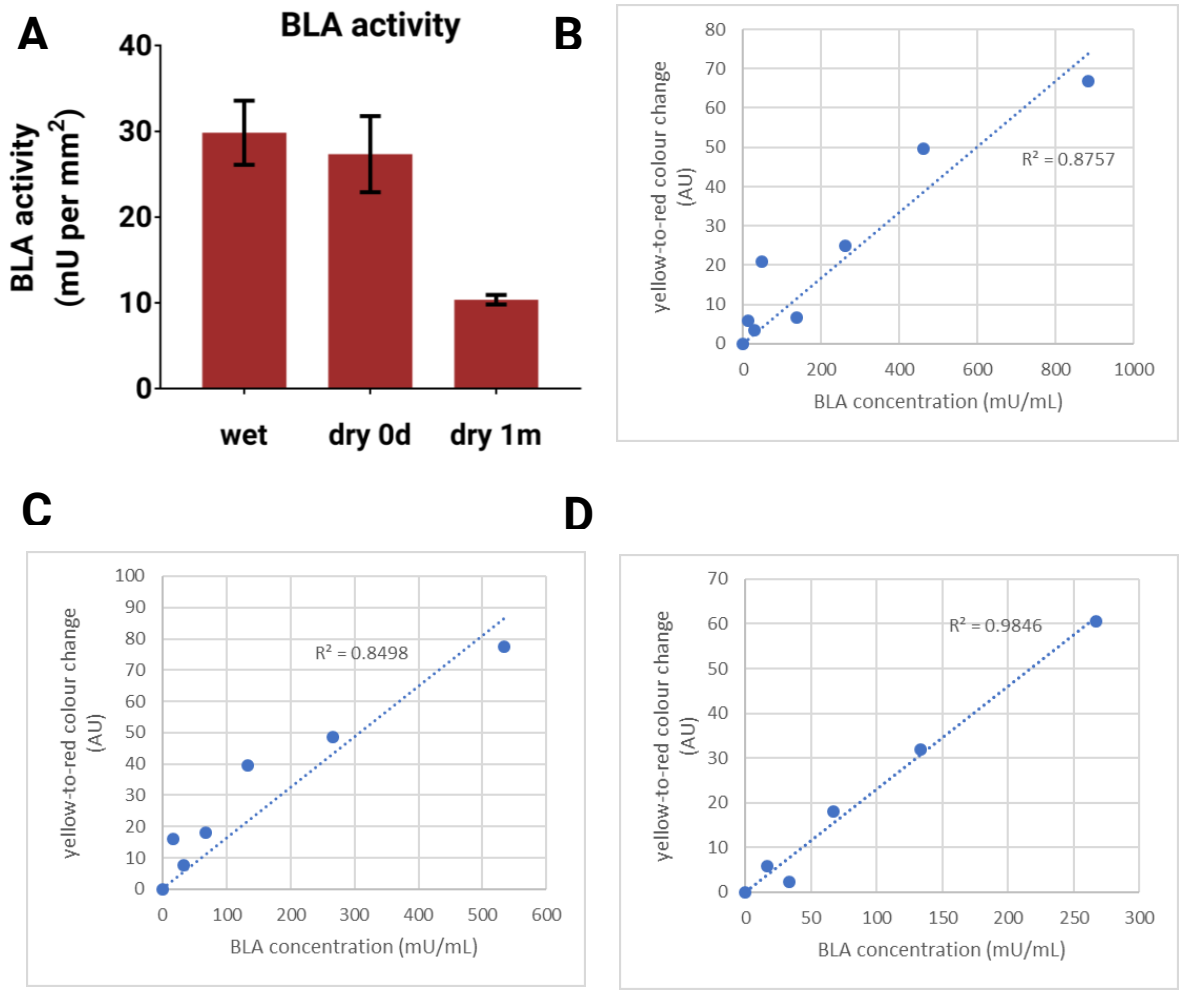

Figure 39 Measuring the stability of β-lactamase following drying and storage of pellicles. A Absolute β-lactamase activities were calculated from native, hydrated pellicles (wet), dried pellicles after no storage (dry 0d) and dried pellicles after one month storage at room temperature (dry 1m). Samples presented here are from pellicles grown in co-culture with yCG05 (BLA-CBD). Since pellicle liquid volume is altered by drying, β-lactamase activity is represented by enzyme activity units per unit of pellicle area, to enable cross-comparison. To obtain absolute β-lactamase activities, standard curves were run alongside wet (**B**), dry 0d (**C**) and dry 1m (**D**) samples. Samples prepared in triplicate, data represent the mean ±1 SD.

In contrast to some techniques for enzyme immobilisation, this approach does not covalently attach the protein to the support material. Instead, we hypothesise that BLA simply diffuses into the BC matrix while BLA-CBD does the same but then becomes bound by an intermolecular interaction. It might, therefore, be anticipated that BLA enzyme would rapidly leach out of the BC material, while BLA-CBD would remain bound stably. To test this, dried pellicles functionalised with BLA and BLA-CBD were subjected to multiple rounds of washes in PBS buffer and then assayed for β-lactamase activity (Figure 40). The activity of β-lactamase in BLA-functionalised pellicles fell sharply after washing. By contrast, BLA-CBD-functionalised pellicles retained a greater proportion of their original β-lactamase activity after washing. This observation is consistent with the CBD providing a specific, stable binding interaction between the enzyme and cellulose.

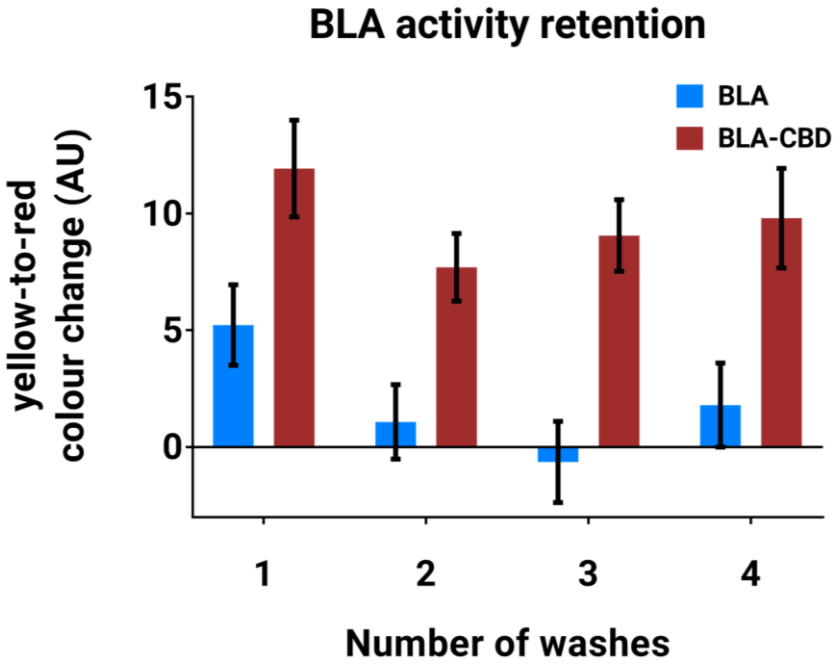

Figure 40 Retention of β-lactamase within functionalised material after washing. Dried pellicles functionalised with BLA or BLA-CBD were subjected to a variable number of washes in PBS buffer and then screened for β-lactamase activity by the nitrocefin assay. Samples prepared in triplicate, data represent the mean ±1 SD.

Interestingly, while immobilised enzymes typically require stable, long-term binding of the enzyme to the support material, alternative applications can be envisioned where leaching might be beneficial – for instance, when using a material to deliver a therapeutic to a

particular site in the body. Therefore, the choice of whether to include a CBD or not, offers flexibility for downstream applications which may require stably functionalised materials or materials able to leach a functional species. However, it will be crucial to consider whether potential applications will require exposure to any conditions that might denature the CBD or disrupt the CBD-cellulose binding interaction – for example, elevated temperatures, low pH, high salt concentrations.

Next, as an alternative to growing thin sheets of material, we asked if we could use our BC balls approach to produce functionalised materials. Co-cultures were prepared as before and grown under shaking conditions with WT, BLA-secreting (yCG04) and BLA-CBD-secreting (yCG05) *S. cerevisiae* strains. The resultant BC balls were assayed for β-lactamase activity (Figure 41). BC balls from co-cultures with BLA- and BLA-CBD-secreting *S. cerevisiae* were positive for active β-lactamase and, once again, an increased activity was observed with BC functionalised with BLA-CBD compared to BLA. Interestingly, many of the supports to which

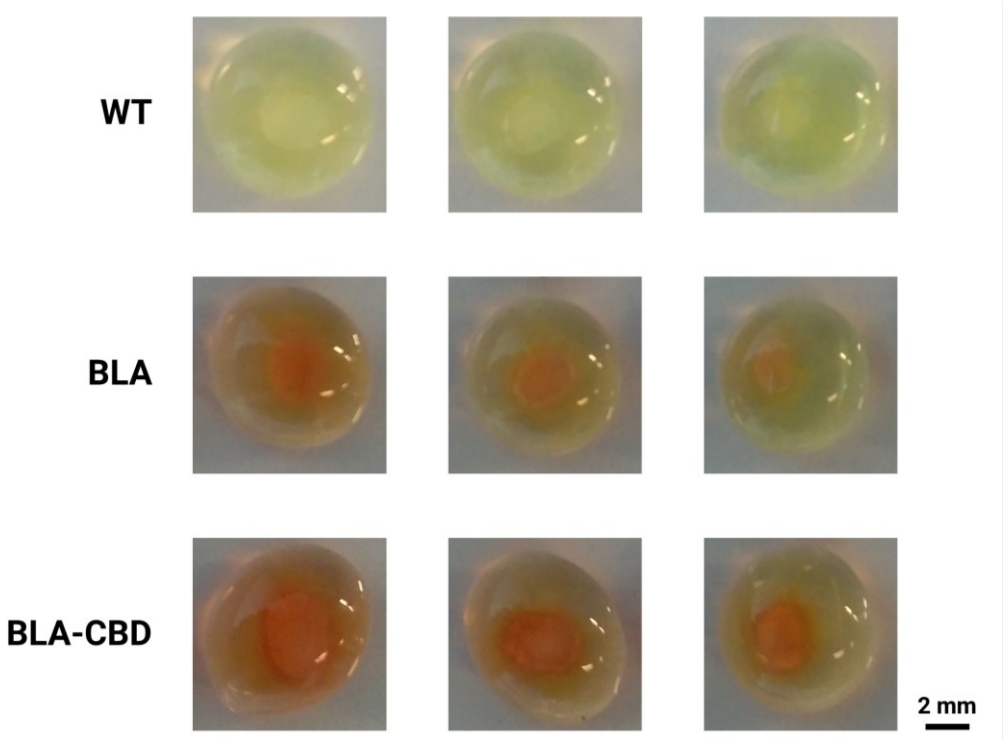

Figure 41 Co-culturing β-lactamase-functionalised balls. Balls of BC were produced using our agitated co-culture procedure with three different *S. cerevisiae* strains: BY4741 (WT), yCG04 (BLA) and yCG05 (BLA-CBD). Balls from these co-cultures were then rinsed and analysed by the nitrocefin assay, which produces a yellow-to-red colour change in the presence of active β-lactamase. Shown above are images of triplicate samples of balls suspended in buffer during the nitrocefin assay (15 minutes incubation at 25▪C). WT leads to no colour change, whereas BLA and BLA-CBD accumulate the red product. The majority of the red product accumulates in the vicinity of the balls.

immobilised enzymes are attached are beads. This therefore represents another potentially useful approach for the production of functionalised materials.

Having demonstrated that BC materials can be functionalised with the enzyme β-lactamase, we set out to explore alternative proteins with which BC might be functionalised. In general, efforts to engineer heterologous protein secretion are more likely to succeed when the protein of interest is secreted from its native host – the *E. coli* TEM1 BLA, for instance, is naturally secreted from its host. Therefore, to select a more challenging protein target we chose a protein that is not secreted in its native host, green fluorescent protein (GFP). In fact, numerous previous attempts have been made to secrete GFP from *S. cerevisiae*, with varying degrees of success[249,250].

Once again, the yeast toolkit (YTK) system was employed to generate strains secreting GFP and GFP fused to CBDcex. Both GFP and GFP-CBD were fused to the *S. cerevisiae* mating factor alpha (MFα) secretion signal peptide and expressed from a strong constitutive promoter (pTDH3), creating *S. cerevisiae* strains yCG01 and yCG02, respectively. As an initial test of our constructs, GFP-secreting (yCG01) and GFP-CBD-secreting (yCG02) *S. cerevisiae* strains were grown in mono-culture under agitation. Supernatants were harvested from these cultures and then imaged for GFP fluorescence under a transluminator (Figure 42A and 42B). A low level of GFP fluorescence was visible in supernatants from both GFP-secreting and GFP-CBD-secreting strains, indicating our engineered strains were able to secrete GFP. However, this fluorescence was only observable after 48 hours of growth and a large amount of GFP was retained within the cellular fraction, suggesting inefficient secretion. To test whether these engineered strains could functionalise BC, co-cultures of *K. rhaeticus* with wild-type, GFP-secreting (yCG01) and GFP-CBD-secreting (yCG02) *S. cerevisiae* were prepared. Since GFP secretion appeared to be inefficient, co-cultures were incubated for an extended period of either 7 or 14 days before pellicles were harvested and screened for GFP fluorescence. However, pellicles from co-cultures with GFP-secreting and GFP-CBD-secreting *S. cerevisiae* exhibited no detectable increase in fluorescence compared to pellicles with wild type *S. cerevisiae* after 7 days or 14 days (Figure 42C and 42D). Therefore, the level of GFP secretion from *S. cerevisiae* appears to be insufficient to result in detectable functionalisation of pellicles during co-culture. Although low levels of GFP secretion were detectable in mono-culture with agitation, the lower cell density of *S. cerevisiae* under co-culture conditions likely

accounts for the low apparent yield of secreted protein. In order to confirm that GFP is in fact secreted under our co-culture conditions, albeit at undetectable levels, anti-GFP antibodies and a variety of immunodetection methods – more sensitive than the fluorescence detection method used here – could be employed in the future. However, this experiment clearly illustrates that, while practicable, using engineered *S. cerevisiae* strains to functionalise BC grown with our co-culture method could be limited to cases where proteins of interest can be efficiently secreted or are highly-active at low yields.

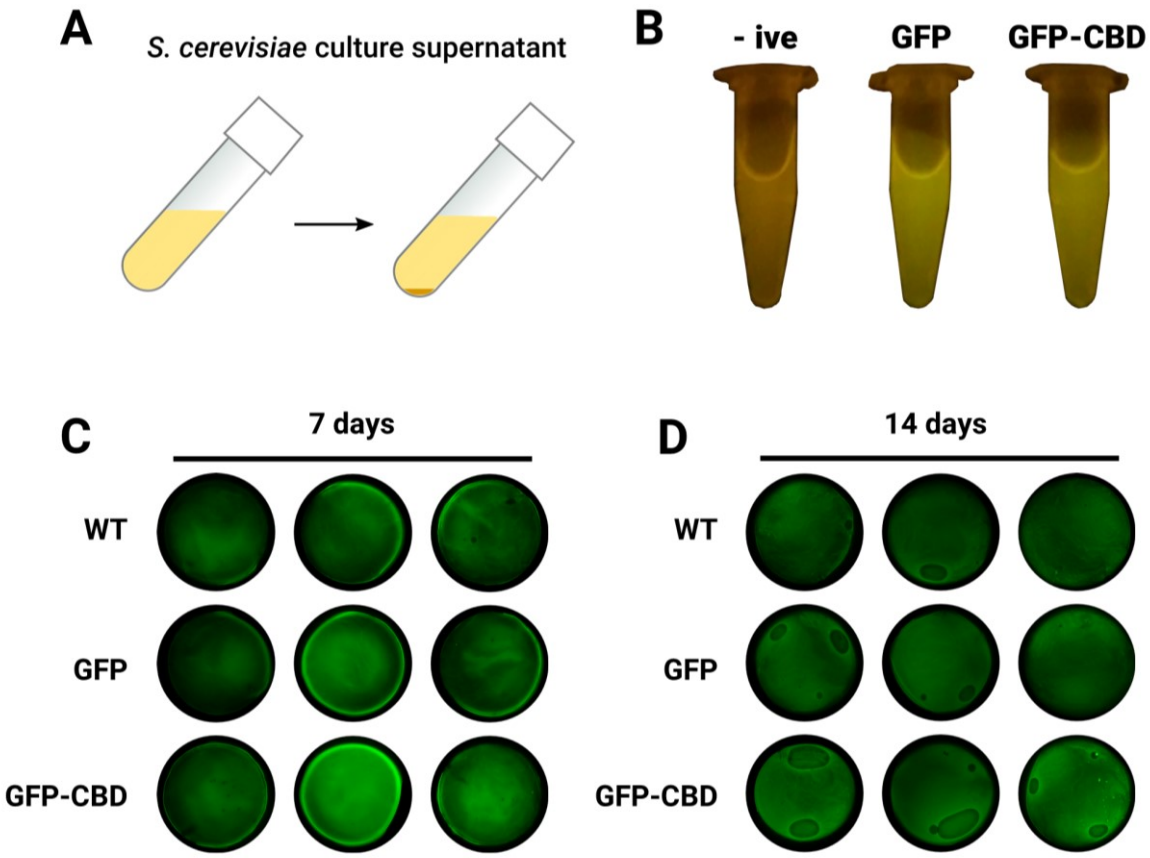

Figure 42 Testing for functionalisation of BC by GFP secretion. Culture supernatants (**A**) of *S. cerevisiae* strains were prepared to isolate secreted protein fraction. **B** Supernatants from three *S. cerevisiae* strains were imaged for GFP fluorescence under a transluminator: yCG04 (-ive), yCG01 (GFP) and yCG02 (GFP-CBD). To test if GFP-secreting strains could functionalise pellicles, co-cultures were prepared with BY4741 (WT), yCG01 (GFP) and yCG02 (GFP-CBD) *S. cerevisiae* strains and grown for 7 days (**C**) or 14 days (**D**) and imaged for GFP fluorescence with a fluorescence laser scanner. Other than mild fluctuations, likely due to slight differences in pellicle thickiness, no difference in GFP signal was observed between samples.

4.2.4 Engineering sense-and-response in BC materials

Another biological function we wished to add to BC materials through engineered *S. cerevisiae* was the ability to sense-and-respond to environmental stimuli. There are numerous published examples of genetic circuits which convert chemical and physical cues to transcriptional responses in *S. cerevisiae*. Therefore, we set out to test if BC materials, into which engineered biosensor *S. cerevisiae* strains were incorporated and functional, could be grown using our co-culture method. To begin with, we selected a chemical inducible system from the literature, in which addition of β-estradiol leads to activation of transcription from the target promoter (Figure 43A). Specifically, transcription is controlled by a synthetic transcription factor (Z_3EV) consisting of three domains: the Zif268 DNA-binding domain, the human estrogen receptor (hER) ligand binding domain, and the transcriptional activation domain of viral protein 16 ($VP16^{AD}$)[251]. When present, β-estadiol binds to the hER ligand binding domain of Z_3EV, releasing it from its basal sequestration in the cytosol and enabling it to translocate into the nucleus. Once in the nucleus, the Zif268 domain binds cognate DNA sequences in engineered promoters and the $VP16^{AD}$ domain activates transcription of downstream genes. Here, we used a previously-engineered *S. cerevisiae* strain (yGPY093) in which Z_3EV is expressed from a constitutive weak strength promoter and GFP is under the control of a β-estradiol responsive promoter – a Gal1 promoter containing six repeats of the Zif268 target sequence (Figure 43B).

We hypothesised that our optiprep method could be used to grow pellicles into which *S. cerevisiae* yGPY093 was incorporated and which could subsequently sense-and-respond to β-estradiol. To test this, co-cultures of *K. rhaeticus* and wild-type or yGPY093 *S. cerevisiae* were prepared in YPS-optiprep medium. The resultant pellicles were rinsed and then incubated in fresh medium in the presence or absence of β-estradiol. After 24 hours incubation with gentle agitation, pellicles were rinsed and imaged for GFP fluorescence. By contrast to pellicles grown with wild-type *S. cerevisiae*, addition of β-estradiol to pellicles containing yGPY093 *S. cerevisiae* yielded a strong GFP signal. While this demonstrates the general principle that engineered biosensor *S. cerevisiae* strains can indeed sense-and-respond to environmental stimuli, there are also potential applications of this approach. For instance, a number of *S. cerevisiae* biosensor strains have been engineered to screen and detect a range of environmental pollutants and pathogens[252–254]. Our approach could,

therefore, be used to create grown biosensor materials for on-site screening of medical or environmental samples.

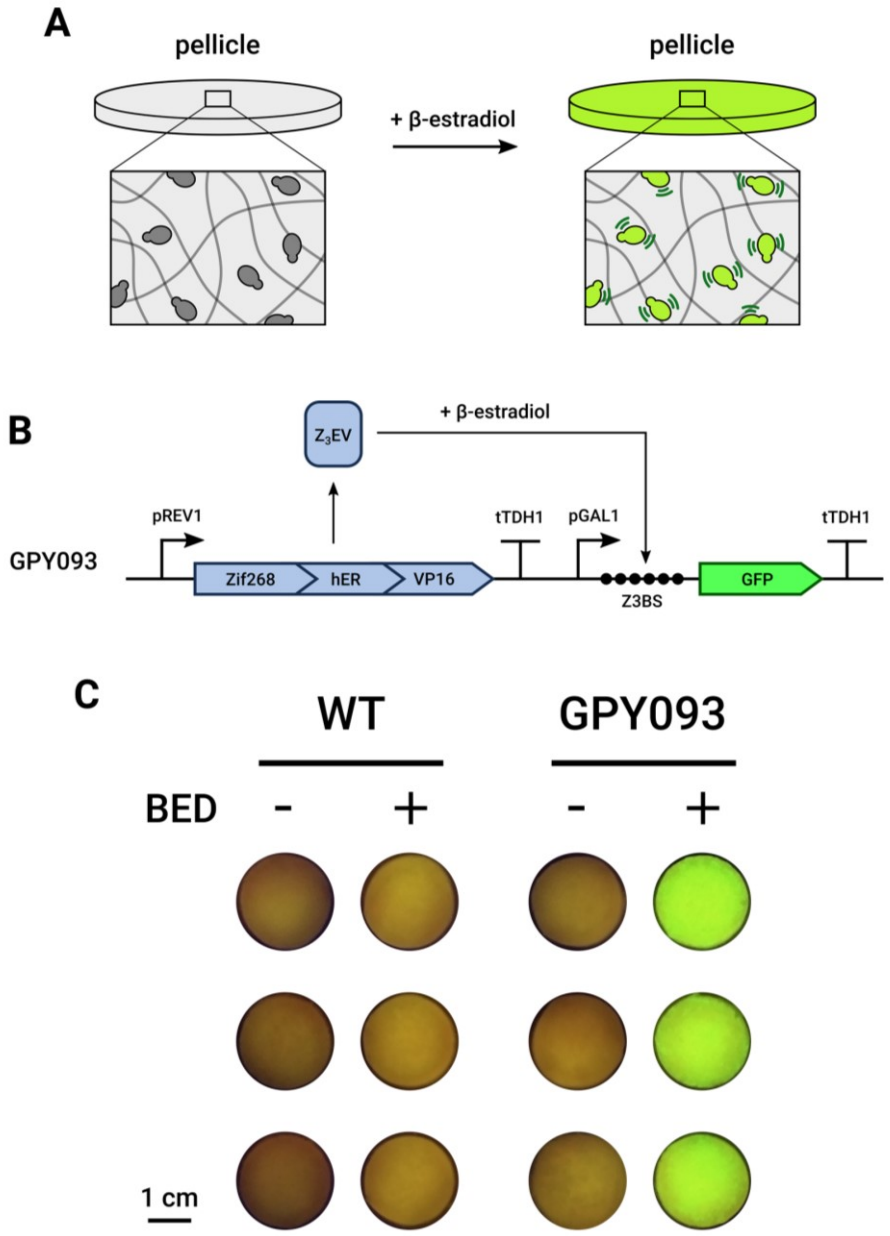

Figure 43 Engineering materials to sense and respond to β-estradiol. A Schematic illustrating biosensor pellicle function. Pellicles contain and engineered *S. cereivisiae* strain (GPY093) that senses the chemical inducer β-estradiol and in response produces the reporter protein GFP. **B** Schematic showing genetic GPY093 circuit. The Z_3EV synthetic transcription factor is expressed from the weak constitutive yeast promoter pREV1. Upon addition of β-estradiol Z_3EV is able to bind Z_3EV binding sites (Z3BSs) in the pGAL1 promoter, activating transcription of GFP. **C** Testing biosensor pellicles. Pellicles with either BY4741 (WT) or β-estradiol responsive (GPY093) *S. cerevisiae* incorporated within the BC matric were grown using the optiprep method. Triplicate samples were washed, then incubated with agitation in fresh media in the presence or absence of β-estradiol (BED). After 24 hours, pellicles were washed and imaged for GFP fluorescence under a transluminator.

However, for this approach to be feasible, biosensor materials would have to be stored without losing their functionality. Therefore, we wondered if *S. cerevisiae* cells incorporated into BC materials could remain viable after drying and long-term storage. To test this, co-cultures were prepared in YPS-optiprep medium to create pellicles into which the GFP-expressing *S. cerevisiae* Sc GFP strain was incorporated (Figure 44A). The resultant pellicles were then dried and stored at room temperature under ambient conditions (Figure 44B). Wet and dried pellicles were degraded enzymatically, plated onto selective medium and cell counts of *S. cerevisiae* determined. While the drying process resulted in a large decrease in the number of viable cells within pellicles, significant numbers of viable *S. cerevisiae* cells remained (Figure 44C). In addition, although at very low levels, viable *S. cerevisiae* cells could be detected in pellicles after 1 month of storage at room temperature under ambient

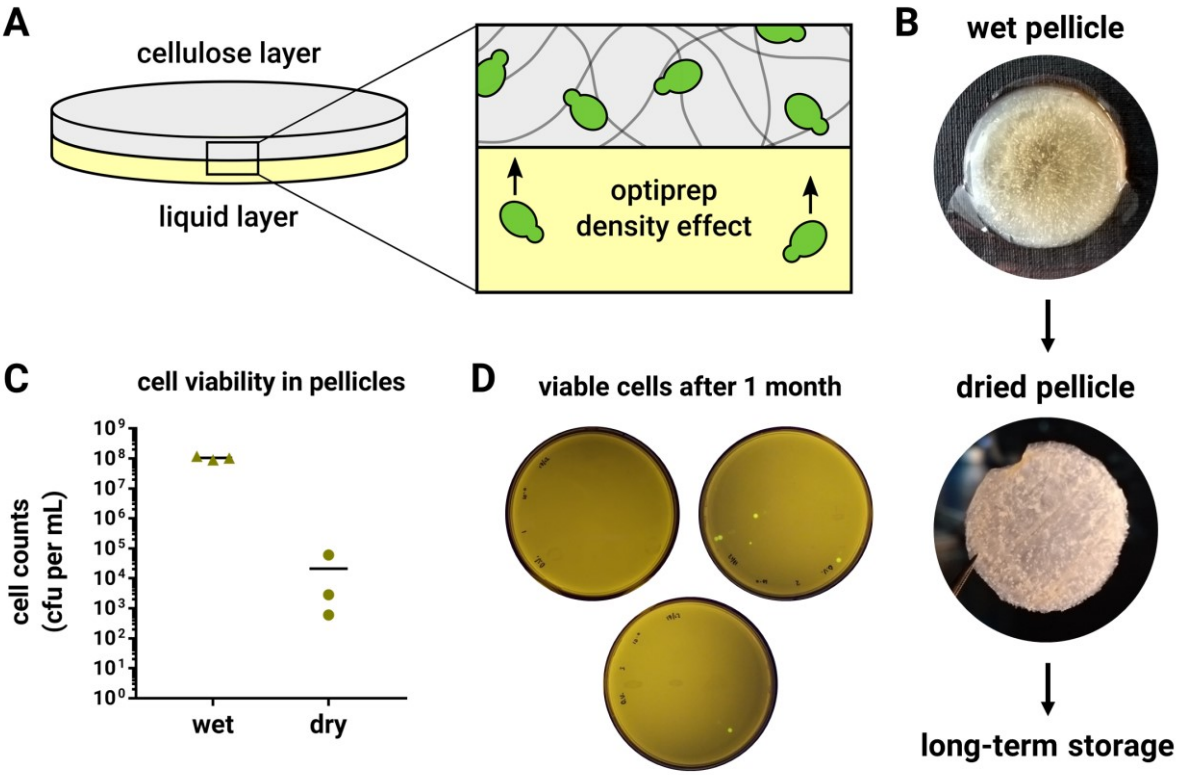

Figure 44 Cell viability in dried pellicles. A Schematic illustrating the effect of optiprep in the culture medium. By increasing culture medium density, *S. cerevisiae* cells become buoyant, rise to the surface and become incorporated into the BC matrix. **B** Pellicles into which *S. cerevisiae* cells have been incorporated can be dried and stored. **C** Cell viability was compared between wet and dried pellicles by enzymatically-degraded pellicles, plating and obtain counts of fluorescent *S. cerevisiae* cells. Bars represent the mean and green dots represent individual values. **D** After storage for 1 month, dried pellicles were enzymatically-degraded and 100 µL samples plated without dilution. The resultant plates are shown here, imaged for GFP fluorescence under translumination. Viable cells were obtained on two of three plates, indicating that a small minority of *S. cerevisiae* cells survive even after 1 month of storage at room temperature.

conditions (Figure 44D). Although the majority of *S. cerevisiae* cells within pellicles did not remain viable after drying, even small numbers of viable cells may be sufficient for biosensor materials to remain functional. Specifically, since biosensor cells are exposed to fresh culture medium and grown, small numbers of viable cells can proliferate and eventually produce a large response. Therefore, biosensor pellicles containing the β-estradiol-responsive *S. cerevisiae* strain yGPY093 were grown, dried and incubated in fresh medium for 24 hours in the presence of absence of β-estradiol (Figure 45A). Notably, to more closely match the potential use of biosensors in an on-site detection setting, pellicles were incubated without

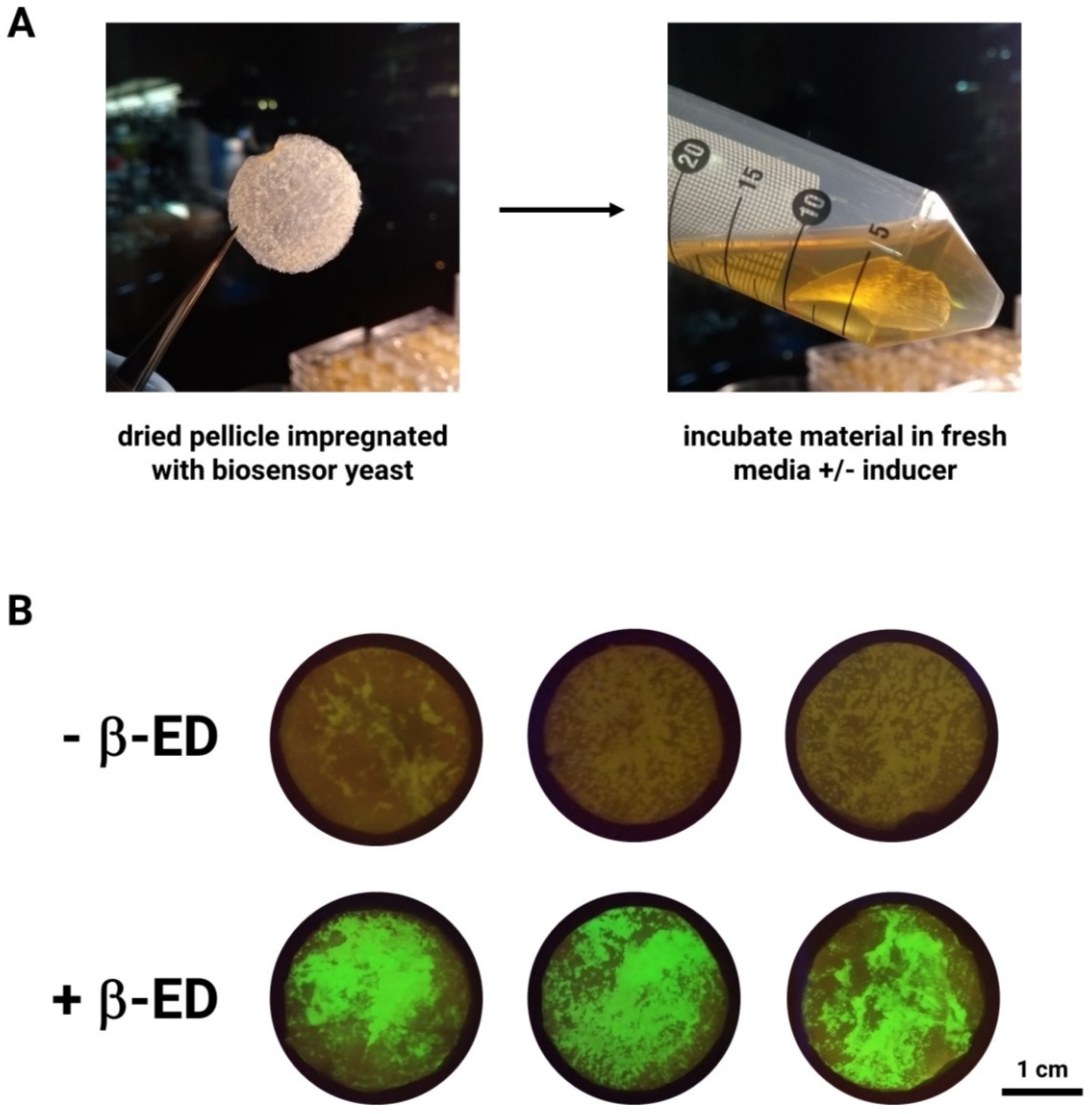

Figure 45 Dried pellicles can function as biosensor materials. A Schematic illustrating the dried pellicle biosensor experimental set up. Dried pellicles into which biosensor *S. cerevisiae* are incorporated are incubated in fresh medium with or without the inducer and later screened for response. **B** Dried pellicles, into which a β-estradiol responsive *S. cerevisiae* strain (GPY093) was incorporated, were incubated in fresh medium without agitation in the presence or absence of β-estradiol (β-ED). After 24 hours, biosensor pellicles were imaged for GFP fluorescence under a transluminator.

agitation in this instance. Pellicles containing yGPY093 *S. cerevisiae* yielded a strong GFP signal in the presence of β-estradiol (Figure 45B). Therefore, despite containing a reduced number of viable cells, dried pellicles can be rehydrated and function as biosensor materials. While these sense-and-response functions require the addition of fresh medium, it may be possible to screen diverse sample types by supplementing with concentrated nutrient stocks. In fact, this approach has been employed previously, enabling *S. cerevisiae* biosensor strains to function in blood, urine and soil[252].

As mentioned above, *S. cerevisiae* strains have been engineered to sense-and-respond to many chemical stimuli other than β-estradiol. One class of *S. cerevisiae* biosensors employs the G protein coupled receptor (GPCR) family of receptors. GPCRs are membrane protein receptors that share a common basic structure, but are able to detect a remarkable range of different chemical and physical stimuli. *S. cerevisiae* possesses a native GPCR signalling cascade, which it uses to sense-and-respond to mating pheromones. By transplanting heterologous GPCRs into this pathway, biosensors with novel targets can be generated. To show that our approach is compatible with GPCR-based signalling, co-cultures were prepared between *K. rhaeticus* and a previously-developed *S. cerevisiae* biosensor strain yWS890. This biosensor strain detects the *S. cerevisiae* mating factor alpha (MFα) peptide through a native GPCR (Ste2) and activating GFP expression in response. Pellicles into which yWS890 and wild type *S. cerevisiae* had been incorporated were grown and dried. Pellicles were then incubated in fresh medium for 24 hours in the presence or absence of MFα and imaged for GFP fluorescence under a transluminator (Figure 46). Biosensor pellicles exhibited a clear increase in GFP signal in the presence of MFα, indicating that the GPCR-based biosensor strain does indeed function well using our grown biosensor approach. Although in some cases it remains a significant challenge to successfully transplant heterologous GPCRs into the native *S. cerevisiae* cellular machinery, numerous studies have succeeded in developing novel GPCR-based *S. cerevisiae* biosensors[252,254]. Using our approach, these and future biosensor strains could, therefore, be employed to create a panel of grown biosensor materials.

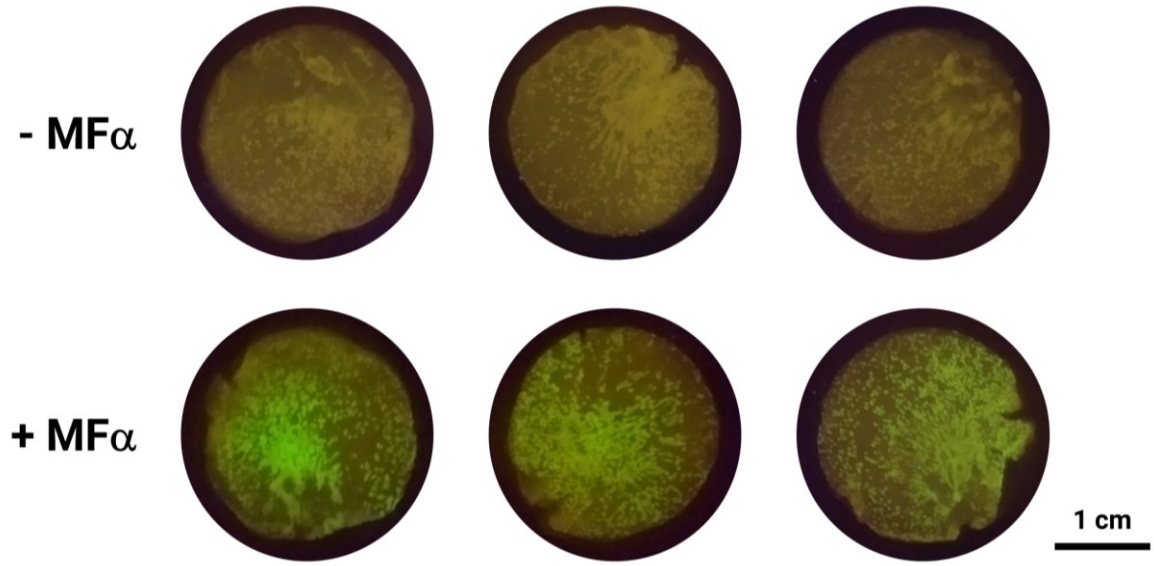

Figure 46 Alternative biosensor strains function when incorporated within pellicles. Dried pellicles, into which a GPCR-based MFα-responsive *S. cerevisiae* strain (yWS890) was incorporated, were incubated in fresh medium without agitation in the presence or absence of MFα. After 24 hours, biosensor pellicles were imaged for GFP fluorescence under a transluminator.

4.3 Conclusions

Here we have demonstrated that stable, kombucha-like co-cultures of two engineerable microbes, *K. rhaeticus* and *S. cerevisiae* can be recreated in the lab. By screening various co-culture conditions, we uncovered an interaction between *K. rhaeticus* and *S. cerevisiae*, resembling a commensal symbiotic interaction, in which the presence of *S. cerevisiae* promotes the growth of *K. rhaeticus* on sucrose medium. Exploiting this interaction, we developed and characterised a standard protocol that enabled reproducible co-culture of *K. rhaeticus* with *S. cerevisiae* and self-assembly of a BC-based biological material. This co-culture system therefore is not only of interest for the development of biological ELMs, but may also represent an interesting model system for synthetic ecology, in which further microbe-microbe interactions could be investigated and engineered.

Using our co-culture method, we demonstrated how the wealth of existing *S. cerevisiae* synthetic biology tools can be leveraged to program functional biological properties into grown BC materials. Firstly, we showed that an enzyme can be secreted from *S. cerevisiae*, become incorporated into the BC material and, therefore, functionalise the material. In addition, we found that functionalised BC materials can be dried and later rehydrated without losing catalytic activity. This approach is highly adaptable – numerous other protein targets could be secreted from *S. cerevisiae* to add various biological properties to the material. However, as exemplified by our inability to secrete detectable levels of GFP from *S. cerevisiae*, it will be important to consider what yields of the target protein are required to confer the desired property and whether those yields will be achievable in our co-culture system. Proteins requiring relatively low yields to bring about functional changes – such as enzymes or antimicrobial peptides – might therefore represent better initial targets than those requiring relatively high yields – such as proteins conferring material properties, like elastin or hydrophobins. Secondly, we showed how *S. cerevisiae* biosensor strains can be incorporated within the BC material to create biosensor materials. While we illustrate this with just two test cases, numerous useful *S. cerevisiae* biosensor strains able to detect pathogens[252], environmental pollutants[253], biomarkers[255] and so on, have been described and could be used in conjunction with our co-culture method. In addition, the ability of cells to sense-and-respond to environmental stimuli underlies a number of interesting properties of natural biological materials, including autonomous patterning and dynamic, responsive

properties. We believe that this system constitutes a novel and useful approach for the development of functional and growable BC-based ELMs.

5 Discussion

This thesis has described two distinct strategies for the development of novel biological ELMs. In this chapter we will first discuss some of the general properties and limitations of each of these approaches, as well as future work to expand their utility. In addition, we will consider the future of the field of biological ELMs more generally.

5.1 *Bacillus subtilis* as a host for *de novo* biological ELM assembly

In section **3** we presented a strategy enabling extracellular conjugation of proteins secreted by *B. subtilis*. As outlined in section **1.5.1**, this work was motivated by a desire to create a modular platform for *de novo* biological ELM assembly. Specifically, to form a *de novo* biological ELM, secreted structural proteins would polymerise to form an extracellular matrix into which functional proteins could then be conjugated. In this section we will discuss the properties and limitations of our approach, as well as future work required to translate our system into a platform for *de novo* biological ELM assembly.

5.1.1 *Bacillus subtilis* protein secretion

We set out to create a modular system for protein secretion and conjugation, into which any heterologous protein could be seamlessly incorporated. A key requirement for this aim is a protein secretion host that can efficiently secrete any protein. We found that *B. subtilis* was able to secrete both native proteins (XynA and CelA) and heterologous proteins (ELP, SpyTag and SpyCatcher). Protein secretion yields were limited to tens of milligrams per litre, sufficient to enable proof of principle experiments and similar to yields obtained for *E. coli* biofilm ELMs. However, going forward, it will be desirable to increase these yields simply to improve the efficiency of biological ELM production. We found that secreted protein yields were hampered, in particular, by extracellular proteolysis (Figure 20). Consistent with previous reports, proteolysis was generally found to be more problematic when secreting heterologous proteins[163]. This is likely due to the fact that native secreted proteins and proteases have co-evolved to minimise excessive degradation. *B. subtilis* naturally secretes at least two quality control proteases and eight feeding proteases. Feeding proteases degrade extracellular proteins to provide amino acid nutrients for the cell. Quality control proteases play an important role in maintaining an optimal cell wall environment, degrading misfolded extracellular proteins which might otherwise block protein secretion translocases or interfere

with cell wall growth. Because of their important functions in maintaining general cell health, deletion of these proteases is detrimental to the cell. Nonetheless, in this study we worked exclusively with a strain in which all eight feeding proteases are deleted. In fact, a strain in which all ten known extracellular proteases are deleted has been developed[256]. This strain, although significantly impaired in cell growth, was able to secrete improved yields of a heterologous protein. In the future, therefore, it will be advantageous to utilise such strains, to optimise the secretion yields of heterologous proteins.

In the future, alternative strategies could be used to improve the spectrum of heterologous proteins which can be secreted from *B. subtilis* and the yields at which they can be produced. For example, it is known that the choice of signal peptide influences the yields of secreted heterologous proteins. However, for a given heterologous protein, the rules determining the optimal choice of signal peptide remain unknown. To solve this issue, one report screened a library of all known *B. subtilis* signal peptides to determine which conferred the highest yields for particular heterologous proteins[161]. It was found that the secretion yields were highly-variable depending on the signal peptide used and that different signal peptides directed different yields for given heterologous proteins. This screening approach could be relatively easily integrated into the genetic toolkit described in section **3.2.3**. A library of different signal peptide parts could be first pre-cloned into part vectors. To optimise the secretion of a given protein, the construct could then be assembled in a Golden Gate reaction using the library of different signal peptide parts. This library could be transformed into *B. subtilis* and the resultant strains screened for the highest secretion yields. However, the simplicity of this approach will be dependent on the ease with which secreted protein yields can be assayed. If the target protein is an enzyme which produces a simple readout such as colour change, high-yielding colonies could be identified easily on an agar plate. However, if the target protein is a structural protein – such as an ELP or spider silk fibroin – screening for high secretion yields may require a more complex method such as dot blotting or SDS-PAGE analysis.

This same strategy could be expanded further to screen for other genetic parts that might improve secretion yields. In this study we have focussed solely on the Sec protein secretion pathway, however, *B. subtilis* also possesses the Tat secretion machinery (described in detail in section **1.5.2**). In contrast to the Sec pathway, the Tat pathway secretes fully-folded

proteins and is therefore better able to handle certain proteins. In fact, many proteins that are incompatible with Sec pathway secretion are well-secreted by the Tat pathway, including fluorescent proteins[156], cofactor-containing proteins[157] and multiprotein complexes[158]. Therefore, in addition to Sec signal peptides, Tat signal peptides could be incorporated into the library of signal peptide parts to expand the versatility of the system. Further, while a single strong inducible expression system was used in this study, overexpression of secreted proteins may reduce cell growth rates and therefore result in decreased secreted protein yields. To find optimal expression levels, libraries of promoters, ribosome binding sites (RBSs) and terminators could be constructed and cloned into our genetic toolkit. Given proteins could then be assembled with these libraries and screened for the combination of promoter, RBS and terminator that result in the highest secretion yields.

Despite all of these possible solutions, there may still be given proteins that cannot be efficiently secreted by *B. subtilis* and therefore will be incompatible with our approach. To attempt to resolve this, it may be possible to transfer our approach to alternative protein secretion host organisms. While *E. coli* is generally not considered an ideal host organism for the secretion of a numerous heterologous proteins, various individual instances of successful protein secretion from *E. coli* have been reported. Notably, these reports include several important structural proteins, such as spider silk, elastin and resilin[224]. Otherwise, as outlined in section **1.5.2**, *S. cerevisiae* yeast is a widely-used heterologous protein secretion host and could be used as an alternative to *B. subtilis*. Importantly, however, it is not known whether the SpyTag-SpyCatcher system will function efficiently when secreted from alternative host organisms. While the SpyTag-SpyCatcher system is simple and versatile, potential obstacles can be envisioned. For instance, in the *S. cerevisiae* protein secretion pathway heterologous proteins can become glycosylated. In the case of the SpyTag-SpyCatcher system, glycosylation could interfere with the correct folding of the SpyCatcher or the reaction between the two domains.

5.1.2 Expanding the toolkit of *de novo* assembly

The results in section **3** demonstrate the feasibility and applicability of our approach in directing extracellular self-assembly. Following on from this, it is now possible to incorporate new genetic parts and designs into this system to expand its functionality.

Here, we have worked exclusively with a single fusion protein architecture, in which a protein of interest is sandwiched between two SpyParts. This design can result in end-to-end conjugation of fusion proteins or cyclisation. However, by varying the number and organisation of SpyParts within fusion proteins, numerous alternative structures could be formed. For instance, Sun et al. showed that mixing two purified SpyPart proteins – one containing three SpyTags and the other containing two SpyCatchers – resulted in the formation of an extended cross-linked polymer matrix[181]. At high concentrations, exceeding 1% protein (w/v), these proteins formed self-standing hydrogel materials. Others have modified the number and orientation of SpyParts within fusion proteins to create nonlinear protein conjugates, producing circular, tadpole, star, and H-shaped structures[215]. Remarkably, SpyParts have even been arranged within fusion proteins to create mechanically-interlocked polypeptide rings, known as catenanes[216]. Our genetic toolkit could be expanded relatively easily to enable the self-assembly of more complex protein-protein conjugate architectures such as these. Additionally, as outlined in section **1.5.3**, a number of orthogonal equivalents to the SpyTag-SpyCatcher system have now been described. Integrating these components into our genetic toolkit would, therefore, further expand users' control over protein-protein conjugate topology.

In this study we worked with just three proteins of interest, two lignocellulosic mass-degrading enzymes, XynA and CelA, and one structural protein, $ELP_{20\text{-}24}$. To further develop our system towards *de novo* biological ELM assembly, new structural and functional protein components can now be incorporated. A variety of structural protein components could be screened for successful secretion and self-assembly to form the material scaffold, such as amyloid fibre-forming proteins, collagens and elastins. However, it should be noted that recreating the natural processes of self-assembly of protein polymers may prove challenging. Taking collagen for example, monomers containing non-standard amino acids must associate into triple helical structures which subsequently self-assemble into fibres and become enzymatically cross-linked. Recreating such complex self-assembly processes in

system may not be feasible. Therefore, initial experiments should focus on relatively simple systems such as amyloid fibre-forming proteins. Interestingly, during biofilm formation, *B. subtilis* naturally secretes two proteins that self-assemble outside the cell: the amyloid-forming protein TasA and the hydrophobin protein BslA. Similarly to CsgA, which forms curli fibres, TasA is secreted into *B. subtilis* biofilms where it self-assembles into amyloid fibres[257]. Interestingly, it has been shown that heterologous proteins, as large as entire fluorescent proteins, can be fused to TasA without interfering with native fibre formation[40]. In addition, BslA plays an important role in the creation of the highly-hydrophobic *B. subtilis* biofilm surface[44]. Monomers of BslA are able to self-assemble into elastic films at oil-water and air-water interfaces[258]. In fact, the SpyTag-SpyCatcher system has been used to create functionalised monolayers of BslA[259]. Since they are both naturally secreted by *B. subtilis*, TasA and BslA may therefore be ideal initial candidates to create extracellular polymeric matrices.

Since it may be a challenge to recreate the self-assembly of natural structural proteins, as an alternative approach, it may be possible to use the SpyTag-SpyCatcher system itself to form protein scaffolds. As described above, SpyPart-containing fusion proteins can be designed to form extended polymeric networks and, at very high yields, hydrogel materials. Therefore *B. subtilis* strains could be engineered to secrete proteins in which SpyTag and SpyCatcher domains direct the extracellular formation of a polymeric protein scaffold. Further, the orthogonal SnoopTag and SnoopCatcher domains could then enable conjugation of additional functional protein domains.

Lastly, going forward, incorporating genetic control circuits into our system will enable control over the morphogenesis and dynamic properties of future *de novo* biological ELMs. As described in section **1.4.2**, various approaches have been developed to enable spontaneous patterning of simple microbial systems. Many of these approaches rely on genetic circuits incorporating quorum-sensing systems. For example, *E. coli* cells engineered to accumulate quorum sensing molecules and simultaneously to detect their presence at threshold levels, produce bullseye patterns on agar plates[126]. Similar genetic circuits could be engineered in *B. subtilis* and combined with *de novo* biological ELM assembly components to create materials with predefined, genetically-programmed morphology. Indeed, synthetic quorum sensing systems have already been engineered in *B. subtilis*[260]. Alternatively, genetic

circuits could be engineered to enable *B. subtilis* to sense various environmental stimuli and, in response, change the material properties of the ELM accordingly. Such genetic circuits could be designed in such a way as to create useful dynamic material properties. For instance, an ELM designed for bioremediation – degradation of environmental toxins or pollutants – could be engineered to screen the environment for the presence of specific chemicals and therefore to only produce degradative enzymes when required, reducing the cellular burden of heterologous protein expression in the absence of the target molecules.

5.2 BC biological ELMs produced by *S. cerevisiae* - *K. rhaeticus* co-cultures

In section **4** we outlined a method for production of BC-based biological ELMs with genetically programmable functional properties. As described in section **1.3** BC is a promising model biological ELM system. However, efforts to genetically engineer new BC material properties have so far remained relatively limited, in part due to a paucity of genetic tools and circuits for BC-producing hosts. Therefore, we set out to expand the capabilities for genetically-engineering BC materials by co-culturing a BC-producing bacterium with the model organism and synthetic biology host *S. cerevisiae*. In this section we discuss the advantages and limitations of our approach and explore future experiments to further extend this approach.

5.2.1 Limitations of the co-culture system

One potential limitation of our approach is the relative abundance of *K. rhaeticus* and *S. cerevisiae* co-cultures. As outlined in section **4.2.4**, our method enables functionalisation of BC using engineered *S. cerevisiae* strains. The efficiency of functionalisation will be highly-dependent not only on the efficiency of protein secretion, but also on the density of *S. cerevisiae* cells in the co-culture. As we found in the case of GFP, the yields of secreted protein were not sufficient to produce detectable levels of GFP-functionalisation. Since the *S. cerevisiae* protein secretion pathway is complex and poorly understood, engineering significantly increased protein secretion yields is likely to be a major challenge. However, it may instead be possible to generate co-cultures in which cell density of *S. cerevisiae* is increased. Based on our initial screening of co-culture conditions (Figure 29), we found that the yield of BC was dependent on the relative inoculation densities of *S. cerevisiae* and *K. rhaeticus*. Specifically, as the *S. cerevisiae* density is increased, the yield of BC decreases. This suggests that higher initial inoculation densities of *S. cerevisiae* result in increased final densities of *S. cerevisiae* and decreased final densities of *K. rhaeticus*. Therefore, simply by changing the relative inoculation densities of *S. cerevisiae* and *K. rhaeticus*, it may be possible to increase the final yields of secreted protein. Alternatively, going forward, it may be possible to genetically-program the final cell densities of *S. cerevisiae* and *K. rhaeticus* in co-culture conditions. Synthetic quorum sensing systems could be engineered into both species, enabling cell-cell communication and detection of cell densities. By coupling these genetic circuits to genes that influence growth rates, such as genes involved in amino acid

metabolism, the relative cell densities of the two species might be controlled and tuned. It should be noted, however, that increasing the *S. cerevisiae* cell density is likely to decrease *K. rhaeticus* cell density and therefore decrease BC yields. For given applications, users will therefore have to strike a balance between BC yields and functionalisation efficiencies.

An additional limitation of our system is the distribution of *S. cerevisiae* cells within the co-culture. As described in section **4.2.3**, the fact that majority of *S. cerevisiae* cells are found in the liquid layer below the pellicle limits the potential of our system. For instance, to engineer autonomous patterning of BC materials or to create dynamic, environmentally-responsive biosensor BC materials, *S. cerevisiae* cells must be incorporated within the BC layer. To solve this problem, we found that optiprep could be added to the culture medium, making *S. cerevisiae* cells buoyant and resulting in their incorporation into BC. However, since optiprep is an expensive reagent unsuitable for industrial scale production, an alternative solution is desirable. As outlined previously, one solution to this problem would be to use a more cost-effective density-modifying reagent. Ideally, incorporation of *S. cerevisiae* into BC could be engineered genetically, obviating the need for any modifications to the culture medium. A variety of genetic approaches could be explored. Firstly, *S. cerevisiae* could be engineered to display cellulose binding domains (CBDs) on its cell surface. Indeed, a number of cell surface anchor proteins have been described that enable the display of heterologous proteins on the *S. cerevisiae* cell surface. Similarly, *K. rhaeticus* and *S. cerevisiae* could be engineered to display cell surface proteins leading to cell-cell adhesion and therefore incorporation of *S. cerevisiae* into the BC layer. Alternatively, *S. cerevisiae* strains could be engineered to naturally float to the surface of the culture medium. It is known, for instance, that *S. cerevisiae* flocculation, directed by expression of the FLO11 protein, leads to the formation of multicellular aggregates. As aggregated cells grow, they accumulate and entrap bubbles of CO_2 which eventually float the aggregates to the surface of liquid cultures[261]. Gas vesicles offer an alternative potential approach to engineering buoyant *S. cerevisiae* cells. Gas vesicles are gas-filled, subcellular proteinaceous compartments. Bourdeau et al. recently demonstrated the successful formation of recombinantly-expressed gas vesicles in *E. coli*[262], resulting in buoyant cells which floated to surfaces of liquid cultures. Expressing the same gas vesicle proteins in *S. cerevisiae* may therefore create naturally buoyant strains, which become incorporated into BC layers.

5.2.2 *S. cerevisiae* - *K. rhaeticus* co-culture interactions

Inspired by kombucha, a pseudo-natural co-culture of yeast and BC-producing bacteria, we created *S. cerevisiae* - *K. rhaeticus* co-cultures in the lab. Interestingly, *S. cerevisiae* and *K. rhaeticus* exhibited an unexpected metabolic interaction when grown on sucrose medium. Specifically, the presence of *S. cerevisiae* significantly promoted the growth of *K. rhaeticus* in sucrose medium. It may be of interest to explore the nature of this metabolic interaction more rigorously using mass spectrometry methods. We speculate that *K. rhaeticus* is unable to efficiently utilise sucrose as a carbon source. When co-cultured with *S. cerevisiae*, which secretes invertase enzymes, extracellular glucose and fructose monosaccharides accumulate, which *K. rhaeticus* can metabolise more efficiently. As described in section **4.2.1** such metabolic co-dependencies are desirable in situations where a stable co-culture is required, ensuring neither species outcompetes the other. In the future, it would be advantageous to engineer co-dependence in our system, in this case by engineering *S. cerevisiae* to depend on the presence of *K. rhaeticus* for normal growth. One potential way to achieve this would be through exometabolite profiling. Here, *K. rhaeticus* would be grown in mono-culture and the spent medium analysed by mass spectrometry to identify accumulated metabolites. Based on this profile, specific auxotrophic mutant strains of *S. cerevisiae* can then be generated which cannot grow in the absence of externally-supplemented metabolites matching those accumulated by *K. rhaeticus*. Therefore, *K. rhaeticus* growth will result in the accumulation of a metabolite upon which *S. cerevisiae* is dependent. Alternatively, a mutant fitness profiling approach could be employed. Firstly, a library of barcoded *S. cerevisiae* mutants would be engineered. This pooled library would then be grown with or without co-cultured *K. rhaeticus*. For each condition, samples would be taken at the start and end of growth and the relative abundances of individual mutant strains at each point determined by DNA microarray hybridisation. Using this data, mutants in which fitness is significantly increased in the presence of *K. rhaeticus* can be identified, in effect, identifying *S. cerevisiae* mutants whose growth is promoted by *K. rhaeticus*. Notably, this method will not detect *S. cerevisiae* strains that are completely dependent on *K. rhaeticus* for growth, since these mutants cannot grow in mono-culture. However, strains which are not completely dependent on the presence of *K. rhaeticus* may, in fact, be preferable, since there will be an early stage

in co-culture in which neither species has grown to sufficient levels to be able to complement the other.

5.2.3 Expanding BC biological engineering

In this study we have focussed on engineering two novel properties into BC-based materials: enzyme functionalisation and sense-and-response. However, going forwards additional properties could be engineered into BC materials through co-cultured *S. cerevisiae* strains. Firstly, for a variety of downstream ELM development efforts, it may be useful to engineer cell-cell communication between *K. rhaeticus* and *S. cerevisiae*. As outlined in section **5.2.1**, synthetic cell-cell communication could enable coordination of *K. rhaeticus* and *S. cerevisiae* growth rates in co-cultures and therefore control over the relative cell densities of each population. Further, cell-cell communication systems are essential components of several forms of synthetic morphogenesis, such as Turing patterns and French Flag patterns. In addition, cross-species communication will enable transmission of signals and states between *K. rhaeticus* and *S. cerevisiae*. For example, it may be desirable to couple the activation of an *S. cerevisiae* biosensor to responses in both *K. rhaeticus* and *S. cerevisiae*. While synthetic cell-cell communication systems have been developed within various species of bacteria and yeast, there are to our knowledge no reports in the literature of yeast-bacteria, synthetic cell-cell communication. In *S. cerevisiae*, cell-cell communication systems have been developed based on peptide signalling and heterologously expressed plant hormones[263]. In *E. coli*, bacterial quorum-sensing systems are commonly used to engineer synthetic cell-cell communication[130]. As an initial step towards developing communication between *K. rhaeticus* and *S. cerevisiae*, bacterial cell-cell communications could be transplanted into yeast and vice versa. However, potential obstacles can be anticipated, for instance, it is not known whether *S. cerevisiae* will be able to synthesise bacteria quorum-sensing small molecules or whether bacterial quorum-sensing transcription factors can be re-engineered to function in *S. cerevisiae*. While it is unclear whether this strategy will be successful, it may be possible instead to engineer completely novel cell-cell communication systems. In principle, all that is needed to create a two-species cell-cell communication system is the molecular machinery to synthesise and also sense some small molecule which can diffuse between cells. One such candidate is cis-cis muconic acid (CCM). Reports in the literature have described how CCM can be both produced and detected in *E. coli*[264,265] and *S. cerevisiae*[266,267]. It may therefore be possible to use CCM to direct cross-species cell-cell communication between *K. rhaeticus* and *S. cerevisiae*.

Secondly, *S. cerevisiae* could be engineered to produce extracellular metabolites to functionalise BC. *S. cerevisiae* is a widely-used host for metabolic engineering and strains have been developed that are able to produce a variety of high value compounds, including vanilin, isobutanol, amorphadiene and many others[268]. While we focussed in section **4.2.4** solely on functionalisation by secretion of proteins, *S. cerevisiae* strains producing metabolites of interest could, therefore, be co-cultured with *K. rhaeticus* to produce BC endowed with novel properties.

5.2.4 Division of labour or a universal single host?

Our primary motivation for creating *S. cerevisiae* - *K. rhaeticus* co-cultures was the wealth of synthetic biology tools that already exist for *S. cerevisiae*. However, it is interesting to consider whether future work to develop BC-based ELMs should aim to divide labour between co-cultured strains or should focus on engineering a single, BC-producing host. The chief advantage of engineering a single, BC-producing host is the simplicity such a system would offer. We found that co-culturing *S. cerevisiae* with *K. rhaeticus* presented new challenges, such as balancing the cell densities of the two species and the localisation of *S. cerevisiae* within the liquid layer. In this respect, a one-species system may be preferable. In addition, BC-producing bacteria can be engineered to control the production of the BC matrix itself. Further, since BC-producing bacteria are naturally incorporated within BC pellicles, they are suitable hosts for controlling autonomous patterning of BC-based materials and for dynamic sense-and-response functions. However, as with all synthetic biology and biotechnology efforts, different host organisms offer distinct advantages and are better or worse suited for individual projects. Here, for example, it is not known whether BC-producing bacteria will be able to efficiently secrete heterologous proteins. By contrast, *S. cerevisiae* is known to be a good choice of host organism for protein secretion. There may in fact be scope to co-culture additional host organisms with *K. rhaeticus*, further expanding biological ELM engineering possibilities. Biological materials or molecules of interest could be incorporated into BC by co-culturing other microorganisms with *K. rhaeticus*, for instance, the electrically-conductive pili of *Geobacter sp.* or calcite precipitated by *Bacillus pasteurii*. Broadly, therefore, it seems clear that developing co-culture systems such as ours will help expand the potential range of BC-based ELM engineering efforts.

5.2.5 Potential applications

While the primary objective of this study was to simply push the boundaries of BC biological ELM engineering, the work presented in section **4.2** has some potential applications. In this section we discuss some of these applications and the obstacles to their development. Firstly, we found that our approach enabled the production of functionalised BC-based materials with a number of conceivable applications. As discussed in section **4.2.4**, several existing industrial processes utilise immobilised enzyme materials. Our system may represent a viable alternative process for manufacturing these and new types of functionalised materials. Theoretically, grown materials might require less manual intervention to manufacture, improving cost-effectiveness. Further, this approach enables functionalisation of a material under mild conditions, without the need for chemical cross-linking methods. However, as exemplified by with GFP, the yields of secreted protein obtained by our method may be limited. For any potential application, it will therefore be important that our approach is able to functionalise materials with sufficient levels of secreted protein. On top of this, our approach relies on the CBD-cellulose interaction to bind functionalising proteins into the BC matrix. Since this interaction is based on the correct folding of the CBD, potential applications must not involve exposure to harsh chemical or physical conditions that might disrupt the CBD fold – such as high temperature or extremes in salt concentration, pH or organic solvents. Lastly, many conceivable applications will require functionalised materials to be sterilised. However, it is difficult to envision a procedure that ensures sterilisation of materials without simultaneously abrogating the function of enzymes incorporated into the material.

In section **4.2.5**, we demonstrate how *S. cerevisiae* biosensor strains can be incorporated into BC to create growable biosensor materials. This system functions well with two different biosensor strains: one based on an intracellular β-estradiol sensitive synthetic transcription factor and one based on a transmembrane GPCR. In theory, numerous other biosensor strains from the literature could be adopted, to create a panel of grown biosensor materials. We have shown that BC-based biosensor materials can be dried under ambient conditions and rehydrated without impacting their sense-and-response function. However, it remains to be seen whether dried biosensor materials remain functional after long periods of storage, although future work is underway to address this question. If current materials are not

suitable for long-term storage, it may be worth exploring alternative methods for drying biosensor materials, such as lyophilisation, or cold storage conditions. While we use GFP as a reporter in this study, for deployment of biosensor materials to act as in-the-field diagnostics simpler, visible outputs will be advantageous. Therefore, biosensor strains could be engineered to couple sensing to the expression of a chromoprotein or chromogenic metabolite. However, we note that there is likely no real case for commercial development of biosensor materials using our approach. There is already precedent in the literature for paper-based *S. cerevisiae* biosensor materials which can detect pathogen markers in blood, soil and urine[252]. This approach used a relatively expensive glass fibre filter paper as a solid substrate (£110 for 100 discs each 75 mm in diameter), but is anticipated to work well on cheaper substrates. Therefore, our approach is unlikely to offer significant cost reduction either in terms of manufacturing processes or raw materials.

5.3 The future of biological ELMs

As outlined in the introduction to this thesis, the growing field of biological ELMs aims to recreate and engineer the natural processes of biological material assembly to develop new and useful materials. It is hoped that this field might eventually lead to a new paradigm in the production of materials. In this vision, clothing, construction materials, tools, furniture and many other everyday objects could be grown by genetically-engineered organisms. As described in section **1.1.2** these materials could have added advantages, such as sustainable production and degradation or the ability to sense and respond to their environment. This vision may seem outlandish, but when we consider the complexity of materials that natural biological systems have evolved to produce, it becomes apparent that biology itself will not be a limiting factor in this endeavour. Instead, impediments to achieving this goal will more likely come from an incomplete understanding of the natural processes of biological material assembly or an inability to precisely and predictable engineer biological systems. It remains an open question whether this vision will be attainable. For the remainder of this section we will discuss the future of the field and some of the obstacles that must be overcome.

As has been discussed in the introduction to this thesis, the majority of current efforts to develop biological ELMs have focussed on simple bacterial systems. This trend is motivated by their simplicity and genetic tractability. Since the field of biological ELM development is still very young, these systems will likely prove ideal testbeds to push the boundaries of what material properties can be engineered. Over the next years, research should focus on expanding the repertoire of biological ELM properties, with a major focus on recreating the processes of autonomous patterning, sense-and-response and functionalisation. For example, some of the strategies used to engineer autonomous pattern of cells, outlined in section **1.4.2**, could be recreated in *E. coli* biofilm and BC materials. In particular, since the field remains relatively immature, there should be an emphasis on developing fundamental, basic science rather than focussing on applications. Over time, as more and more complex properties can be engineered, real-world applications will be achievable.

In this thesis, we have explored two distinct approaches to develop biological ELMs: engineering a naturally-existing biological material and engineering a biological ELM *de novo*. In general, is one strategy likely to be more productive than the other? As is evident from the literature so far, working with relatively simple, naturally-existing biological

materials is an ideal starting point. Both BC materials and *E. coli* biofilm materials have been engineered to produce a variety of novel biological ELMs. In the future, attention may turn to more complex natural biological systems – marine molluscs could be engineered to produce modified mineralised materials, trees could be engineered to produce modified wood. However, since natural biological material systems have evolved in their host organisms, their biological and physical properties are, to an extent, predetermined and therefore limited. By contrast, engineering biological ELMs *de novo* presents a major challenge – in fact, there are to our knowledge no reports of this in the literature. However, if *de novo* biological ELM assembly were possible, this approach would, in theory, offer a far more flexible platform. Therefore, on-going advances in enabling technologies, such as DNA synthesis, DNA sequencing, automation and high-throughput screening, will likely be vital to efforts to develop *de novo* biological ELMs. Going forwards, it is likely that a combination of the two approaches will be productive. For instance, natural biological material systems can be reduced to their minimal components, removing natural regulatory components. Similarly, the development of *de novo* biological ELMs might be accelerated by looking to natural biological materials for inspiration.

One major potential obstacle to the application of biological ELMs is the presence of genetically-engineered cells within these materials. As has been discussed, many of the advantageous properties of biological ELMs rely on the fact that they contain living cells. For instance, living cells within a construction material could enable self-healing of damaged materials. Alternatively, living cells within a textile could detect increases in temperature and remodel the material to make it more breathable. However, it is unclear how genetically-engineered organisms will fit into public perception and legal framework in the future. These challenges remain distant, but must be addressed if biological ELMs are to become real-world materials.

Bibliography

(1) Wang, Q., Nemoto, M., Li, D., Weaver, J. C., Weden, B., Stegemeier, J., Bozhilov, K. N., Wood, L. R., Milliron, G. W., Kim, C. S., Dimasi, E., and Kisailus, D. (2013) Phase transformations and structural developments in the radular teeth of *Cryptochiton stelleri*. *Adv. Funct. Mater. 23*, 2908–2917.

(2) Su, R. S. C., Kim, Y., and Liu, J. C. (2014) Resilin: Protein-based elastomeric biomaterials. *Acta Biomater. 10*, 1601–1611.

(3) Malvankar, N. S., Vargas, M., Nevin, K., Tremblay, P., Evans-lutterodt, K., and Nykypanchuk, D. (2015) Structural basis for metallic-like conductivity in microbial nanowires. *MBio 6*, 1–10.

(4) Chessher, A., Breitling, R., and Takano, E. (2015) Bacterial microcompartments: biomaterials for synthetic biology-based compartmentalization strategies. *ACS Biomater. Sci. Eng.* 150518142250000.

(5) Rothschild, L. J. (2016) Synthetic biology meets bioprinting: enabling technologies for humans on Mars (and Earth). *Biochem. Soc. Trans. 44*, 1158–1164.

(6) Geyer, R., Jambeck, J. R., and Law, K. L. (2017) Production, use, and fate of all plastics ever made. *Sci. Adv. 3*, e1700782.

(7) Römer, L., and Scheibel, T. (2008) The elaborate structure of spider silk: structure and function of a natural high performance fiber. *Prion 2*, 154–161.

(8) Bolt Threads – Bolt Threads Brings a Glimpse of the Future of Advanced Materials to SXSW.

(9) Modern Meadow Launches Zoa, the First Ever Biofabricated Leather Material Brand On view this Fall at SoHo Pop-Up and the Museum of Modern Art.

(10) Chen, A. Y., Zhong, C., and Lu, T. K. (2015) Engineering living functional materials. *ACS Synth. Biol. 4*, 8–11.

(11) Nguyen, P. Q. (2017) Synthetic biology engineering of biofilms as nanomaterials factories. *Biochem. Soc. Trans. 45*, 585–597.

(12) Nguyen, P. Q., Courchesne, N. D., Duraj-thatte, A., Praveschotinunt, P., and Joshi, N. S. (2018) Engineered living materials: prospects and challenges for using biological systems to direct the assembly of smart materials. *Adv. Mater. 1704847*, 1–34.

(13) Sunde, M., Serpella, L., Bartlama, M., Frasera, P., Pepysa, M., and Blakea, C. (1997) Common core structure of amyloid fibrils by synchrotron X-ray diffraction. *J. Mol. Biol. 273*, 729–739.

(14) Jimenez, J. L., Nettleton, E. J., Bouchard, M., Robinson, C. V., Dobson, C. M., and Saibil, H. R. (2002) The protofilament structure of insulin amyloid fibrils. *Proc. Natl. Acad. Sci. 99*, 9196–9201.

(15) Fowler, D. M., Koulov, A. V., Balch, W. E., and Kelly, J. W. (2007) Functional amyloid - from bacteria to humans. *Trends Biochem. Sci. 32*, 217–224.

(16) Blanco, L. P., Evans, M. L., Smith, D. R., Badtke, M. P., and Chapman, M. R. (2012) Diversity, biogenesis and function of microbial amyloids. *Trends Microbiol. 20*, 66–73.

(17) Knowles, T. P., Fitzpatrick, A. W., Meehan, S., Mott, H. R., Vendruscolo, M., Dobson, C. M., and Welland, M. E. (2007) Role of intermolecular forces in protein nanofibrils. *Science 318*, 1900–1903.

(18) Chapman, M. R., Robinson, L. S., Pinkner, J. S., Roth, R., Heuser, J., Hammar, M., Normark, S., and Hultgren, S. J. (2002) Role of *Escherichia coli* curli operons in directing amyloid fibre formation. *Science (80-.). 295*, 851–855.

(19) Hall-Stoodley, L., Costerton, J. W., and Stoodley, P. (2004) Bacterial biofilms: From the natural environment to infectious diseases. *Nat. Rev. Microbiol. 2*, 95–108.

(20) Cao, B., Zhao, Y., Kou, Y., Ni, D., Zhang, X. C., and Huang, Y. (2014) Structure of the nonameric bacterial amyloid secretion channel. *Proc. Natl. Acad. Sci. 111*, E5439–E5444.

(21) Barnhart, M. M., and Chapman, M. R. (2006) Curli biogenesis and function. *Annu. Rev. Microbiol. 60*, 131–47.

(22) Chen, A. Y., Deng, Z., Billings, A. N., Seker, U. O. S., Lu, M. Y., Citorik, R. J., Zakeri, B., and Lu, T. K. (2014) Synthesis and patterning of tunable multiscale materials with engineered cells. *Nat. Mater. 13*, 515–23.

(23) Nguyen, P. Q., Botyanszki, Z., Tay, P. K. R., and Joshi, N. S. (2014) Programmable biofilm-based materials from

engineered curli nanofibres. *Nat. Commun. 5*, 4945.

(24) Zakeri, B., Fierer, J. O., Celik, E., Chittock, E. C., Schwarz-Linek, U., Moy, V. T., and Howarth, M. (2012) Peptide tag forming a rapid covalent bond to a protein, through engineering a bacterial adhesin. *Proc. Natl. Acad. Sci.*

(25) Botyanszki, Z., Tay, P. K. R., Nguyen, P. Q., Nussbaumer, M. G., and Joshi, N. S. (2015) Engineered catalytic biofilms: Site-specific enzyme immobilization onto *E. coli* curli nanofibers. *Biotechnol. Bioeng. 110*, 2016–2024.

(26) Nussbaumer, M. G., Nguyen, P. Q., Tay, P. K. R., Naydich, A., Hysi, E., Botyanszki, Z., and Joshi, N. S. (2017) Bootstrapped biocatalysis: biofilm-derived materials as reversibly functionalizable multi-enzyme surfaces. *ChemCatChem 9*, 4328–4333.

(27) Dorval Courchesne, N.-M., Duraj-Thatte, A., Tay, P. K. R., Nguyen, P. Q., and Joshi, N. S. (2016) Scalable production of genetically engineered nanofibrous macroscopic materials via filtration. *ACS Biomater. Sci. Eng.* acsbiomaterials.6b00437.

(28) Seker, U. O. S., Chen, A. Y., Citorik, R. J., and Lu, T. K. (2017) Synthetic biogenesis of bacterial amyloid nanomaterials with tunable inorganic-organic interfaces and electrical conductivity. *ACS Synth. Biol. 6*, 266–275.

(29) Reardon, P. N., and Mueller, K. T. (2013) Structure of the type IVa major pilin from the electrically conductive bacterial nanowires of *Geobacter sulfurreducens*. *J. Biol. Chem. 288*, 29260–29266.

(30) Tan, Y., Adhikari, R. Y., Malvankar, N. S., Pi, S., Ward, J. E., Woodard, T. L., Nevin, K. P., Xia, Q., Tuominen, M. T., and Lovley, D. R. (2016) Synthetic biological protein nanowires with high conductivity. *Small* 4481–4485.

(31) Kalyoncu, E., Ahan, R. E., Olmez, T. T., and Safak Seker, U. O. (2017) Genetically encoded conductive protein nanofibers secreted by engineered cells. *RSC Adv. 7*, 32543–32551.

(32) Zhong, C., Gurry, T., Cheng, A. a, Downey, J., Deng, Z., Stultz, C. M., and Lu, T. K. (2014) Strong underwater adhesives made by self-assembling multi-protein nanofibres. *Nat. Nanotechnol. 9*, 858–866.

(33) Lin, Q., Gourdon, D., Sun, C. J., Holten-Andersen, N., Anderson, T. H., Waite, J. H., and Israelachvili, J. N. (2007) Adhesion mechanisms of the mussel foot proteins mfp-1 and mfp-3. *Proc. Natl. Acad. Sci. U. S. A. 104*, 3782–3786.

(34) Wei, W., Yu, J., Broomell, C., Israelachvili, J. N., and Waite, J. H. (2013) Hydrophobic enhancement of dopa-mediated adhesion in a mussel foot protein. *J. Am. Chem. Soc. 135*, 377–383.

(35) Lu, Q., Danner, E., Waite, J. H., Israelachvili, J. N., Zeng, H., and Hwang, D. S. (2013) Adhesion of mussel foot proteins to different substrate surfaces. *J. R. Soc. Interface 10*, 20120759.

(36) Tay, P. K. R., Nguyen, P. Q., and Joshi, N. S. (2017) A synthetic circuit for mercury bioremediation using self-assembling functional amyloids. *ACS Synth. Biol. 6*, 1841–1850.

(37) Hidalgo, G., Chen, X., Hay, A. G., and Lion, L. W. (2010) Curli produced by *Escherichia coli* phl628 provide protection from hg(ii)∇ . *Appl. Environ. Microbiol. 76*, 6939–6941.

(38) Van Gerven, N., Goyal, P., Vandenbussche, G., De Kerpel, M., Jonckheere, W., De Greve, H., and Remaut, H. (2014) Secretion and functional display of fusion proteins through the curli biogenesis pathway. *Mol. Microbiol. 91*, 1022–1035.

(39) Cairns, L. S., Hobley, L., and Stanley-Wall, N. R. (2014) Biofilm formation by *Bacillus subtilis*: new insights into regulatory strategies and assembly mechanisms. *Mol. Microbiol. 93*, 587–598.

(40) Vogt, C. M., Schraner, E. M., Aguilar, C., and Eichwald, C. (2016) Heterologous expression of antigenic peptides in *Bacillus subtilis* biofilms. *Microb. Cell Fact.* 1–12.

(41) van Dijl, J. M., and Hecker, M. (2013) *Bacillus subtilis*: from soil bacterium to super-secreting cell factory. *Microb. Cell Fact. 12*, 3.

(42) Epstein, A. K., Pokroy, B., Seminara, A., and Aizenberg, J. (2011) Bacterial biofilm shows persistent resistance to liquid wetting and gas penetration. *Proc. Natl. Acad. Sci. 108*, 995–1000.

(43) Hobley, L., Ostrowski, A., Rao, F. V, Bromley, K. M., Porter, M., Prescott, A. R., MacPhee, C. E., van Aalten, D. M. F., and Stanley-Wall, N. R. (2013) BslA is a self-assembling bacterial hydrophobin that coats the *Bacillus subtilis* biofilm. *Proc. Natl. Acad. Sci. 110*, 13600–13605.

(44) Kobayashi, K., and Iwano, M. (2012) BslA(YuaB) forms a hydrophobic layer on the surface of *Bacillus subtilis* biofilms. *Mol. Microbiol. 85*, 51–66.

(45) Liu, J., Prindle, A., Humphries, J., Gabalda-Sagarra, M., Asally, M., Lee, D. Y. D., Ly, S., Garcia-Ojalvo, J., and Süel, G. M. (2015) Metabolic co-dependence gives rise to collective oscillations within biofilms. *Nature 523*, 550–554.

(46) Prindle, A., Liu, J., Asally, M., Ly, S., Garcia-Ojalvo, J., and Süel, G. M. (2015) Ion channels enable electrical communication in bacterial communities. *Nature 527*, 59–63.

(47) Humphries, J., Xiong, L., Liu, J., Prindle, A., Yuan, F., Arjes, H. A., Tsimring, L., and Süel, G. M. (2017) Species-independent attraction to biofilms through electrical signaling. *Cell 168*, 200–209.e12.

(48) Liu, J., Martinez-Corral, R., Prindle, A., Lee, D. Y. D., Larkin, J., Gabalda-Sagarra, M., Garcia-Ojalvo, J., and Süel, G. M. (2017) Coupling between distant biofilms and emergence of nutrient time-sharing. *Science (80-.). 356*, 638–642.

(49) Dueholm, M. S., Albertsen, M., Otzen, D., and Nielsen, P. H. (2012) Curli functional amyloid systems are phylogenetically widespread and display large diversity in operon and protein structure. *PLoS One 7*, e51274.

(50) Klemm, D., Heublein, B., Fink, H. P., and Bohn, A. (2005) Cellulose: Fascinating biopolymer and sustainable raw material. *Angew. Chemie - Int. Ed. 44*, 3358–3393.

(51) Römling, U., and Galperin, M. Y. (2015) Bacterial cellulose biosynthesis: Diversity of operons, subunits, products, and functions. *Trends Microbiol. 23*, 545–557.

(52) Jang, W. D., Hwang, J. H., Kim, H. U., Ryu, J. Y., and Lee, S. Y. (2017) Bacterial cellulose as an example product for sustainable production and consumption. *Microb. Biotechnol.*

(53) De Roos, J., and De Vuyst, L. (2018) Acetic acid bacteria in fermented foods and beverages. *Curr. Opin. Biotechnol. 49*, 115–119.

(54) Lee, K. Y., Buldum, G., Mantalaris, A., and Bismarck, A. (2014) More than meets the eye in bacterial cellulose: Biosynthesis, bioprocessing, and applications in advanced fiber composites. *Macromol. Biosci. 14*, 10–32.

(55) Huang, Y., Zhu, C., Yang, J., Nie, Y., Chen, C., and Sun, D. (2014) Recent advances in bacterial cellulose. *Cellulose 21*, 1–30.

(56) Morgan, J. L. W., Strumillo, J., and Zimmer, J. (2013) Crystallographic snapshot of cellulose synthesis and membrane translocation. *Nature 493*, 181–186.

(57) Hestrin, S., and Schramm, M. (1954) Synthesis of cellulose by *Acetobacter xylinum* 2 Preparation of freeze-dried cells capable of polymerizing glucose to cellulose. *Biochem. J. 58*, 345–352.

(58) Zaar, K. (1979) Visualization of pores (export sites) correlated with cellulose production in the envelope of the gram-negative bacterium *Acetobacter xylinum*. *Cell 80*.

(59) Brown, R. M., Willison, J. H., and Richardson, C. L. (1976) Cellulose biosynthesis in *Acetobacter xylinum:* visualization of the site of synthesis and direct measurement of the in vivo process. *Proc. Natl. Acad. Sci. U. S. A. 73*, 4565–4569.

(60) Ross, P., Mayer, R., and Benziman, M. (1991) Cellulose biosynthesis and function in bacteria. *Microbiol. Rev. 55*, 35–58.

(61) Picheth, G. F., Pirich, C. L., Sierakowski, M. R., Woehl, M. A., Sakakibara, C. N., de Souza, C. F., Martin, A. A., da Silva, R., and de Freitas, R. A. (2017) Bacterial cellulose in biomedical applications: A review. *Int. J. Biol. Macromol. 104*, 97–106.

(62) Yano, H. (2005) Optically transparent composites reinforced with networks of bacterial nanofibers. *Adv. Mater. 17*.

(63) Hsieh, Y. C., Yano, H., Nogi, M., and Eichhorn, S. J. (2008) An estimation of the Young's modulus of bacterial cellulose filaments. *Cellulose 15*, 507–513.

(64) Meirovitch, S., Shtein, Z., Ben-Shalom, T., Lapidot, S., Tamburu, C., Hu, X., Kluge, J. A., Raviv, U., Kaplan, D. L., and Shoseyov, O. (2016) Spider silk-CBD-cellulose nanocrystal composites: Mechanism of assembly. *Int. J. Mol. Sci. 17*.

(65) Li, W., Guo, R., Lan, Y., Zhang, Y., Xue, W., and Zhang, Y. (2014) Preparation and properties of cellulose nanocrystals reinforced collagen composite films. *J. Biomed. Mater. Res. - Part A 102*, 1131–1139.

(66) Wan, Z., Wang, L., Ma, L., Sun, Y., and Yang, X. (2017) Controlled hydrophobic biosurface of bacterial cellulose

nanofibers through self-assembly of natural zein protein. *ACS Biomater. Sci. Eng. 3*, 1595–1604.

(67) Saska, S., Teixeira, L. N., Tambasco de Oliveira, P., Minarelli Gaspar, A. M., Lima Ribeiro, S. J., Messaddeq, Y., and Marchetto, R. (2012) Bacterial cellulose-collagen nanocomposite for bone tissue engineering. *J. Mater. Chem. 22*, 22102.

(68) Li, Y., Jiang, H., Zheng, W., Gong, N., Chen, L., Jiang, X., and Yang, G. (2015) Bacterial cellulose–hyaluronan nanocomposite biomaterials as wound dressings for severe skin injury repair. *J. Mater. Chem. B 3*, 3498–3507.

(69) Kirdponpattara, S., Khamkeaw, A., Sanchavanakit, N., Pavasant, P., and Phisalaphong, M. (2015) Structural modification and characterization of bacterial cellulose-alginate composite scaffolds for tissue engineering. *Carbohydr. Polym. 132*, 146–155.

(70) Wan, Y., Gao, C., Han, M., Liang, H., Ren, K., Wang, Y., and Luo, H. (2011) Preparation and characterization of bacterial cellulose/heparin hybrid nanofiber for potential vascular tissue engineering scaffolds. *Polym. Adv. Technol. 22*, 2643–2648.

(71) Wang, J., Wan, Y., and Huang, Y. (2012) Immobilisation of heparin on bacterial cellulose-chitosan nano-fibres surfaces via the cross-linking technique. *IET Nanobiotechnology 6*, 52.

(72) Fürsatz, M., Skog, M., Sivlér, P., Palm, E., Aronsson, C., Skallberg, A., Greczynski, G., Khalaf, H., Bengtsson, T., and Aili, D. (2017) Functionalization of bacterial cellulose wound dressings with the antimicrobial peptide ε-poly-L-Lysine. *Biomed. Mater.* 0–16.

(73) Saska, S., Scarel-Caminaga, R. M., Teixeira, L. N., Franchi, L. P., Santos, R. A. Dos, Gaspar, A. M. M., De Oliveira, P. T., Rosa, A. L., Takahashi, C. S., Messaddeq, Y., Ribeiro, S. J. L., and Marchetto, R. (2012) Characterization and in vitro evaluation of bacterial cellulose membranes functionalized with osteogenic growth peptide for bone tissue engineering. *J. Mater. Sci. Mater. Med. 23*, 2253–2266.

(74) Shi, Q., Li, Y., Sun, J., Zhang, H., Chen, L., Chen, B., Yang, H., and Wang, Z. (2012) The osteogenesis of bacterial cellulose scaffold loaded with bone morphogenetic protein-2. *Biomaterials 33*, 6644–6649.

(75) Andrade, F. K., Costa, R., Domingues, L., Soares, R., and Gama, M. (2010) Improving bacterial cellulose for blood vessel replacement: Functionalization with a chimeric protein containing a cellulose-binding module and an adhesion peptide. *Acta Biomater. 6*, 4034–4041.

(76) Pertile, R., Moreira, S., Andrade, F., Domingues, L., and Gama, M. (2012) Bacterial cellulose modified using recombinant proteins to improve neuronal and mesenchymal cell adhesion. *Biotechnol. Prog. 28*, 526–532.

(77) Stumpf, T. R., Yang, X., Zhang, J., and Cao, X. (2016) In situ and ex situ modifications of bacterial cellulose for applications in tissue engineering. *Mater. Sci. Eng. C 82*, 372–383.

(78) Couso, Ro. O., Ielpi, L., and Dankert, M. A. (1987) A Xanthan-gum-like polysaccharide from *Acetobacter xylinum*. *J. Gen. Microbiol. 133*, 2123–2135.

(79) Ishida, T., Sugano, Y., Nakai, T., and Shoda, M. (2002) Effects of acetan on production of bacterial cellulose by *Acetobacter xylinum*. *Biosci. Biotechnol. Biochem. 66*, 1677–81.

(80) Wu, R. Q., Li, Z. X., Yang, J. P., Xing, X. H., Shao, D. Y., and Xing, K. L. (2010) Mutagenesis induced by high hydrostatic pressure treatment: A useful method to improve the bacterial cellulose yield of a *Gluconoacetobacter xylinus* strain. *Cellulose 17*, 399–405.

(81) Kuo, C. H., Teng, H. Y., and Lee, C. K. (2015) Knock-out of glucose dehydrogenase gene in *Gluconacetobacter xylinus* for bacterial cellulose production enhancement. *Biotechnol. Bioprocess Eng. 20*, 18–25.

(82) Mangayil, R., Rajala, S., Pammo, A., Sarlin, E., Luo, J., Santala, V., Karp, M., and Tuukkanen, S. (2017) Engineering and characterization of bacterial nanocellulose films as low cost and flexible sensor material. *ACS Appl. Mater. Interfaces 9*, 19048–19056.

(83) Yadav, V., Paniliatis, B. J., Shi, H., Lee, K., Cebe, P., and Kaplan, D. L. (2010) Novel in vivo-degradable cellulose-chitin copolymer from metabolically engineered *Gluconacetobacter xylinus*. *Appl. Environ. Microbiol. 76*, 6257–6265.

(84) Fang, J., Kawano, S., Tajima, K., and Kondo, T. (2015) *In vivo* curdlan/cellulose bionanocomposite synthesis by genetically modified *Gluconacetobacter xylinus*. *Biomacromolecules 16*, 3154–3160.

(85) McIntosh, M., Stone, B. A., and Stanisich, V. A. (2005) Curdlan and other bacterial (1→3)-β-D-glucans. *Appl.*

Microbiol. Biotechnol. 68, 163–173.

(86) Florea, M., Hagemann, H., Santosa, G., Abbott, J., Micklem, C. N., Spencer-Milnes, X., de Arroyo Garcia, L., Paschou, D., Lazenbatt, C., Kong, D., Chughtai, H., Jensen, K., Freemont, P. S., Kitney, R., Reeve, B., and Ellis, T. (2016) Engineering control of bacterial cellulose production using a genetic toolkit and a new cellulose-producing strain. *Proc. Natl. Acad. Sci.* 201522985.

(87) Freitas, F., Alves, V. D., and Reis, M. A. M. (2011) Advances in bacterial exopolysaccharides: From production to biotechnological applications. *Trends Biotechnol. 29*, 388–398.

(88) Thongsomboon, W., Serra, D. O., Possling, A., Hadjineophytou, C., Hengge, R., and Cegelski, L. (2018) Phosphoethanolamine cellulose: A naturally produced chemically modified cellulose. *Science (80-.). 359*, 334–338.

(89) Florea, M., Reeve, B., Abbott, J., Freemont, P. S., and Ellis, T. (2016) Genome sequence and plasmid transformation of the model high-yield bacterial cellulose producer *Gluconacetobacter hansenii* ATCC 53582. *Sci. Rep. 6*, 1–9.

(90) Goers, L., Freemont, P., and Polizzi, K. M. (2014) Co-culture systems and technologies: taking synthetic biology to the next level. *J. R. Soc. Interface 11*.

(91) Hays, S. G., Patrick, W. G., Ziesack, M., Oxman, N., and Silver, P. A. (2015) Better together: Engineering and application of microbial symbioses. *Curr. Opin. Biotechnol. 36*, 40–49.

(92) Zhou, K., Qiao, K., Edgar, S., and Stephanopoulos, G. (2015) Distributing a metabolic pathway among a microbial consortium enhances production of natural products. *Nat. Biotechnol. 33*, 377–383.

(93) Qin, G., Panilaitis, B. J., and Kaplan, Z. S. D. L. (2014) A cellulosic responsive "living" membrane. *Carbohydr. Polym. 100*, 40–45.

(94) Drachuk, I., Harbaugh, S., Geryak, R., Kaplan, D. L., Tsukruk, V. V., and Kelley-Loughnane, N. (2017) Immobilization of recombinant *e. coli* cells in a bacterial cellulose-silk composite matrix to preserve biological function. *ACS Biomater. Sci. Eng. 3*, 2278–2292.

(95) Greenwalt, C. J., Steinkraus, K. H., and Ledford, R. a. (2000) Kombucha, the fermented tea: microbiology, composition, and claimed health effects. *J. Food Prot. 63*, 976–981.

(96) May, A. N., Medina, J., Alcock, J., Maley, C., and Aktipis, A. (2017) Kombucha as a model system for multispecies microbial cooperation: theoretical promise, methodological challenges and new solutions "in solution." *bioRxiv* 214478.

(97) Jayabalan, R., Malbaša, R. V., Lončar, E. S., Vitas, J. S., and Sathishkumar, M. (2014) A review on kombucha tea-microbiology, composition, fermentation, beneficial effects, toxicity, and tea fungus. *Compr. Rev. Food Sci. Food Saf. 13*, 538–550.

(98) Coton, M., Pawtowski, A., Taminiau, B., Burgaud, G., Deniel, F., Coulloumme-Labarthe, L., Fall, A., Daube, G., and Coton, E. (2017) Unraveling microbial ecology of industrial-scale Kombucha fermentations by metabarcoding and culture-based methods. *FEMS Microbiol. Ecol. 93*, 1–16.

(99) Teoh, A. L., Heard, G., and Cox, J. (2004) Yeast ecology of Kombucha fermentation. *Int. J. Food Microbiol. 95*, 119–126.

(100) Chen, C., and Liu, B. Y. (2000) Changes in major components of tea fungus metabolites during prolonged fermentation. *J. Appl. Microbiol. 89*, 834–839.

(101) Dufresne, C., and Farnworth, E. (2000) Tea, Kombucha, and health: A review. *Food Res. Int. 33*, 409–421.

(102) Liu, C. H., Hsu, W. H., Lee, F. L., and Liao, C. C. (1996) The isolation and identification of microbes from a fermented tea beverage, Haipao, and their interactions during Haipao fermentation. *Food Microbiol. 13*, 407–415.

(103) Dima, S. O., Panaitescu, D. M., Orban, C., Ghiurea, M., Doncea, S. M., Fierascu, R. C., Nistor, C. L., Alexandrescu, E., Nicolae, C. A., Trica, B., Moraru, A., and Oancea, F. (2017) Bacterial nanocellulose from side-streams of kombucha beverages production: Preparation and physical-chemical properties. *Polymers (Basel). 9*, 5–10.

(104) Podolich, O., Zaets, I., Kukharenko, O., Orlovska, I., Reva, O., Khirunenko, L., Sosnin, M., Haidak, A., Shpylova, S., Rabbow, E., Skoryk, M., Kremenskoy, M., Demets, R., Kozyrovska, N., and de Vera, J.-P. (2017) Kombucha multimicrobial community under simulated spaceflight and martian conditions. *Astrobiology 17*, 459–469.

(105) Aizenberg, J. (2004) Crystallization in patterns: A bio-inspired approach. *Adv. Mater. 16*, 1295–1302.

(106) Kröger, N., and Poulsen, N. (2008) Diatoms—from cell wall biogenesis to nanotechnology. *Annu. Rev. Genet. 42*, 83–107.

(107) Bozarth, A., Maier, U. G., and Zauner, S. (2009) Diatoms in biotechnology: Modern tools and applications. *Appl. Microbiol. Biotechnol. 82*, 195–201.

(108) Hildebrand, M. (2005) Prospects of Manipulating Diatom Silica Nanostructure. *J. Nanosci. Nanotechnol. 5*, 146–157.

(109) Sumper, M., and Brunner, E. (2008) Silica biomineralisation in diatoms: The model organism *Thalassiosira pseudonana*. *ChemBioChem 9*, 1187–1194.

(110) Ford, N. R., Hecht, K. A., Hu, D. H., Orr, G., Xiong, Y., Squier, T. C., Rorrer, G. L., and Roesijadi, G. (2016) Antigen binding and site-directed labeling of biosilica-immobilized fusion proteins expressed in diatoms. *ACS Synth. Biol. 5*, 193–199.

(111) Poulsen, N., Berne, C., Spain, J., and Kröger, N. (2007) Silica immobilization of an enzyme through genetic engineering of the diatom *Thalassiosira pseudonana*. *Angew. Chemie - Int. Ed. 46*, 1843–1846.

(112) Sheppard, V. C., Scheffel, A., Poulsen, N., and Kröger, N. (2012) Live diatom silica immobilization of multimeric and redox-active enzymes. *Appl. Environ. Microbiol. 78*, 211–218.

(113) Kröger, N. (2007) Prescribing diatom morphology: toward genetic engineering of biological nanomaterials. *Curr. Opin. Chem. Biol. 11*, 662–669.

(114) Bazylinski, D., and Schu, D. (2009) Biomineralization and assembly of the bacterial magnetosome chain. *Microbe 4*, 124–130.

(115) Yan, L., Zhang, S., Chen, P., Liu, H., Yin, H., and Li, H. (2012) Magnetotactic bacteria, magnetosomes and their application. *Microbiol. Res. 167*, 507–19.

(116) Ohuchi, S., and Schüler, D. (2009) In vivo display of a multisubunit enzyme complex on biogenic magnetic nanoparticles. *Appl. Environ. Microbiol. 75*, 7734–7738.

(117) Pollithy, A., Romer, T., Lang, C., Müller, F. D., Helma, J., Leonhardt, H., Rothbauer, U., and Schüler, D. (2011) Magnetosome expression of functional camelid antibody fragments (nanobodies) in *Magnetospirillum gryphiswaldense*. *Appl. Environ. Microbiol. 77*, 6165–6171.

(118) Borg, S., Hofmann, J., Pollithy, A., Lang, C., and Schüler, D. (2014) New vectors for chromosomal integration enable high-level constitutive or inducible magnetosome expression of fusion proteins in *Magnetospirillum gryphiswaldense*. *Appl. Environ. Microbiol. 80*, 2609–2616.

(119) Kolinko, I., Lohße, A., Borg, S., Raschdorf, O., Jogler, C., Tu, Q., Pósfai, M., Tompa, E., Plitzko, J. M., Brachmann, A., Wanner, G., Müller, R., Zhang, Y., and Schüler, D. (2014) Biosynthesis of magnetic nanostructures in a foreign organism by transfer of bacterial magnetosome gene clusters. *Nat. Nanotechnol. 9*, 193–7.

(120) Dhami, N. K., Reddy, M. S., and Mukherjee, A. (2013) Biomineralization of calcium carbonates and their engineered applications: a review. *Front. Microbiol. 4*, 314.

(121) Bang, S. S., Lippert, J. J., Yerra, U., Mulukutla, S., and Ramakrishnan, V. (2010) Microbial calcite, a bio-based smart nanomaterial in concrete remediation. *Int. J. Smart Nano Mater. 1*, 28–39.

(122) Fujita, Y., Redden, G. D., Ingram, J. C., Cortez, M. M., Ferris, F. G., and Smith, R. W. (2004) Strontium incorporation into calcite generated by bacterial ureolysis. *Geochim. Cosmochim. Acta 68*, 3261–3270.

(123) Warren, L. A., Maurice, P. A., Parmar, N., and Ferris, F. G. (2001) Microbially mediated calcium carbonate precipitation: Implications for Interpreting calcite precipitation and for solid-phase capture of inorganic contaminants. *Geomicrobiol. J. 18*, 93–115.

(124) Teague, B. P., Guye, P., and Weiss, R. (2016) Synthetic morphogenesis. *Cold Spring Harb. Perspect. Biol. 8*, 1–16.

(125) Scholes, N. S., and Isalan, M. (2017) A three-step framework for programming pattern formation. *Curr. Opin. Chem. Biol. 40*, 1–7.

(126) Basu, S., Gerchman, Y., Collins, C. H., Arnold, F. H., and Weiss, R. (2005) A synthetic multicellular system for

programmed pattern formation. *Nature 434*, 1130–1134.

(127) Sohka, T., Heins, R. A., and Ostermeier, M. (2009) Morphogen-defined patterning of *Escherichia coli* enabled by an externally tunable band-pass filter. *J. Biol. Eng. 3*, 1–9.

(128) Grant, P. K., Dalchau, N., Brown, J. R., Federici, F., Rudge, T. J., Yordanov, B., Patange, O., Phillips, A., and Haseloff, J. (2016) Orthogonal intercellular signaling for programmed spatial behavior. *Mol. Syst. Biol. 12*, 849–849.

(129) Boehm, C. R., Grant, P. K., and Haseloff, J. (2017) Programmed hierarchical patterning of bacterial populations. *bioRxiv* 204925.

(130) Scott, S. R., and Hasty, J. (2016) Quorum sensing communication modules for microbial consortia. *ACS Synth. Biol.*

(131) Borek, B., Hasty, J., and Tsimring, L. (2016) Turing patterning using gene circuits with gas-induced degradation of quorum sensing molecules. *PLoS One 11*, e0153679.

(132) Cachat, E., Liu, W., Martin, K. C., Yuan, X., Yin, H., Hohenstein, P., and Davies, J. A. (2016) 2- and 3-Dimensional synthetic large-scale de novo patterning by mammalian cells through phase separation. *Sci. Rep. 6*, 1–8.

(133) Maître, J. L., and Heisenberg, C. P. (2013) Three functions of cadherins in cell adhesion. *Curr. Biol. 23*, 626–633.

(134) Payne, S., Li, B., Cao, Y., Schaeffer, D., Ryser, M. D., and You, L. (2013) Temporal control of self-organized pattern formation without morphogen gradients in bacteria. *Mol. Syst. Biol. 9*, 1–10.

(135) Liu, C., Fu, X., Liu, L., Ren, X., Chau, C. K. L., Li, S., Xiang, L., Zeng, H., Chen, G., Tang, L. H., Lenz, P., Cui, X., Huang, W., Hwa, T., and Huang, J. D. (2011) Sequential establishment of stripe patterns in an expanding cell population. *Science (80-.). 334*, 238–241.

(136) Rudge, T. J., Federici, F., Steiner, P. J., Kan, A., and Haseloff, J. (2013) Cell polarity-driven instability generates self-organized, fractal patterning of cell layers. *ACS Synth. Biol. 2*, 705–714.

(137) Nuñez, I. N., Matute, T. F., Del Valle, I. D., Kan, A., Choksi, A., Endy, D., Haseloff, J., Rudge, T. J., and Federici, F. (2017) Artificial symmetry-breaking for morphogenetic engineering bacterial colonies. *ACS Synth. Biol. 6*, 256–265.

(138) Keeley, F. W., Bellingham, C. M., and Woodhouse, K. a. (2002) Elastin as a self-organizing biomaterial: use of recombinantly expressed human elastin polypeptides as a model for investigations of structure and self-assembly of elastin. *Philos. Trans. R. Soc. Lond. B. Biol. Sci. 357*, 185–189.

(139) Elvin, C. M., Carr, A. G., Huson, M. G., Maxwell, J. M., Pearson, R. D., Vuocolo, T., Liyou, N. E., Wong, D. C. C., Merritt, D. J., and Dixon, N. E. (2005) Synthesis and properties of crosslinked recombinant pro-resilin. *Nature 437*, 999–1002.

(140) Cosgriff-Hernandez, E., Hahn, M. S., Russell, B., Wilems, T., Munoz-Pinto, D., Browning, M. B., Rivera, J., and Höök, M. (2010) Bioactive hydrogels based on Designer Collagens. *Acta Biomater. 6*, 3969–3977.

(141) Rouse, J. G., and Van Dyke, M. E. (2010) A review of keratin-based biomaterials for biomedical applications. *Materials (Basel). 3*, 999–1014.

(142) Spiess, K., Lammel, A., and Scheibel, T. (2010) Recombinant spider silk proteins for applications in biomaterials. *Macromol. Biosci. 10*, 998–1007.

(143) Heim, M., Römer, L., and Scheibel, T. (2010) Hierarchical structures made of proteins. The complex architecture of spider webs and their constituent silk proteins. *Chem. Soc. Rev. 39*, 156–64.

(144) Pédelacq, J.-D., Cabantous, S., Tran, T., Terwilliger, T. C., and Waldo, G. S. (2006) Engineering and characterization of a superfolder green fluorescent protein. *Nat. Biotechnol. 24*, 79–88.

(145) Viswanath, B., Rajesh, B., Janardhan, A., Kumar, A. P., and Narasimha, G. (2014) Fungal laccases and their applications in bioremediation. *Enzyme Res. 2014*.

(146) Chung, W. J., Kwon, K. Y., Song, J., and Lee, S. W. (2011) Evolutionary screening of collagen-like peptides that nucleate hydroxyapatite crystals. *Langmuir 27*, 7620–7628.

(147) Marin, F., Roy, N. Le, and Marie, B. (2012) The formation and mineralization of mollusk shell 1099–1125.

(148) Hiew, S. H., and Miserez, A. (2016) Squid sucker ring teeth: multiscale structure–property relationships,

sequencing, and protein engineering of a thermoplastic biopolymer. *ACS Biomater. Sci. Eng.* acsbiomaterials.6b00284.

(149) Ståhl, S., Gräslund, T., Eriksson Karlström, A., Frejd, F. Y., Nygren, P.-Å., and Löfblom, J. (2017) Affibody molecules in biotechnological and medical applications. *Trends Biotechnol. 35*, 691–712.

(150) Alves, D., and Olívia Pereira, M. (2014) Mini-review: Antimicrobial peptides and enzymes as promising candidates to functionalize biomaterial surfaces. *Biofouling 30*, 483–499.

(151) Harwood, C. R., and Cranenburgh, R. (2008) *Bacillus* protein secretion: an unfolding story. *Trends Microbiol. 16*, 73–79.

(152) Harwood, C. R., Pohl, S., Smith, W., and Wipat, A. (2013) *Bacillus subtilis*. Model gram-positive synthetic biology chassis. *Methods Microbiol.*

(153) Lycklama a Nijeholt, J. a., and Driessen, a. J. M. (2012) The bacterial Sec-translocase: structure and mechanism. *Philos. Trans. R. Soc. B Biol. Sci. 367*, 1016–1028.

(154) Whitaker, N., Bageshwar, U., and Musser, S. M. (2013) Effect of cargo size and shape on the transport efficiency of the bacterial Tat translocase. *FEBS Lett. 587*, 912–6.

(155) Fisher, A. C., Kim, J. Y., Perez-Rodriguez, R., Tullman-Ercek, D., Fish, W. R., Henderson, L. a., and Delisa, M. P. (2008) Exploration of twin-arginine translocation for expression and purification of correctly folded proteins in *Escherichia coli*. *Microb. Biotechnol. 1*, 403–415.

(156) Thomas, J. D., Daniel, R. a., Errington, J., and Robinson, C. (2001) Export of active green fluorescent protein to the periplasm by the twin-arginine translocase (Tat) pathway in *Escherichia coli*. *Mol. Microbiol. 39*, 47–53.

(157) Natale, P., Brüser, T., and Driessen, a. J. M. (2008) Sec- and Tat-mediated protein secretion across the bacterial cytoplasmic membrane-Distinct translocases and mechanisms. *Biochim. Biophys. Acta - Biomembr. 1778*, 1735–1756.

(158) Rodrigue, A., Chanal, A., Beck, K., Müller, M., Wu, L., and Mu, M. (1999) Co-translocation of a periplasmic enzyme complex by a hitchhiker mechanism through the bacterial tat pathway. *J. Biol. Chem. 274*, 13223–13228.

(159) DeLisa, M. P., Tullman, D., and Georgiou, G. (2003) Folding quality control in the export of proteins by the bacterial twin-arginine translocation pathway. *Proc. Natl. Acad. Sci. 100*, 6115–6120.

(160) Tjalsma, H., Bolhuis, a, Jongbloed, J. D., Bron, S., and van Dijl, J. M. (2000) Signal peptide-dependent protein transport in *Bacillus subtilis*: a genome-based survey of the secretome. *Microbiol. Mol. Biol. Rev. 64*, 515–547.

(161) Brockmeier, U., Caspers, M., Freudl, R., Jockwer, A., Noll, T., and Eggert, T. (2006) Systematic screening of all signal peptides from *Bacillus subtilis*: a powerful strategy in optimizing heterologous protein secretion in gram-positive bacteria. *J. Mol. Biol. 362*, 393–402.

(162) Degering, C., Eggert, T., Puls, M., Bongaerts, J., Evers, S., Maurer, K. H., and Jaeger, K. E. (2010) Optimization of protease secretion in *Bacillus subtilis* and *Bacillus licheniformis* by screening of homologousand heterologous signal peptides. *Appl. Environ. Microbiol. 76*, 6370–6376.

(163) Pohl, S., and Harwood, C. R. (2010) Heterologous protein secretion by *Bacillus* species. From the cradle to the grave. *Adv. Appl. Microbiol.* 1st ed. Elsevier Inc.

(164) Idiris, A., Tohda, H., Kumagai, H., and Takegawa, K. (2010) Engineering of protein secretion in yeast: Strategies and impact on protein production. *Appl. Microbiol. Biotechnol. 86*, 403–417.

(165) Kjeldsen, T. (2000) Yeast secretory expression of insulin precursors. *Appl. Microbiol. Biotechnol. 54*, 277–286.

(166) Miyanohara, A., Toh-e, A., Nozaki, C., Hamada, F., Ohtomo, N., and Matsubara, K. (1983) Expression of hepatitis B surface antigen gene in yeast. *Proc. Natl. Acad. Sci. U. S. A. 80*, 1–5.

(167) Huang, M., Bao, J., Hallström, B. M., Petranovic, D., and Nielsen, J. (2017) Efficient protein production by yeast requires global tuning of metabolism. *Nat. Commun. 8*.

(168) Veggiani, G., Zakeri, B., and Howarth, M. (2014) Superglue from bacteria: unbreakable bridges for protein nanotechnology. *Trends Biotechnol. 32*, 506–512.

(169) Reddington, S. C., and Howarth, M. (2015) Secrets of a covalent interaction for biomaterials and biotechnology: SpyTag and SpyCatcher. *Curr. Opin. Chem. Biol. 29*, 94–99.

(170) Woolfson, D. N. (2005) The design of coiled-coil structures and assemblies. *Adv. Protein Chem.*

(171) Fontes, C. M. G. A., and Gilbert, H. J. (2010) Cellulosomes: highly efficient nanomachines designed to deconstruct plant cell wall complex carbohydrates. *Annu. Rev. Biochem. 79*, 655–681.

(172) Brune, K. D., Leneghan, D. B., Brian, I. J., Ishizuka, A. S., Bachmann, M. F., Draper, S. J., Biswas, S., and Howarth, M. (2016) Plug-and-Display: decoration of Virus-Like Particles via isopeptide bonds for modular immunization. *Sci. Rep. 6*, 19234.

(173) Schoene, C., Fierer, J. O., Bennett, S. P., and Howarth, M. (2014) SpyTag/SpyCatcher cyclization confers resilience to boiling on a mesophilic enzyme. *Angew. Chem. Int. Ed. Engl. 53*, 6101–4.

(174) Wang, J., Wang, Y., Wang, X., Zhang, D., Wu, S., and Zhang, G. (2016) Enhanced thermal stability of lichenase from *Bacillus subtilis* 168 by SpyTag/SpyCatcher-mediated spontaneous cyclization. *Biotechnol. Biofuels 9*, 79.

(175) Schoene, C., Bennett, S. P., and Howarth, M. (2016) SpyRing interrogation : analyzing how enzyme resilience can be achieved with phytase and distinct cyclization chemistries. *Sci. Rep.* 1–12.

(176) Alves, N. J., Turner, K. B., Daniele, M. A., Oh, E., Medintz, I. L., and Walper, S. A. (2015) Bacterial nanobioreactors-directing enzyme packaging into bacterial outer membrane vesicles. *ACS Appl. Mater. Interfaces 7*, 24963–24972.

(177) Alves, N. J., Turner, K. B., Medintz, I. L., and Walper, S. A. (2016) Protecting enzymatic function through directed packaging into bacterial outer membrane vesicles. *Sci. Rep. 6*, 24866.

(178) Fierer, J. O., Veggiani, G., and Howarth, M. (2014) SpyLigase peptide-peptide ligation polymerizes affibodies to enhance magnetic cancer cell capture. *Proc. Natl. Acad. Sci. U. S. A. 111*, E1176-81.

(179) Lakshmanan, A., Farhadi, A., Nety, S. P., Lee-Gosselin, A., Bourdeau, R. W., Maresca, D., and Shapiro, M. G. (2016) Molecular engineering of acoustic protein nanostructures. *ACS Nano 10*, 7314–7322.

(180) Giessen, T. W., and Silver, P. (2016) A catalytic nanoreactor based on in vivo encapsulation of multiple enzymes in an engineered protein nanocompartment. *ChemBioChem 17*, 1931–1935.

(181) Sun, F., Zhang, W.-B., Mahdavi, A., Arnold, F. H., and Tirrell, D. a. (2014) Synthesis of bioactive protein hydrogels by genetically encoded SpyTag-SpyCatcher chemistry. *Proc. Natl. Acad. Sci. U. S. A. 111*.

(182) Wang, R., Yang, Z., Luo, J., Hsing, I.-M., and Sun, F. (2017) B_{12} -dependent photoresponsive protein hydrogels for controlled stem cell/protein release. *Proc. Natl. Acad. Sci. 114*, 5912–5917.

(183) Kou, S., Yang, Z., Luo, J., and Sun, F. (2017) Entirely recombinant protein-based hydrogels for selective heavy metal sequestration. *Polym. Chem.*

(184) Tan, L. L., Hoon, S. S., and Wong, F. T. (2016) Kinetic controlled Tag-Catcher interactions for directed covalent protein assembly. *PLoS One 11*, 1–15.

(185) Veggiani, G., Nakamura, T., Brenner, M. D., Gayet, R. V, Yan, J., Robinson, C. V, and Howarth, M. (2016) Programmable polyproteams built using twin peptide superglues. *Proc. Natl. Acad. Sci. U. S. A. 113*, 1202–7.

(186) Buldun, C. M., Jean, J., Bedford, M. R., and Howarth, M. (2018) SnoopLigase catalyzes peptide-peptide locking and enables solid-phase conjugate isolation. *J. Am. Chem. Soc.* jacs.7b13237.

(187) Brune, K. D., Buldun, C. M., Li, Y., Taylor, I. J., Brod, F., Biswas, S., and Howarth, M. (2017) Dual plug-and-display synthetic assembly using orthogonal reactive proteins for twin antigen immunization. *Bioconjug. Chem. 28*, 1544–1551.

(188) Zakeri, B., and Howarth, M. (2010) Spontaneous intermolecular amide bond formation between side chains for irreversible peptide targeting. *J. Am. Chem. Soc. 132*, 4526–4527.

(189) Peng, Y. Y., Yoshizumi, A., Danon, S. J., Glattauer, V., Prokopenko, O., Mirochnitchenko, O., Yu, Z., Inouye, M., Werkmeister, J. a., Brodsky, B., and Ramshaw, J. a M. (2010) A *Streptococcus pyogenes* derived collagen-like protein as a non-cytotoxic and non-immunogenic cross-linkable biomaterial. *Biomaterials 31*, 2755–2761.

(190) Parmar, P. A., Chow, L. W., St-Pierre, J.-P., Horejs, C.-M., Peng, Y. Y., Werkmeister, J. A., Ramshaw, J. A. M., and Stevens, M. M. (2015) Collagen-mimetic peptide-modifiable hydrogels for articular cartilage regeneration. *Biomaterials 54*, 213–225.

(191) Liu, C. C., and Schultz, P. G. (2010) Adding new chemistries to the genetic code. *Annu. Rev. Biochem. 79*,

413–44.

(192) Chin, J. W., Martin, A. B., King, D. S., Wang, L., and Schultz, P. G. (2002) Addition of a photocrosslinking amino acid to the genetic code of *Escherichia coli*. *Proc. Natl. Acad. Sci. U. S. A. 99*, 11020–4.

(193) Bundy, B. C., and Swartz, J. R. (2010) Site-specific incorporation of p-propargyloxyphenylalanine in a cell-free environment for direct protein-protein click conjugation. *Bioconjug. Chem. 21*, 255–263.

(194) Torres-Kolbus, J., Chou, C., Liu, J., and Deiters, A. (2014) Synthesis of non-linear protein dimers through a genetically encoded Thiol-ene reaction. *PLoS One 9*, e105467.

(195) Albayrak, C., and Swartz, J. R. (2014) Direct polymerization of proteins. *ACS Synth. Biol. 3*, 353–62.

(196) Shih, H.-W., Kamber, D. N., and Prescher, J. a. (2014) Building better bioorthogonal reactions. *Curr. Opin. Chem. Biol. 21C*, 103–111.

(197) Lajoie, M., Rovner, A., and Goodman, D. (2013) Genomically recoded organisms expand biological functions. *Science (80-.).*

(198) Zhang, W. H., Otting, G., and Jackson, C. J. (2013) Protein engineering with unnatural amino acids. *Curr. Opin. Struct. Biol. 23*, 581–7.

(199) Lee, M. E., DeLoache, W. C., Cervantes, B., and Dueber, J. E. (2015) A highly-characterized yeast toolkit for modular, multi-part assembly. *ACS Synth. Biol. 4*, 150414151809002.

(200) Li, L., Fierer, J. O., Rapoport, T. a, and Howarth, M. (2014) Structural analysis and optimization of the covalent association between SpyCatcher and a peptide Tag. *J. Mol. Biol. 426*, 309–17.

(201) Lee, M. E., DeLoache, W. C., Cervantes, B., and Dueber, J. E. (2015) A highly-characterized yeast toolkit for modular, multi-part assembly. *ACS Synth. Biol. 4*, 975–986.

(202) Bellingham, C. M., Woodhouse, K. A., Robson, P., Rothstein, S. J., and Keeley, F. W. (2001) Self-aggregation characteristics of recombinantly expressed human elastin polypeptides. *Biochim. Biophys. Acta - Protein Struct. Mol. Enzymol. 1550*, 6–19.

(203) Cormack, B. P., Valdivia, R. H., and Falkow, S. (1996) FACS-optimized mutants of the green fluorescent protein (GFP). *Gene 173*, 33–38.

(204) Winston, F., Dollard, C., and Ricupero-Hovasse, S. L. (1995) Construction of a set of convenient *Saccharomyces cerevisiae strains* that are isogenic to S288C. *Yeast 11*, 53–55.

(205) Florea, M., Hagemann, H., Santosa, G., Abbott, J., Micklem, C. N., Spencer-Milnes, X., de Arroyo Garcia, L., Paschou, D., Lazenbatt, C., Kong, D., Chughtai, H., Jensen, K., Freemont, P. S., Kitney, R., Reeve, B., and Ellis, T. (2016) Engineering control of bacterial cellulose production using a genetic toolkit and a new cellulose-producing strain. *Proc. Natl. Acad. Sci.* 201522985.

(206) Hartwell, L. H., Hopfield, J. J., Leibler, S., and Murray, A. W. (1999) From molecular to modular cell biology. *Nature 402*, C47–C52.

(207) Myhrvold, C., Polka, J. K., and Silver, P. A. (2016) Synthetic lipid-containing scaffolds enhance production by colocalizing enzymes. *ACS Synth. Biol. 5*, 1396–1403.

(208) Thrane, S., Janitzek, C. M., Matondo, S., Resende, M., Gustavsson, T., de Jongh, W. A., Clemmensen, S., Roeffen, W., van de Vegte-Bolmer, M., van Gemert, G. J., Sauerwein, R., Schiller, J. T., Nielsen, M. A., Theander, T. G., Salanti, A., and Sander, A. F. (2016) Bacterial superglue enables easy development of efficient virus-like particle based vaccines. *J. Nanobiotechnology 14*, 30.

(209) Liu, Z., Zhou, H., Wang, W., Tan, W., Fu, Y.-X., and Zhu, M. (2014) A novel method for synthetic vaccine construction based on protein assembly. *Sci. Rep. 4*, 7266.

(210) Kan, S.-H., Aoyagi-Scharber, M., Le, S. Q., Vincelette, J., Ohmi, K., Bullens, S., Wendt, D. J., Christianson, T. M., Tiger, P. M. N., Brown, J. R., Lawrence, R., Yip, B. K., Holtzinger, J., Bagri, A., Crippen-Harmon, D., Vondrak, K. N., Chen, Z., Hague, C. M., Woloszynek, J. C., Cheung, D. S., Webster, K. A., Adintori, E. G., Lo, M. J., Wong, W., Fitzpatrick, P. A., LeBowitz, J. H., Crawford, B. E., Bunting, S., Dickson, P. I., and Neufeld, E. F. (2014) Delivery of an enzyme-IGFII fusion protein to the mouse brain is therapeutic for mucopolysaccharidosis type IIIB. *Proc. Natl. Acad. Sci. U. S. A. 111*, 14870–5.

(211) Chen, X., Zaro, J. L., and Shen, W.-C. (2013) Fusion protein linkers: property, design and functionality. *Adv.*

Drug Deliv. Rev. 65, 1357–69.

(212) Yang, H., Liu, L., and Xu, F. (2016) The promises and challenges of fusion constructs in protein biochemistry and enzymology. *Appl. Microbiol. Biotechnol. 100*, 8273–8281.

(213) Zhang, M., Lin, S., Song, X., Liu, J., Fu, Y., Ge, X., Fu, X., Chang, Z., and Chen, P. R. (2011) A genetically incorporated crosslinker reveals chaperone cooperation in acid resistance. *Nat. Chem. Biol. 7*, 671–7.

(214) Hudak, J. E., Barfield, R. M., Dehart, G. W., Grob, P., Nogales, E., Bertozzi, C. R., and Rabuka, D. (2012) Synthesis of heterobifunctional protein fusions using copper-free click chemistry and the aldehyde tag. *Angew. Chemie - Int. Ed. 51*, 4161–4165.

(215) Zhang, W.-B., Sun, F., Tirrell, D. a, and Arnold, F. H. (2013) Controlling macromolecular topology with genetically encoded SpyTag-SpyCatcher chemistry. *J. Am. Chem. Soc. 135*, 13988–97.

(216) Wang, X. W., and Zhang, W. Bin. (2016) Cellular Synthesis of Protein Catenanes. *Angew. Chemie - Int. Ed. 55*, 3442–3446.

(217) Gao, X., Fang, J., Xue, B., Fu, L., and Li, H. (2016) Engineering protein hydrogels using spycatcher-spytag chemistry. *Biomacromolecules 17*, 2812–2819.

(218) Bedbrook, C. N., Kato, M., Ravindra kumar, S., Lakshmanan, A., Nath, R. D., Sun, F., Sternberg, P. W., Arnold, F. H., and Gradinaru, V. (2015) Genetically encoded spy peptide fusion system to detect plasma membrane-localized proteins in vivo. *Chem. Biol. 22*, 1108–1121.

(219) Moon, H., Bae, Y., Kim, H., and Kang, S. (2016) Plug-and-playable fluorescent cell imaging modular toolkits using the bacterial superglue, SpyTag/SpyCatcher. *Chem. Commun. 52*, 14051–14054.

(220) Dovala, D., Sawyer, W. S., Rath, C. M., and Metzger, L. E. (2016) Rapid analysis of protein expression and solubility with the SpyTag-SpyCatcher system. *Protein Expr. Purif. 117*, 44–51.

(221) Schloss, A. C., Liu, W., Williams, D. M., Kaufman, G., Hendrickson, H. P., Rudshteyn, B., Fu, L., Wang, H., Batista, V. S., Osuji, C., Yan, E. C. Y., and Regan, L. (2016) Fabrication of Modularly Functionalizable Microcapsules Using Protein-Based Technologies. *ACS Biomater. Sci. Eng.* acsbiomaterials.6b00447.

(222) Peschke, T., Rabe, K. S., and Niemeyer, C. M. (2017) Orthogonal surface tags for whole-cell biocatalysis. *Angew. Chemie Int. Ed.* 1–5.

(223) Mergulhão, F. J. M., Summers, D. K., and Monteiro, G. a. (2005) Recombinant protein secretion in *Escherichia coli*. *Biotechnol. Adv. 23*, 177–202.

(224) Azam, A., Li, C., Metcalf, K. J., and Tullman-Ercek, D. (2015) Type III secretion as a generalizable strategy for the production of full-length biopolymer-forming proteins. *Biotechnol. Bioeng. 9999*, 1–8.

(225) Brenner, K., You, L., and Arnold, F. H. (2008) Engineering microbial consortia: a new frontier in synthetic biology. *Trends Biotechnol. 26*, 483–9.

(226) Jones, J. A., Vernacchio, V. R., Sinkoe, A. L., Collins, S. M., Ibrahim, M. H. A., Lachance, D. M., Hahn, J., and Koffas, M. A. G. (2016) Experimental and computational optimization of an *Escherichia coli* co-culture for the efficient production of flavonoids. *Metab. Eng. 35*, 55–63.

(227) Scott, C. P., Abel-Santos, E., Wall, M., Wahnon, D. C., and Benkovic, S. J. (1999) Production of cyclic peptides and proteins in vivo. *Proc. Natl. Acad. Sci. 96*, 13638–13643.

(228) Trabi, M., and Craik, D. J. (2002) Circular proteins - no end in sight. *Trends Biochem. Sci. 27*, 132–138.

(229) Iwai, H., and Plu, A. (1999) Circular L-lactamase : stability enhancement by cyclizing the backbone. *FEBS Lett. 459*, 166–172.

(230) Waldhauer, M. C., Schmitz, S. N., Ahlmann-Eltze, C., Gleixner, J. G., Schmelas, C. C., Huhn, A. G., Bunne, C., Büscher, M., Horn, M., Klughammer, N., Kreft, J., Schäfer, E., Bayer, P. A., Krämer, S. G., Neugebauer, J., Wehler, P., Mayer, M. P., Eils, R., and Di Ventura, B. (2015) Backbone circularization of *Bacillus subtilis* family 11 xylanase increases its thermostability and its resistance against aggregation. *Mol. Biosyst. 11*, 3231–43.

(231) Schoene, C., Bennett, S. P., and Howarth, M. (2016) SpyRings Declassified: A Blueprint for Using Isopeptide-Mediated Cyclization to Enhance Enzyme Thermal Resilience. *Pept. Protein Enzym. Des.* 1st ed. Elsevier Inc.

(232) Kumar, V., Marín-Navarro, J., and Shukla, P. (2016) Thermostable microbial xylanases for pulp and paper

industries: trends, applications and further perspectives. *World J. Microbiol. Biotechnol. 32*, 1–10.

(233) Juturu, V., and Wu, J. C. (2012) Microbial xylanases: Engineering, production and industrial applications. *Biotechnol. Adv. 30*, 1219–1227.

(234) Kuhad, R. C., Gupta, R., and Singh, A. (2011) Microbial cellulases and their industrial applications. *Enzyme Res. 2011*, 280696.

(235) Zhang, X. Z., and Zhang, Y. H. P. (2010) One-step production of biocommodities from lignocellulosic biomass by recombinant cellulolytic Bacillus subtilis: Opportunities and challenges. *Eng. Life Sci. 10*, 398–406.

(236) Moraïs, S., Barak, Y., Caspi, J., and Hadar, Y. (2010) Cellulase-xylanase synergy in designer cellulosomes for enhanced degradation of a complex cellulosic substrate. *MBio 1*, 3–10.

(237) Arai, T., Matsuoka, S., Cho, H.-Y., Yukawa, H., Inui, M., Wong, S.-L., and Doi, R. H. (2007) Synthesis of *Clostridium cellulovorans* minicellulosomes by intercellular complementation. *Proc. Natl. Acad. Sci. U. S. A. 104*, 1456–1460.

(238) Moraïs, S., Shterzer, N., Lamed, R., Bayer, E. A., and Mizrahi, I. (2014) A combined cell-consortium approach for lignocellulose degradation by specialized *Lactobacillus plantarum* cells. *Biotechnol. Biofuels 7*, 112.

(239) Stahl, S. W., Nash, M. A., Fried, D. B., Slutzki, M., Barak, Y., Bayer, E. A., and Gaub, H. E. (2012) Single-molecule dissection of the high-affinity cohesin-dockerin complex. *Proc. Natl. Acad. Sci. 109*, 20431–20436.

(240) Abe, H., Wakabayashi, R., Yonemura, H., Yamada, S., Goto, M., and Kamiya, N. (2013) Split Spy0128 as a potent scaffold for protein cross-linking and immobilization. *Bioconjug. Chem. 24*, 242–250.

(241) Dorval Courchesne, N.-M., Duraj-Thatte, A., Tay, P. K. R., Nguyen, P. Q., and Joshi, N. S. (2016) Scalable production of genetically engineered nanofibrous macroscopic materials via filtration. *ACS Biomater. Sci. Eng.* acsbiomaterials.6b00437.

(242) Jayabalan, R., Malini, K., Sathishkumar, M., Swaminathan, K., and Yun, S. E. (2010) Biochemical characteristics of tea fungus produced during kombucha fermentation. *Food Sci. Biotechnol. 19*, 843–847.

(243) Kosina, S. M., Danielewicz, M. A., Mohammed, M., Ray, J., Suh, Y., Yilmaz, S., Singh, A. K., Arkin, A. P., Deutschbauer, A. M., and Northen, T. R. (2016) Exometabolomics Assisted Design and Validation of Synthetic Obligate Mutualism. *ACS Synth. Biol. 5*, 569–576.

(244) Baldwin, W., and Kubitschek, H. E. (1984) Buoyant density variation during the cell cycle of *Saccharomyces cerevisiae*. *J. Bacteriol. 158*, 701–704.

(245) Ong, E., Gilkes, N. R., Miller, R. C., Warren, R. a, and Kilburn, D. G. (1993) The cellulose-binding domain (CBD(Cex)) of an exoglucanase from *Cellulomonas fimi*: production in *Escherichia coli* and characterization of the polypeptide. *Biotechnol. Bioeng. 42*, 401–9.

(246) Harju, M., Kallioinen, H., and Tossavainen, O. (2012) Lactose hydrolysis and other conversions in dairy products: Technological aspects. *Int. Dairy J. 22*, 104–109.

(247) Bhosale, S. H., Rao, M. B., and Deshpande, V. V. (1996) Molecular and industrial aspects of glucose isomerase. *Microbiol. Rev. 60*, 280–300.

(248) DiCosimo, R., McAuliffe, J., Poulose, A. J., and Bohlmann, G. (2013) Industrial use of immobilized enzymes. *Chem. Soc. Rev. 42*, 6437.

(249) Li, J., Xu, H., Bentley, W. E., and Rao, G. (2002) Impediments to secretion of green fluorescent protein and its fusion from *Saccharomyces cerevisiae*. *Biotechnol. Prog. 18*, 831–838.

(250) Huang, D., and Shusta, E. V. (2005) Secretion and surface display of green fluorescent protein using the yeast *Saccharomyces cerevisiae*. *Biotechnol. Prog. 21*, 349–357.

(251) McIsaac, R. S., Gibney, P. A., Chandran, S. S., Benjamin, K. R., and Botstein, D. (2014) Synthetic biology tools for programming gene expression without nutritional perturbations in *Saccharomyces cerevisiae*. *Nucleic Acids Res. 42*, 1–8.

(252) Ostrov, N., Jimenez, M., Billerbeck, S., Brisbois, J., Matragrano, J., Ager, A., and Cornish, V. W. (2017) A modular yeast biosensor for low-cost point-of-care pathogen detection. *Sci. Adv. 3*, e1603221.

(253) Jarque, S., Bittner, M., Blaha, L., and Hilscherova, K. (2016) Yeast Biosensors for Detection of Environmental

Pollutants: Current State and Limitations. *Trends Biotechnol. 34*, 408–419.

(254) Adeniran, A., Sherer, M., and Tyo, K. E. J. (2015) Yeast-based biosensors: Design and applications. *FEMS Yeast Res. 15*, 1–15.

(255) Adeniran, A., Stainbrook, S., Bostick, J., and Tyo, K. (2018) Detection of a peptide biomarker by engineered yeast receptors. *ACS Synth. Biol.* acssynbio.7b00410.

(256) Pohl, S., Bhavsar, G., Hulme, J., Bloor, A. E., Misirli, G., Leckenby, M. W., Radford, D. S., Smith, W., Wipat, A., Williamson, E. D., Harwood, C. R., and Cranenburgh, R. M. (2013) Proteomic analysis of *Bacillus subtilis* strains engineered for improved production of heterologous proteins. *Proteomics 13*, 3298–3308.

(257) Hobley, L., Harkins, C., MacPhee, C. E., and Stanley-Wall, N. R. (2015) Giving structure to the biofilm matrix: an overview of individual strategies and emerging common themes. *FEMS Microbiol. Rev. 39*, 649–669.

(258) Hobley, L., Ostrowski, A., Rao, F. V, Bromley, K. M., Porter, M., Prescott, A. R., MacPhee, C. E., van Aalten, D. M. F., and Stanley-Wall, N. R. (2013) BslA is a self-assembling bacterial hydrophobin that coats the *Bacillus subtilis* biofilm. *Proc. Natl. Acad. Sci. 110*, 13600–13605.

(259) Schloss, A. C., Liu, W., Williams, D. M., Kaufman, G., Hendrickson, H. P., Rudshteyn, B., Fu, L., Wang, H., Batista, V. S., Osuji, C., Yan, E. C. Y., and Regan, L. (2016) Fabrication of modularly functionalizable microcapsules using protein-based technologies. *ACS Biomater. Sci. Eng. 2*, 1856–1861.

(260) Zhang, F., Kwan, A., Xu, A., and Süel, G. M. (2015) A synthetic quorum sensing system reveals a potential private benefit for public good production in a biofilm. *PLoS One* (Meijler, M. M., Ed.) *10*, e0132948.

(261) Zara, S., Bakalinsky, A. T., Zara, G., Pirino, G., Demontis, M. A., and Budroni, M. (2005) FLO11-based model for air-liquid interfacial biofilm formation by *Saccharomyces cerevisiae*. *Appl. Environ. Microbiol. 71*, 2934–9.

(262) Bourdeau, R. W., Lee-Gosselin, A., Lakshmanan, A., Farhadi, A., Kumar, S. R., Nety, S. P., and Shapiro, M. G. (2018) Acoustic reporter genes for noninvasive imaging of microorganisms in mammalian hosts. *Nature 553*, 86–90.

(263) Chen, M.-T., and Weiss, R. (2005) Artificial cell-cell communication in yeast *Saccharomyces cerevisiae* using signaling elements from Arabidopsis thaliana. *Nat. Biotechnol. 23*, 1551–5.

(264) Weber, C., Brückner, C., Weinreb, S., Lehr, C., Essl, C., and Boles, E. (2012) Biosynthesis of cis,cis-muconic acid and its aromatic precursors, catechol and protocatechuic acid, from renewable feedstocks by *Saccharomyces cerevisiae*. *Appl. Environ. Microbiol. 78*, 8421–8430.

(265) Rogers, J. K., and Church, G. M. (2016) Genetically encoded sensors enable real-time observation of metabolite production. *Proc. Natl. Acad. Sci. 113*, 2388–2393.

(266) Curran, K. A., Leavitt, J. M., Karim, A. S., and Alper, H. S. (2013) Metabolic engineering of muconic acid production in *Saccharomyces cerevisiae*. *Metab. Eng. 15*, 55–66.

(267) Skjoedt, M. L., Snoek, T., Kildegaard, K. R., Arsovska, D., Eichenberger, M., Goedecke, T. J., Rajkumar, A. S., Zhang, J., Kristensen, M., Lehka, B. J., Siedler, S., Borodina, I., Jensen, M. K., and Keasling, J. D. (2016) Engineering prokaryotic transcriptional activators as metabolite biosensors in yeast. *Nat. Chem. Biol. 12*, 951–958.

(268) Borodina, I., and Nielsen, J. (2014) Advances in metabolic engineering of yeast *Saccharomyces cerevisiae* for production of chemicals. *Biotechnol. J. 9*, 609–620.

(269) Manukyan, L., Montandon, S. A., Fofonjka, A., Smirnov, S., and Milinkovitch, M. C. (2017) A living mesoscopic cellular automaton made of skin scales. *Nature 544*, 173–179.

(270) McNamara, J. T., Morgan, J. L. W., and Zimmer, J. (2015) A Molecular Description of Cellulose Biosynthesis. *Annu. Rev. Biochem. 84*, 895–921.

Appendix

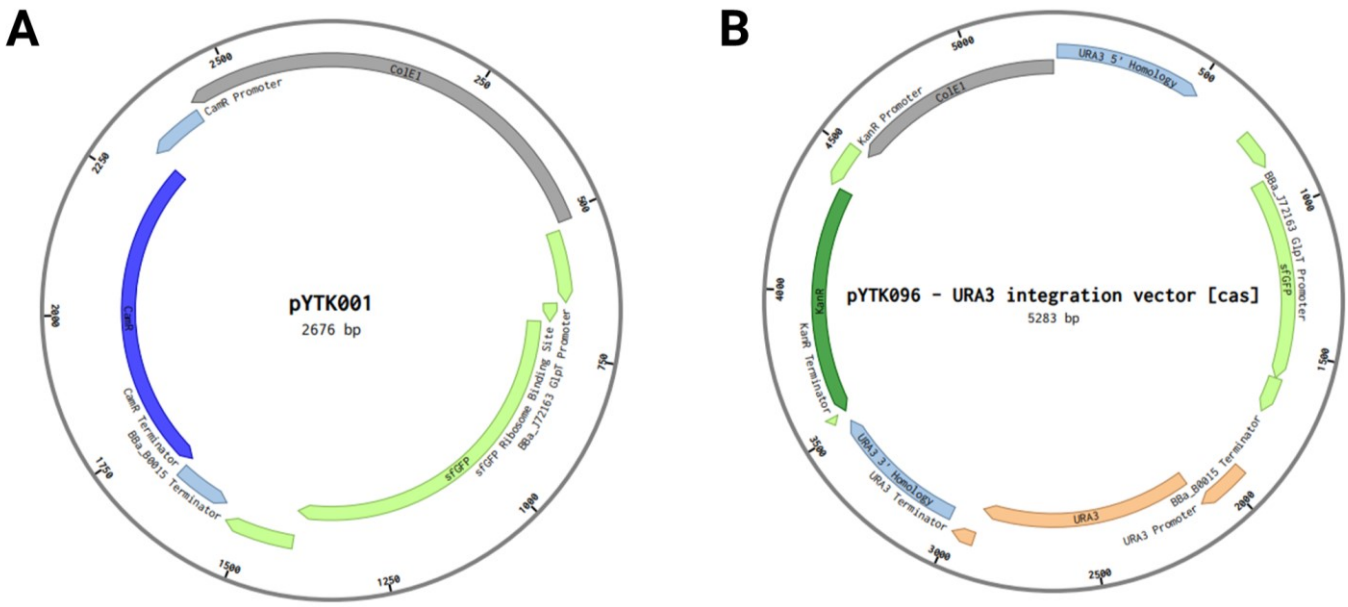

Appendix Figure 1. **Plasmid maps of YTK cloning vectors. A** The YTK entry vector pYKT001. The ColE1 and CamR sequences on the pYTK001 plasmid backbone enable plasmid replication and selection in E. coli. A constitutive GFP expressing 'dropout' part is included. When new parts are cloned into the pYTK001 vector using BsmBI golden gate reactions, the GFP dropout part is excised and replaced by the new part. Therefore, simple green-white selection enables discrimination of plasmids into which new parts have been cloned and unwanted re-ligate pYTK001 plasmids. **B** The YTK destination vector pYTK096. To improve cloning efficiency, multiple YTK parts can be pre-assembled to form a destination vector. In this case, YTK parts enabling plasmid replication and selection in E. coli (KanR and ColE1) and YTK parts enabling integrative transformation into the URA3 locus in S. cerevisiae (URA3 5' homology, URA3 3' homology and URA3 expression cassette) have been pre-assembled. Another GFP dropout part is present, spanning part positions 2 (promoter), 3 (protein coding sequence) and 4 (terminator). Therefore, to create integrative constructs for protein expression in S. cerevisiae, promoter parts, terminator parts and protein coding parts are selected from the YTK system and assembled into pYTK096 using a BsaI golden gate reaction. For clarity, sequences of 2-3-4 parts used in this study are shown in Appendix Table 1.

Appendix Table 1. Annotated DNA sequences of inserts used to create S. cerevisiae protein expression constructs. Promoter sequences are highlighted in grey (part 2, pTDH1), mating factor alpha coding sequences are highlighted in turquoise (part 3a, MFα), sfGFP coding sequences are highlighted in green (part 3b, sfGFP), TEM1 BLA coding sequences are highlighted in red (part 3b, BLA), CBDcex coding sequences are highlighted in teal (part 4a, CBDcex) and terminator coding sequences are highlighted in yellow (part 4b or 4, tTDH1). Overhangs created during golden gate assembly are underlined.

Construct	2-3-4 insert DNA sequence
yCG01	AACGCAGTTCGAGTTTATCATTATCAATACTGCCATTTCAAAGAATACGTAAATAATTAATAGTAGTGATTTTCCTAAC TTTATTTAGTCAAAAAATTAGCCTTTTAATTCTGCTGTAACCCGTACATGCCCAAAATAGGGGGCGGGTTACACAGAAT ATATAACATCGTAGGTGTCTGGGTGAACAGTTTATTCCTGGCATCCACTAAATATAATGGAGCCCGCTTTTTAAGCTGG CATCCAGAAAAAAAAAAGAATCCCAGCACCAAAATATTGTTTTCTTCACCAACCATCAGTTCATAGGTCCATTCTCTTAG CGCAACTACAGAGAACAGGGGCACAAACAGGCAAAAAACGGGCACAACCTCAATGGAGTGATGCAACCTGCCTGGAGTA AATGATGACACAAGGCAATTGACCCACGCATGTATCTATCTCATTTTCTTACACCTTCTATTACCTTCTGCTCTCTCTG ATTTGGAAAAAGCTGAAAAAAAAGGTTGAAACCAGTTCCCTGAAATTATTCCCCTACTTGACTAATAAGTATATAAAGA CGGTAGGTATTGATTGTAATTCTGTAAATCTATTTCTTAAACTTCTTAAATTCTACTTTTATAGTTAGTCTTTTTTTTA GTTTTAAAACACCAAGAACTTAGTTTCGAATAAACACACATAAACAAACAAAAGATCTATGAGATTTCCTTCAATTTTT ACTGCAGTTTTATTCGCAGCATCCTCCGCATTAGCTGCTCCAGTCAACACTACAACAGAAGATGAAACGGCACAAATTC CGGCTGAAGCTGTCATCGGTTACTTAGATTTAGAAGGGGATTTCGATGTTGCTGTTTTGCCATTTTCCAACAGCACAAA TAACGGGTTATTGTTTATAAATACTACTATTGCCAGCATTGCTGCTAAAGAAGAAGGGGTATCTTTGGATAAAAGAGGT TCTATGTCCAAGGGTGAAGAGCTATTTACTGGGGTTGTACCCATTTTGGTAGAACTGGACGGAGATGTAAACGGACATA AATTCTCTGTTAGAGGTGAGGGCGAAGGCGATGCCACCAATGGTAAATTGACTCTGAAGTTTATATGCACTACGGGTAA ATTACCTGTTCCTTGGCCAACCCTAGTAACAACTTTGACATATGGTGTTCAATGTTTCTCAAGATACCCAGACCATATG AAAAGGCATGATTTCTTTAAAAGTGCTATGCCAGAAGGCTACGTGCAAGAGAGAACTATCTCCTTTAAGGATGACGGTA CGTATAAAACACGAGCAGAAGTGAAATTCGAAGGGGATACACTAGTTAATCGCATCGAATTAAAGGGTATAGACTTTAA GGAAGATGGTAATATTCTCGGCCATAAACTTGAGTATAATTTCAACTCGCATAATGTGTACATTACAGCTGACAAACAA AAGAACGGAATTAAAGCGAATTTTAAAATCAGGCACAACGTCGAAGATGGGTCTGTTCAACTTGCCGATCATTATCAGC AAAACACCCCTATTGGTGATGGTCCAGTCTTGTTACCCGATAATCACTACTTAAGCACACAGTCTAGATTGTCAAAAGA TCCGAATGAAAAGCGTGATCACATGGTTTTATTGGAATTTGTCACCGCTGCAGGAATAACTCACGGAATGGACGAGCTT TATAAGGGATCCTAACTCGAGATAAAGCAATCTTGATGAGGATAATGATTTTTTTTTGAATATACATAAATACTACCGT TTTTCTGCTAGATTTTGTGATGACGTAAATAAGTACATATTACTTTTTAAGCCAAGACAAGATTAAGCATTAACTTTAC CCTTTTCTTTTCTAAGTTTCAATATTAGTTATCACTGTTTAAAAGTTATGGCGAGAACGTCGGCGGTTAAAATATATTAC CCTGAACGGCTG
yCG02	AACGCAGTTCGAGTTTATCATTATCAATACTGCCATTTCAAAGAATACGTAAATAATTAATAGTAGTGATTTTCCTAAC TTTATTTAGTCAAAAAATTAGCCTTTTAATTCTGCTGTAACCCGTACATGCCCAAAATAGGGGGCGGGTTACACAGAAT ATATAACATCGTAGGTGTCTGGGTGAACAGTTTATTCCTGGCATCCACTAAATATAATGGAGCCCGCTTTTTAAGCTGG CATCCAGAAAAAAAAAAGAATCCCAGCACCAAAATATTGTTTTCTTCACCAACCATCAGTTCATAGGTCCATTCTCTTAG CGCAACTACAGAGAACAGGGGCACAAACAGGCAAAAAACGGGCACAACCTCAATGGAGTGATGCAACCTGCCTGGAGTA AATGATGACACAAGGCAATTGACCCACGCATGTATCTATCTCATTTTCTTACACCTTCTATTACCTTCTGCTCTCTCTG ATTTGGAAAAAGCTGAAAAAAAAGGTTGAAACCAGTTCCCTGAAATTATTCCCCTACTTGACTAATAAGTATATAAAGA CGGTAGGTATTGATTGTAATTCTGTAAATCTATTTCTTAAACTTCTTAAATTCTACTTTTATAGTTAGTCTTTTTTTTA GTTTTAAAACACCAAGAACTTAGTTTCGAATAAACACACATAAACAAACAAAAGATCTATGAGATTTCCTTCAATTTTT ACTGCAGTTTTATTCGCAGCATCCTCCGCATTAGCTGCTCCAGTCAACACTACAACAGAAGATGAAACGGCACAAATTC CGGCTGAAGCTGTCATCGGTTACTTAGATTTAGAAGGGGATTTCGATGTTGCTGTTTTGCCATTTTCCAACAGCACAAA TAACGGGTTATTGTTTATAAATACTACTATTGCCAGCATTGCTGCTAAAGAAGAAGGGGTATCTTTGGATAAAAGAGGT TCTATGTCCAAGGGTGAAGAGCTATTTACTGGGGTTGTACCCATTTTGGTAGAACTGGACGGAGATGTAAACGGACATA AATTCTCTGTTAGAGGTGAGGGCGAAGGCGATGCCACCAATGGTAAATTGACTCTGAAGTTTATATGCACTACGGGTAA ATTACCTGTTCCTTGGCCAACCCTAGTAACAACTTTGACATATGGTGTTCAATGTTTCTCAAGATACCCAGACCATATG AAAAGGCATGATTTCTTTAAAAGTGCTATGCCAGAAGGCTACGTGCAAGAGAGAACTATCTCCTTTAAGGATGACGGTA CGTATAAAACACGAGCAGAAGTGAAATTCGAAGGGGATACACTAGTTAATCGCATCGAATTAAAGGGTATAGACTTTAA GGAAGATGGTAATATTCTCGGCCATAAACTTGAGTATAATTTCAACTCGCATAATGTGTACATTACAGCTGACAAACAA AAGAACGGAATTAAAGCGAATTTTAAAATCAGGCACAACGTCGAAGATGGGTCTGTTCAACTTGCCGATCATTATCAGC AAAACACCCCTATTGGTGATGGTCCAGTCTTGTTACCCGATAATCACTACTTAAGCACACAGTCTAGATTGTCAAAAGA TCCGAATGAAAAGCGTGATCACATGGTTTTATTGGAATTTGTCACCGCTGCAGGAATAACTCACGGAATGGACGAGCTT TATAAGGGATCCGGCGGACCCGCTGGGTGCCAAGTGTTATGGGGGGTCAATCAGTGGAATACTGGTTTCACGGCTAACG TCACTGTCAAGAACACTTCCTCTGCCCCTGTTGACGGCTGGACACTAACTTTCAGTTTCCCATCCGGTCAACAGGTTAC CCAGGCATGGTCCTCCACTGTAACTCAATCCGGTAGTGCTGTCACTGTAAGGAATGCACCTTGGAATGGCAGCATCCCT GCCGGAGGGACTGCACAATTCGGCTTCAACGGGAGTCACACCGGTACAAACGCGGCTCCAACAGCATTCAGCCTAAACG GTACGCCATGCACCGTAGGGGGTAGTACTGGTTAACTCGAGTGGCATAAAGCAATCTTGATGAGGATAATGATTTTTTT TTGAATATACATAAATACTACCGTTTTTCTGCTAGATTTTGTGATGACGTAAATAAGTACATATTACTTTTTAAGCCAA GACAAGATTAAGCATTAACTTTACCCTTTTCTTTCTAAGTTTCAATATTAGTTATCACTGTTTAAAAGTTATGGCGAGA ACGTCGGCGGTTAAAATATATTACCCTGAACGGCTG

yCG04	AACGCAGTTCGAGTTTATCATTATCAATACTGCCATTTCAAAGAATACGTAAATAATTAATAGTAGTGATTTTCCTAAC TTTATTTAGTCAAAAAATTAGCCTTTTAATTCTGCTGTAACCCGTACATGCCCAAAATAGGGGGCGGGTTACACAGAAT ATATAACATCGTAGGTGTCTGGGTGAACAGTTTATTCCTGGCATCCACTAAATATAATGGAGCCCGCTTTTTAAGCTGG CATCCAGAAAAAAAAAAGAATCCCAGCACCAAAATATTGTTTTCTTCACCAACCATCAGTTCATAGGTCCATTCTCTTAG CGCAACTACAGAGAACAGGGGCACAAACAGGCAAAAAACGGGCACAACCTCAATGGAGTGATGCAACCTGCCTGGAGTA AATGATGACACAAGGCAATTGACCCACGCATGTATCTATCTCATTTTCTTACACCTTCTATTACCTTCTGCTCTCTCTG ATTTGGAAAAAGCTGAAAAAAAAGGTTGAAACCAGTTCCCTGAAATTATTCCCCTACTTGACTAATAAGTATATAAAGA CGGTAGGTATTGATTGTAATTCTGTAAATCTATTTCTTAAACTTCTTAAATTCTACTTTTATAGTTAGTCTTTTTTTTA GTTTTAAAACACCAAGAACTTAGTTTCGAATAAACACACATAAACAAACAAAAGATCTATGAGATTTCCTTCAATTTTT ACTGCAGTTTTATTCGCAGCATCCTCCGCATTAGCTGCTCCAGTCAACACTACAACAGAAGATGAAACGGCACAAATTC CGGCTGAAGCTGTCATCGGTTACTTAGATTTAGAAGGGGATTTCGATGTTGCTGTTTTGCCATTTTCCAACAGCACAAA TAACGGGTTATTGTTTATAAATACTACTATTGCCAGCATTGCTGCTAAAGAAGAAGGGGTATCTTTGGATAAAAGAGGT TCTCACCCAGAAACGCTGGTGAAAGTAAAAGATGCTGAAGATCAGTTGGGTGCACGAGTGGGTTACATCGAACTGGATC TCAACAGCGGTAAGATCCTTGAGAGTTTTCGCCCCGAAGAACGTTTTCCAATGATGAGCACTTTTAAAGTTCTGCTATG TGGCGCGGTATTATCCCGTATTGACGCCGGGCAAGAGCAACTCGGTCGCCGCATACACTATTCTCAGAATGACTTGGTT GAGTACTCACCAGTCACAGAAAAGCATCTTACGGATGGCATGACAGTAAGAGAATTATGCAGTGCTGCCATAACCATGA GTGATAACACTGCGGCCAACTTACTTCTGACAACGATCGGAGGACCGAAGGAGCTAACCGCTTTTTTGCACAACATGGG GGATCATGTAACTCGCCTTGATCGTTGGGAACCGGAGCTGAATGAAGCCATACCAAACGACGAGCGTGACACCACGATG CCTGTAGCAATGGCAACAACGTTGCGCAAACTATTAACTGGCGAACTACTTACTCTAGCTTCCCGGCAACAATTAATAG ACTGGATGGAGGCGGATAAAGTTGCAGGACCACTTCTGCGCTCGGCCCTTCCGGCTGGCTGGTTTATTGCTGATAAATC TGGAGCCGGTGAGCGTGGGTCCCGCGGTATCATTGCAGCACTGGGGCCAGATGGTAAGCCCTCCCGTATCGTAGTTATC TACACGACGGGGAGTCAGGCAACTATGGATGAACGAAATAGACAGATCGCTGAGATAGGTGCCTCACTGATTAAGCATT GGGGATCCTAACTCGAGATAAAGCAATCTTGATGAGGATAATGATTTTTTTTTGAATATACATAAATACTACCGTTTTT CTGCTAGATTTTGTGATGACGTAAATAAGTACATATTACTTTTTAAGCCAAGACAAGATTAAGCATTAACTTTACCCTT TTCTTTCTAAGTTTCAATATTAGTTATCACTGTTTAAAAGTTATGGCGAGAACGTCGGCGGTTAAAATATATTACCCTG AACGGCTG
yCG05	AACGCAGTTCGAGTTTATCATTATCAATACTGCCATTTCAAAGAATACGTAAATAATTAATAGTAGTGATTTTCCTAAC TTTATTTAGTCAAAAAATTAGCCTTTTAATTCTGCTGTAACCCGTACATGCCCAAAATAGGGGGCGGGTTACACAGAAT ATATAACATCGTAGGTGTCTGGGTGAACAGTTTATTCCTGGCATCCACTAAATATAATGGAGCCCGCTTTTTAAGCTGG CATCCAGAAAAAAAAAAGAATCCCAGCACCAAAATATTGTTTTCTTCACCAACCATCAGTTCATAGGTCCATTCTCTTAG CGCAACTACAGAGAACAGGGGCACAAACAGGCAAAAAACGGGCACAACCTCAATGGAGTGATGCAACCTGCCTGGAGTA AATGATGACACAAGGCAATTGACCCACGCATGTATCTATCTCATTTTCTTACACCTTCTATTACCTTCTGCTCTCTCTG ATTTGGAAAAAGCTGAAAAAAAAGGTTGAAACCAGTTCCCTGAAATTATTCCCCTACTTGACTAATAAGTATATAAAGA CGGTAGGTATTGATTGTAATTCTGTAAATCTATTTCTTAAACTTCTTAAATTCTACTTTTATAGTTAGTCTTTTTTTTA GTTTTAAAACACCAAGAACTTAGTTTCGAATAAACACACATAAACAAACAAAAGATCTATGAGATTTCCTTCAATTTTT ACTGCAGTTTTATTCGCAGCATCCTCCGCATTAGCTGCTCCAGTCAACACTACAACAGAAGATGAAACGGCACAAATTC CGGCTGAAGCTGTCATCGGTTACTTAGATTTAGAAGGGGATTTCGATGTTGCTGTTTTGCCATTTTCCAACAGCACAAA TAACGGGTTATTGTTTATAAATACTACTATTGCCAGCATTGCTGCTAAAGAAGAAGGGGTATCTTTGGATAAAAGAGGT TCTCACCCAGAAACGCTGGTGAAAGTAAAAGATGCTGAAGATCAGTTGGGTGCACGAGTGGGTTACATCGAACTGGATC TCAACAGCGGTAAGATCCTTGAGAGTTTTCGCCCCGAAGAACGTTTTCCAATGATGAGCACTTTTAAAGTTCTGCTATG TGGCGCGGTATTATCCCGTATTGACGCCGGGCAAGAGCAACTCGGTCGCCGCATACACTATTCTCAGAATGACTTGGTT GAGTACTCACCAGTCACAGAAAAGCATCTTACGGATGGCATGACAGTAAGAGAATTATGCAGTGCTGCCATAACCATGA GTGATAACACTGCGGCCAACTTACTTCTGACAACGATCGGAGGACCGAAGGAGCTAACCGCTTTTTTGCACAACATGGG GGATCATGTAACTCGCCTTGATCGTTGGGAACCGGAGCTGAATGAAGCCATACCAAACGACGAGCGTGACACCACGATG CCTGTAGCAATGGCAACAACGTTGCGCAAACTATTAACTGGCGAACTACTTACTCTAGCTTCCCGGCAACAATTAATAG ACTGGATGGAGGCGGATAAAGTTGCAGGACCACTTCTGCGCTCGGCCCTTCCGGCTGGCTGGTTTATTGCTGATAAATC TGGAGCCGGTGAGCGTGGGTCCCGCGGTATCATTGCAGCACTGGGGCCAGATGGTAAGCCCTCCCGTATCGTAGTTATC TACACGACGGGGAGTCAGGCAACTATGGATGAACGAAATAGACAGATCGCTGAGATAGGTGCCTCACTGATTAAGCATT GGGGATCCGGCGGACCCGCTGGGTGCCAAGTGTTATGGGGGGTCAATCAGTGGAATACTGGTTTCACGGCTAACGTCAC TGTCAAGAACACTTCCTCTGCCCCTGTTGACGGCTGGACACTAACTTTCAGTTTCCCATCCGGTCAACAGGTTACCCAG GCATGGTCCTCCACTGTAACTCAATCCGGTAGTGCTGTCACTGTAAGGAATGCACCTTGGAATGGCAGCATCCCTGCCG GAGGGACTGCACAATTCGGCTTCAACGGGAGTCACACCGGTACAAACGCGGCTCCAACAGCATTCAGCCTAAACGGTAC GCCATGCACCGTAGGGGGTAGTACTGGTTAACTCGAGTGGCATAAAGCAATCTTGATGAGGATAATGATTTTTTTTTGA ATATACATAAATACTACCGTTTTTCTGCTAGATTTTGTGATGACGTAAATAAGTACATATTACTTTTTAAGCCAAGACA AGATTAAGCATTAACTTTACCCTTTTCTTTCTAAGTTTCAATATTAGTTATCACTGTTTAAAAGTTATGGCGAGAACGT CGGCGGTTAAAATATATTACCCTGAACGGCTG